General Disclaimer

One or more of the Following Statements may affect this Document

- This document has been reproduced from the best copy furnished by the organizational source. It is being released in the interest of making available as much information as possible.

- This document may contain data, which exceeds the sheet parameters. It was furnished in this condition by the organizational source and is the best copy available.

- This document may contain tone-on-tone or color graphs, charts and/or pictures, which have been reproduced in black and white.

- This document is paginated as submitted by the original source.

- Portions of this document are not fully legible due to the historical nature of some of the material. However, it is the best reproduction available from the original submission.

Produced by the NASA Center for Aerospace Information (CASI)

MCR-71-1 (Vol II) Copy No. C3

CONTRACT JPL 952811

FINAL
STUDY
REPORT

JUPITER ATMOSPHERIC ENTRY MISSION STUDY

N71 24338
(ACCESSION NUMBER)
353
(PAGES)
CR 118022
(NASA CR OR TMX OR AD NUMBER)
(THRU)
G-3
(CODE)
30
(CATEGORY)
FACILITY FORM 602

Volume II
Mission and System Evolution

April 1971

MARTIN MARIETTA
DENVER DIVISION

MCR-71-1

Contract JPL 952811

JUPITER ATMOSPHERIC ENTRY MISSION STUDY

FINAL REPORT

Volume II

Mission and System Evolution

April 1971

Approved

Stephen J. Ducsai
Study Manager

MARTIN MARIETTA CORPORATION
Denver Division
Denver, Colorado

This work was performed for the Jet Propulsion Laboratory, California Institute of Technology, sponsored by the National Aeronautics and Space Administration under Contract NAS7-100.

FOREWORD

This report has been prepared in accordance with requirements of Contract JPL 952811 to present data and conclusions resulting from a six-month study effort performed for the Jet Propulsion Laboratory by the Martin Marietta Corporation, Denver Division. The report is divided into the following volumes:

Volume I - Management Summary

Volume II - Mission and System Evolution

Volume III - Supporting Technical Studies

The report is arranged so that Volume I (Management Summary) will provide a concise overview of the study, Volume II (Mission and System Evolution) will provide an appreciation of the major mission and system integration and trade sensitivities, and Volume III (Supporting Technical Studies) will provide the detailed supporting tradeoff studies down to the subsystem level. Volume III also includes the Appendixes with additional detailed data.

CONTENTS

		Page
Foreword		ii
Contents		iii
Abbreviations and Symbols		vi thru xii
I.	Introduction to Volume II	I-1
II.	Environmental Models	II-1
	A. Micrometeoroid Model	II-2
	B. Jupiter Radiation Belt Model	II-6
	C. Decameter and Decimeter Radiation Models	II-11
	D. Jupiter Atmospheric Models	II-12
	E. Atmospheric Attenuation Model	II-28 thru II-30
III.	Science Selection Rationale	III-1
	A. Introduction	III-1
	B. Scientific Objectives and Basic Questions for Jupiter	III-2
	C. Measurement Performance Requirements	III-9
	D. Instrumental Techniques	III-20
	E. Mission and System Science Performance Requirements and Tradeoffs	III-27
	F. Science Payload Descriptions and Capabilities	III-43 thru III-55
IV.	Mission Concept Evolution	IV-1
	A. Navigation and Trajectory Evolution	IV-3
	B. Engineering Concept Evolution	IV-18
	C. Engineering Experiment	IV-43
	D. Mission Effectiveness Studies	IV-48 thru IV-54

V. Baseline Parametric Study V-1

A. Introduction V-1

B. Science Payload and Descent Profiles V-2

C. Selection of Parameter Ranges V-5

D. Ground Rule Summary V-8

E. Results and Observations V-17

F. Influence of Mission Parameters on Survival Depth, Probe System Weight and Power Requirements V-26

G. Use of Pioneer Spacecraft with the Probes of the Parametric Study V-37

H. Deflection Implementation Accuracy Impact on Probe Parametric Study Results V-42

I. Impact of Heat Shield Weight Fraction Uncertainties on Parametric Study Results . . V-45

J. Impact of the Cool Dense Model Atmosphere on Communications Parameters for the Baseline Parametric Study V-47

K. Impact of Cool Dense Model Atmosphere on Probe System Weights . . . . . V-52 and V-53

VI. Design Example Mission VI-1

A. Design Example Selection Rationale VI-1

B. Profile of the Design Example Mission VI-2

C. Sequence of Events VI-6

D. Configuration Summary - Design Example Case VI-13

E. Mechanical and Support Systems VI-13

F. Telecommunications, Data Handling and Power (DE Mission) . . . . . VI-31 thru VI-57

VII. Sample Missions VII-1

A. Mission A Selection Rationale VII-2

B. Mission B Selection Rationale VII-23

C. Mission C Selection Rationale VII-44

D. Mission D Selection Rationale VII-47

E. Mission E Selection Rationale VII-60

F. Mission F Selection Rationale . . . . . VII-77 thru VII-106

VIII. Reliability Requirements and Magnetic Cleanliness Requirements VIII-1

A. Reliability Requirements VIII-1

B. Magnetic Cleanliness Requirements . . . . . VIII-2 and VIII-3

ABBREVIATIONS AND SYMBOLS

A	reference area, ft^2 (m^2)
	ampere, electrical unit of current
	atmosphere (pressure) (1 atmosphere = 1.013×10^6 dynes/cm^2)
	(subscript) ambient
Å	Angstrom unit (= 10^{-4} μ)
ACS	attitude control system
A/D	analog to digital
ADC	analog to digital converter
Alt.	altitude
AMU	atomic mass unit
A/S	aeroshell
B	impact parameter, km
	ballistic coefficient, Kg/m^2
	bandwidth
	(subscript) body
b	bar, (pressure) (1 bar = 10^6 dynes/cm^2)
	bit
B_{LO}	tracking loop bandwidth
bps	bits per second (also B/S)
C	capacity (battery, ampere hours)
C_3	injection energy, km^2/sec^2
c	free space propagation velocity of light
°C	temperature, degrees Celsius
C_D	drag coefficient
cg	center of gravity

cm	centimeter
CP	center of pressure
c_p	specific heat
D	diameter
db	decibel
dbm	decibels above 1 milliwatt
deg	degrees
DLA	declination of launch asymptote
DS	dark side
DSIF	Deep Space Instrumentation Facility
DSN	Deep Space Net
E	electrical voltage
	modulus of elasticity
	(subscript) entry
	(subscript) Earth
e	eccentricity
EJ	(subscript) deflection-ejection
EV	entry vehicle
EZ	equatorial zone (of Jupiter)
EMI	electromagnetic interference
E/NO	Energy per data bit per noise power density
F	solar flux
	frequency, Hz
FS	full scale
FSK	frequency shift keyed
°F	temperature, degrees Fahrenheit

f	(subscript) flight
$\dot{f}$	frequency rate of change
GSFC	Goddard Space Flight Center
G	(prefix) giga (1×10^9)
GC/MS	gas chromatograph/mass spectrometer
g	acceleration of gravity, (Earth reference)
gm	gram
H	altitude
	(subscript) horizontal
HE	(subscript) (V_{HE} - hyperbolic excess velocity referred to Earth)
HP	(subscript) (V_{HP} referred to planet)
h	heat transmission coefficient
hr	hour
Hz	Hertz
I	electrical current
	moment of inertia
i	inclination to ecliptic
IR	infrared
J	(subscript) Jupiter (also 4)
JPL	Jet Propulsion Laboratory
JUN	Jupiter-Uranus-Neptune (Grand Tour Mission)
°K	temperature, degrees Kelvin
K	constraint length (of code)
k	thermal conductivity
	(prefix) kilo (1×10^3)
km	kilometer
LS	light side

M	Mach number
	(prefix) Mega (1×10^6)
m	mass
	meter
	(prefix) milli- (1×10^{-3})
mb	millibar
MCD	main chute deployment
MOS	metal oxide semiconductor
MMC	Martin Marietta Corporation
mps	meters per second
N	refractivity
N	(subscript) noise
n	index of refraction
nm	nautical miles
NASA	National Aeronautics and Space Administration
NEB	North Equatorial Belt (of Jupiter)
P	pressure
	(subscript) periapsis
p	roll rate
PCM	phase change material
	pulse code modulation
P/L	payload
PLL	phase lock loop
PM	phase modulation
Pr	Prandtl number
ppm	parts per million

psf	pounds per ft^2
psi	pounds per $in.^2$
psia	pounds per $in.^2$ (absolute)
PV	planetary vehicle
q	dynamic pressure
R	radius (reference R_J = 71420 km)
	(subscript) relative
°R	temperature, degrees Rankine
RA	right ascension
Re	Reynolds number
RF	radio frequency
rpm	revolutions per minute
RTG	radioisotope thermoelectric generator
S/C	spacecraft
S/H	sample and hold
Sl	slugs
SNR	Signal-to-noise ratio
SP	South Pole
SS	subsolar
T	time
t_L	lead time
TOPS	Thermoelectric Outer Planets Spacecraft
TR	Temperate Region (of Jupiter)
t_s	time of staging
TTL	transistor transistor logic
TWT	traveling wave tube
UV	ultraviolet

V	velocity
	volume
	electrical voltage
	(subscript) vertical
W	watts
X	displacement
α	solar absorptivity
α_E	angle of attack at entry
Γ	polarization
γ	inertial flight path angle
γ_E	entry angle
Δ	(prefix) increment of change
ϵ	2.71828
	dielectric constant
	infrared emissivity
θ_o	solar zenith angle
θ	ray launch angle
λ	wavelength
	longitude
	lead angle
μ	micron
	(prefix) micro (1×10^{-6})
	gravitational constant of Jupiter (1.26077×10^8 km^3/sec^2)
	viscosity
π	3.1416

ρ	density
σ	standard deviation
	Stefan-Boltzmann constant
τ	application angle (for ΔV_{EJ})
ϕ	latitude
ϕ_t	trap angle of communications ray
ψ	angle at which a ray emerges from the atmosphere.
	probe aspect angle measured from zenith
ω	angular velocity,
	frequency, radians per second
$\sim$	approximately
$\propto$	varies as
$\frac{\partial(y)}{\partial(x)}$	(partial derivative) sensitivity of y to changes in x
φ	Aries (direction of the vernal equinox)

I. INTRODUCTION TO VOLUME II

This volume contains the rationale and describes the evolution of mission and system concepts for Jupiter atmospheric entry missions. In addition to the descriptions of the environmental models, the chapters include the science criteria selection rationale, the mission and system concept evolution, the baseline parametric mission study, a detailed design example mission from the parametric study, and a variety of illustrative sample missions.

The environmental models and the science criteria established the fundamental design factors for the implementation of the engineering designs. The mission and system concepts evolved within the bounds established by feasible engineering solutions. From these concepts, the baseline parametric study was developed, and a Design Example mission was selected from this study to be defined in detail in order to illustrate the subsystem and system integration and interfaces. Other sample missions are defined in less detail, and illustrate some of the unique problems and solutions associated with particular mission options.

The contents of this volume are based on the supporting technical studies of Volume III.

II. ENVIRONMENTAL MODELS

Environmental models of the planet Jupiter for use in the study were specified in the Statement of Work. Some of the models were revised during the course of the study. The models used, summaries of additional investigative work performed during the study, and implications to various Jupiter missions are described in this chapter.

A. Micrometeoroid Model

1. Descriptive Uncertainties

The risk of penetration by a micrometeoroid of significant size ($\sim$ 0.01 gm) on a Jupiter mission can be considered to be the sum of the risks associated with the near earth region, the interplanetary region and the region of the asteroid belt. It is shown by Volkoff[1] that on a Jupiter mission the risk per unit time in the near earth region is at least an order of magnitude greater than in the asteroid belt and several orders of magnitude greater than in other regions. Volkoff also makes an informative comparison of the protective requirements for a Jupiter mission for three widely different micrometeoroid distributions over the trajectory. It is shown that overall protective requirements are relatively ($\sim$ 15%) insensitive to the micrometeoroid distribution model selected.

2. Protective Requirements

A Jupiter entry probe designed to withstand pressures and temperatures at significant depths is inherently insensitive to micrometeoroid penetration during interplanetary cruise. For example, the upper probe of the trial mission was designed for a depth of 45.5 atmospheres. The resulting pressure vessel design can be represented in terms of micrometeoroid penetration as being equivalent to 0.25 inches of carbon, 0.025 inches of aluminum and 0.080 inches of titanium. This can be converted to an equivalent thickness of 0.20 inches of aluminum. Then based on an empirical formula contained in reference (2) below, the threshold mass of a micrometeoroid particle to just penetrate the assembly (with reasonable allowances for the constants in the formula) can be computed. The threshold mass

---

(1) Protection Requirements for the Resistance of Meteoroid Penetration Damage of Interplanetary Spacecraft Systems. Technical Report No. 32-410. Jet Propulsion Laboratory, Pasadena. July 1, 1964.

(2) Frost, V. C., Aerospace Meteoroid Environment and Penetration Criteria. TOR 269 (4560-40)-2. Aerospace Corporation, El Segundo. 17 August 1964.

of the particle turns out to be 0.06 grams. This is consistent with the impact design value for the TOPS spacecraft which is stated in reference (3) to be for particles of less than 10^{-2} gram mass. This reference also states that 1.3×10^{-3} total integrated impacts (per square meter) from particles greater than 10^{-2} grams are expected during 10 year TOPS missions. With allowance for a three year interplanetary mission to Jupiter, the greater concentrations in the asteroid belt, and the projected area of this upper probe (0.2 sq.m.) this places the total number of expected impacts of particles with mass greater than 10^{-2} grams in the order of 10^{-4}.

Differences in total time of exposure may also have some effect on the choice between a Type I and Type II interplanetary trajectory. On the basis of data contained in reference (4), the risk per unit time in traversing from the orbit of Mars to the orbit of Jupiter can be considered as twice the risk in traversing a path outside this region. Figure IIA-1 shows typical durations of 100 days to the orbit of Mars and 750 days to the orbit of Jupiter for a Type I trajectory. A Type II trajectory typically adds another 250 days of unit-risk exposure. A simple calculation shows that a Type II trajectory, as compared to a Type I, has an increased risk of approximately 15%. It, therefore, appears that possible meteoroid damage should not be a major factor affecting the choice of trajectories.

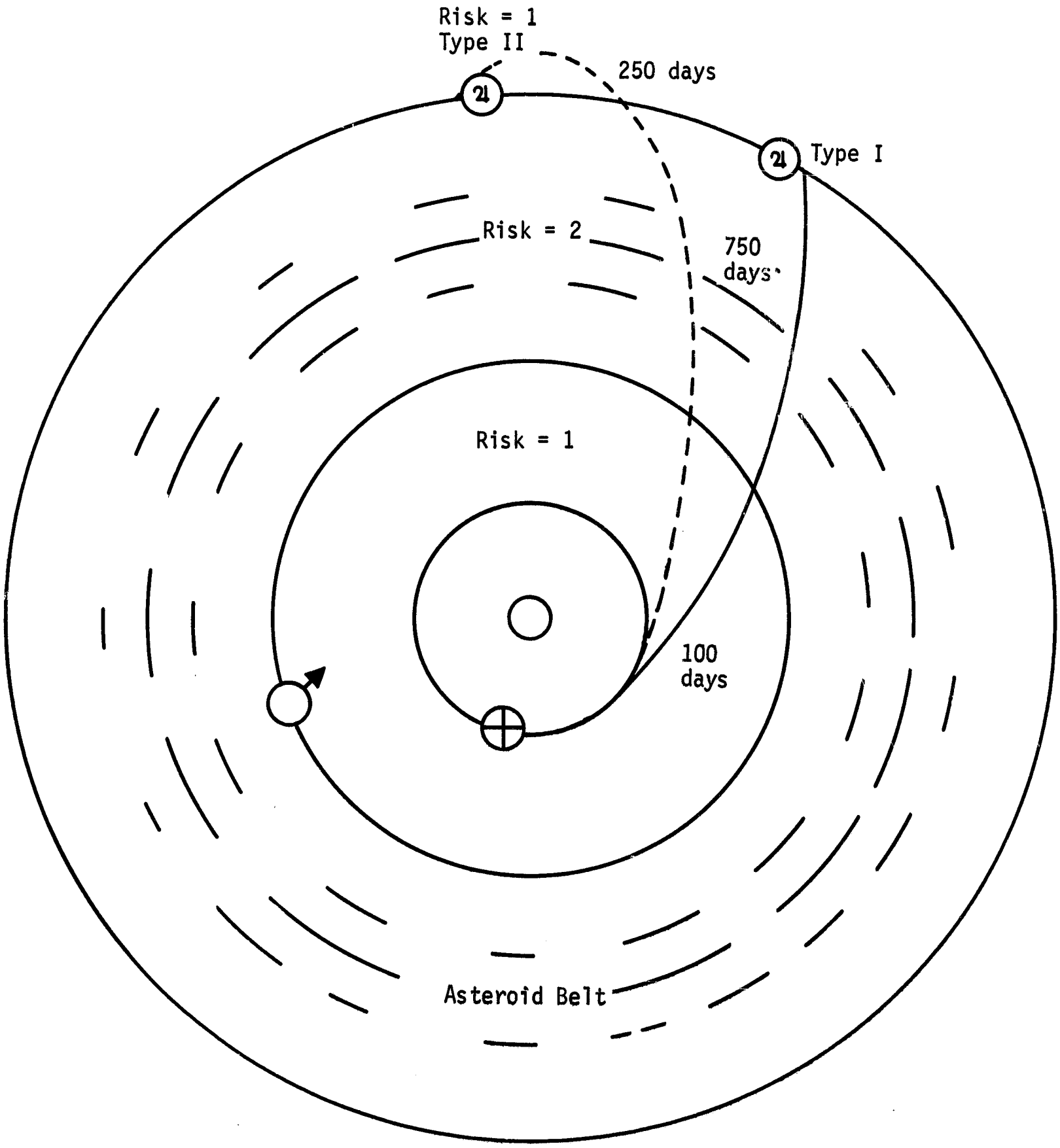
All of the preceding analyses have indicated that the conceived designs are compatible with acceptable risk of micrometeoroid penetration of the pressure vessel. An area that remains to be investigated is the heat shield of the entry vehicle. The graphite is somewhat less effective than the aluminum for an equal thickness due to the lower values of density and Young's modulus.

The heat shield is in greater jeopardy because the projected area of the heat shield can be 8 or 9 times as great as the area of the pressure vessel considered. Another consideration is that the empirical formula of reference (2) contains

---

(3) Devita, E. L., et.al.,"TOPS Spacecraft and the Missions", Astronautics and Aeronautics. September, 1970.

(4) Space Environment Criteria Guidelines for Use in Space Vehicle Development 1969 Revision, 2nd Edition, August 26, 1970, NASA TMX 53957.



Exposure to Meteoroids for
Type I and Type II Trajectories

Figure II A-1

constants that tend to mask uncertainties in a composite design, and the uncertainties can be reduced by tests of candidate heat shields. It, therefore, seems necessary to plan the heat shield qualification test program to include bombardment by high velocity particles so that possible modes of failure can be identified and samples of the bombarded material can be functionally compared with material that has not been bombarded.

B. Jupiter Radiation Belt Model

1. Descriptive Uncertainties

The radiation belt model used for the study consisted of material provided by JPL (1), Subject: "Jupiter Trapped Radiation Material from (Draft of Space Vehicles Design Criteria 'The Planet Jupiter (1970)') Monograph."

An abstract of the material reads as follows:

On the basis of earth observations of the HF and UHF radio emission generated near Jupiter, the presence of energetic charged particles trapped in the planet's dipole magnetic field has been inferred. For electrons, energies of the order of 10 MeV and peak fluxes of the order of 10^{7} cm^{-2} sec^{-1} about two planetary radii from the dipole are implied. An engineering model which describes the distributions of relativistic electrons has been developed, including reasonable uncertainty estimates. Models have also been developed for energetic protons and for low energy particles, but these models are not securely based on observational data. The uncertainties associated with these models are very broad, and could be reduced only by considerable further study and/or direct detection by spacecraft. A consistent presentation of particle concentrations and fluxes for space vehicle design purposes has been generated for these environments.

2. Integrated Doses for Typical Missions

The radiation models were applied to the entry probes of the Trial Mission using the probe configuration of Figure IIB-1, with data on the properties of materials contained in (2) below.

---

(1) JPL letter 290-RGN:cth from R. G. Nagler, to S. Ducsai dated 28 August 1970.

(2) M. J. Berger and S. M. Seltzer: Additional Stopping Power and Range Tables for Protons Mesons and Electronics. NASA SP-3036. National Bureau of Standards, 1966.

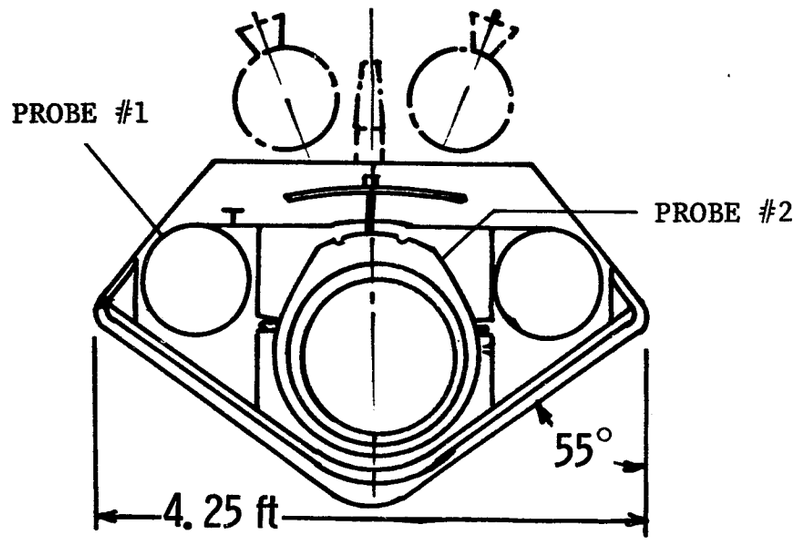


Figure IIB-1 Trial Mission Entry Vehicle

Additional assumptions included the following:

a. The approach trajectory was as defined for the Trial Mission in Volume III, Chapter VII.

(Periapsis radius of 2.0 R_j,
Entry angle of γ_E -10°,
Deflection velocity of 197 M/S
At an angle, γ, of -115°, coast time of 12 days)

b. Spherical analysis (probes and spacecraft were represented by spherical shells for shielding analysis).

1) Probe number 1 is shielded by 0.25 inches of carbon (representing the aft heat shield), 0.025 inches of aluminum, and 0.080 inches of titanium.

2) Probe number 2 is shielded by 0.25 inches of carbon, 0.125 inches of aluminum, and 0.50 inches of steel.

3) Spacecraft shielding equals 1.0 gram per square centimeter.

Calculations of expected dosage at the centers of the respective spheres are shown in Table IIB-1.

3. Implications to Design

Threshold damage levels shown in Table IIB-2 were used for assessment of expected damage.

When comparing the information presented in the tables, it becomes obvious that the minimum environment is insignificant and that the maximum environment implies extremely heavy shielding. The nominal environment, although it presents a problem, can be shielded against with some local protection around individual black boxes.

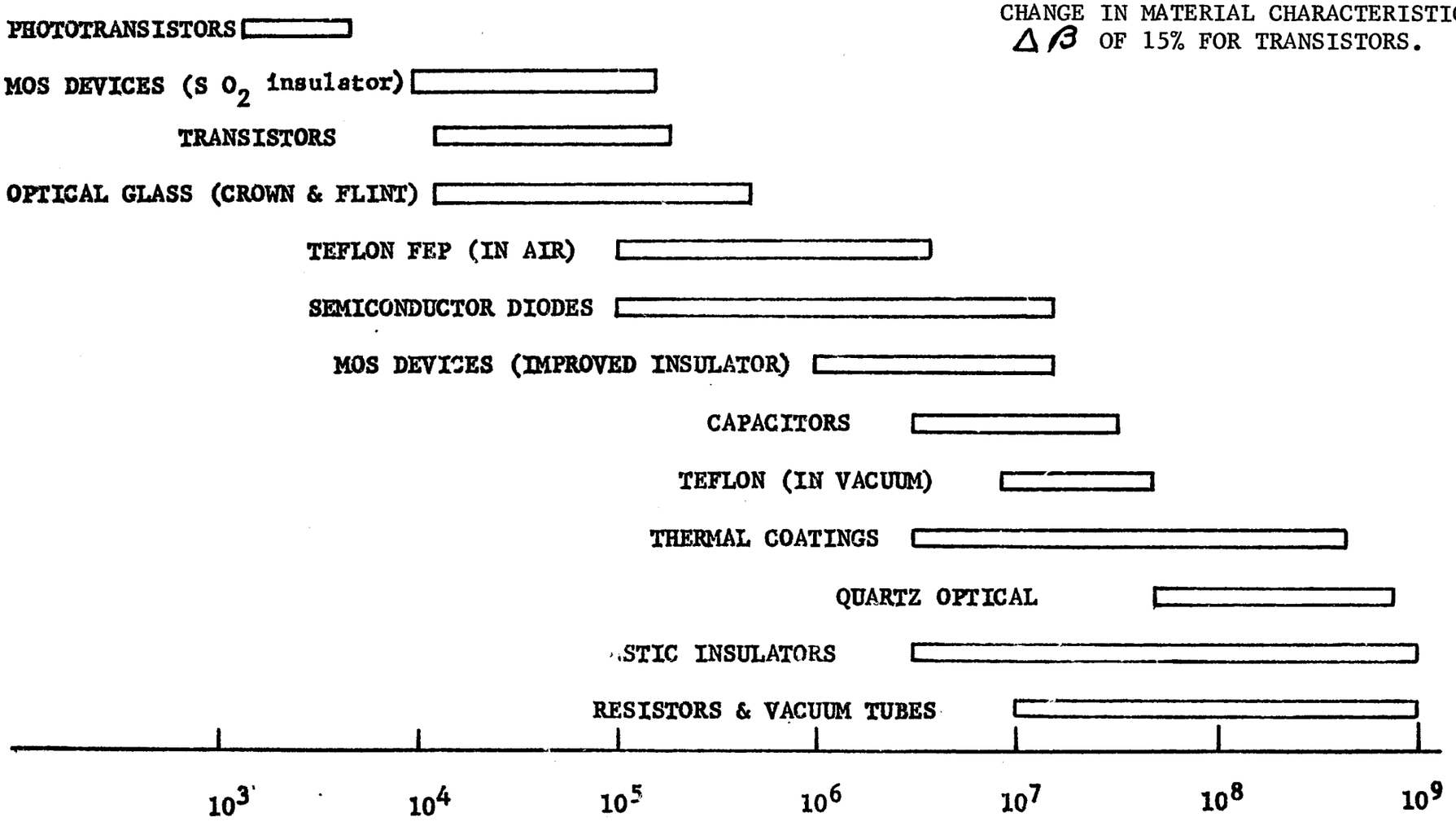
TABLE IIB-1
TRIAL MISSION JUPITER PROBE RADIATION ANALYSIS

MODULE	DOSE ~ RADS SILICON JPL ENVIRONMENTS		
	MAXIMUM	NOMINAL	MINIMUM
Spacecraft	1.23×10^5	2.30×10^3	4.4×10^1
Probe #1	9.17×10^4	1.66×10^3	2.1×10^1
Probe #2	5.15×10^4	4.43×10^2	0
Surface Dose	1.94×10^5	7.01×10^4	4.9×10^2

Integrated doses will change somewhat for missions other than the Trial Mission trajectory assumed for this analysis. The spacecraft dose will be significantly reduced for flyby radii greater than about 3 R_J. For the probe, a brief check of trajectory parameters shows that the flight time through the radiation belt is most sensitive to entry angle. The total time required for the probe to traverse from 3.0 R_J to entry at an entry of -10° is about 1.4 hours. At an entry angle of -60° the flight time is about 1.0 hour. The total radiation dose, although not directly proportional to time alone, will be reduced about 30% for the -60° γ_E compared to the -10° γ_E.

TABLE IIB-2
IONIZATION DAMAGE THRESHOLDS

THRESHOLDS INDICATE SIGNIFICANT CHANGE IN MATERIAL CHARACTERISTICS. $\Delta\beta$ OF 15% FOR TRANSISTORS.



C. Decameter and Decimeter Radiation Models

The models for these sources of radiation are derived from NASA SP-3031, "Handbook of the Physical Properties of the Planet Jupiter". The decameter radiation is not an important factor in the mission design. There are numerous hypotheses for the origin of decameter radiation, with the postulated location of the source ranging from deep in the atmosphere to far out in the magnetosphere. Much of the uncertainty about the origin of this radiation could be resolved by a properly instrumented probe and spacecraft. However, this has not been given high priority, and except for the lightning detectors on Missions B, C, and E, the necessary instruments are not included on the probes.

Decimeter radiation occurs within the frequency band of interest for the probe communications sytems, so it imposes a major constraint on mission design, by introducing noise into the communication links. Its source is the Jovian magnetosphere, extending out to 3 or more R_j. The noise temperature vs frequency curve on page 56 of NASA SP-3031 was used in our communication link designs. The sharp rise in temperature with decreasing frequency shown in this curve places a lower limit on frequencies that can be considered for the probe to spacecraft relay links. It also has some effect on the probe-to-probe links used for split probe missions.

Computation of antenna temperatures is discussed in Volume III, Chapter IV.K.

One major problem caused by decimeter radiation is that it limits the effectiveness of earth-based radiometry in the decimeter frequency band where significant penetration of the upper atmosphere would be possible.

D. Jupiter Atmospheric Models

The preliminary model atmospheres defined in JPL Section Document 131-10 (Reference IID-1) were specified as the design criteria for this study. Two improved sets of model atmospheres have been circulated (References IID-2, IID-3) since the study began but the Nominal models in the three sets are essentially the same. The Nominal model defined in Reference IID-2 was used as the baseline engineering design model for all analyses and system designs. However, the effects of encountering other models were also investigated and one sample mission was designed to survive in either the Nominal and Cool models of Reference IID-2. The following sections discuss the uncertainties in the atmospheric environment and their effects on the mission, system, and subsystem designs.

1. Descriptive Uncertainties: Present and Future

The size, shape, and mass of Jupiter suggest that it is composed mainly of H_2 and He (mean density = 1.35 g/cm^3). Spectroscopy confirms the presence of large amounts of H_2 but He is unobservable from earth. Methane (CH_4) and ammonia (NH_3) have also been detected spectroscopically. Visual observation shows pastel-colored bands of clouds with continual changes in shape, detail, color, and motion. These clouds are presumably ammonia with the coloration due to trace molecules of an unknown nature. Temperatures and pressures in the vicinity of the visible cloud tops have been inferred from spectra and radiometry. The resulting temperatures and pressures near the equatorial cloud tops range from about 125°K to 200°K and a few tenths of an atmosphere to several atmospheres. Microwave and IR observations indicate that the temperature increases with depth as expected but the lapse rate is unknown.

Conditions in the upper and lower atmosphere must be inferred from theory and the rather uncertain knowledge of conditions near the cloud tops. The models of References IID-1, IID-2, IID-3 assume pressures of 0.2, 0.3, and 0.5 atm at the 125°K level (correspondence

level) and extrapolate up and down assuming a range of lapse rates and compositions. Table IID-1 shows the parameters used in Reference IID-2. Note that the tropospheric lapse rates are constant down to 1000 atm but are different for each model. Reference IID-1 assumed the same composition and lapse rate for all three models while Reference IID-3 takes the variation of lapse rate with temperature (and composition) into account.

The pressure-temperature profiles for the models of references IID-1 and IID-2 are shown in Figures IID-1 and IID-2. The small differences between the extreme models of Reference IID-1 (dashed lines) do not adequately reflect our present ignorance of the Jovian atmosphere; nor do they result in any significant design penalties in the lower atmosphere. On the other hand, while the Cool and Nominal models of Reference IID-2 are quite plausible, the Warm model is highly improbable since it is superadiabatic.

An upper bound on the temperature versus pressure is given by a dry adiabatic lapse rate for pure H_2 (the addition of He and condensing clouds decreases the rate of change of temperature with pressure). Since we know there are clouds on Jupiter and there is almost certainly a significant amount of He present, the temperature at a given pressure will be less than that given by a dry adiabat. Figure IID-3 compares the models of Reference IID-2 to dry adiabats for two extreme compositions. As can be seen, the Warm model overestimates the temperature at 1000 atm by at least 1500°K to 2000°K. Reference IID-3 takes the variation of lapse rate with temperature and composition into account to obtain a more plausible Warm Model ($\sim$1840°K at 1000 atm). This improved model did not become available until after most of the parametric analyses were already performed so it was not used in the study.

The atmospheric parameters for the Nominal and Cool models used in the study are given in Tables IID-2 and IID-3. The small deviations from the models of Reference IID-2 are due to a difference in

computational technique and are insignificant. For purposes of the present study, these models represent an adequate range of conditions although small expansions to cooler and warmer models (e.g. Reference IID-3) should be considered for future studies.

It is doubtful that the range of possible lower atmosphere pressure-temperature profiles will be significantly reduced until an entry probe actually descends below the 1 to 10 atmosphere level since the Pioneers F and G occultation experiments are not expected to probe below about 1 atm. The uncertainties in the upper atmosphere profiles and composition will probably be significantly reduced by the expected data return from Pioneers F and G and perhaps by the planned observations of the occultation of β Scorpio by Jupiter in 1971.

The uncertainties in the H_2O content and the pressure-temperature profiles results in a significant difference in the depth of the expected H_2O cloud bottoms. The locations of the levels where H_2O condensation begins are shown in Figure IID-4 for the Nominal and Cool models. Note that the cloud thicknesses are also different for the two models.

TABLE IID-1

Composition and Other Parameters

for Jupiter Model Atmospheres

(Reference IID-2, 8 May 1970)

Parameter		Cool Model	Nominal Model	Warm Model	Units
Fraction by number (or volume)	H_2	0.68454	0.86578	0.93754	
	He	0.31057	0.13214	0.06143	
	CH_4	0.00145	0.00062	0.00028	
	NH_3	0.00035	0.00015	0.00007	
	H_2O	0.00240	0.00102	0.00048	
	Ne	0.00031	0.00013	0.00006	
	Others	0.00038	0.00016	0.00008	
Mean molecular mass		2.70	2.30	2.14	g/mole
Acceleration of gravity		2700	2500	2300	m/sec^2
Effective temperature		128	134	140	^oK
Radius at 1 atm level		71420	71420	71420	Km
Correspondence level temperature		125	125	125	^oK
Pressure		0.5	0.3	0.2	atm
Troposphere:					
Temperature lapse rate		-1.75	-2.07	-2.37	$^oK/Km$
d(ln T)/d(ln P)		0.2	0.3	0.4	—
H_2O cloud bottom (or H_2O-NH_3 sol'n)		~ 80	~ 4	~ 1	atm
Stratosphere temperature		108	113	118	^oK
Scale heights above stratosphere		12.3	21.0	20 to 70	Km

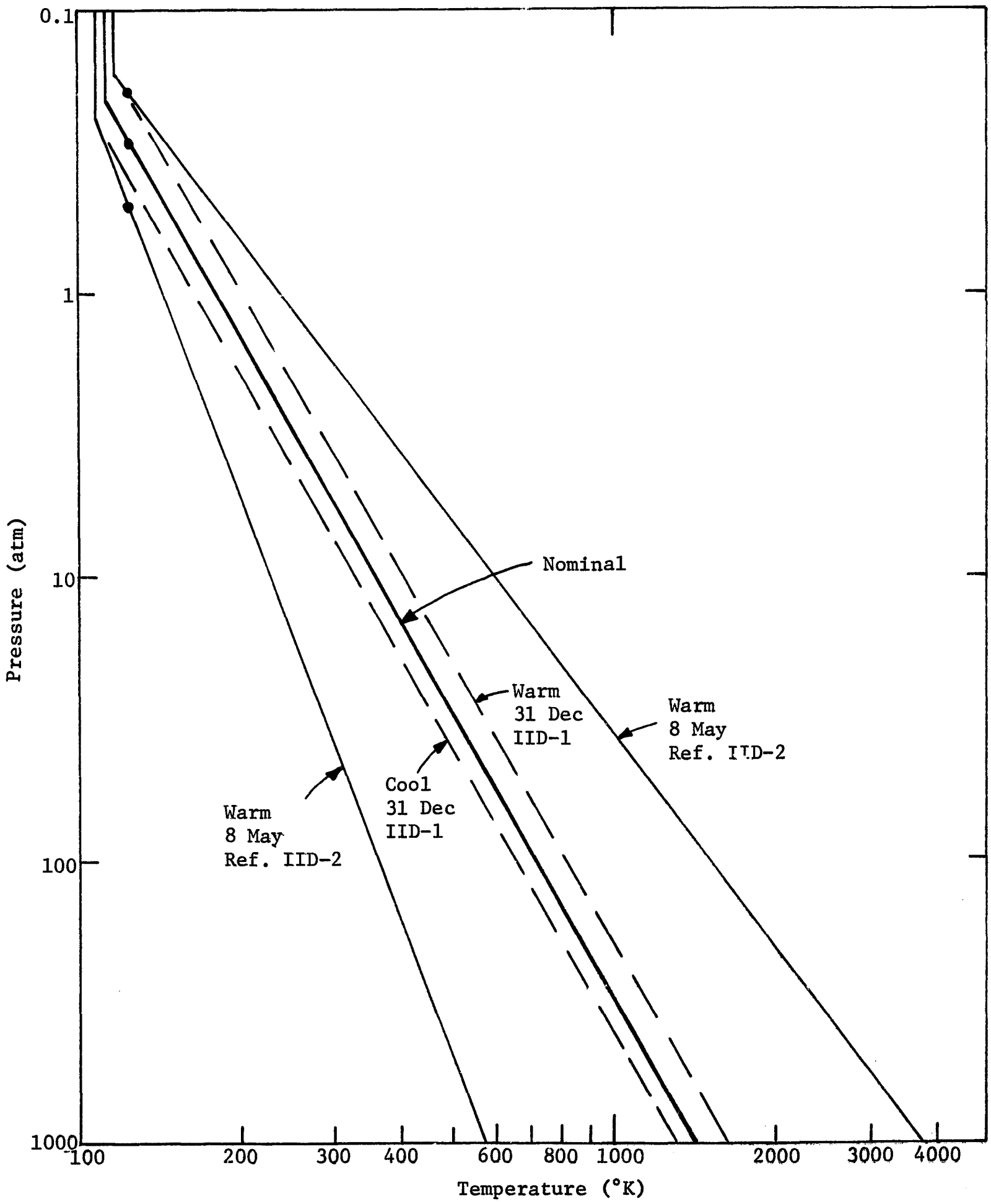


Figure IID-1 Lower Atmosphere Structure

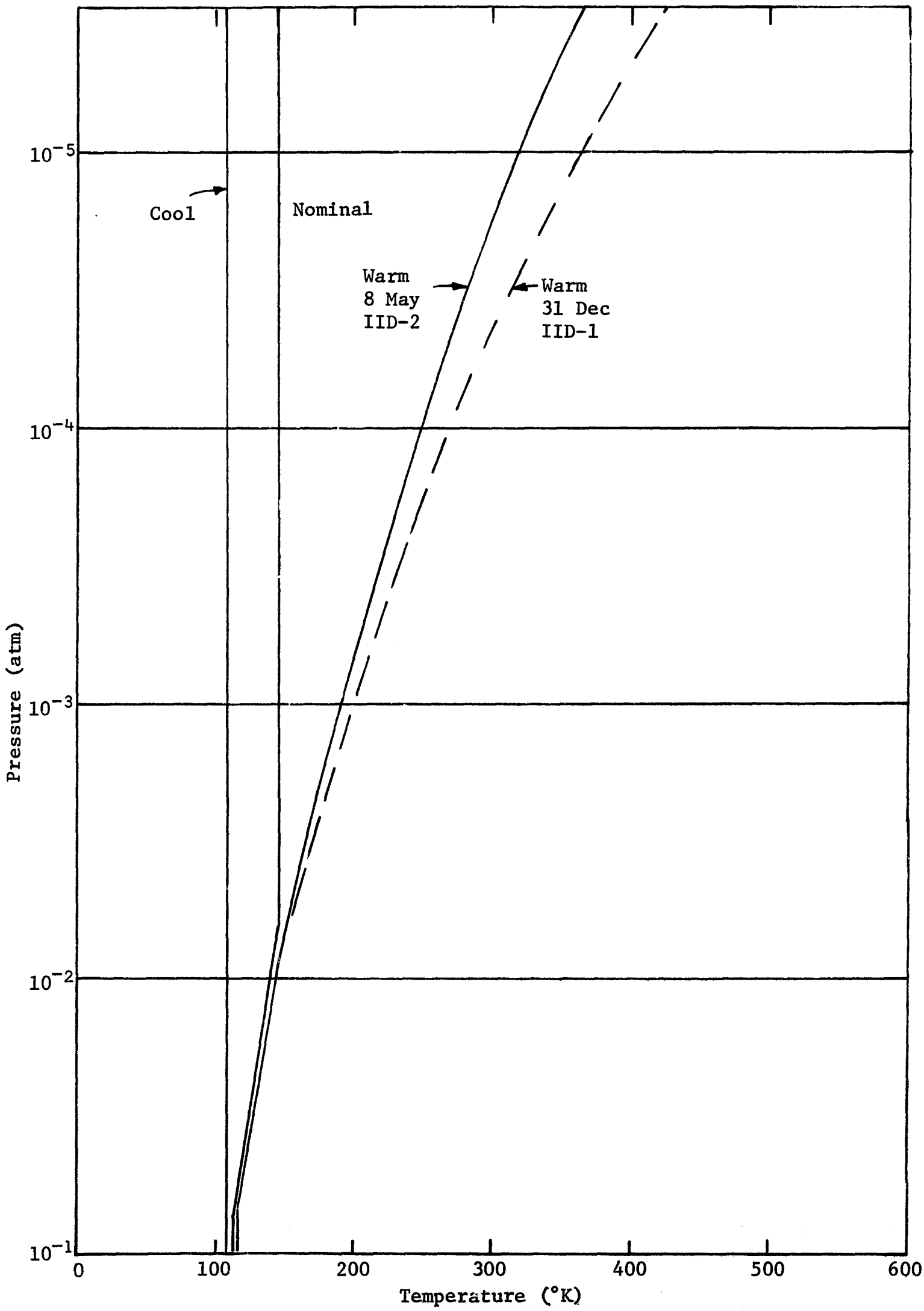


Figure IID-2. Upper Atmosphere Structure

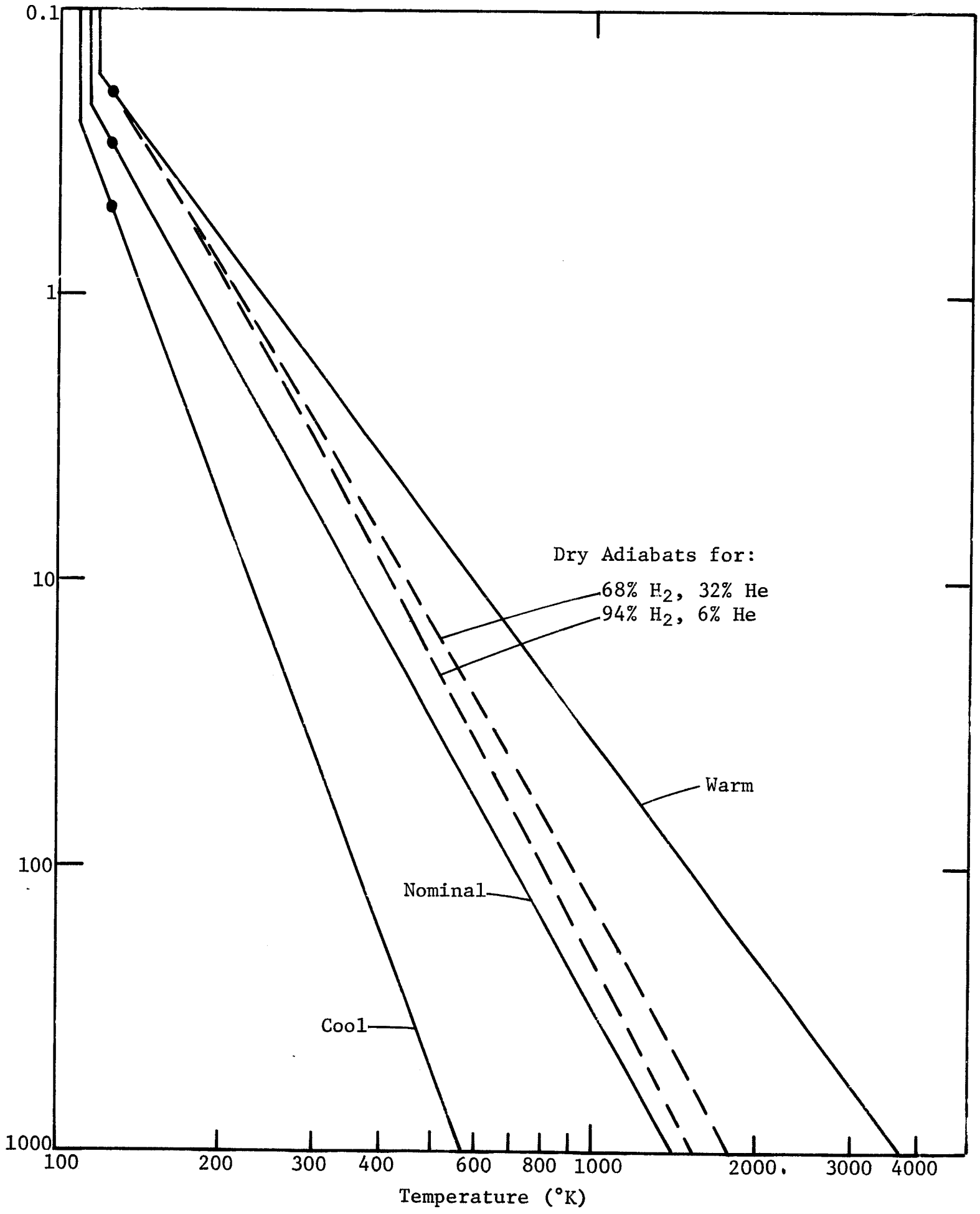


Figure IID-3. Dry Adiabatic Models Compared to Models of Ref IID-2.

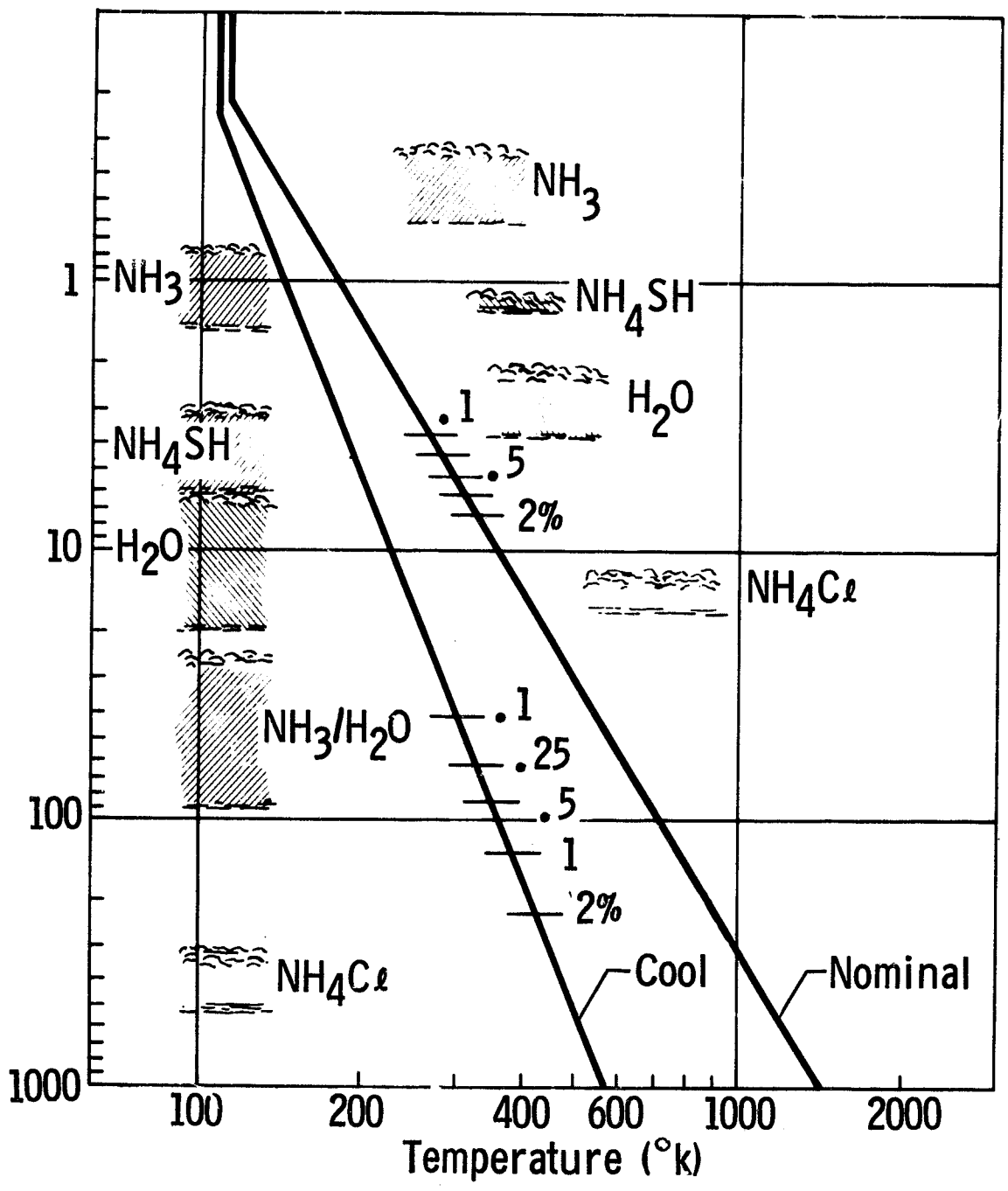


Figure IID-4. Cloud Layering in Study Models

TABLE IID-2

JUPITER MODEL ATMOSPHERE NO 8 MAY NOM DATE 30 JULY 1970
MEAN MOLECULAR MASS = 2.30 GRAMS/MOLE
INITIAL PRESSURE =0.303975E 06 DYNES/SQCM AT 71446.20 KM RADIUS
PRINT INTERVAL = 10. KM

ALTITUDE IS ABOVE 71420.0 KM RADIUS

RADIUS KM	ALTITUDE KM	TEMPERATURE KELVIN	TEMPERATURE FAHREN	PRESSURE DYNE/CM2	PRESSURE ATMOSPHERES	DENSITY GM/CM3
70818.00	-602.000	1426.966	2108.870	0.101420E 10	0.100093E 04	0.196612E-01
70828.00	-592.000	1406.241	2071.565	0.965383E 09	0.952759E 03	0.189907E-01
70838.00	-582.000	1385.516	2034.260	0.918256E 09	0.906248E 03	0.183338E-01
70848.00	-572.000	1364.791	1996.955	0.872784E 09	0.861370E 03	0.176905E-01
70858.00	-562.000	1344.066	1959.650	0.828930E 09	0.818091E 03	0.170608E-01
70868.00	-552.000	1323.341	1922.345	0.786662E 09	0.776375E 03	0.164444E-01
70878.00	-542.000	1302.616	1885.040	0.745943E 09	0.736189E 03	0.158413E-01
70888.00	-532.000	1281.891	1847.735	0.706740E 09	0.697498E 03	0.152514E-01
70898.00	-522.000	1261.166	1810.430	0.669019E 09	0.660270E 03	0.146746E-01
70908.00	-512.000	1240.441	1773.125	0.632746E 09	0.624472E 03	0.141109E-01
70918.00	-502.000	1219.716	1735.819	0.597887E 09	0.590068E 03	0.135600E-01
70928.00	-492.000	1198.991	1698.514	0.564409E 09	0.557029E 03	0.130220E-01
70938.00	-482.000	1178.266	1661.209	0.532280E 09	0.525319E 03	0.124968E-01
70948.00	-472.000	1157.541	1623.904	0.501466E 09	0.494908E 03	0.119841E-01
70958.00	-462.000	1136.816	1586.599	0.471935E 09	0.465764E 03	0.114840E-01
70968.00	-452.000	1116.091	1549.294	0.443656E 09	0.437854E 03	0.109963E-01
70978.00	-442.000	1095.366	1511.989	0.416595E 09	0.411148E 03	0.105210E-01
70988.00	-432.000	1074.641	1474.684	0.390722E 09	0.385613E 03	0.100579E-01
70998.00	-422.000	1053.916	1437.379	0.366006E 09	0.361220E 03	0.960692E-02
71008.00	-412.000	1033.191	1400.074	0.342415E 09	0.337937E 03	0.916799E-02
71018.00	-402.000	1012.466	1362.769	0.319918E 09	0.315734E 03	0.874098E-02
71028.00	-392.000	991.741	1325.464	0.298485E 09	0.294582E 03	0.832581E-02
71038.00	-382.000	971.016	1288.159	0.278086E 09	0.274450E 03	0.792238E-02
71048.00	-372.000	950.291	1250.854	0.258691E 09	0.255308E 03	0.753057E-02
71058.00	-362.000	929.566	1213.549	0.240271E 09	0.237129E 03	0.715028E-02
71068.00	-352.000	908.841	1176.244	0.222795E 09	0.219882E 03	0.678141E-02
71078.00	-342.000	888.116	1138.939	0.206235E 09	0.203538E 03	0.642386E-02
71088.00	-332.000	867.391	1101.634	0.190563E 09	0.188071E 03	0.607752E-02
71098.00	-322.000	846.666	1064.328	0.175749E 09	0.173451E 03	0.574228E-02
71108.00	-312.000	825.941	1027.023	0.161766E 09	0.159651E 03	0.541803E-02
71118.00	-302.000	805.216	989.718	0.148586E 09	0.146643E 03	0.510467E-02
71128.00	-292.000	784.490	952.413	0.136180E 09	0.134400E 03	0.480209E-02
71138.00	-282.000	763.765	915.108	0.124523E 09	0.122895E 03	0.451017E-02
71148.00	-272.000	743.040	877.803	0.113586E 09	0.112101E 03	0.422880E-02
71158.00	-262.000	722.315	840.498	0.103344E 09	0.101993E 03	0.395787E-02
71168.00	-252.000	701.590	803.193	0.937698E 08	0.925436E 02	0.369727E-02
71178.00	-242.000	680.865	765.888	0.848369E 08	0.837275E 02	0.344687E-02
71188.00	-232.000	660.140	728.583	0.765200E 08	0.755194E 02	0.320657E-02
71198.00	-222.000	639.415	691.278	0.687938E 08	0.678942E 02	0.297624E-02
71208.00	-212.000	618.690	653.973	0.616330E 08	0.608270E 02	0.275576E-02
71218.00	-202.000	597.965	616.668	0.550129E 08	0.542935E 02	0.254501E-02
71228.00	-192.000	577.240	579.363	0.489091E 08	0.482695E 02	0.234387E-02
71238.00	-182.000	556.515	542.058	0.432974E 08	0.427312E 02	0.215222E-02
71248.00	-172.000	535.790	504.753	0.381540E 08	0.376551E 02	0.196991E-02
71258.00	-162.000	515.065	467.448	0.334555E 08	0.330180E 02	0.179683E-02
71268.00	-152.000	494.340	430.143	0.291788E 08	0.287972E 02	0.163284E-02

TABLE IID-2

JUPITER MODEL ATMOSPHERE NO 8 MAY NOM DATE 30 JULY 1970
MEAN MOLECULAR MASS = 2.30 GRAMS/MOLE
INITIAL PRESSURE =0.303975E 06 DYNES/SQCM AT 71446.20 KM RADIUS
PRINT INTERVAL = 10. KM

ALTITUDE IS ABOVE 71420.0 KM RADIUS

RADIUS	ALTITUDE	TEMPERATURE		PRESSURE		DENSITY
KM	KM	KELVIN	FAHREN	DYNE/CM2	ATMOSPHERES	GM/CM3
71278.00	-142.000	473.615	392.837	0.253012E 08	0.249703E 02	0.147780E-02
71288.00	-132.000	452.890	355.532	0.218002E 08	0.215151E 02	0.133158E-02
71298.00	-122.000	432.165	318.227	0.186538E 08	0.184099E 02	0.119404E-02
71308.00	-112.000	411.440	280.922	0.158405E 08	0.156334E 02	0.106503E-02
71318.00	-102.000	390.715	243.617	0.133389E 08	0.131645E 02	0.944417E-03
71328.00	-92.000	369.990	206.312	0.111282E 08	0.109827E 02	0.832029E-03
71338.00	-82.000	349.265	169.007	0.918791E 07	0.906776E 01	0.727718E-03
71348.00	-72.000	328.540	131.702	0.749791E 07	0.739986E 01	0.631326E-03
71358.00	-61.999	307.815	94.397	0.603859E 07	0.595962E 01	0.542684E-03
71368.00	-51.999	287.090	57.092	0.479076E 07	0.472811E 01	0.461624E-03
71378.00	-41.999	266.365	19.787	0.373566E 07	0.368681E 01	0.387965E-03
71388.00	-31.999	245.640	-17.517	0.285501E 07	0.281768E 01	0.321522E-03
71398.00	-21.999	224.915	-54.822	0.213101E 07	0.210315E 01	0.262102E-03
71408.00	-11.999	204.190	-92.127	0.154638E 07	0.152615E 01	0.209499E-03
71418.00	-1.999	183.465	-129.432	0.108435E 07	0.107017E 01	0.163500E-03
71428.00	8.000	162.740	-166.737	0.728744E 06	0.719214E 00	0.123874E-03
71438.00	18.000	142.015	-204.042	0.463972E 06	0.457905E 00	0.903774E-04
71448.00	28.000	121.290	-241.347	0.275096E 06	0.271499E 00	0.627426E-04
71452.00	32.000	113.000	-256.270	0.217583E 06	0.214738E 00	0.532659E-04
71458.00	38.000	113.000	-256.270	0.151119E 06	0.149143E 00	0.369950E-04
71468.00	48.000	113.000	-256.270	0.823257E 05	0.812492E-01	0.201539E-04
71468.30	48.300	113.000	-256.270	0.808394E 05	0.797823E-01	0.197900E-04
71478.00	58.000	119.689	-244.228	0.456153E 05	0.450188E-01	0.105428E-04 -
71488.00	68.000	126.586	-231.814	0.261285E 05	0.257868E-01	0.570993E-05 -
71498.00	78.000	133.482	-219.401	0.154179E 05	0.152162E-01	0.319523E-05 -
71508.00	88.000	140.379	-206.987	0.934414E 04	0.922195E-02	0.184135E-05 -
71514.70	94.700	145.000	-198.670	0.677258E 04	0.668402E-02	0.129207E-05 -
71518.00	98.000	145.000	-198.670	0.579452E 04	0.571875E-02	0.110548E-05
71528.00	108.000	145.000	-198.670	0.361237E 04	0.356513E-02	0.689171E-06
71538.00	118.000	145.000	-198.670	0.225229E 04	0.222284E-02	0.429694E-06
71548.00	128.000	145.000	-198.670	0.140447E 04	0.138611E-02	0.267947E-06
71558.00	138.000	145.000	-198.670	0.875915E 03	0.864461E-03	0.167107E-06
71568.00	148.000	145.000	-198.670	0.546344E 03	0.539200E-03	0.104231E-06
71578.00	158.000	145.000	-198.670	0.340822E 03	0.336365E-03	0.650223E-07
71588.00	168.000	145.000	-198.670	0.212641E 03	0.209860E-03	0.405678E-07
71598.00	178.000	145.000	-198.670	0.132685E 03	0.130950E-03	0.253138E-07
71608.00	188.000	145.000	-198.670	0.828051E 02	0.817222E-04	0.157976E-07
71618.00	198.000	145.000	-198.670	0.516830E 02	0.510071E-04	0.986011E-08
71620.00	200.000	145.000	-198.670	0.470340E 02	0.464190E-04	0.897319E-08

TABLE IID-3

JUPITER MODEL ATMOSPHERE NO 8 MAY COOL DATE 30 JULY 1970
MEAN MOLECULAR MASS = 2.70 GRAMS/MOLE
INITIAL PRESSURE =0.506625E 06 DYNES/SQCM AT 71430.60 KM RADIUS
PRINT INTERVAL = 10. KM

ALTITUDE IS ABOVE 71420.0 KM RADIUS

RADIUS	ALTITUDE	TEMPERATURE		PRESSURE		DENSITY
KM	KM	KELVIN	FAHREN	DYNE/CM2	ATMOSPHERES	GM/CM3
71177.00	-243.000	569.453	565.346	0.101684E 10	0.100354E 04	0.579875E-01
71187.00	-233.000	551.927	533.800	0.868721E 09	0.857361E 03	0.511135E-01
71197.00	-223.000	534.402	502.253	0.738445E 09	0.728789E 03	0.448733E-01
71207.00	-213.000	516.876	470.707	0.624344E 09	0.616180E 03	0.392261E-01
71217.00	-203.000	499.350	439.160	0.524851E 09	0.517988E 03	0.341325E-01
71227.00	-193.000	481.824	407.614	0.438507E 09	0.432773E 03	0.295546E-01
71237.00	-183.000	464.298	376.068	0.363954E 09	0.359195E 03	0.254558E-01
71247.00	-173.000	446.773	344.521	0.299934E 09	0.296012E 03	0.218010E-01
71257.00	-163.000	429.247	312.975	0.245283E 09	0.242076E 03	0.185566E-01
71267.00	-153.000	411.721	281.428	0.198926E 09	0.196325E 03	0.156901E-01
71277.00	-143.000	394.195	249.882	0.159877E 09	0.157786E 03	0.131708E-01
71287.00	-133.000	376.670	218.336	0.127230E 09	0.125566E 03	0.109690E-01
71297.00	-123.000	359.144	186.789	0.100160E 09	0.988511E 02	0.905664E-02
71307.00	-113.000	341.618	155.243	0.779178E 08	0.768989E 02	0.740685E-02
71317.00	-103.000	324.092	123.697	0.598222E 08	0.590399E 02	0.599420E-02
71327.00	-93.000	306.567	92.150	0.452626E 08	0.446707E 02	0.479460E-02
71337.00	-83.000	289.041	60.604	0.336915E 08	0.332510E 02	0.378529E-02
71347.00	-73.000	271.515	29.057	0.246217E 08	0.242997E 02	0.294484E-02
71357.00	-62.999	253.989	-2.488	0.176223E 08	0.173919E 02	0.225313E-02
71367.00	-52.999	236.463	-34.034	0.123158E 08	0.121548E 02	0.169137E-02
71377.00	-42.999	218.938	-65.581	0.837385E 07	0.826435E 01	0.124205E-02
71387.00	-32.999	201.412	-97.127	0.551378E 07	0.544168E 01	0.889000E-03
71397.00	-22.999	183.886	-128.674	0.349541E 07	0.344970E 01	0.617286E-03
71407.00	-12.999	166.360	-160.220	0.211722E 07	0.208953E 01	0.413289E-03
71417.00	-2.999	148.835	-191.766	0.121294E 07	0.119708E 01	0.264652E-03
71427.00	7.000	131.309	-223.313	0.648111E 06	0.639636E 00	0.160284E-03
71437.00	17.000	113.783	-254.859	0.316586E 06	0.312446E 00	0.903548E-04
71440.30	20.300	108.000	-265.270	0.243897E 06	0.240708E 00	0.733367E-04
71447.00	27.000	108.000	-265.270	0.141622E 06	0.139770E 00	0.425840E-04
71457.00	37.000	108.000	-265.270	0.629310E 05	0.621080E-01	0.189225E-04
71467.00	47.000	108.000	-265.270	0.279701E 05	0.276044E-01	0.841026E-05
71477.00	57.000	108.000	-265.270	0.124343E 05	0.122717E-01	0.373885E-05
71487.00	67.000	108.000	-265.270	0.552906E 04	0.545676E-02	0.166251E-05
71497.00	77.000	108.000	-265.270	0.245910E 04	0.242695E-02	0.739421E-06
71507.00	87.000	108.000	-265.270	0.109396E 04	0.107965E-02	0.328939E-06
71517.00	97.000	108.000	-265.270	0.486771E 03	0.480405E-03	0.146365E-06
71527.00	107.000	108.000	-265.270	0.216643E 03	0.213810E-03	0.651418E-07
71537.00	117.000	108.000	-265.270	0.964418E 02	0.951806E-04	0.289987E-07
71547.00	127.000	108.000	-265.270	0.429420E 02	0.423805E-04	0.129121E-07
71557.00	137.000	108.000	-265.270	0.191248E 02	0.188747E-04	0.575060E-08
71567.00	147.000	108.000	-265.270	0.851947E 01	0.840807E-05	0.256169E-08
71577.00	157.000	108.000	-265.270	0.379399E 01	0.374635E-05	0.114140E-08
71587.00	167.000	108.000	-265.270	0.169174E 01	0.166962E-05	0.508685E-09
71597.00	177.000	108.000	-265.270	0.754125E 00	0.744264E-06	0.226755E-09
71607.00	187.000	108.000	-265.270	0.336240E 00	0.331843E-06	0.101103E-09
71617.00	197.000	108.000	-265.270	0.149952E 00	0.147991E-06	0.450887E-10
71620.00	200.000	108.000	-265.270	0.117696E 00	0.116157E-06	0.353898E-10

2. Implications to Entry Trajectory

The effects of atmospheric model variation on the descent profile have been analyzed for an entry angle of -10° and an entry ballistic coefficient of 1.5 slug/ft^2. Entries into the Nominal, Cool and Warm atmospheres, as defined in Reference IID-1 (31 Dec 69) were investigated. Entry into the Cool atmosphere of Reference IID-2 was also investigated.

For each of these atmospheres, Table IID-4 details the time and altitude at which the major events occur during descent. The altitudes at which each of these events occur are largest for the warm model and decrease by approximately 50% for the coolest model. Conversely, the maximum deceleration and dynamic pressure experienced by the entry probe is approximately 55% greater for the Cool model of Reference IID-2 than for the Warm model of Reference IID-1. Differences in scale height produce the different environments shown. Despite the wide variation in the entry environment for each of the atmosphere models, the mach number at the staging pressure of 200 mb is essentially unchanged. However, the time from .1 g to the staging altitude exhibits a variation of 39 seconds between the atmosphere models.

The effect of these variations on science objectives and hardware implementation are discussed elsewhere in this chapter of the report.

IID-1 Preliminary Model Atmospheres for Jupiter, JPL Section Document 131-10, Dec 31, 1969.

IID-2 Jupiter Model Atmospheres, JPL IOM 2947-617, N. Divine, May 8, 1970.

IID-3 Draft of Space Vehicle Design Criteria Monograph "The Planet Jupiter (1970)," Supplied by R. G. Nagler.

TABLE IID-4

EFFECTS OF ATMOSPHERIC MODEL VARIATION ON ENTRY

ENTRY CONDITIONS	FLIGHT PATH ANGLE γ_{I_e} = -10°	V_{Ie} = 19557 (fps) = 59.62 km/sec	BALLISTIC COEFFICIENT B_e = 1.5 slug/ft^2	FRACTION OF MASS ABLATED m_a/m_e = .25

Atmosphere	31 Dec 69 Warm	Nominal*	31 Dec 69 Cool	8 May 70 Cool*
Max Deceleration (g's)	393	449	552	718
Max Dynamic Pressure (psf)	15,110	17,235	21,293	27,878
Altitude of Max Deceleration and Dynamic Pressure (ft,km)	327,122=99.7	279,314=85.2	268,113=81.7	189,182=57.7
Time of Max Deceleration and	40.5	42	42	44.5
Altitude of g = .1 (ft,km)	1,364,170=416	903,847=276	759,117=231	584,370=178
Time of g = .1 (sec)	7	21	25.5	31.0
Maximum Relative Velocity (fps, km/sec)	154,702=47.2	154,882=47.2	154,946=47.2	155,029=47.3
Altitude of Max Relative Velocity (ft,km)	1,082,947=330	807,196=246	679,401=207	521,416=159
Time of Max Relative Vel (sec)	15.5	24	28	33
Altitude of M = 1.0 (ft,km)	168,926=51.5	145,349=44.3	140,878=42.9	99,452=30.3
Time of M = 1.0 (sec)	81.5	79	78.5	73.5
Mach Number at 200 mb	.65	.66	.66	.66
Time at 200 mb (sec)	108	104	103.5	93

*Models used as Design Criteria

3. Implications to Low Altitude Descent

The effects of the model atmosphere uncertainties on the descent velocities and times to various pressure levels are illustrated in Table IID-5. The Cool model gives a slower descent velocity but a given pressure level is reached quicker since the vertical distances are less. A more complete discussion of the effects on the descent is given in Chapter VI for the design example mission.

4. Implications to Science Mission

A major science mission requirement is that the probe descend to well below the base of the predicted H_2O cloud. This requires that the probe reach the 5 to 10 atm levels in the Nominal model or 80 to 100 atm in the Cool model. Thus a probe designed to survive to just below the H_2O cloud in the Nominal model would be crushed if the Cool model were encountered and many of the primary objectives would not be accomplished.

The uncertainties also affect the altitude sampling resolution obtained by the instruments although the effect is not so drastic. Figure IID-5 illustrates the slight degradation in altitude resolution that results when the Nominal model is expected but the Cool model is encountered. However, since the clouds are more extensive in the Cool model, the resolution is still sufficient to give measurements above and below each cloud layer. The effects of the atmospheric uncertainties on the sampling are discussed more completely for the design example mission (see Chapter VI).

TABLE IID- 5

MODEL EFFECTS ON LOW ALTITUDE DESCENT

Model Cool = C Nominal = N	Pressure (atm.)	Altitude (km)	Velocity (m/sec)	Time* (min)	Temp (°K)	Time Difference (min)
N	10	-87	100.2	12.1	359.6	3.6
C		-48	76.44	8.52	227.7	
N	30	-155	68.3	26.0	500.5	8.75
C		-79.7	49.35	17.25	283.3	
N	50	-195	57.1	36.7	583.5	13
		-97	40.25	23.7	313.5	
N	100	-260	44.8	58.3	718	21.9
		-23.5	30.5	36.4	360	
N	500	-474	25.6	167.3	116.1	70.5
C		-201	16	96.8	496	
N	1000	-602	20.1	262.0	1427	115.5
C		-242	12.1	146.5	569	

*Time is from deployment at 0.2 atm

Ballistic coefficient = 1 slug/ft^2, $V(B) \sim \sqrt{B}\, V(B=1)$

$t(B) \sim t(B=1)/\sqrt{B}$

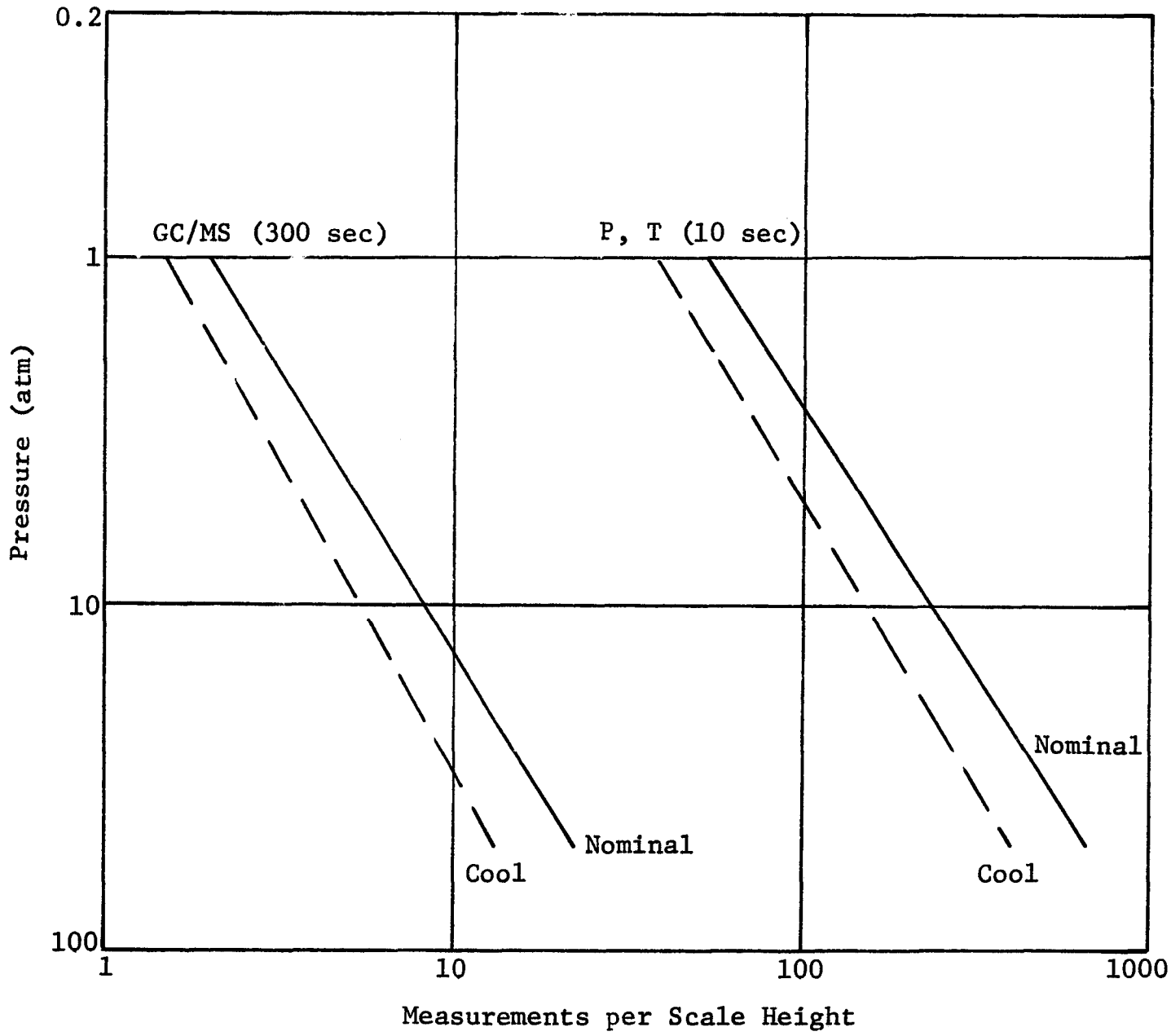


Figure IID-5 Typical altitude resolution profiles for B = 0.05 slugs/sq ft showing the effects of atmosphere uncertainties.

E. Atmospheric Attenuation Model

Computation of atmospheric losses is treated in detail in Volume III, Chapter IV.K. Of the 6 possible sources of loss, the ionosphere, clouds, defocusing, pressure-induced absorption in nonpolar gasses, fading due to atmospheric turbulence, and pressure-broadening of absorption lines in the polarized gasses NH_3 and H_2O, only the last is significant in the nominal atmosphere, with about 90% of the loss due to NH_3. The coolest models have massive H_2O-NH_3 solution droplet clouds which also give significant attenuation.

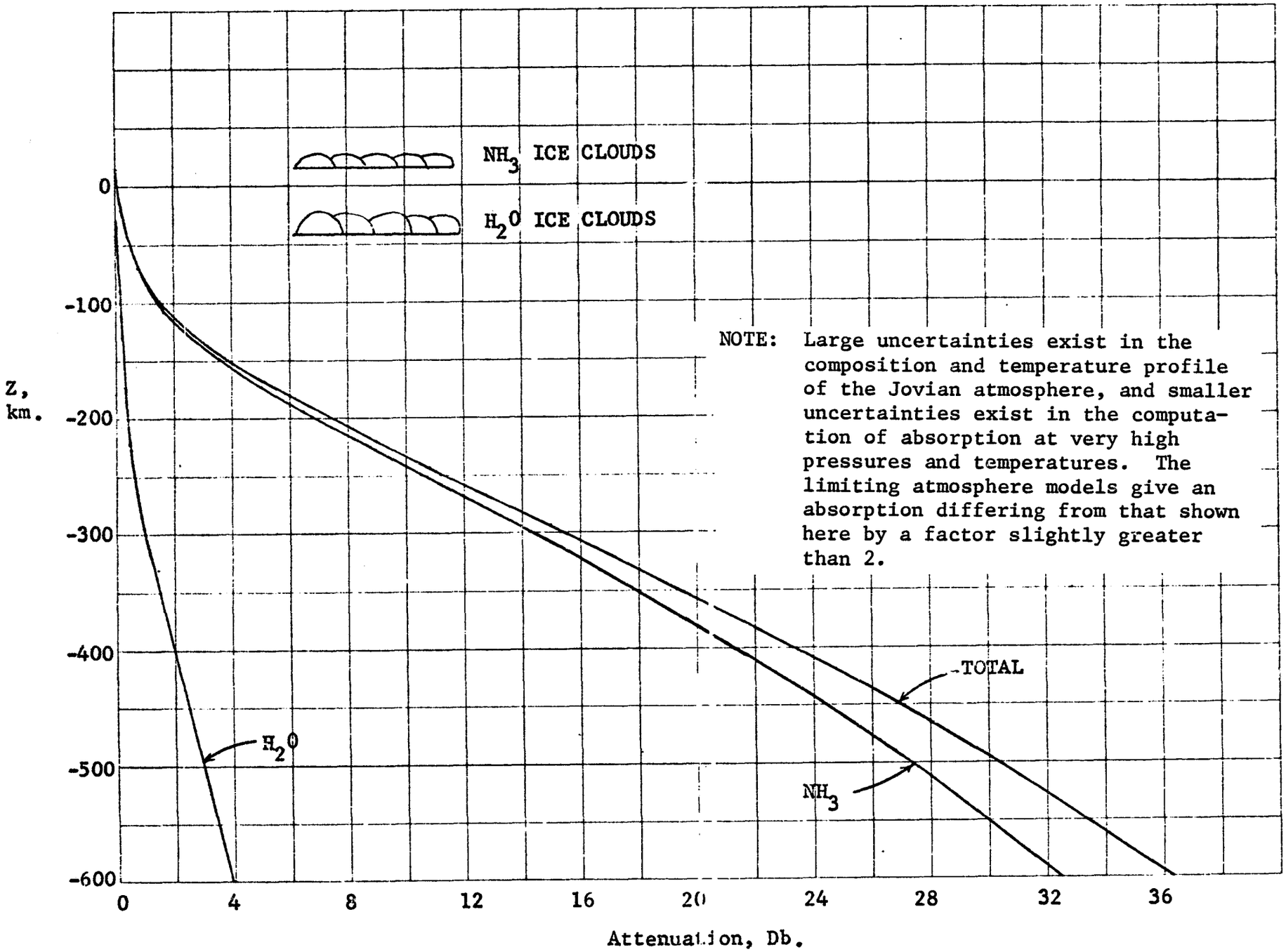
Zenith absorption vs depth for the nominal atmosphere at f = 2.3 GHz is shown in figure II.E-1. This curve was used as the basis for our communication link designs. Absorption scales as the square of frequency, which indicates that lower frequencies should be used. However, this is offset by increasing magnetosphere noise and antenna size with lower frequencies, so an optimum frequency exists for each mission. These optimum frequencies were determined by computer runs covering all necessary parameters over the mission duration.

Given non-zenith communications paths, the absorption increases approximately as sec ψ, where ψ is the probe aspect angle measured from zenith. This has major consequences on the separation and targeting strategy for both relay and direct links. The ideal trajectory would give a near-zenith aspect angle and a minimum communications range at the point of deepest penetration of the probe. Mission designs approximate this ideal while staying within the constraints imposed by mission duration, spacecraft fly-by trajectories, and accuracy considerations.

The very high attenuation given by deep penetrations led to the development of the split-probe concept for these missions. The advantage of a split probe design arises from the fact that the bulk of the absorption occurs on the relatively short (~500 km) probe-to-probe link where power requirements are low, while the long probe-to-spacecraft link has a comparatively low loss due to absorption.

Constraints imposed by atmospheric absorption on a direct link are particularly severe. The latter portion of the mission must be carried out close to the subearth point because of the sec ψ effect. Penetration is limited to a maximum of about 30 atmospheres.

There are some uncertainties in the accuracy of the computations used to determine the atmospheric absorption, particularly at higher pressures. These are due to inadequate experimental data, departure from ideal gas laws, and imperfectly understood behavior of gasses at very high pressures. These uncertainties are believed to be small down to 1000 atmospheres, on the order of 10% of the total zenith attenuation at most. The major uncertainty is in the atmosphere model itself, with a 5 to 1 spread in NH_3 abundance in various models as well as widely varying temperature profiles over these models. These uncertainties can only be resolved by further observation and analysis. Losses given by several other models are shown in Volume III, Chapter IV.K. Loss given by the coolest models is greater than that given by the nominal model by a factor slightly larger than 2.



NOTE: Large uncertainties exist in the composition and temperature profile of the Jovian atmosphere, and smaller uncertainties exist in the computation of absorption at very high pressures and temperatures. The limiting atmosphere models give an absorption differing from that shown here by a factor slightly greater than 2.

Figure II E-1 Zenith Attenuation Assuming the Nominal Atmosphere of this Study and a 2.3 GHz Signal

III. SCIENCE SELECTION RATIONALE AND TRADEOFFS

A. Introduction

The science studies were primarily concerned with (1) establishing the mission, system, subsystem and measurement requirements dictated by the scientific objectives for Jupiter, (2) investigating instrumentation and methods for performing the desired measurements from descent probes, and (3) establishing value curves for making the measurements as a function of depth, entry location, and frequency for use in the mission effectiveness modeling. The basic scientific questions defined in JPL Section Document 131-07 were first translated into observables or relevant measurements which might be performed from a descent probe. This preliminary list of observables was reviewed by five consulting scientists* and a final list including their suggestions was compiled. The performance requirements for each of the observables (e.g. resolution, targeting, depth, etc.) were then defined, again with comments and suggestions from the consultants included. The applicability of instruments defined in JPL Section Document 131-07 (Nominal payload) was reviewed and other instrumental techniques compatible with descent probes suggested by the consultants. These observables, performance requirements, and instrumental techniques were then translated into specific mission and probe system requirements (e.g. descent probe ballistic coefficients, entry sites, deployment altitude, typical payloads and approximate bit rates, etc.). Concurrently, the detailed characteristics and availability of the various instruments were investigated and the performance requirements were translated into value curves for the mission effectiveness modeling. The latter entailed defining, for each observable, the applicable instruments and their potential values for that observable; the value of making a measurement with these instruments as a function of pressure in the Nominal model and as a function of latitude and longitude; and the optimum number of measurements per scale height versus pressure. These were used as criteria for estimating the effectiveness of various mission concepts in accomplishing the scientific objectives.

---

* The five scientists were S. I. Rasool, D. M. Hunten, T. Owen, C. Sagan, and R. Goody.

B. Scientific Objectives and Basic Questions for Jupiter

The major scientific areas of interest for a first generation atmospheric descent probe to Jupiter were specified in JPL Section Document 131-07 as a set of basic questions concerning the lower atmosphere and clouds (Table IIIB-1). In order to establish specific design requirements, these questions were translated into a set of relevant measurements or observables which are compatible with the descent probe concept (Table IIIB-2). The major constraint on defining these observables was that they not be determinable by remote sensing (from earth or spacecraft) due to the greater difficulty and cost of delivering instrumentation through entry to the lower atmosphere of Jupiter. Thus, the emphasis for this study is on objectives which can be accomplished only by in situ measurements, particularly below the visible clouds since much of what lies above the cloud can be inferred from remote sensing or non-survivable entry pro[illegible].

The scientific objectives for an exploration of the outer planets (particularly Jupiter) have been delineated in previous studies (References IIIB-1 and IIIB-2). The basic questions shown in Table IIIB-1 were derived from those studies; the observables given in Table IIIB-2 represent the measurements that will contribute to answering those questions. Complete answers to even these few questions or the determination of all the relevant observables is, unfortunately, impossible for a first generation mission and new questions will undoubtedly arise. The purpose of this study is to investigate the cost and relative feasibility of answering the present questions to various degrees with atmospheric entry probes. The observables serve as specific criteria for the probe system and mission designs.

In general, there is no exact one-to-one correspondence between the questions and observables. Some questions require many kinds of measurements while a single measurement may contribute to several questions. The questions themselves are strongly interrelated and an answer to one requires at least partial answers to others, for example, the questions of whether complex molecules are present and the nature and origin of the colors both require a knowledge of the cloud composition and the pressure-temperature structure. Table IIIB-3 relates the questions to the

observables. As can be seen, relatively few of the observables represent direct answers to the questions; most would give only partial answers or are at best speculative investigations of a possible cause. For example, the colors may be due to any one or a combination of several factors (e.g., photochemical processes, electric discharges and shock waves) or to some unknown process in the deep atmosphere. Even the cloud particle sizes, number densities, and vertical structure probably have some effect on the colors as seen from above the atmosphere.

TABLE IIIB-1

Basic Scientific Questions for Jupiter
(JPL Section Document 131-07)

1. What are the relative abundances of hydrogen, deuterium, helium, neon, and other elements, and what are their isotopic compositions?
2. What are the present-day atmospheric composition and altitude profiles of pressure, temperature, and density, and what effect do they have on the radiation balance?
3. What are the chemical composition and vertical distribution of the clouds?
4. Do complex molecules exist in the atmosphere of Jupiter?
5. What are the nature and origin of the colors observed in Jupiter's atmosphere?
6. *What is the magnetic field strength in the lower atmosphere?
7. *What is the level of turbulence in the atmosphere?

*Supplementary questions added after start of contract.

TABLE IIIB-2

Relevant Measurements or Observables
Derived from Basic Questions

1. Determine the relative abundances of H and He in the lower atmosphere (below the turbopause).

2. Determine the isotopic ratios H/D, $^{3}He/^{4}He$, $^{20}Ne/^{23}Ne$, $^{36}A/^{40}A$, $^{12}C/^{13}C$ in the lower atmosphere (below the turbopause).

3. Determine the atmospheric mean molecular weight and identify the major contributing gases (i.e., determine whether H_2 and He are indeed the only major constituents and, if not, what the other gases are).

4. Determine the concentration profiles (versus pressure and temperature) of the minor atmospheric gases (e.g., Ne, A, N_2, etc. and CH_4, NH_3, H_2O, H_2S, etc.) from above the visible cloud tops down to several hundred bars.

5. Determine the temperature versus pressure (and time) profile from above the cloud tops down to well below the condensation level of H_2O with a precision sufficient to determine whether the lapse rate is adiabatic.

6. Determine the vertical distribution and structure of the cloud layers with respect to pressure and temperature (particularly, locate the cloud tops).

7. Determine the chemical composition of the cloud particles in each layer.

8. Determine the color of each of the cloud layers.

9. Determine the intensity distribution of the incoming solar flux (direct and diffuse) at several wavelengths as a function of pressure and temperature from above the visible clouds down to at least several tens of bars.

10. Determine the thermal radiation (IR) flux profiles at several wavelengths from above the cloud tops down to several hundred bars.

11. Determine whether specific complex molecules are present in the region between the cloud tops and the condensation level of H_2O.

TABLE IIIB-2 (Continued)

12. Determine the frequency of occurrence of electric discharges and the nature of any thunder as a function of pressure and temperature down to at least the condensation level of H_2O.
13. Determine the physical characteristics (number density and size distribution) of the cloud particles in each layer (particularly through the cloud tops).
14. Determine the scales and the magnitude and frequency spectra of any atmospheric turbulence from above the cloud tops down to at least several tens of bars.
15. Determine the magnetic field strength and variations versus depth from above the ionosphere down through the lower atmosphere to as deep as possible.
16. Determine the electric conductivity of the deep atmosphere.
17. Determine the relative abundances and isotopic ratios of Li, Be, B.
18. Determine the composition profiles of the ionic species through the upper atmosphere.
19. Determine the exospheric/ionospheric temperature profiles.
20. Locate the source of decametric radiation (with respect to radius).

TABLE IIIB-3

QUESTIONS RELATED TO OBSERVABLES

Observable	1 H/He etc?	2 Structure & Composition?	3 Clouds?	4 Complex Molec?	5 Colors?	6 Magnetic Field?	7 Turbulence?
1. H/He ratio	D	R					
2. Isotopic Ratios	D						
3. Mean Molecular Weight	R	R					R
4. Minor Constituents	D	D	R	R	R		R
5. Temperature/Pressure		D	R	R	R		R
6. Cloud Layering		R	D	R	R		R
7. Cloud Composition		R	D	R	R		
8. Cloud Colors			R	R	R		R
9. Solar Flux		R	R	R	R		R
10. IR Flux		R	R				R
11. Complex Molecules			R	D	R		
12. Lightning/Thunder			R	R	R		R
13. Cloud Particle Sizes			R	R	R		R
14. Turbulence		R	R	R	R		D
15. Magnetic Fields		R?				D	R
16. Conductivity		R?				R	R
17. Li, Be, B ratios	D						
18. Ionosphere Composition		D					
19. Upper Atm Temperature		D					
20. Decameter Radiation							

D: direct determination
R: related

The question of relative elemental abundances and isotopic ratios requires several types of composition measurements. The simplest is a determination of the H/He ratio at several levels below the turbopause (at least 4 for redundancy). This was listed separately (as observable 1) from the determination of the other elemental abundances due to its extreme importance to theories of the origin of the solar system and to cosmology (see Reference IIIB-1). The relative abundances of other elements (e.g. C, Ne, A) up to mass 40 and their isotopic ratios are also fundamental to origin and evolution theories. Due to the different requirements for measurements, these are further separated into three categories (observables 2, 4, 17). The relative elemental abundances of carbon through argon can be determined from measurements of the composition at any level below the turbopause. Their isotopic ratios (especially H/D, He^3/He^4, C^{12}/C^{13}) require a more refined instrument. The abundances and isotopic ratios of Li, Be, and B would give an upper limit as the past temperature of Jupiter but would require a very deep probe. However, convective penetration from very deep regions may carry these elements (as compounds) up to the probe level and isotopic ratios might be measurable. This would require yet another step in the instrument refinement since these elements have a low cosmic abundance and would not be in gaseous form.

A determination of the mean molecular weight would give a gross indication of the H/He ratio since these are thought to be the major constituents and is therefore related to the first question.

The second question, concerning the atmospheric composition profile and structure, requires at least 4 types of in situ measurements (observables 4, 5, 18, 19) through both the upper and lower atmosphere. The upper atmosphere structure and composition could be partially inferred from remote sensing (e.g., RF occultation, Lyman -α) but an unambiguous answer requires an entry probe -- or at least a pre-entry probe. The lower atmosphere structure and composition can only be determined from a probe which descends below the clouds, preferably to a depth at least below the condensation level of H_2O. While the mean molecular mass is expected to

be relatively uniform in the lower atmosphere, the abundance of minor constituents will vary with depth (and perhaps location) due to phase changes, photochemical processes, or non-equilibrium processes. An understanding of the structure and composition in terms of these processes (or vice-versa) will require a knowledge of the radiative flux profiles, the cloud structure, the dynamics and, if MHD effects exist in the lower atmosphere, the magnetic fields and electric conductivity in the deep atmosphere. Thus, observables 6, 7, 9, 10, 14, and perhaps 15 and 16 are all relevant to the structure and composition profiles (or vice-versa).

The questions concerning the cloud composition and structure are directly answerable by determining the cloud particle composition (GC/MS) and the aerosol density (nephelometer) versus altitude (pressure). However, many other types of measurements (i.e., observables 4 through 14) are also required in order to understand the cloud properties in terms of the atmospheric structure, composition, and dynamics. An understanding of the origin of the colors and the presence (or absence) of complex molecules is even more dependent on making a number of different but related types of measurements since there are many possible causes for both of these phenomena.

The determination of the magnetic fields in the deep atmosphere was included to attack the question of whether magnetohydrodynamics plays a role in the atmospheric dynamics as suggested by Hide.* Measurements of the magnetic fields and electrical conductivity would indicate the importance of MHD effects if the probe could descend to the proper depths. However, it appears that the regions where the conductivity becomes significant are well below 1000 atm and, if the probe were to descend through such regions, radio communications would be impossible.

---

*Hide, R. "Dynamics of the Atmospheres of the Major Planet." Journal of Atmospheric Sciences. Vol 26, No. 5, Part I, September 1969.

C. Measurement Performance Requirements

In order for the observables to be useful as mission design and evaluation criteria, statements of the specific conditions that must be met for a measurement to be properly "relevant" are required. Obviously, the weight, power, volume, data rate, etc. requirements of the necessary instruments must be considered but these are the subject of a following section. The present section discusses the locations (or targets), the range of pressure levels (depths), and the altitude sampling intervals appropriate to each the observables. The requirements for each of the observables are summarized in Table IIIC-1. These are based on present theories of what is expected or thought to be possible on Jupiter. However, the present gamut of theory and speculation concerning Jupiter makes it impossible to cover all theories while keeping the requirements within reason.

1. Targeting

For first generation probe mission to a planet, it is customary to stipulate an entry site thought to be both most relevant to the desired objectives and "typical" of the planet as a whole in order to extrapolate the measurements over the rest of the planet. In the case of Jupiter, it is difficult to define such a location. Some locations are probably "typical" only of themselves (e.g., the Great Red Spot (GRS) or one of the transient "bright ovals") while any location other than the GRS is probably "typical" for measurements of the gross composition or the pressure-temperature-density profiles in the deep atmosphere. However, the cloud structure and compositions (colors), the P-T relations near the cloud tops, and, most obviously, the dynamics and circulations vary markedly with latitude and time. Thus, a location relevant to one question may be neither typical of the planet nor relevant to other questions. For example, Lewis argued that only the GRS may be stagnant enough to accumulate complex molecules; however, this is the most obviously atypical region on Jupiter so very little, if any, information on the questions concerning the clouds and colors in the belts and zones would be expected; even the P-T profiles there may be atypical of the rest of the

TABLE IIIC-1

SUMMARY OF PERFORMANCE REQUIREMENTS FOR OBSERVABLES

Observable	Targets	Pressure Depth	Sampling
1. H/He ratio	Any	Below Turbopause	At least 4
2. Isotopic Ratios	Any	Below Turbopause	At least 4
3. Mean Molecular Weight	Any	To 5 atm or more	At least 4
4. Minor Constituents	Any	To 100 atm or more	2 to 5 per scale height
5. Temperature/Pressure	EZ, NEB, TR, Poles	To 1000 atm	50 to 100 per scale height
6. Cloud layering	EZ, NEB, TR, Poles	To 100 atm or more	100 " "
7. Cloud composition	EZ, NEB, TR, Poles	To 100 atm or more	2 to 5 " "
8. Cloud colors	EZ, NEB, TR, Poles	To 100 atm or more	100 " "
9. Solar Flux	Subsolar or LS	To 10 atm	100 " "
10. IR Flux	Any	To 100 atm or more	50 to 100 "
11. Complex Molecules	GRS, Any	To H_2O cloud (5 to 100 atm)	2 to 5 per scale height
12. Lightning/Thunder	Any	To H_2O cloud (5 to 100 atm)	10 to 20 per scale height
13. Cloud Particle Sizes	EZ, NEB, TR, Poles	To 100 atm or more	100 per scale height
14. Turbulence	EZ, NEB, Poles	To H_2O cloud (5 to 100 atm)	10 to 20 per scale height
15. Magnetic Fields	Poles, GRS or Any	To 1000 atm or more	2 per scale height
16. Conductivity	Poles, GRS or Any	To 1000 atm or more	2 per scale height
17. Li, Be, B ratios	Any	~10,000 atm	At least 4
18. Ionosphere Composition	Subsolar, LS, DS	Pre-entry	2 per scale height
19. Upper atm temperature	LS, DS	Pre-entry	2 per scale height
20. Decameter Radiation	Any	To 100 atm or more	-

Targets: EZ = Equatorial Zone; GRS = Great Red Spot; NEB = North Equatorial Belt
LS = Lightside; TR = North or South Temperate Regions DS = Darkside
Any = Any target expect GRS

planet. Therefore, we exclude the GRS as a primary target for a first-generation probe on the basis of its being both atypical and least relevant to most of the specified questions. The polar regions are also excluded as primary targets on the basis of their being least relevant to the stated objectives and because the cloud structure appears to be quite different from that of the equatorial regions. The wide variety of apparently unique features on Jupiter indicates the eventual need for many entry probes targeted to different latitudes, but there appears to be no strong need for them to be simultaneous.

This study was thus limited to a consideration of two of the obviously different and more apparent and constant features on the planet -- the north equatorial belt (NEB) and the equatorial zone (EZ). Depending on the explanation of these features, one or the other is probably most relevant to the questions for a first-generation probe. According to Ingersoll, the bands are probably convective cells with rising, cloud-forming fluid in the light zones and clear, descending fluid in the dark belts with meridional flow from zones to belts. This hypothesis is supported by Westphal's measurement of higher temperatures in the dark belt implying that lower, and therefore hotter, levels are being observed. If this is indeed the case, then the EZ may be the most suitable entry site since the darker colored bands can be interpreted as low clouds (possibly of complex organic molecules) that will presumably be present below the light-colored higher altitude clouds as well. The question of choice was posed to our consultants and their concensus was that either would be suitable for a first mission although 3 of the 5 had a slight preference for the NEB.

For the purposes of a baseline mission definition for this study the center of the North Equatorial Zone was specified as the prime target with the NEB, the GRS, and a pole following in order of priority (and difficulty).

Most observables are independent of solar lighting conditions and can be satisfied by either a lightside or darkside entry. However, the solar flux attenuation measurements require a light side entry, preferably within $\pm 30^{o}$ of the subsolar point. Other observables

(e.g., ionospheric profiles, influence of photochemical processes, etc.) prefer, but do not require a lightside entry since the rapid rotation of Jupiter tends to minimize diurnal variations. As is discussed in other sections of this report, an entry within 30° of subsolar is undesirable in terms of weight penalty and the subsequent degradation of science capability for accomplishing most other objectives. However, a lightside entry within 50° to 60° of subsolar as shown in Figure IIIC-1 gives a reasonable compromise for all objectives.

In summary, an entry point within 50° to 60° of the subsolar point and in either the North Equatorial Zone or Belt will satisfy the requirements of the observables. If practical considerations preclude a light side entry, the solar flux measurements will obviously be excluded but a satisfactory accomplishment of most of the remaining objectives is still obtained by entry on the dark side.

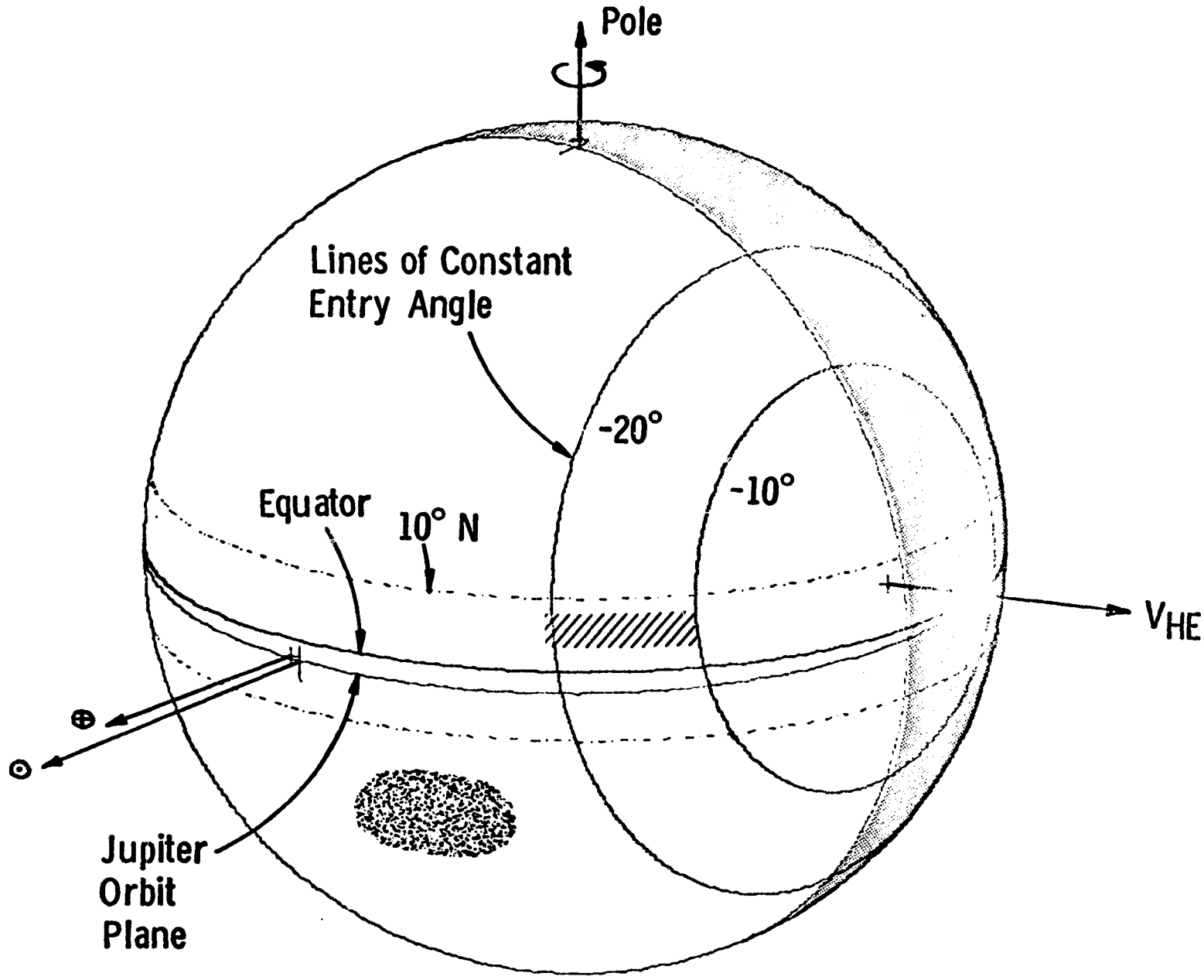


Figure IIIC-1. Preferred Entry Locations. The Entry Points which Give the Best Compromise for all Observables are Bounded by the North and South Equatorial Zones and the -20° and -10° Entry Point Loci.

2. Pressure-Depth Requirements

The depths or pressure levels through which the measurements must be made are summarized in Table IIIC-1 for each of the observables. The upper atmosphere magnetic field and decameter radiation measurements (observables 15, 18, 19, 20) should begin at least 2 to 3 Jupiter radii out and continue until entry. The magnetic field and decameter radiation measurements should begin again as soon after entry as possible and continued down to as deep as practical. The severe entry environment precludes making measurements other than the decelerations during that period. Whether the deceleration history can be interpreted in terms of a density profile remains to be seen but such measurements are desired for engineering purposes in any event.

All other measurements should begin above the clouds (P$\sim$ 0.1 to 0.3 atm) in order to locate the cloud tops and to correlate with remote sensing data (e.g., UV, IR, or visual imaging). The H/H_e ratio and the isotopic ratios could be adequately determined from several ($\sim$ 4) measurements well below the turbopause in the mixed region (preferably $\lesssim$ 0.1 to 1 atm). The same might apply to a determination of the mean molecular mass but measurements to lower levels (the H_2O cloud base) would be desirable since this quantity is required to within 1% or better and may be variable with depth due to phase changes. The determination of the minor constituent profiles, cloud layering, colors and composition and the search for complex molecules and electric discharges should be carried out down to at least the condensation level of H_2O. Most of the cloud layers proposed by Lewis (except NH_4Cl) occur above this level. The environmental conditions most favorable to the abiogenic (or perhaps biogenic) production of organic compounds would also occur above and in the H_2O cloud. A determination of the true NH_3 and H_2O abundances and the problem of the trace coloring matter also require descent below this level. Depending on the nature of the cloud, the solar flux may or may not penetrate to this level. Measurements of the pressure-temperature structure, the level of

turbulence and the IR flux below the clouds are required for dynamical theories. Thus, most of the observables require a descent to a depth below the condensatian level of H_2O. Depending on the model atmosphere assumed, the cloud bottoms lie somewhere between about 1 atm and 100 atm and perhaps as low as 200 to 300 atm. The only firm requirements for descent below the 100 to 300 atmosphere levels are for a determination of the P-T profiles for extrapolation to the interior, an attempt to measure the Li, Be, B isotopic ratios, a search for other clouds, MHD effects, and curiousity. The search for a "surface" or an investigation of the proposed silicate clouds would require descent to 10,000 to 100,000 atmospheres.

In summary, there are several identifiable levels of descent required by the obserables. These are: (1) below the turbopause to determine the H/H_e ratio and gross atmospheric composition, (2) the 1 to 10 atm levels to obtain information on the pressure-temperature profiles and clouds, (3) the 100 to 300 atm levels to satisfy the requirements of most of the observables, and (4) the 500 to 1000 atm levels to satisfy curiosity.

3. Sampling Interval Requirements

The observables fall into several sampling interval categories: (1) those that require only a few (4 for redundancy) measurements in the mixed lower atmosphere such as the H/H_e and isotope ratios or the mean molecular mass, (2) those that require a few (2 to 5) measurements per scale height such as the gross pressure-temperature structure, or the cloud composition and minor constituent profiles; (3) those that require averaging or integrating over an interval such as average turbulence or lightning measurements; (4) those that require 50 to 100 measurements per scale height such as the detailed thermal and turbulence structure; and (5) those that require very detailed profiles (100 to 200 per scale height) such as the cloud structure and physical properties measurements. These are summarized in Table IIIC-1 for each observable. Many of the

sampling requirements could be relaxed and still give useful information. For example, a detailed pressure-temperature profile down to the 100 atm level combined with a few precise composition measurements near 100 atm might allow an inference of the cloud layering above the 100 atm level.

4. Mission Effectiveness Model Inputs

The measurement performance requirements discussed above were translated into value curves and statements for use in estimating the relative effectiveness of the various mission concepts for accomplishing the scientific objectives. The value curves and other criteria are described in Volume III, Chapter VI.

The instrumentation required for each observable was defined and each instrument or group of instruments assigned a potential value less than or equal to one. This potential value could be realized in the model only if all measurement performance requirements were met. For example, the concentration profiles of the minor constituents (observable 4) can be only be partially determined with a mass spectrometer due to mass number ambiguities so the potential value of this instrument is less than one (0.8) for that observable even if all sampling, depth, and targeting requirements are satisfied.

The values of making measurements with the appropriate instrument versus entry location and pressure-depth were given in the form of curves such as shown in Figures IIIC-2 and IIIC-3. Figure IIIC-2 shows the value of making photometer measurements of the solar flux (observable 9) as a function of latitude and angle from the subsolar point while Figure IIIC-3 shows the value of making the same measurements as a function of depth. The values are highest near the subsolar point and through the cloud tops decreasing to zero at the terminator and below 50 atmospheres.

The sampling interval criteria were specified as in Table IIIC-1; fewer measurements per scale height give a value less than one while the required number or more give a maximum value of one. Folding all values together results in the value contributed to an observable by an instrument on a particular mission. The detailed process for obtaining a relative mission value is described in Volume III, Chapter VI.

Figure IIIC-4 shows a comparison of the various missions studied (See Chapters VI and VII for the mission descriptions).

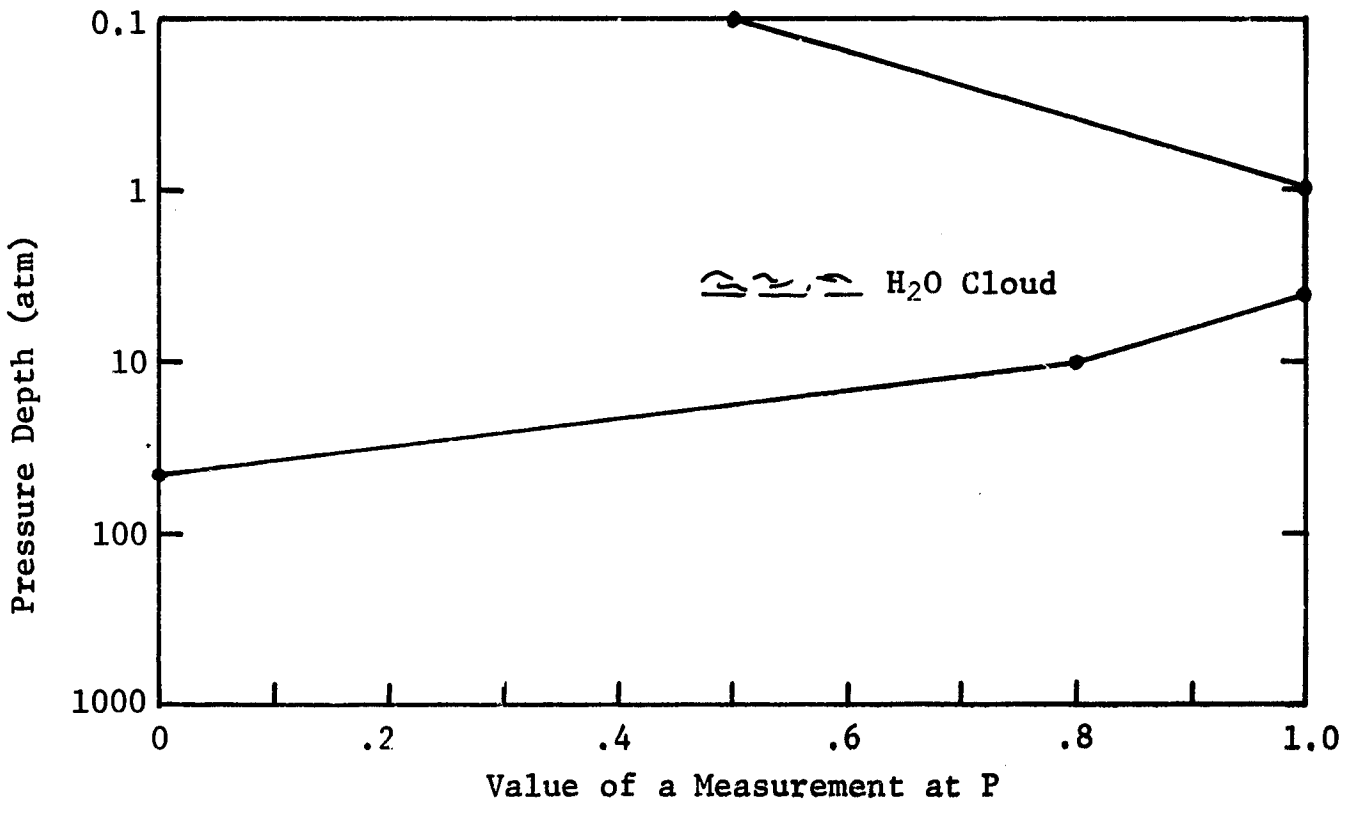


Figure IIIC-3 Value Curve for Making Photometer Measurements Versus Depth

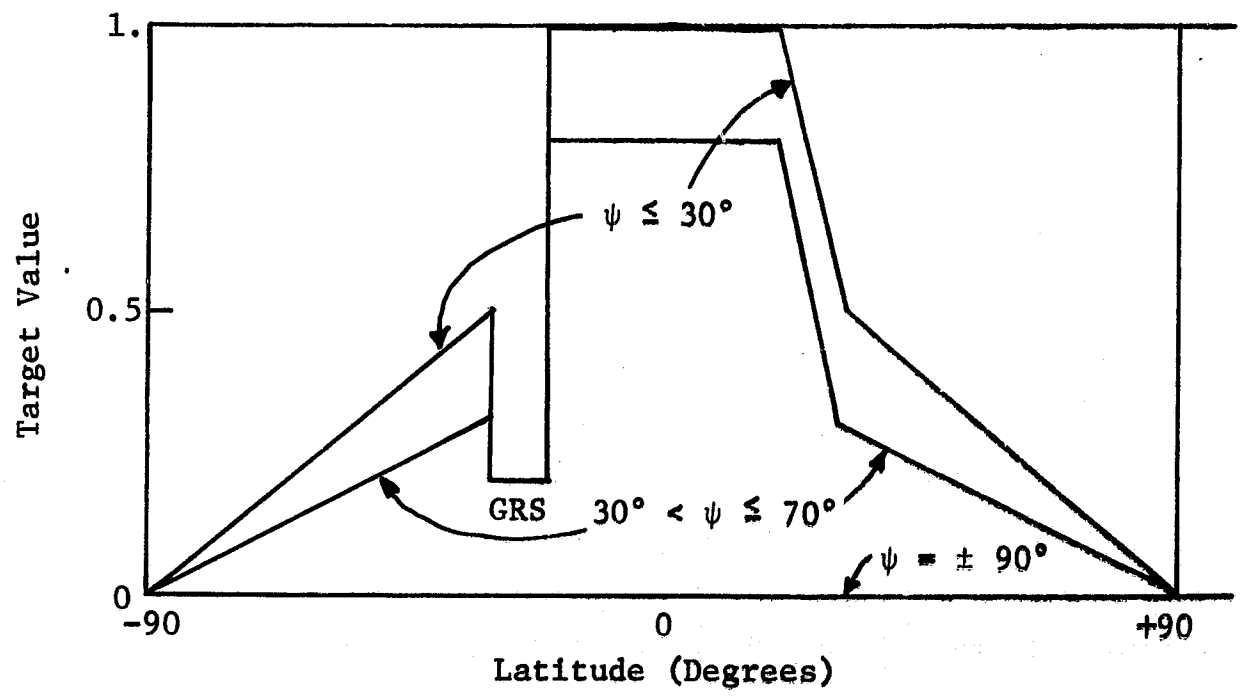


Figure IIIC-2 Value of Making Photometer Measurements Versus Target Latitude nd Angle ψ from Subsolar

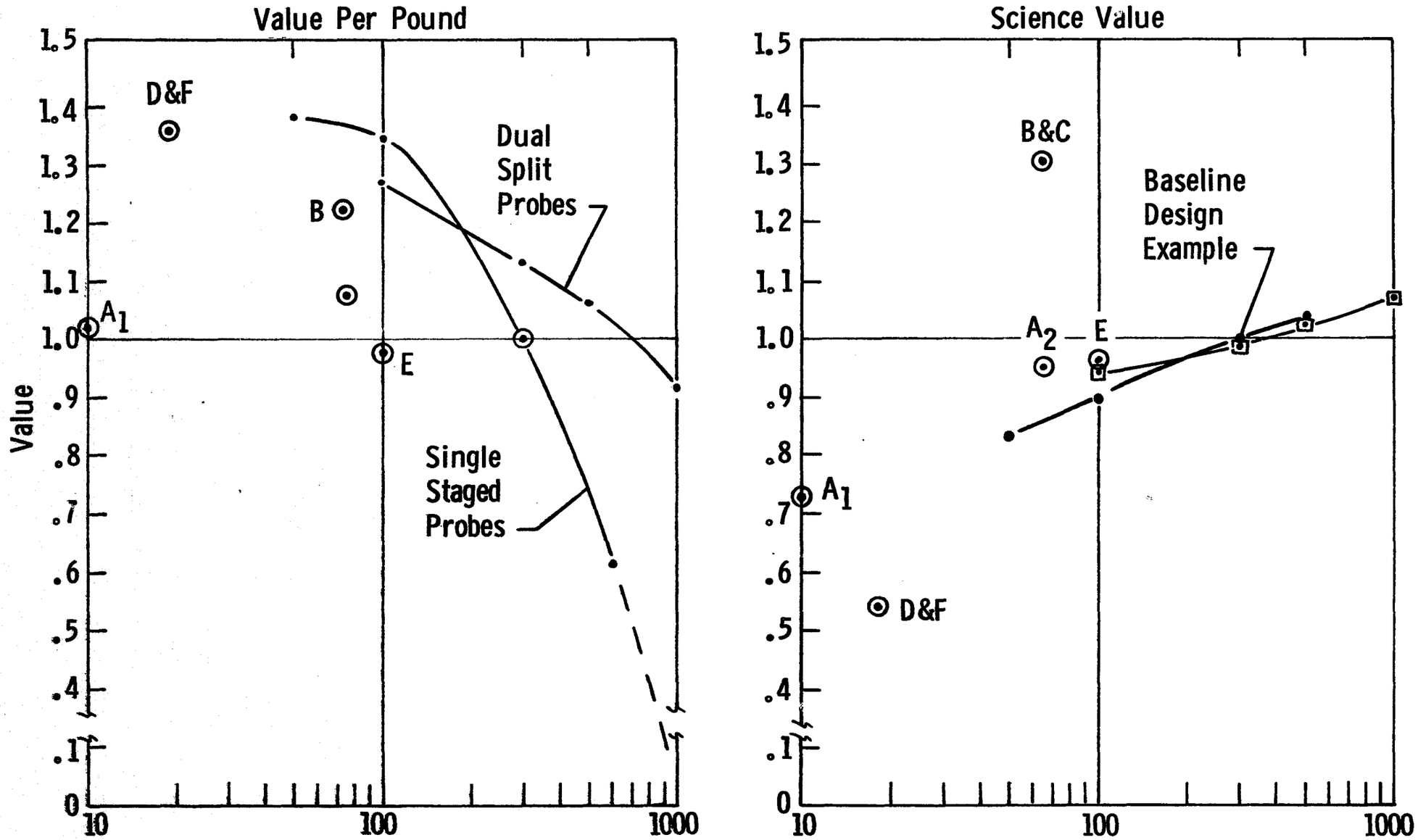


Figure III C-4 Mission Values from Effectiveness Model

D. Instrumental Techniques

The major part of this study was concerned with the definition of probe system capabilities for carrying the Nominal payload (Table IIID-1) to various depths in the Nominal model atmosphere. However, other instrumental techniques appropriate to the observables were also investigated and missions with payloads smaller and larger than the Nominal were defined. The instrumental techniques considered are listed in Table IIID-2; the instrument descriptions and tradeoffs are given in Volume III, Chapter II.

The required composition measurements can be performed to varying degrees of completeness with a wide range of instruments from simple spectrophotometers to a complex gas chronatograph-mass spectrometer combination with cloud particle collecting and processing gear. The GC/MS proposed for the Nominal payload (Reference IIID-1) appears to be the best compromise of versatility and complexity since it could make measurements contributory to all the observables requiring a composition determination. An expanded GC/MS with a few more gas chromatograph columns would be desirable in searching for complex organic molecules but the sample processing times would severely limit the number of measurements. Cloud particle collecting and processing apparatus to concentrate the sample before presenting it to the GC/MS would increase the probability of determining the nature of the coloring matter but again, the number of samples would be limited. In the other direction, a mass spectrometer alone is of limited usefulness due to the mass number ambiguities discussed in Reference IIID-1. However, a small instrument for determining the H/H_e ratio would be desirable for missions with limited payload and/or depth capability. Such an instrument, delivered into the atmospheres of two or more of the outer planets from a Grand Tour mission would be of extreme value to theories of the origin of the solar system. A limited range of 1 to 4 m/e plus $m/e \geq 5$ would give the H/He ratio, an indication of the mean molecular mass and, if the dynamic range is great enough, an indication of the NH_3 and H_2O abundances during descent through the clouds. A better determination of H/D/He could be obtained with the addition of a

TABLE IID-1 BASELINE PAYLOAD INSTRUMENT SPECIFICATIONS AND REQUIREMENTS

Instrument	Volume ($in.^3$)	Weight (lb)	Power (watts)	Sampling Interval (meters)	Word Size (bits)	Words Per Sample	Bits Per Sample
Aerometry: Temperature Gauge (Range-Switched)	15	7	0.2	300	8	1	8
Aerometry: Pressure Gauge (5) (Switched)	10		0.1	300	8	1	8
Aerometry: Accelerometers (4)	24		4	Entry only Δt - 0.2 sec	10	4	40
Ion Mass Spectrometer	80 ($2\frac{1}{2}$"x4"x8")	3	1	1 scan every 2 sec	← 20 words per sec 8 bits per word →		
Gas Chromatograph/Neutral	320 (4"x8"x10")	7	12	1000*	15	40	600
Photometer (6 channels)	36 total (1"x1"x6" per channel)	2	1	100	10	6	60

*Each analysis by the gas chromatograph requires from 2 to 5 minutes. A minimum of four analyses, at altitudes below the region of gravitational separation of atmosphere constituents, are required.

TABLE IIID-2

INSTRUMENTAL TECHNIQUES FOR OBSERVABLES

Observable	Instrumental Techniques
1. H/He ratio	a. Palladium column GC/1 to 4 + ≥ 5 m/e MS b. 1 to 4 + ≥ 5 m/e MS c. Nominal GC/MS d. Expanded GC/MS
2. Isotopic ratios	a. Nominal GC/MS b. Expanded GC/MS c. H/D photometer (4.55 μ CH_3D)
3. Mean molecular mass	2a or 2b above/possibly 1b
4. Minor constituents	2a or 2b above CH_4, NH_3 absorption photometers
5. Temperature/Pressure	a. Pressure gauges of various types b. Immersion thermometers (thermocouples, Pt wire) c. 10 μ radiometer for relative temp to ± 0.1°k
6. Cloud layering	a. Nephelometer b. Aerosol photometer (cloud tops only) c. IR radiometers (5 μ & 10 μ) d. Pressure/temperature - very precise
7. Cloud composition	a. Nominal or Expanded GC/MS b. Pressure, Temperature, Nephelometer
8. Cloud colors	a. Nephelometer with color wheel b. Photometers (solar) with color wheel
9. Solar flux	a. Photometers with various filter
10. IR flux	b. Up & down looking IR photometers (various wavelength bands).
11. Complex molecules	a. Nominal or Expanded GC/MS b. UV spectrophotometer with light source
12. Lightning	a. RF lightning detector and microphone b. Optical flash detectors
13. Cloud particle sizes, etc.	a. Cloud particle counter b. Nephelometer

TABLE IIID-2 (Continued)

14. Turbulence	a. Accelerometers b. Pressure/temperature fluctuations
15. Magnetic fields	Various magnetometers
16. Electric conductivity	a. Electrometer b. Loss of RF communications link
17. Li, Be, B ratios	a. Nominal or Expanded GC/MS
18. Ionosphere composition	a. Ion mass spectrometer b. Neutral mass spectrometer
19. Upper atm. temperature	a. Electron density probe and ion and neutral scale heights.
20. Decameter radiation	a. Receivers on probe and spacecraft.

palladium GC column with Kr carrier but the weight and analysis times would increase significantly.

The "expanded" GC/MS referred to in Table IIID-2 is a hypothetical instrument with 3 or 4 GC columns added to the Nominal GC/MS' several columns to search for specific complex molecules and one Palladium column with Kr carrier for making H/D/He analyses. Only 2 to 4 analyses with each of the columns are performed and an impactor type aerosol collector is used to concentrate the samples for the complex molecule columns.

A simpler but less definitive way to search for complex molecules would be to use a UV spectrophotometer viewing a suitable light source through a short (∿ 10 to 50 cm) atmospheric path. Many of the proposed molecules have strong absorption features in the near UV to around 2000 Å to 2600 Å.

The filtered photometers to determine the CH_4, NH_3 and CH_3D (H/D) abundances would be very unsatisfactory as primary instruments but might be useful for backup measurements to resolve ambiguities. The palladium GC column with a Kr carrier is preferable for an H/D/He analysis.

The pressure and temperature sensors should cover the ranges 0.1 to 1000 at m and 100°K to 2000°K, respectively, with the upper limit depending on the design depth. This will require several sensors and range switching. The absolute accuracy should be about ±0.5% for both pressure and temperature (± 5mb at 1000 mb and ± 1°K at 200°K). The vertical temperature gradient should be determined to within 1% or better to be useful for dynamical theories (i.e., to within 0.02°K/km). This may require temperature measurements with a relative accuracy of ± 0.1°K over a 20°K range for 15 minutes or ± 1°K over a 200°K range for 60 minutes. An IR radiometer (at 10μ) can be used in conjunction with an immersion temperature sensor to obtain these relative accuracies.

The pressure and temperature sensors are also used to provide reference for the other measurements. A relative altitude reference is obtained by integrating the hydrostatic equation. This can be related (within 50 to 100 km) to the planetocentric radius by determining the pressure and temperature at the detected cloud top.

The fact that an aerosol is present (nephelometer) at a given pressure/temperature level can be used to infer the aerosol composition by examining the phase relations for the condensibles (NH_3, H_2O, H_2S, etc.) expected on Jupiter.

The sidelooking nephelometer is to be preferred for determining the cloud structure or layering during descent on either the lightside or dark side. A modulated light source is required to distinguish between the signal and the solar flux on the lightside. A range of about 10 to 25 meters is desired but a 1 to 5 meter range would be adequate to indicate the presence of significant amounts of aerosol.

The aerosol photometer of the Nominal payload would be useful only on the light side and, even then, only for locating the cloud tops and perhaps one or two layers just below the cloud tops. The nephelometer with its own light source, can sense the presence of aerosol at any depth below the cloud tops.

The addition of a downlooking 5μ channel to the 10μ IR radiometer would permit another means of determining the cloud layering. The 10μ channel senses the blackbody radiation from the atmosphere in the immediate vicinity of the probe while the 5μ channel senses radiation from an opaque cloud layer below the probe (if it is within about optical depth 1 at 5μ). The 5 and 10 micron channel temperatures will be equal when the probe reaches the top of the cloud layer and will change again when the probe passes out the bottom of the layer.

The dual channel radiometer should be capable of resolving temperature differences of the order of 1°K or less at temperatures up to at least 350°K. This would allow the precise location of cloud layers above the condensation levels of H_2O. At greater depths, a resolution of at least 5° K at temperatures up to 500°K would be sufficient to detect a NH_4Cl cloud.

A determination of the cloud colors could be made by using a filter wheel in front of the nephelometer detector. At least 2 color filters (yellow and red) plus one clear would be required.

The nephelometer might provide some information on the cloud particle size distribution, but an instrument which actually detects and

counts individual particles is preferred. One such instrument is currently under development at NCAR. Particles streaming through a small volume are illuminated and their shadows observed on a fiber optic background. While this would give both the number density and size distribution of the particles, the instrumentation is complicated and requires at least 20 bps.

While the flash photometer of the Nominal payload would indicate whether and how frequently electrical discharges are occurring within about 10 to 20 km of the probe, no information is obtained on the magnitude or frequency of the shock waves (thunder) resulting from the discharges. The shock waves are thought to be the important factor in the production of non-equilibrium chemical species and/or complex organic molecules. For this reason a microphone is suggested to investigate the frequency and magnitude of thunder. An RF click detector would extend the range of detectable electrical discharges to the order of several hundred kilometers.

E. Mission and System Science Performance Requirements and Tradeoffs

The implementation of the measurement performance requirements and instrumental techniques is discussed in detail in the following chapters. This section outlines some of the specific science mission and system requirements and tradeoffs that result from the measurement performance requirements.

1. Implications for Targeting

A targeting accuracy of about ±3° in latitude is required to ensure entry near the center of a belt or zone. While ± 10° in longitude is sufficient for the measurement purposes, a much closer tolerance would be desirable to minimize the entry flight path angle (and entry weight) while avoiding skipout.

In general, the desired light side entry within ±30° of subsolar requires steep entry angles for both Type I and Type II transfers (see Section IV) but the angles are shallower for a Type II. A light side entry (50° to 60° from subsolar) at shallow angles (-10° to -20°) can be achieved with a Type II but not with a Type I. Thus, the desired subsolar targeting implies a significant weight penalty for the heat shield and structure; an acceptable light side entry implies a Type II transfer (i.e., an increased mission time). The least penalty is obtained with a dark side entry (Type I and shallow entry angle). However, since a subsolar entry is required by only one observable and the associated weight penalties would degrade accomplishment of the other objectives, a light side entry near the terminator would be the best compromise.

The entry should be far enough from the evening terminator to allow the probe to descend well below the cloud tops before reaching 70° to 75° from subsolar. Figure IIIE-1 shows the time in sunlight versus entry longitude. The probe ballistic coefficient determines the depth of descent in a given time while the entry point determines the time in the sun. Thus, the entry point and ballistic coefficient can be matched to reach a desired depth while remaining within the required angle from subsolar. However, the ballistic coefficient must also meet several other requirements as discussed below.

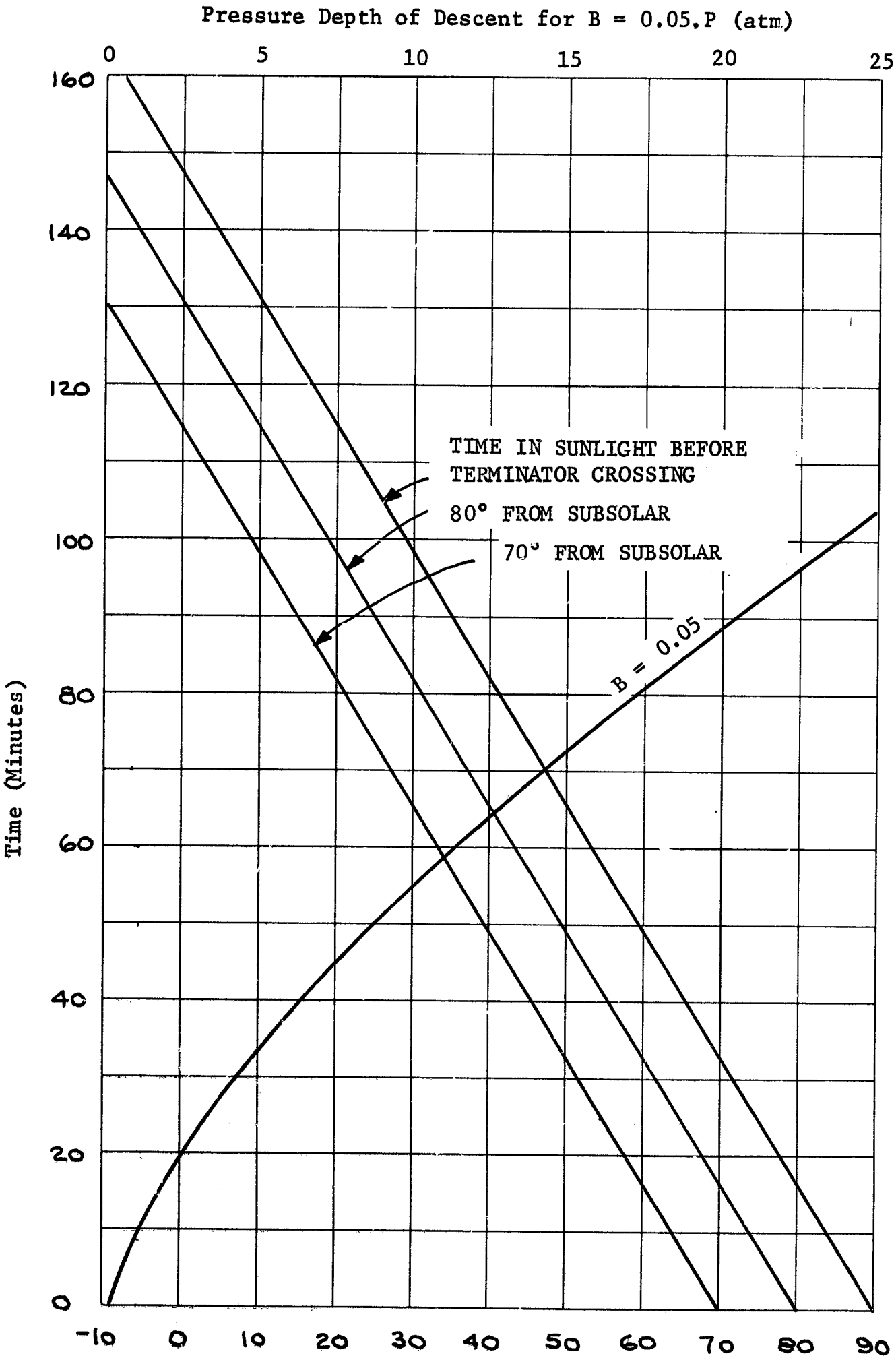


Figure IIIE-1

2. Implications for Probe Ballistic Coefficients

The effect of the descent probe ballistic coefficient (B) on the descent velocity and times to various pressure levels in the Nominal atmosphere is shown in Figures IIIE-2 and IIIE-3. The instrument capabilities, the required sampling intervals, and the required descent depths all influence the choice of B. The descent velocity should be well below Mach 0.5 to minimize instrumental effects. Since some instruments require a minimum integrating or sample processing time (e.g., 5 min for the GC/MS) the velocity should also be low enough to permit the required number of samples per scale height. In general, most science requirements point to the choice of a low ballistic coefficient (i.e., a parachute). However, practical considerations of the thermal control, power, and communications subsystems limit the allowable time for reaching a given depth. Depending on the mission details, the maximum time is on the order of 2.5 to 3.5 hours or less due to the large relay communications ranges and atmospheric attenuation. While it is possible to reach the 1000 atm level within 2.5 hours (with B >3), the velocity at the 1 atm level is so high ($v \gtrsim 400$ meters/sec) that the instruments cannot obtain the required altitude resolution (samples/scale height).

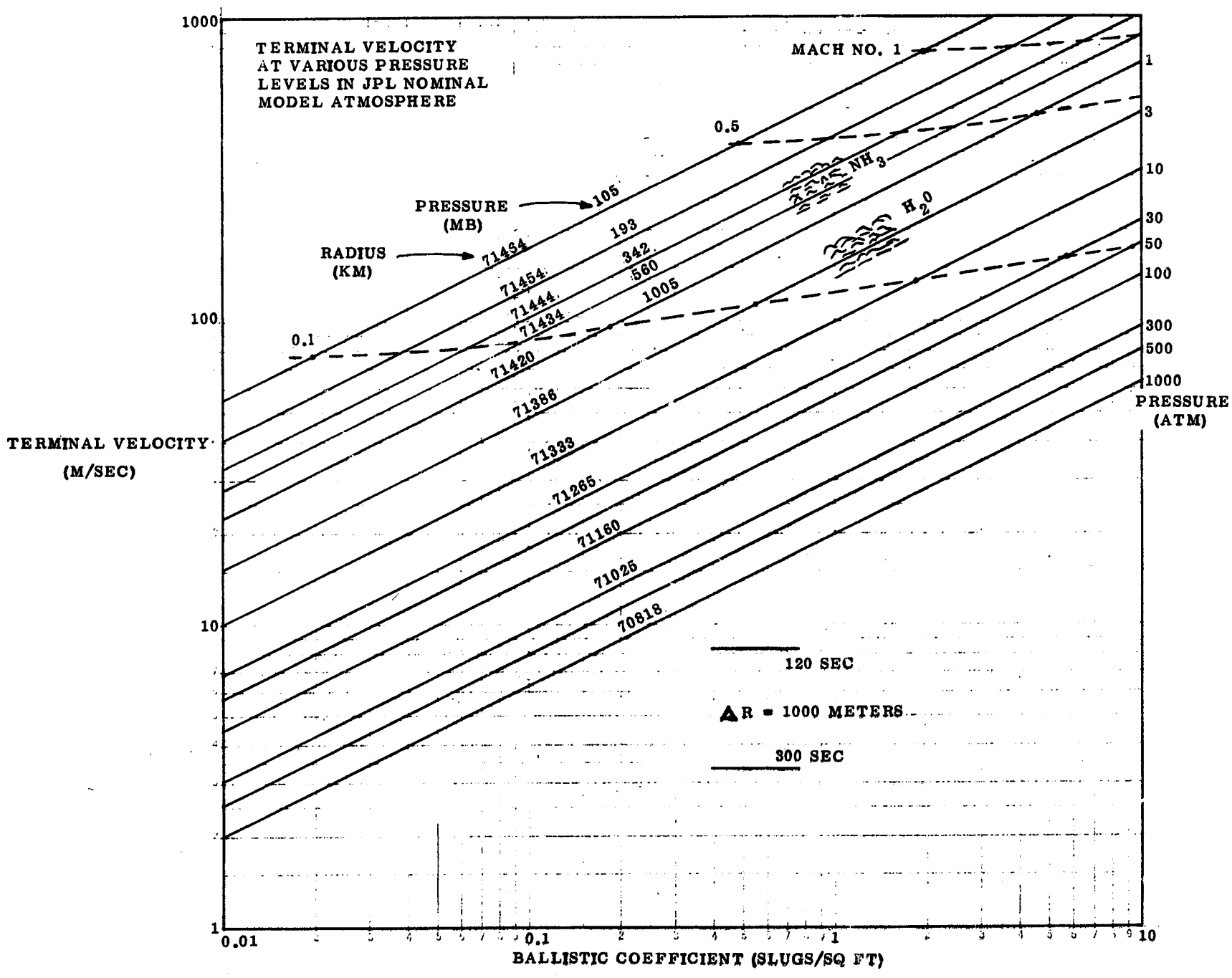


Figure IIIE-2

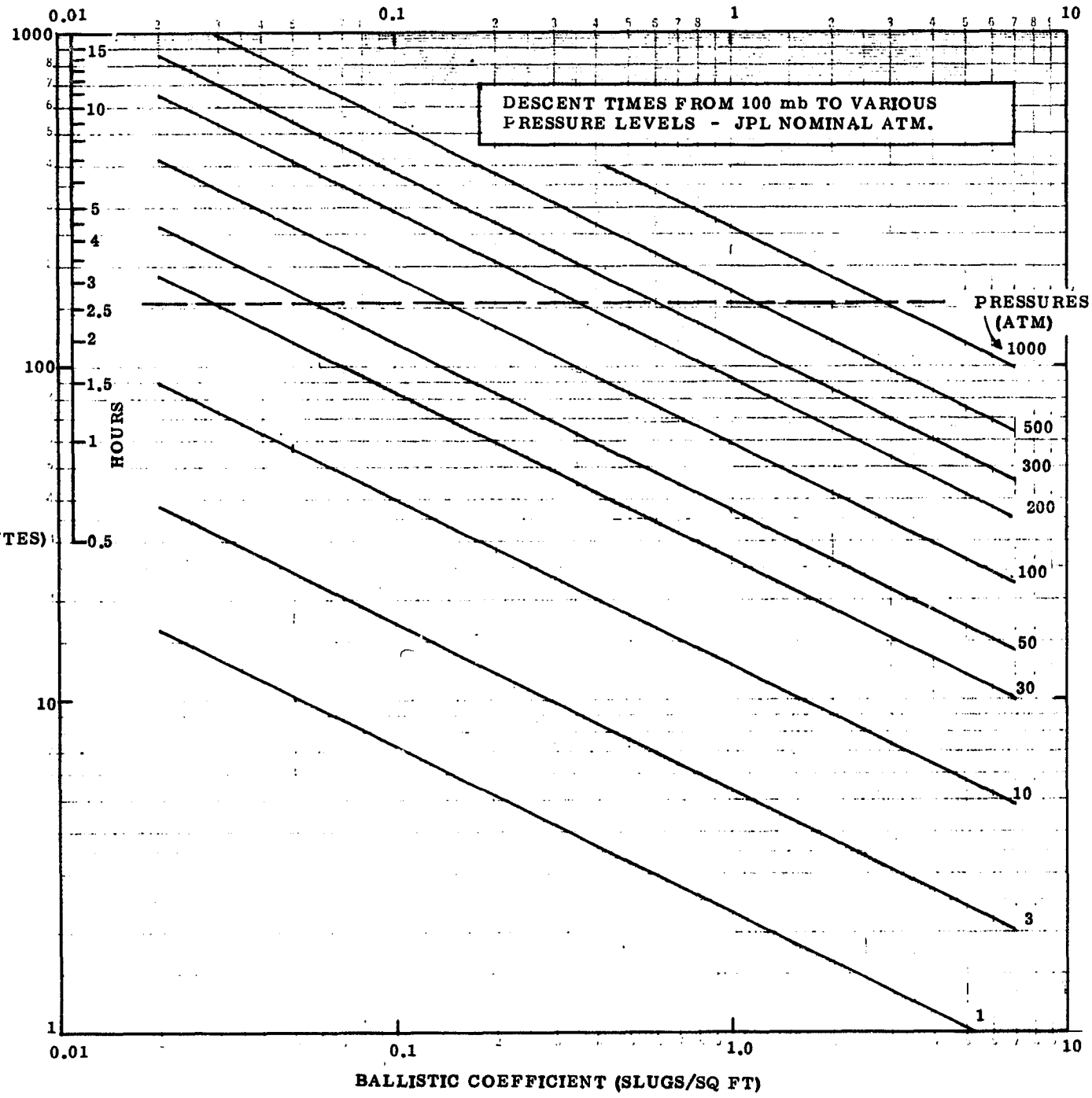


Figure IIIE-3

The GC/MS has the greatest impact on the selection of a ballistic coefficient which gives the required number of samples/ scale height at and below the one atmosphere level since it requires a long sample processing time ($\gtrsim$ 300 sec). The ballistic coefficient required to obtain 1, 2, and 5 samples per scale height at 5 min intervals as a function of pressure in the Nominal atmosphere is shown in Figure IIIE-4. Two samples per scale height are taken as the minimum acceptable since this would give measurements just above and just below the thinnest of the predicted cloud layers; 5 analyses per scale height would give a profile through a layer while one analysis per scale height might miss a thin layer. The requirement to obtain 2 samples/ scale height at the 1 atm level thus results in the choice of B = 0.05 slugs per square foot (i.e., a parachute). This is also a practical choice for meeting the requirements of the pressure-temperature, nephelometer, and other measurements; figure IIIE-5 shows the number of measurements per scale height versus ballistic coefficient for 5 and 10 second sampling intervals typical of temperature measurements.

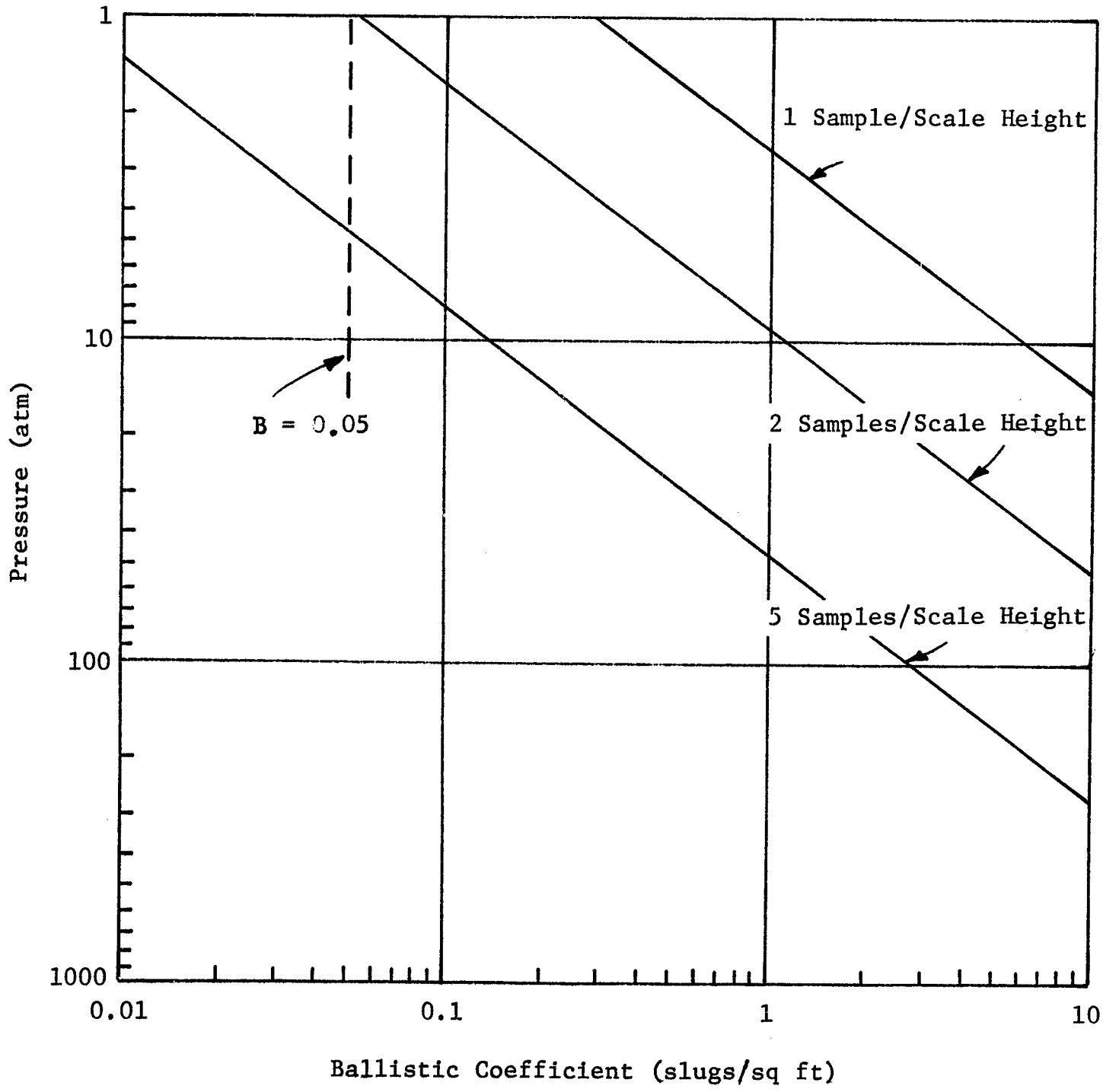


Figure IIIE-4 Ballistic coefficient required to obtain 1, 2, 5 samples per scale height with 5 minute GC/MS analysis time. Nominal model atmosphere.

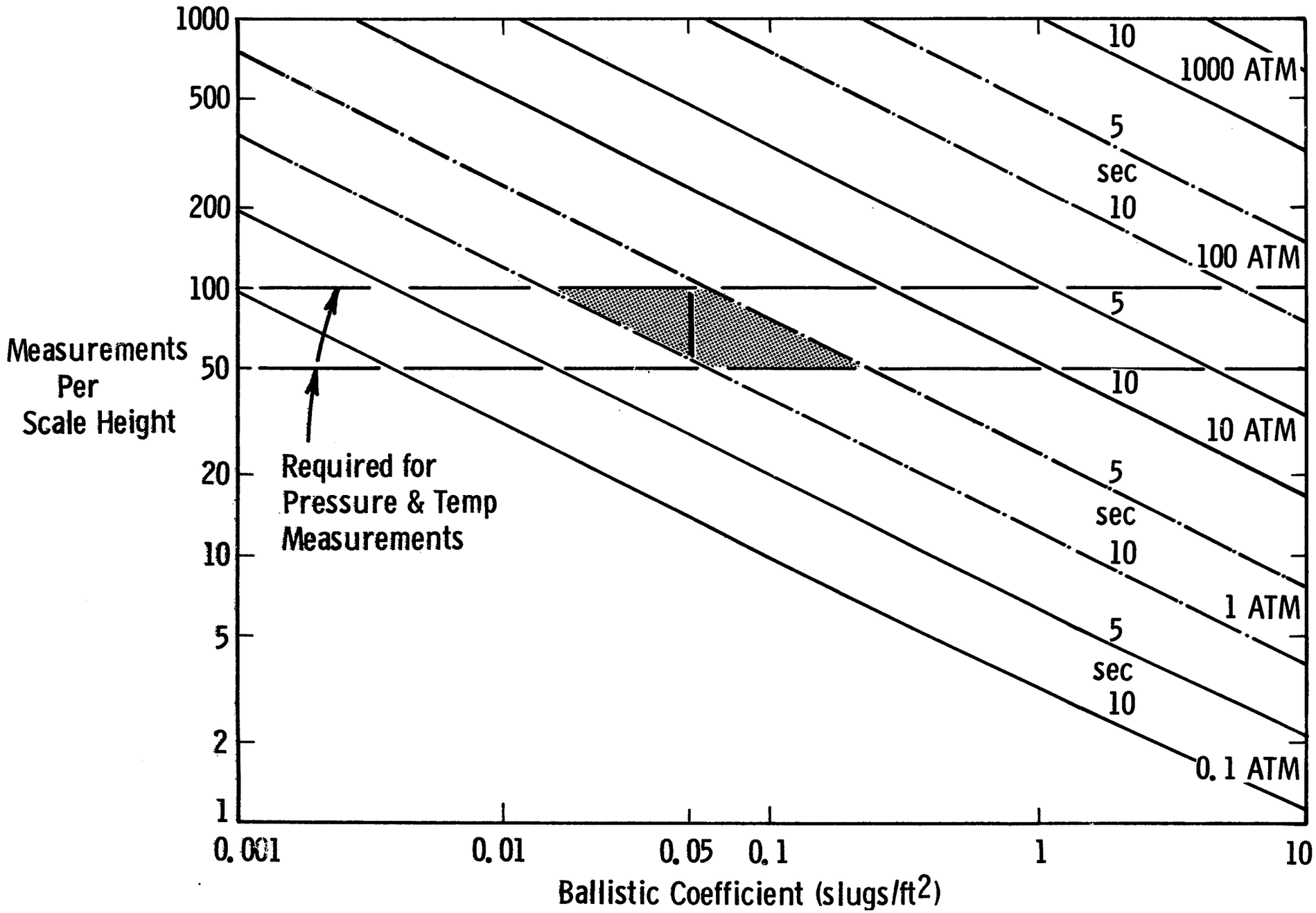


Figure IIIE-5 Measurements per scale height obtained with 5 and 10 sec time intervals.

Keeping a ballistic coefficient of 0.05 throughout the mission would only allow descent to about 45 to 70 atmospheres within 2.5 to 3.5 hours. However, since the probe velocity decreases as the pressure increases, the ballistic coefficient can be increased at lower levels. If it were practical to continuously increase the ballistic coefficient to keep the number of measurements per scale height constant as shown in Figure IIIE-4, the minimum descent time would be obtained. However, practical considerations limit the variation of ballistic coefficient to an upper (parachute) stage with B = 0.05 and one lower stage (aerodynamic fairings) with the ballistic coefficient and staging level chosen to minimize the descent time while always obtaining 2 or more samples per scale height with the GC/MS.

For purposes of the parametric studies, descent probes to final pressures of 50, 100, 300, 500, and 1000 atmospheres were examined. The second stage ballistic coefficients and staging altitudes which meet the minimum descent time and sampling interval requirements are summarized in Tables IIIE-1 and IIIE-2 and Figure IIIE-6. The minimum descent time to 50 atmospheres is obtained by staging at about 7 atm to a B of 0.7 slugs/sq ft. However, this requires a parachute for the second stage while a B of 1.1 slugs/sq ft does not. Therefore B = 1.1 was selected to eliminate the added complexity of a second parachute at a cost of only a few added minutes in mission time.

TABLE IIIE-1

DESCENT TIMES AND BALLISTIC COEFFICIENTS FOR STAGED PROBES TO VARIOUS PRESSURES

Final Pressure P_2 (atm)	1st Stage B(slugs/ft^2)	Staging at P_1 (atm)	Staging Time (Min.)	2nd Stage B(Slugs/ft^2)	Time From P_1 to P_2 (atm)	Total Time to P_2 (Min)
50	0.05	5	33	0.44	44	77
		6	38	0.56	38	76
		7	44	0.70	32	76
		* 10	55	1.1	23	78
100	0.05	* 10	55	1.1	56	99
		12	62	1.4	38	100
		15	72	1.9	31	103
300	0.05	10	55	1.1	103	158
		* 15	72	1.9	76	148
		20	92	2.8	60	152
500	0.05	15	72	1.9	110	182
		* 20	92	2.8	90	182
		25	106	3.70	76	182
		30	118	4.7	66	184

NOTE: Times are approximate, to within ± 1%, * Preferred combinations.

GROUND RULES: (1) Minimum descent times

(2) Obtain more than 2 samples per scale height at all levels below 1 atmosphere.

(3) No more than 2 ballistic coefficient stages

(4) Nominal Jupiter model atmosphere.

TABLE IIIE-2

SINGLE STAGED PROBE TO 1000 ATM

1st Stage B(sl/sq ft)	Staging at P_1 (atm)	Staging time (min)	2nd Stage B(sl/sq ft)	Time from P_1 to P_2 (min)	Total Time to P_2 (min)	Δ P when Sampling is less than criterion
0.035	10	66	3.5	133	199	14 (10 to 24 atm)
0.05	10 10	55 55	1.1 2.5	238 158	293 213	0 9 (10 to 19 atm)
	15 15	72 72	1.9 3.3	178 136	250 208	0 8 (15 to 23 atm)
	20 20	92 92	2.7 4.0	143 120	235 212	0 6 (20 to 26 atm)
	25 25	106 106	3.7 5.4	124 103	230 209	0 8 (25 to 33 atm)
Preferred →	30 30	118 118	4.8 7.0	108 90	226 208	0 10 (30 to 40 atm)
	35	130 130	5.8 8.6	98 80	228 210	0 12 (35 to 47 atm)

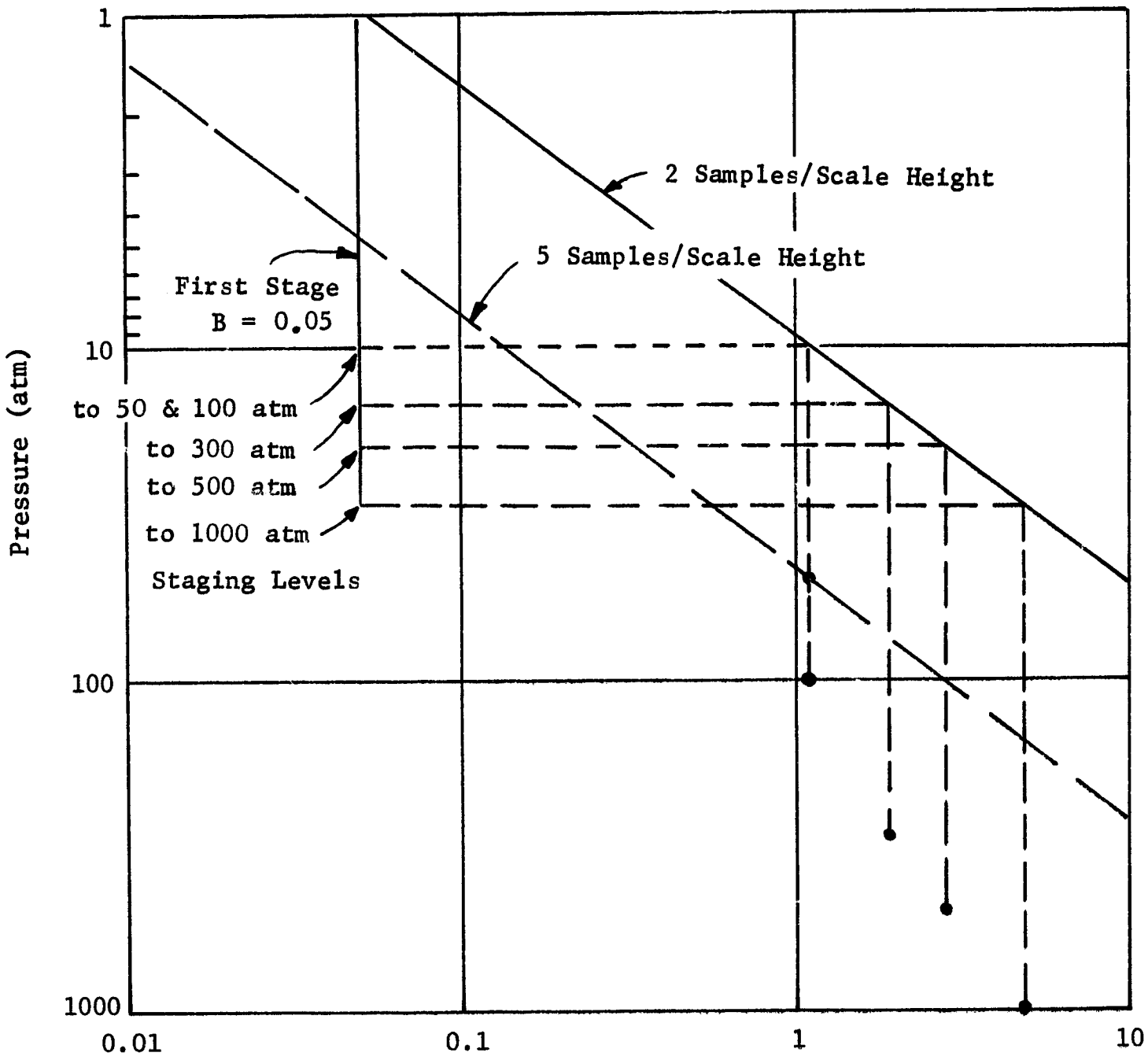


Figure IIIE-6 Staging levels and ballistic coefficients for staged probes to 50, 100, 300, 500, and 1000 atm.

A two stage descent to 1000 atmospheres requires a minimum time of about 225 minutes or 3.75 hours unless the sampling interval requirements can be relaxed as shown in Table IIIE-2. As discussed in Chapter IV, a "split" probe concept evolved to alleviate the communications and power problems associated with deep probes and/or relay spacecraft with large periapsis radii. The split probe concept also allows a strict adherence to the sampling interval criteria down to 1000 atm in reasonable times.

The "split" probe mission consists of two descent probes with different ballistic coefficients deployed simultaneously from the same entry vehicle at about 200 mb. The "upper" probe has a ballistic coefficient of 0.05 as for the single probe but acts as relay link for the "lower" probe which has a high ballistic coefficient, and hence, descends rapidly. The lower probe ballistic coefficient is chosen to obtain the required sampling intervals at the lowest depth reached by the upper probe. That is, if the upper probe descends to 10 atm, the lower probe should begin to obtain 2 samples per scale height there. The lower probe ballistic coefficients required to meet the sampling criteria are listed in Table IIIE-3. The minimum mission time allowed versus the lower probe depth is shown in Figure IIIE-7. As can be seen, a significant reduction in mission time (and hence relay communications range) is obtained. Figure IIIE-8 shows the descent profiles that reach the various levels in the minimum times permitted by the sampling interval criteria. Other sections discuss the other advantages and the disadvantages of the split probe concept.

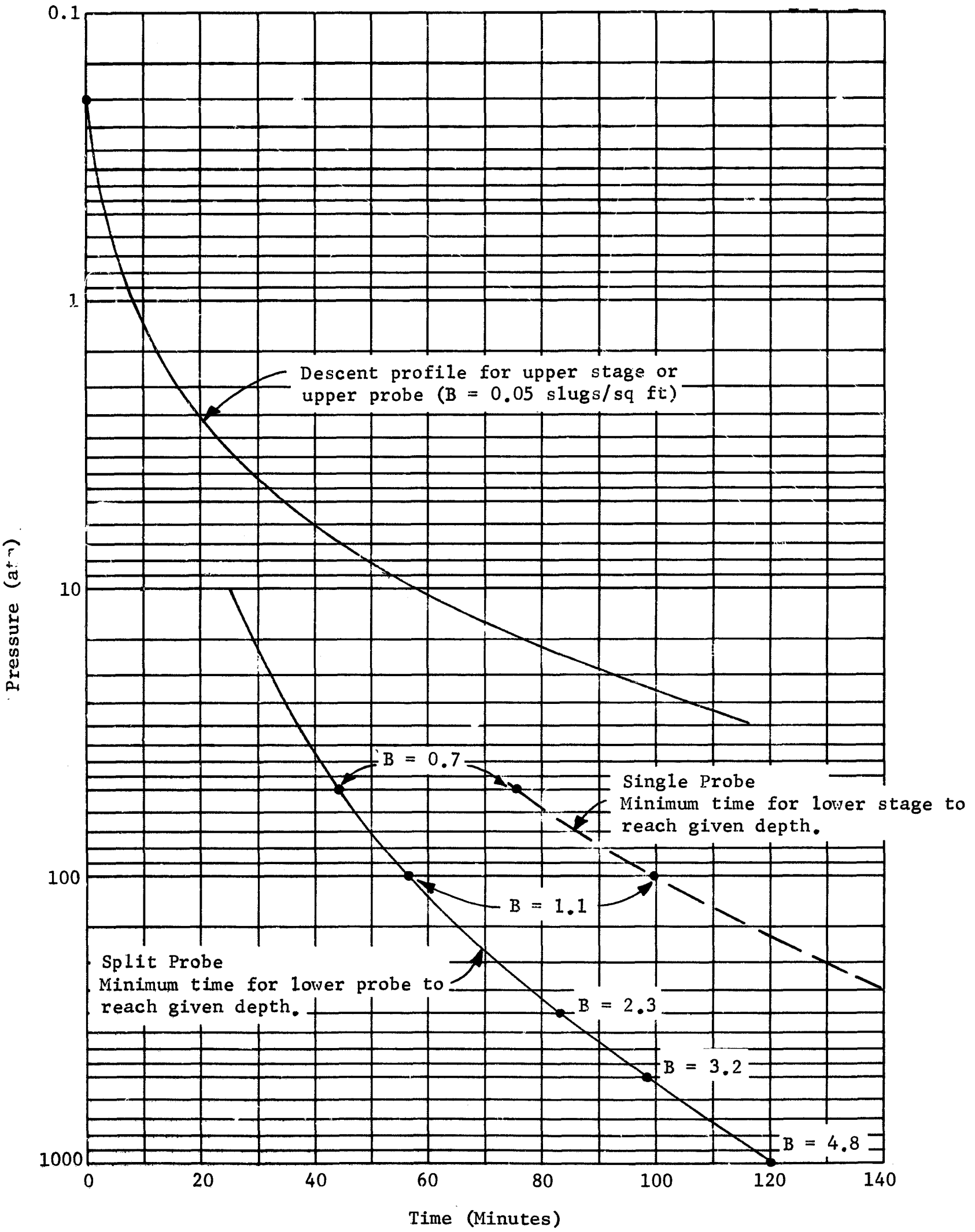


Figure IIIE-7 Minimum time to reach a given depth while meeting sampling interval criteria.

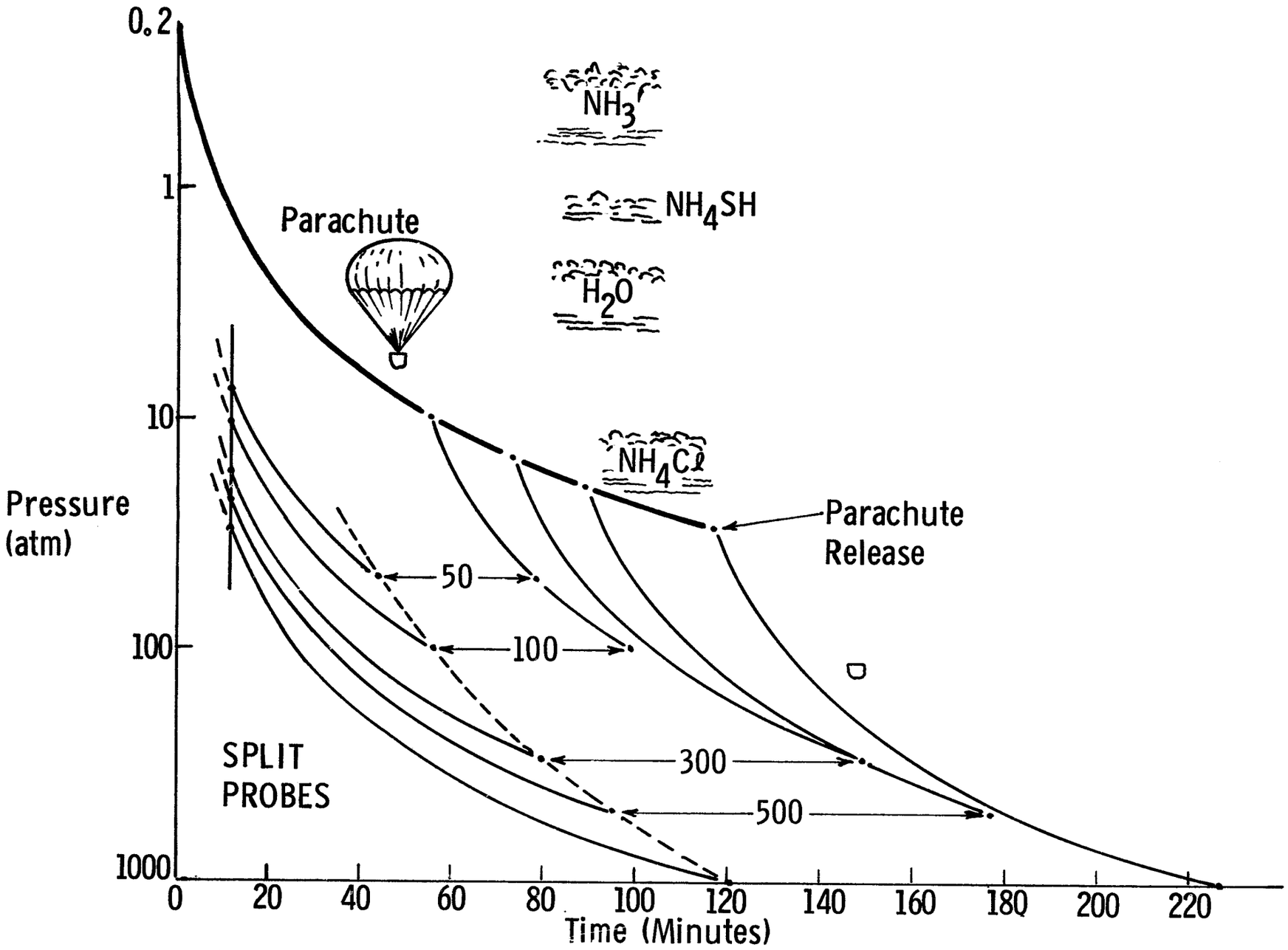


Figure IIIE-8 Parametric Study Descent Profiles
(See Tables IIIE-1 and IIIE-2 also)

TABLE LIIE-3

SPLIT PROBES TO VARIOUS DEPTHS

UPPER PROBE B = 0.05 SLUGS/FT^2

Lower Probe Final Pressure (atm)	Lower Probe B (slugs/ft^2)	Mission Time (min)	Upper Probe Final Pressure (atm)
50	0.7	44	7
100	1.1	56	10
300	2.3	80	17
500	3.2	95	22
1000	4.8	120	31

F. Science Payload Descriptions and Capabilities

This section describes the instrument payloads for the Baseline and two Sample missions (B and D). The Baseline or Nominal payload is that defined by JPL Section Document 131-07. It was used for the parametric mission studies and the design example mission in order to examine the feasibility and costs of obtaining measurements as a function of depth from 50 to 1000 atm. For Sample mission B, the Baseline payload was modified and expanded to maximize the accomplishment of the objectives. It represents the maximum payload considered in the study.

The minimum payload resulted from a desire to evaluate a reduced science capability, a minimum weight probe, and a potential for multiple probes. On review by several of our consultants, it was concluded that a single more capable Jupiter probe was preferred over reduced capability multiple Jupiter probes. However, the thought of utilizing the first probe at Jupiter and the second at a subsequent planet from a Grand Tour Spacecraft did evoke a measure of interest. In the minimum payload, the photometers and accelerometers are eliminated. The GCMS is replaced by a reduced range mass spec.

1. Nominal (Baseline) Payload

The Nominal or Baseline payload was described in Reference IIIF-1. The instrument characteristics are summarized in Table IIIF-1 and detailed instrument descriptions are given in Volume III, Chapter II. Since the Baseline parametric studies covered both single, staged and dual, split probes the payload compositions were modified accordingly. Table IIIF-2 summarizes the payloads for the staged and split probe types.

In the design example (Chapter VI), the Nominal payload is carried to 300 atmospheres with a single staged probe configuration. The 0.05 slugs/sq ft parachute is released at 15 atmospheres and the B = 1.9 slugs/sq ft probe descends to 300 atmospheres in 150 minutes (93 minutes in the Cool model). The instrument sampling times and resulting data rates are shown in Table IIIF-3. The number of measurements obtained per scale height vs pressure are shown in Figure IIIF-1 for both the Nominal and Cool models.

TABLE IIIF-1 BASELINE AND DESIGN EXAMPLE SCIENCE INSTRUMENTS

(Reference JPL Section Document 131-07)

Instrument	Weight (lbs.)	Power (watts)	Bits/Per Sample	Meas. Ranges	Meas. Accuracy	Usage	Remark
Pressure Sensors 3 sensors 2 sensors (range switched)	 1.2 0.8	 0.2 0.2	 8 8	 0.1 to 50 atm 30 to 1000 atm	 0.5% of fullscale	 Upper Lower	Diaphragm transducers
Temperature 4 ranges 2 ranges	 0.5 0.5	 0.2 0.2	 8 8	 100°K to 600°K 400°K to 1500°K	1% of range absolute 0.5% relative	 Upper Lower	Pt wire sensor
Accelerometers triad + one off c.g. Turbulence (2 axis)	 4.0 2.0	 4 2.0	 40 30	 1000 g's ± 5 m/sec^2	 0.1% F.S. 0.1% F.S.	 Entry only Upper	200 bps into storage for entry decelerations Turbulence average, maximum, frequency
GC/MS	7	12	600	0.1 ppm	±5% and ±20% of reading for major and minor gases	Upper Lower	300 sec minimum analysis time; gaseous constituents only.
Optical Flash Detectors (down & side) Absorption & Aerosol photometers	2	1	60	10^{-3} to 10^4 foot-candles dynamic range, 10^2	± 30% of reading ± 10% of reading	Upper Upper	
Ion Mass Spec	3	1	320	1 to 20 m/e 5 to 10^6/cm^3		Pre-entry	160 bps from 2 R_J

TABLE IIIF-2

BASELINE PARAMETRIC PAYLOAD WEIGHTS*

Instruments	Staged Probes	Split Probes	
	Upper and Lower	Upper	Lower
Pressure Sensors	2.0	1.2	0.8
Temperature Sensors	1.0	0.5	0.5
Accelerometers	4.0 turbulence	2.0 turbulence	(4.0)+ entry only
GC/MS	7.0	7.0	7.0
Photometers	2.0	2.0	-
Total descent Weight	16	12.7	12.3

*Ion mass spectrometer ejected at 0.1 g increasing

+CG of entry vehicle located inside lower probe so other accelerometers must be used for upper probe turbulence measurements.

TABLE IIIF-3

NOMINAL PAYLOAD DATA RATES

Instrument	Bits Per Sample	Sample Intervals (sec)		Bit Rates	
		0.2 to 30 atm	30 to 300 atm	0.1 to 30 atm	30 to 300 atm
Pressure	8	10	10	.8	.8
Temperature	8	10	10	.8	.8
Accelerometers	30	10	0	3	0
Photometers	60	2.5	0	24	0
GC/MS	600	300	300	2	2
Entry Accelerometer	20,000	-	-	30.6 2.0	3.6 28 (30 to 105 atm)
Data in Storage	(+6175)				0 (105 to 300 atm)
				32.6	31.6 (3.6)

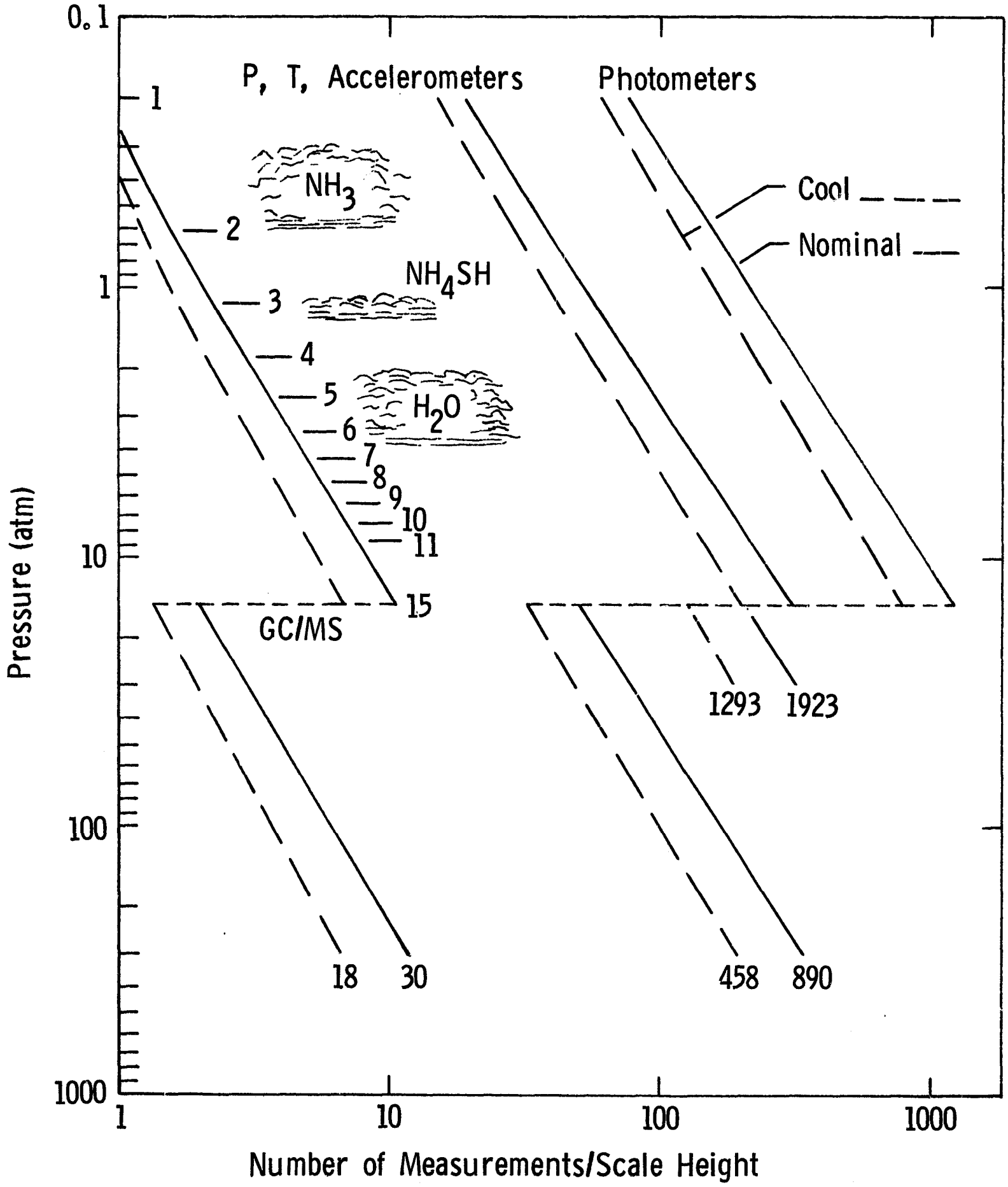


Figure IIIF-1 Measurement Profile for Design Example Mission with Baseline Payload

2. Sample Mission B (Expanded) Payload

The expanded payload is shown in Table IIIF-4. The addition of several GC columns (see Section D above) and a cloud particle collector increases the capability for analyzing complex molecules and gives a definitive H/D/He analysis. The photometers of the nominal payload are replaced by: (1) A nephelometer with color filters to determine the presence of cloud material and its color independent of solar radiation; (2) Visual photometers to determine the solar flux attenuation with depth; (3) 5μ and 10μ IR radiometers to give more information on the cloud layering and to determine the relative ambient temperature; and (4) an RF lightning detector and microphone to provide information on the influence of electric discharges and shock waves on the formation of complex molecules.

The number of measurements per scale height obtained with each of the instruments is shown in Figure IIIF-2 for the sample mission B descent profile.

TABLE IIIF-4

SAMPLE MISSION B (Expanded) PAYLOAD

Instrument	Weight	Power	Bits Per Sample	Time (sec)	Bit Rate bps
Expanded GC/MS	14	20	1200	300 (300)	4 (4)
Pressure	1.0	0.5	10	5 (10)	2 (1)
Temperature	0.75	0.5	10	5 (10)	2 (1)
Nephelometer (3 color filters)	4	3	30	5 (5)	6 (6)
Visual Photometers (3 channel)	0.75	0.5	30	5 (∞)	6 (0)
IR radiometers (5 & 10 , downlooking)	3	2.5	30	5 (5)	6 (6)
RF lightning Detector & Microphone	1.5	1.0	40	40 (40)	1 (1)
Accelerometers (turbulence)	2.0	2.0	30	10 (∞)	3 (0)
	27	30			30 (19)

NOTE: ( ) indicates possible bit rate change below 10 atm; this was not necessary for sample mission B.

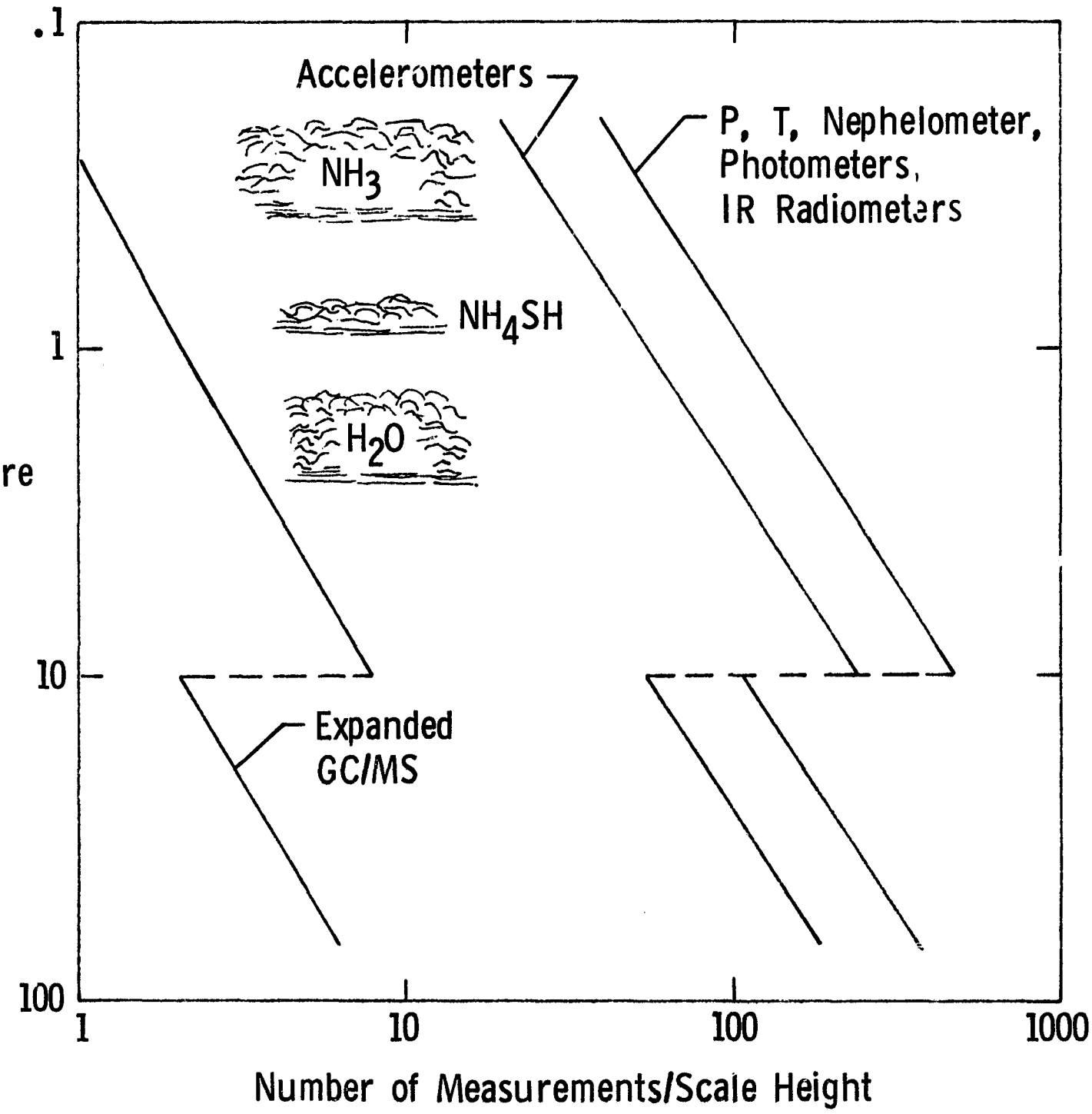


Figure IIIF-2 Measurement Profile for Sample Mission B Expanded Payload

3. Sample Mission D (Contracted) Payload

This payload was defined to be compatible with missions having a limited payload and/or depth capability. It would be suitable for mission with limited capability at Jupiter (one small probe) or for a Grand Tour mission with the capability to deposit one small probe at two or more of the Outer planets. The group of instruments shown in Table IIIF-5 attack the most important questions concerning the Outer Planets. Namely, the H/He ratio, the pressure-temperature structure, and the cloud structure and composition. While there is no direct cloud composition measurement, the composition might be inferred from the pressure and temperature at which the aerosol appears to be condensing. The NH_3 and H_2O clouds might also give an increase in the H fractions in the mass spectrometer.

As used for sample mission D, the mini payload is carried to 18.6 atmospheres in one hour on a probe with B = 0.1 slugs/sq ft. This results in the measurement profile shown in Figure IIIF-3.

TABLE IIIF-5

SAMPLE MISSION D (Contracted) PAYLOAD

	Weight (lbs.)	Bits Per Sample	Sample Time (sec)	Data Rate bps
Mass Spectrometer (1 to 4 amu + ≥ 5 amu)	3.5	60	60	1
Pressure	1.5	10	5	2
Temperature	1.0	10	5	2
Nephelometer	4	30	5	6
	10.0			11

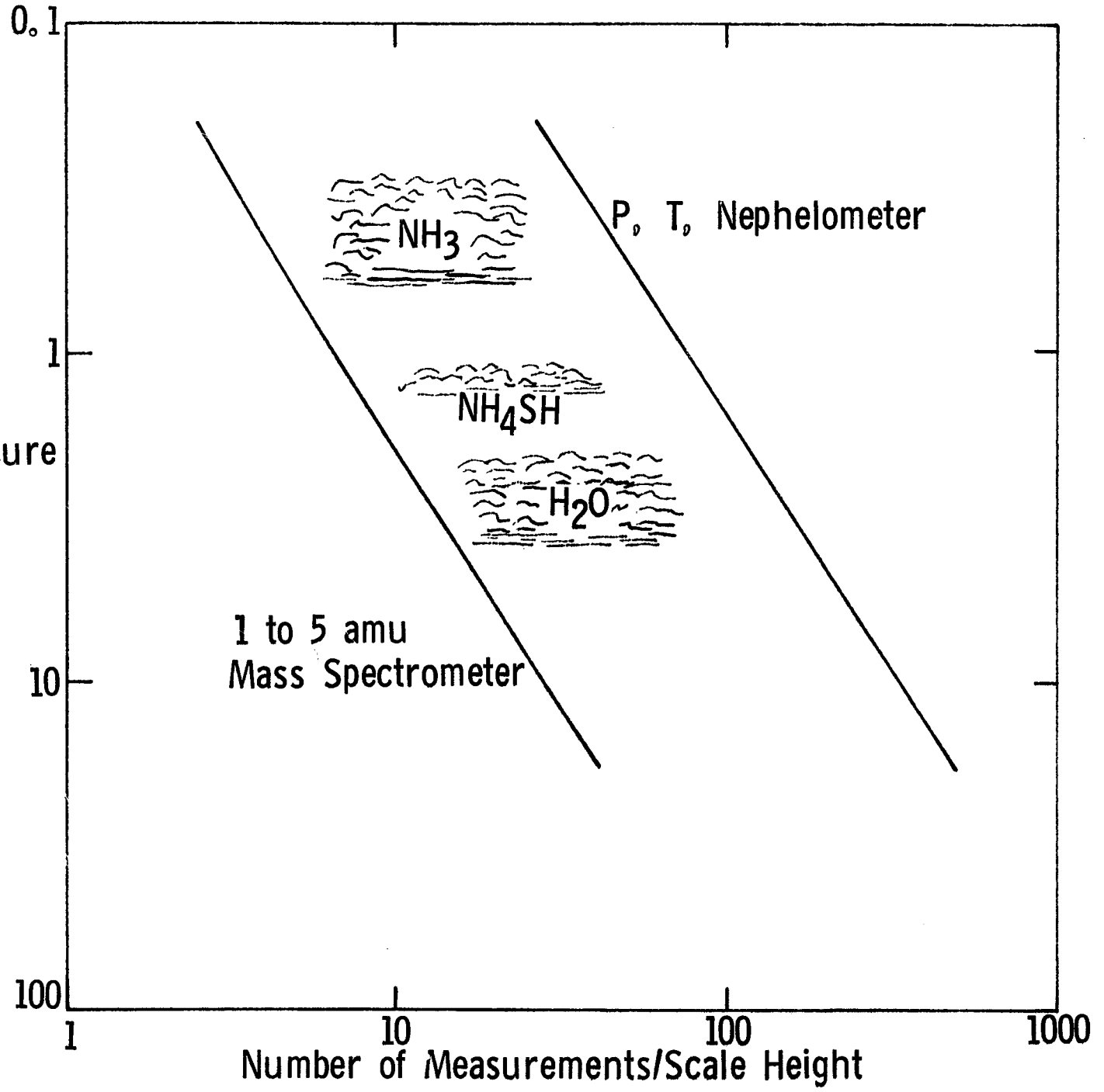


Figure IIIF-3 Measurement Profile for Sample Mission D Mini Payload

REFERENCES

IIIB-1. *The Outer Solar System. A Program for Exploration.* Report of a Study by the Space Science Board, National Academy of Sciences, June 1969.

IIIB-2. *Scientific Questions for the Exploration of the Terrestrial Planets and Jupiter.* JPL TM33-410. October 1, 1968.

IIIF-1. *Science Criteria for Jupiter Entry Missions.* JPL Section Document 131-07. December 31, 1969.

IV. MISSION CONCEPT EVOLUTION

The mission and engineering system concepts evolved from three fundamental considerations. The first is the study requirement for in situ measurements within the atmosphere of Jupiter. The second is the extreme distance between Jupiter and Earth which results in major demands on launch energy, and communications system capability. The third is a composite of the effects of Jupiter's high gravity field, rapid rotation rate and severe attenuation of radio signals by the atmosphere.

The design for in situ measurements within the atmosphere is bounded by the depth required to answer the science questions versus the engineering feasibility of penetrating to sufficient depths to accomplish those measurements. Although the science questions in effect imply the deeper the better, the major questions can be satisfied by penetrating through the bottom of the primary cloud layers or about a pressure level of 5 to 50 atmospheres in the nominal atmosphere model and 100-300 atmospheres in the cool model. However, in order to establish a broad range of engineering trades, depths to 1000 atmospheres were included.

The extreme distances between Jupiter and Earth result in large space losses in the communications link and requirements for large launch energies. Launch vehicle capabilities up to that of the Titan IIID/7 segment solid/ Centaur/Burner II were within the study constraints resulting in payloads of the order of 2000 lbs.

In addition to the communications system space loss, the Jupiter atmosphere attenuates the signals from the probe as it descends. Also, the rapid rotation of Jupiter carries the atmospheric probe through a large aspect angle, thus further attenuating the signal as the probe antenna pointing angle varies away from zero or from the receiver.

The planetary environment, in addition to attenuating the communications signals through atmospheric and planet rotation effects, has two other major influences on probe engineering design. The first is the design penalty incurred during the extremely severe entry and the second is the design penalty incurred protecting the descent probe equipment from the high pressure and temperature encountered during the terminal descent phase.

The following sections of this chapter describe the evolution of mission and engineering design concepts which provide feasible system design options for a Jupiter atmospheric entry mission. The environmental models of Chapter II and the science criteria of Chapter III provide the basis for the engineering design requirements. Section A discusses the Navigation and Trajectory evolution, Section B discusses the Engineering Concept evolution, Section C discusses the Engineering Experiment Rationale, and Section D discusses the Mission Effectiveness studies.

A. NAVIGATION AND TRAJECTORY EVOLUTION

This section of the report presents the development of mission definitions and the evaluation of the knowledge and control uncertainties associated with these missions. The parametric analyses of the constraints and mission design choices are presented in Section III of Volume III and significant results are summarized in the following paragraphs. The evolution of the Design Example Mission is described as being representative of the processes leading to any mission definition.

The mission design parameters and their principal influence on navigation and trajectory evolution are shown in Table IVA-1. The atmospheric descent portion of the mission is established to meet the science requirements for data sampling and as a consequence is not considered an independent mission parameter. The booster constraints of launch period and declination of the launch asymptote, DLA, restrict the launch and arrival dates slightly and result in a requirement for variable arrival dates. The variable arrival dates, in turn, result in a communication requirement to consider ranges greater than 5 AU and generally approaching a maximum value of near 6.4 AU.

The spacecraft (TOPS or PIONEER) is a factor in booster selection from the standpoint of weight. The spacecraft also influences relay communications link geometry according to its ability to point the antennas.

The science requirement for light side entry is a factor in the selection of Type I or Type II trajectories. Type II trajectories yield light side entry at smaller entry path angles than Type I. Type II trajectories also exhibit more payload capabilities than Type I. However, the Type I paths are on the order of 18 months shorter in duration than the Type II paths.

The mission year affects the payload for single planet missions. The 1978 launch opportunities exhibit smaller payload capabilities than the later years of 1979 and 1980-81. In multiple planet flyby missions the launch year affects the periapsis radius, R_p, that can be reasonably achieved. Entry dispersions and deflection velocity increment increase with increasing R_p of the spacecraft. The relay link communication range is increased and aspect angle variations are reduced. The communications

TABLE IVA - I MISSION PARAMETERS

PARAMETER	SIGNIFICANCE WEAK	AVERAGE	STRONG	AREAS AFFECTED IN THIS STUDY
Launch Period		x		Payload, Launch and Arrival Dates, Variable Arrival Geometry, Communications Range
Minimum DLA	x			None
Maximum DLA	x			Payload, Launch and Arrival Dates
Spacecraft		x		Payload, Booster Selection, Communications Geometry
Science (light-dark)		x		Type I, Type II
Trajectory Type (I, II)		x		Payload, Mission Duration, Lighting, Entry Angle
Launch Year			x	Payload, R_P
Launch and Interplanetary Navigation	x			None
Velocity at Encounter ($V/_{HP}$)	x			None
Post Encounter Objectives			x	Payload, R_P
Periapsis Radius			x	Accuracy, Communications, ΔV_{EJ}
Deflection Radius	x			ΔV, Lead Time Errors ($10^7 < R_{EJ} < 4.8 \times 10^7$)
Lead Time			x	Communications Geometry
Entry Path Angle			x	Probe Weight, Accuracy, ΔV_{EJ}, Communication Geometry
Deflection Accuracy			x	Communications System, Minimum Entry Path Angle

time is generally reduced for a relay link as the R_p increases.

Launch and interplanetary navigation and the study of midcourse correction strategy was not a part of the Jupiter probe study and therefore was not a factor in the mission design. Studies of the probe deflection maneuver indicate that the implementation errors dominate the picture and navigation errors may be neglected in the Jupiter missions.

The encounter geometry includes the V_{HP}, B, R_p, and the direction of approach. Factors affecting R_p (and B) have been noted above. The magnitude of the V_{HP} has little effect on the mission design. The direction of approach is a function of trajectory type and is established by requirements for light during entry and limits on the entry path angle.

The deflection maneuver is perhaps the most important mission phase other than the actual scientific portion of the mission. The deflection maneuver achieves the proper probe entry conditions and establishes the desired probe-spacecraft relative geometry for relay communications. The deflection maneuver radius is not a major factor; controlling only the magnitude of the maneuver velocity and affecting the lead time dispersions slightly. However the maximum radius should be less than the Sphere-of-Influence radius (approximately 4.8×10^7 km) for accuracy and greater than 10^7 km to maintain reasonable velocity increments. The requirement for the angle between the Earth-Sun line and the Earth-spacecraft line to be greater than 15° for good communications limits the encounter geometry and can influence the choice of deflection radius as noted in the discussion of the Design Example Mission.

The parameters of velocity increment and deflection angle are dependent on the mission requirements and geometry and as such are not independent variables but are calculated to give the desired result when all other constraints have been imposed.

The communication geometry results from a combination of lead time and R_p. The best compromise of total time, aspect angles and range comes when the spacecraft passes directly over the probe at periapsis passage and the R_p is about 2 Jupiter radii. The average angular rates of both the probe and the spacecraft are matched. If lead time is too great then the planet rotation will take the probe beyond the horizon before a reasonable communication link time has elapsed and range at entry will be large.

If the lead time is too short then the range and aspect angles grow too rapidly and short communication periods result. Large negative lead times are not usable for communication relay patterns because the spacecraft is beyond the probe when the essential data is collected.

Now consider the Design Example Mission and the mission design processes that must be followed to evolve an effective mission.

Entry and Descent

The mission definition starts with a definition of the science objectives and necessary descent profiles to collect the data desired. The methods and results of this procedure are discussed in Chapter III. These descent profiles have no real impact upon the initial mission parameters beyond indicating an altitude at which staging must be achieved. Then the required entry ballistic coefficients and range of entry angles can be selected to achieve this initial staging.

To experience the smallest impact of the aerothermodynamic environment, the entry is achieved with the planetary rotation and at the smallest possible angle commensurate with accuracy, communications geometry and lighting requirements. A minimum entry angle of -10 deg is assumed to allow for dispersions and avoid skipout. The upper limit is set at about -50 deg to avoid excessive weight penalties for the deflection system and environmental protection. This range of entry angles also reduces the problems associated with initial staging. These limits are iterated throughout the study to improve accuracy, communications geometry and mission achievement.

Targeting of the entry point influences the possible entry angles. If daylight during entry and for the first hour of descent is desired the entry site must be 56.57 deg from the terminator. This assumes that sufficient lighting angles exist only up to 70° from the subsolar point.

From Figure IVA-1 it can be seen that the likely Type II arrival dates fall between November 1981 and October 1982 while likely Type I arrivals fall between May 1980 and August 1981. Requirements for launch period will extend the arrival dates over most of this range. Then, utilizing Figure IVA-2, the direction of the V_{HP} vector can be shown to fall between 50 deg on the dark side and the terminator for Type I paths and between 7 deg

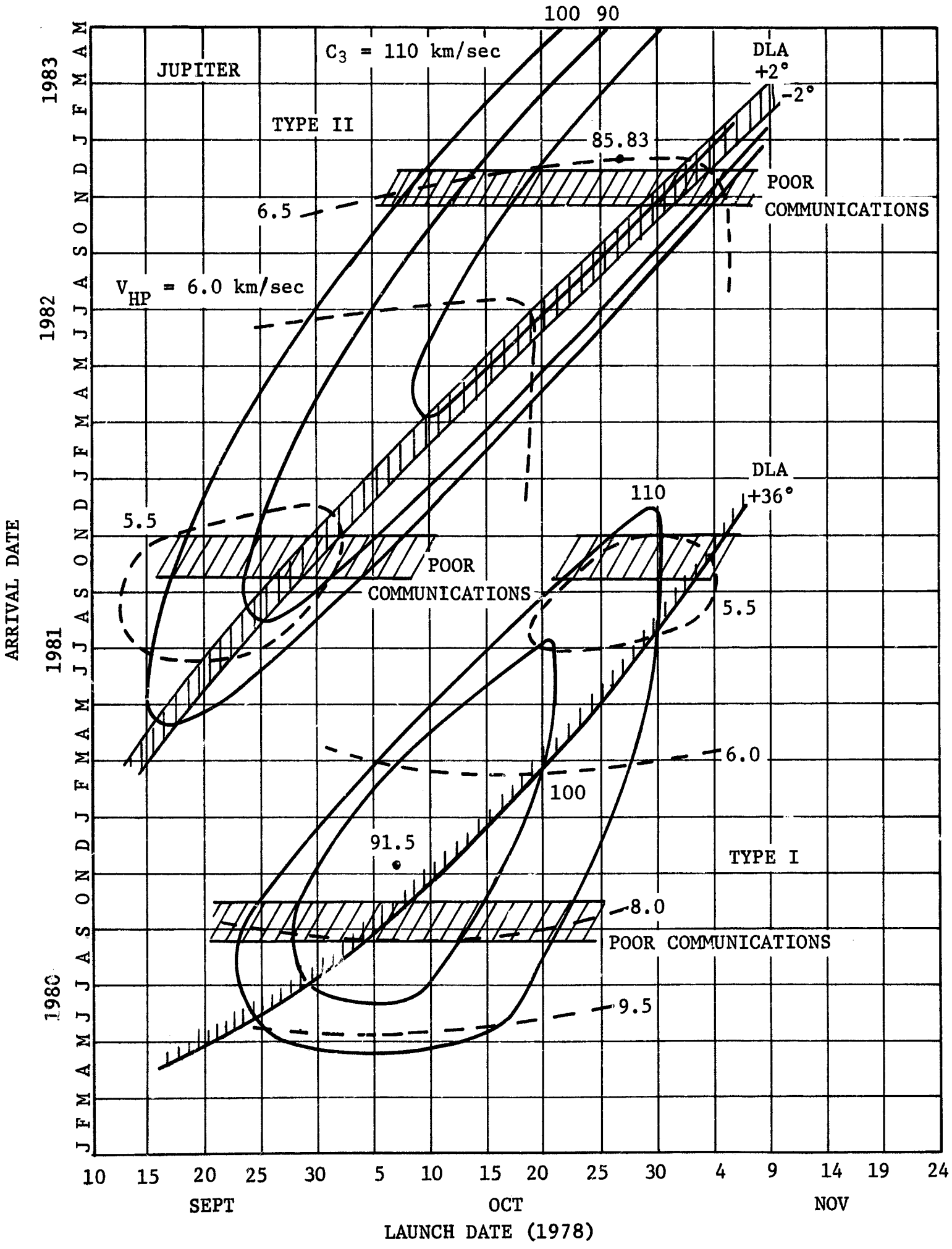

JUPITER
TYPE II
C_3 = 110 km/sec
V_{HP} = 6.0 km/sec
100 90
DLA
+2°
-2°
85.83
6.5
POOR
COMMUNICATIONS
110
DLA
+36°
5.5
POOR
COMMUNICATIONS
5.5
6.0
100
91.5
TYPE I
8.0
POOR COMMUNICATIONS
9.5
1983
1982
1981
1980
J F M A M J J A S O N D J F M A M J J A S O N D J F M A M J J A S O N D
ARRIVAL DATE
10 15 20 25 30 5 10 15 20 25 30 4 9 14 19 24
SEPT
OCT
NOV
LAUNCH DATE (1978)

Figure IVA-1

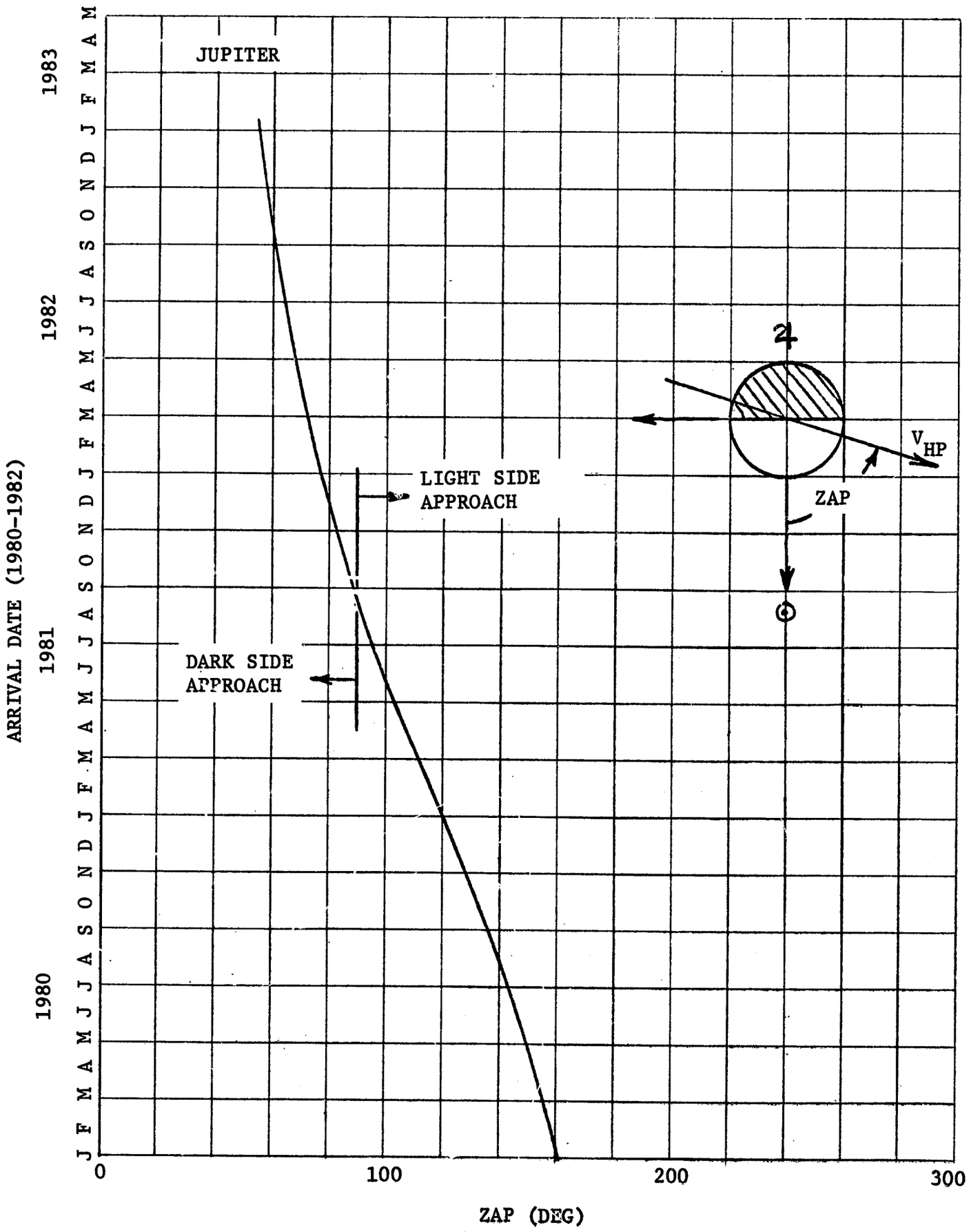

JUPITER
LIGHT SIDE
APPROACH
DARK SIDE
APPROACH
ZAP
V_{HP}
ARRIVAL DATE (1980-1982)
1980
1981
1982
1983
J F M A M J J A S O N D J F M A M J J A S O N D J F M A M J J A S O N D J F M A M
0
100
200
300
ZAP (DEG)

Figure IVA-2

into the light side and 33 deg into the light side for Type II paths. Adding for Type I or subtracting for Type II the 56.57 deg mentioned above puts the entry point between 56.57 deg and 106.57 deg from the direction of the V_{HP} for Type I paths and 49.57 and 23.57 deg from the direction of the V_{HP} for Type II paths. Therefore the entry angles which are a function of displacement from the V_{HP} (Figure IVA-3) will be between -24 deg and -48 deg for the Type I path and a minimum of 1 hour of daylight descent time and between -7 deg and -20 deg for Type II. On this basis a Type II path with a -20 deg entry angle has been selected for the Design Example. The -20 deg entry angle also is associated with the earliest arrival date in the window and must be the design condition if a significant launch period is to be considered. Other launch years considered will yield similar results.

Encounter and Deflection

The encounter geometry is a result of the path selected for lighting and the launch period requirements. As noted above the Design Example arrival dates fall between November 1981 and October 1982. From Figure IVA-1 it can be determined that a reasonable payload capability (C_3 = 100 km^2/sec^2) for these arrival dates requires that the launch dates fall between September 25 and November 2, 1978 permitting 20 to 30 day launch periods. A nominal September 25, 1978 launch and November 4, 1981 arrival is considered for the Design Example. The launch and arrival geometry for this mission is shown in Figure IVA-4. It should be noted that at entry the Earth is a full 15 deg past conjunction and acceptable communications exist. However some portion of the coast from deflection to entry will occur out of sight of the Earth. A constraint then is imposed on the deflection maneuver if it is to be seen from Earth. The deflection maneuver must occur 30 deg or about 30 days before entry. Also the maneuvers should occur within the sphere of influence or less than 81 days before entry. A radius of deflection of 2.6×10^7 km is safely more than 30 days prior to entry and within the sphere of influence. Adjusting the arrival date while considering the requirements of payload and launch period will obviate this deflection radius consideration for the nominal launch date. However, since arrival dates vary by nearly a year the problem will come up again late in the launch period.

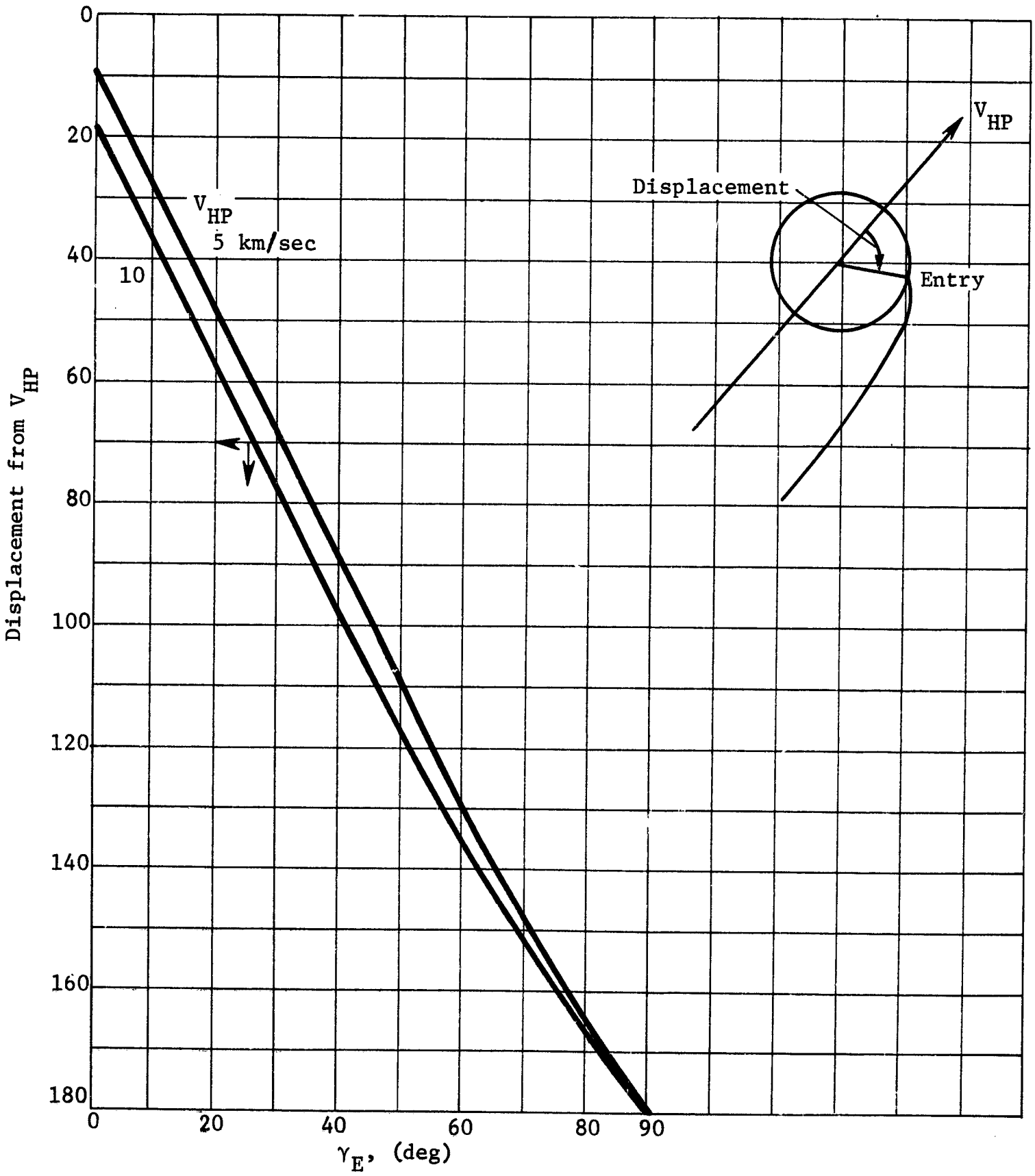

0
20
40
60
80
100
120
140
160
180
Displacement from V_{HP}
V_{HP}
5 km/sec
10
V_{HP}
Displacement
Entry
0
20
40
60
80
90
γ_E, (deg)

Figure IVA-3

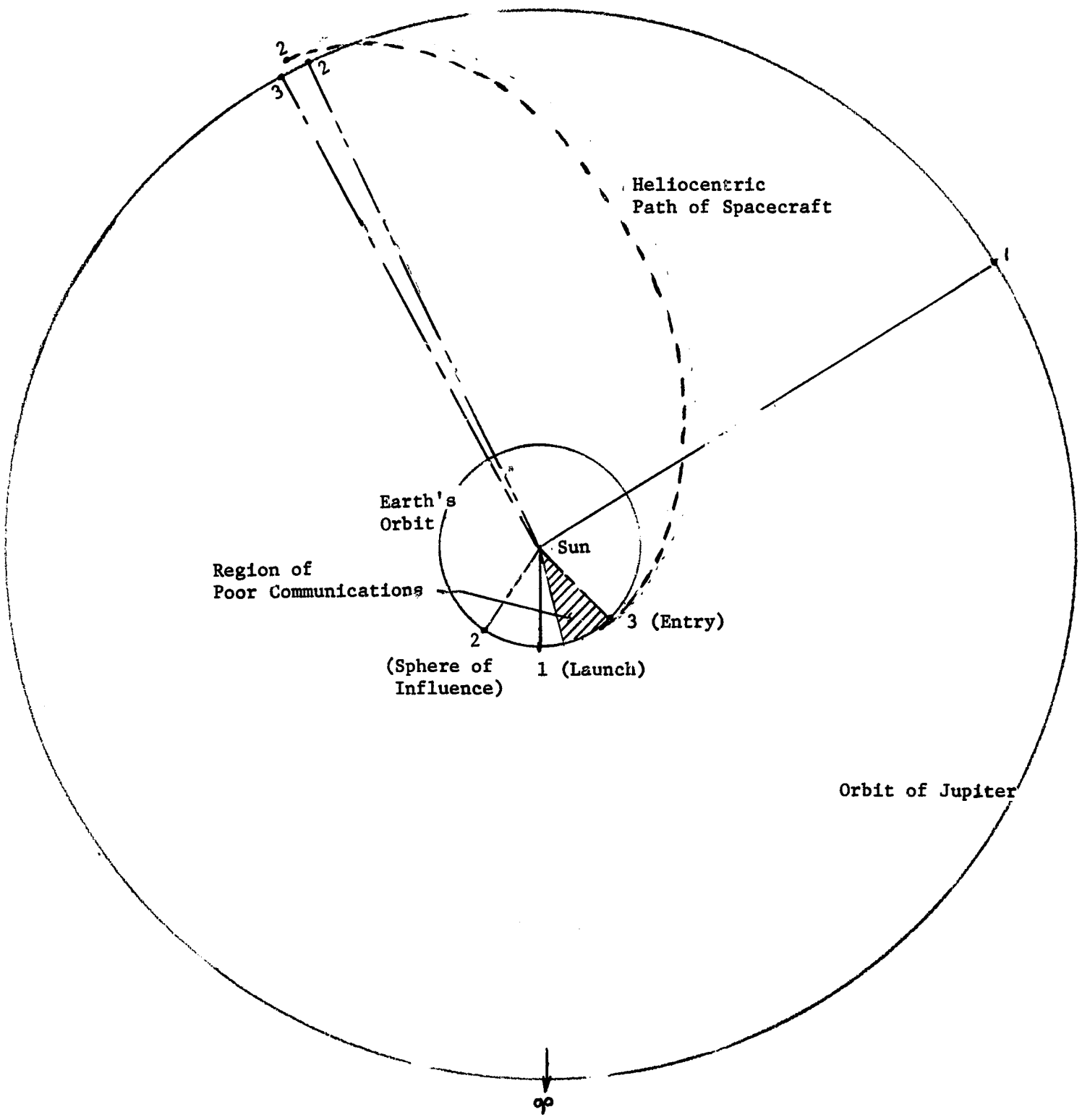


Figure IVA-4 Mission Geometry

To yield good communications geometry for 1-2 hours after entry the periapsis radius should be near 2 Jupiter radii and the spacecraft should be over the probe at periapsis passage. The deflection parameters of velocity increment and application angle are calculated to yield this geometry and achieve the -20 deg entry angle specified earlier for lighting. Figure IVA-5 presents this geometry. The trade-offs resulting in this optimization are discussed in Section III of Volume III and the parameters include range, range rate, first derivative of range rate, probe aspect angle history and spacecraft aspect angle. No constraint on spacecraft antenna pointing is considered.

Utilizing a Pioneer spacecraft instead of a TOPS applies an additional constraint to the relay link goemetry. If the spinning spacecraft is equipped with simple antennas the pointing area is severely restricted. In this case the probe is sent well ahead of the spacecraft and reduced mission time is accepted. Higher entry angles result as a consequence of achieving the best possible relay link.

Navigation and Accuracy

From the parametric data of Section III Volume III it has been concluded that navigation errors and uncertainties in Jupiter's gravitational constant can be ignored. Spacecraft on-board sensors contribute nothing to this mission under the assumption that navigation errors are minor factors. Errors in the radius of the atmosphere affect the entry angle dispersions but do not influence the communication geometry. The deflection errors, then, are the dominant quantities. These deflection errors (3σ) cannot be larger than 1% proportionally and 1.5 deg pointing or the communications dispersions become unmanageable. Larger deflection errors can be handled from the entry path angle aspect by increasing the nominal angle but this does not improve the communication geometry dispersions. With these deflection errors the -20 deg entry angle can be achieved to a high level of probability and the other aspects of the mission appear workable.

At periapsis radii greater than 2 Jupiter radii the minimum entry angle increases. At periapsis distances of 6.8 Jupiter radii the minimum entry angle for 1% proportionality and 1.5 deg pointing errors is -15 deg.

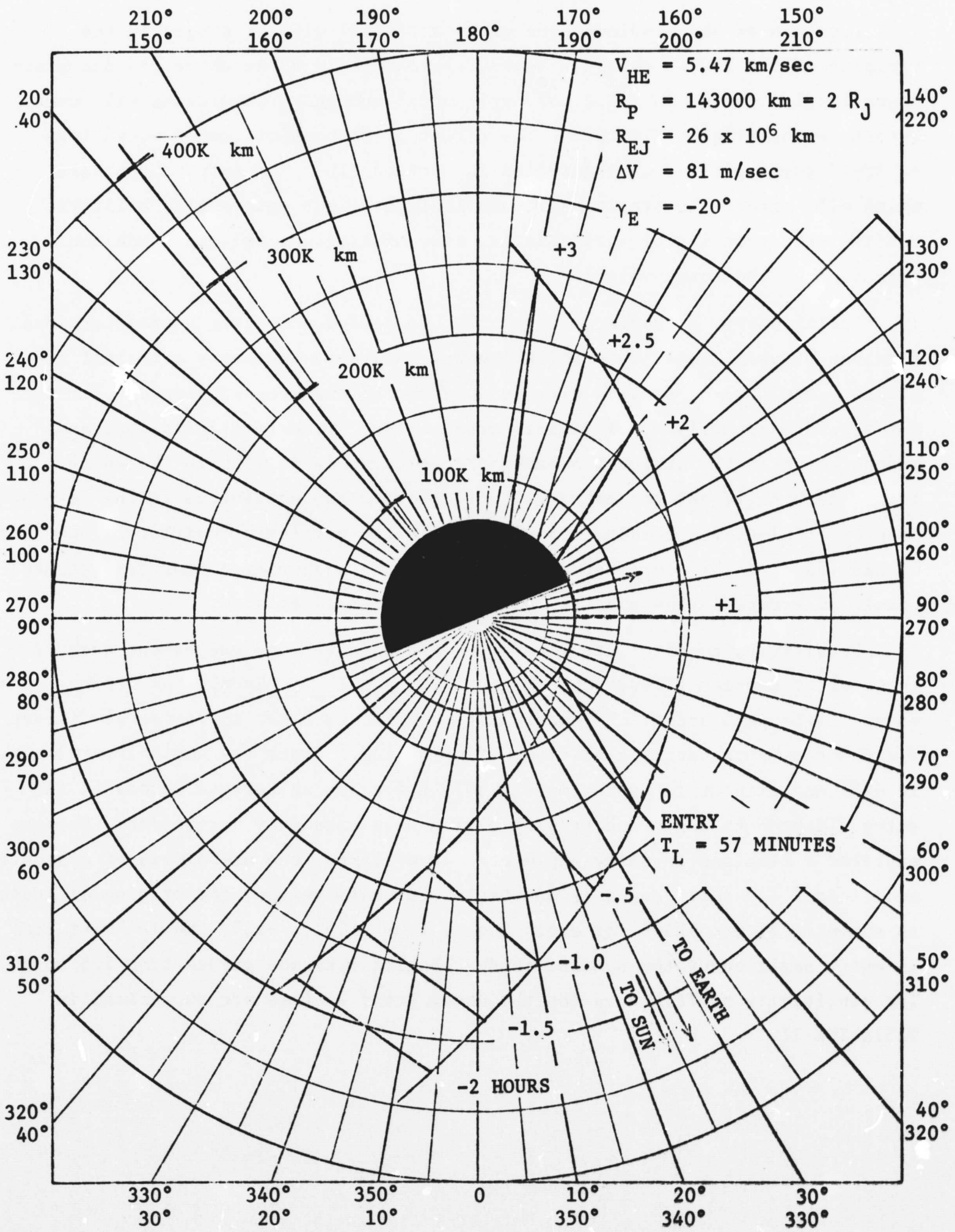


Figure IVA-5 Design Example - Approach Geometry

For each of the missions, the entry aeroshell will be staged in the vicinity of the 200 mb pressure level, approximately 33 km above the one atmosphere level. Errors in the atmospheric model and entry conditions will cause errors in the staging altitude. The effect of atmospheric model variations on the descent profile were detailed in Section IID. The entry parameters which will affect the staging altitude include flight path angle, ballistic coefficient, quantity of mass ablated, time of staging, and magnitude and direction of the entry velocity.

During entry, a deceleration of .1 g is sensed and after a predetermined time has elapsed (based on preflight entry analyses) the entry aeroshell is staged. The time of staging will be in error if the deceleration of .1 g is not sensed accurately or if timing errors exist. Tracking limitations and inaccuracies in the deflection maneuver can cause deviations in the entry flight path angle and the entry velocity vector. Uncertainties in the aeroshell's drag coefficient may result in variations in the ballistic coefficient, and lack of knowledge of the aero/thermodynamic processes occurring during descent may result in errors in the quantity of heat shield mass ablated.

Sensitivity coefficients were developed to determine the extent each of these error sources affects the staging altitude (h_s). Except for errors in the entry flight path angle, the sensitivity coefficients are approximately linear for changes in the entry conditions of up to 10%. Since the nominal entry angle is -20° and skipout is approximately -4°, the relation between errors in the entry flight path angle and staging altitude is extremely non-linear. Because the expected variations in entry angle are rather large, the usefulness of a sensitivity coefficient for entry angle is doubtful. For this reason, the staging altitude is shown in Figure IVA-6 for entry angles from -10° to -30°; the 10° variation in entry angle about the nominal causes staging altitude errors from 7.5 to 20.5 km. The sensitivity coefficients for the other error sources are summarized in Table IVA-II.

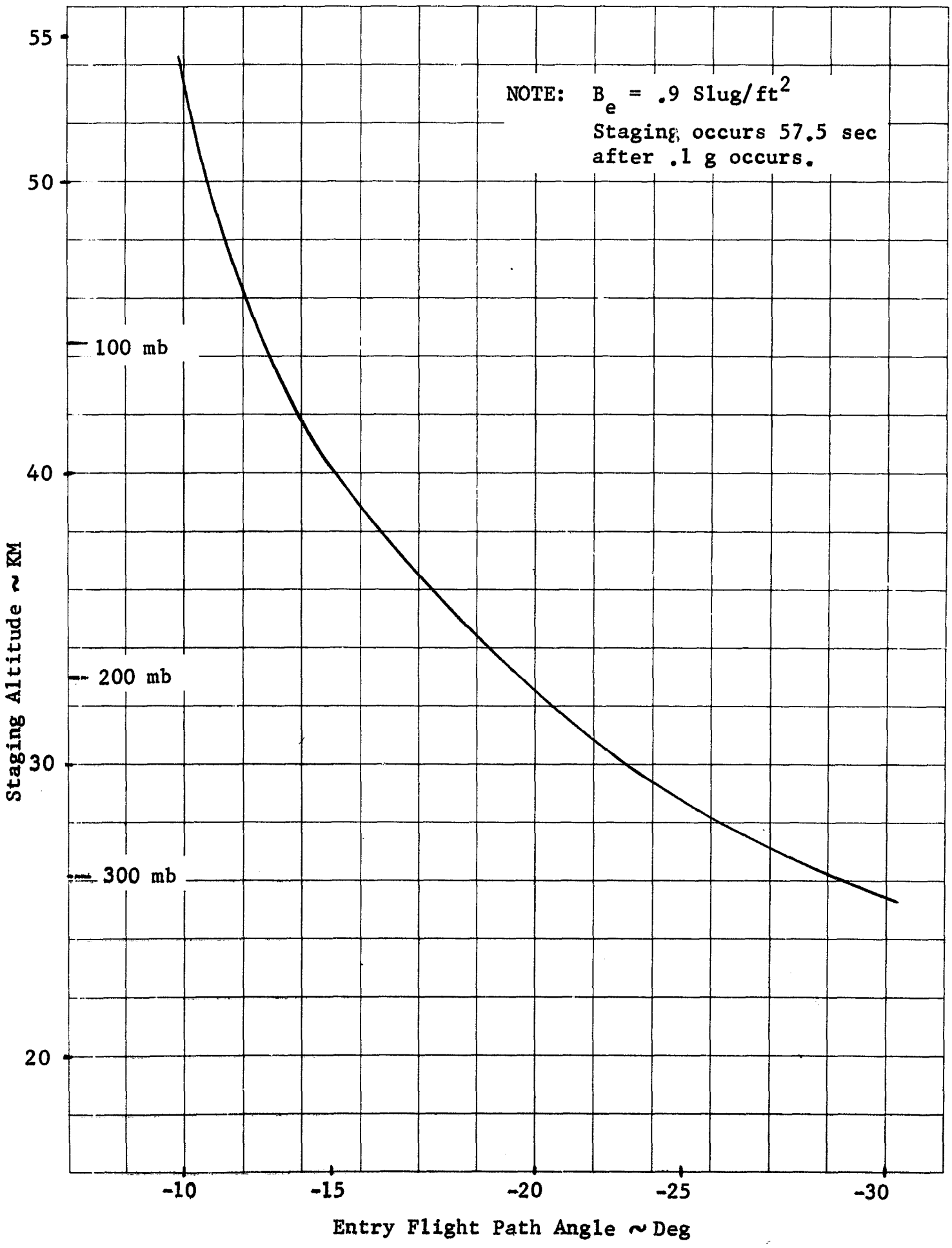


Figure IVA-6 Effect of Entry Angle Errors on Staging Altitude

TABLE IVA-II

Error Source	
Ballistic Coefficient (B_e)	$\Delta h_s/\Delta B_e$ = -18 km/slug/ft^2
Entry Velocity Magnitude (V_e)	$\Delta h_s/\Delta V_e$ = -.2 sec
Ablated Mass Fraction (m_a/m_e)	$\Delta h_s/\Delta(m_a/m_e$ = 19.5 km
Time of Staging (t_s)	$\Delta h_s/\Delta t_s$ = -.38 km/sec
Azimuth of Entry Velocity (A_V)	$\Delta h_s/\Delta A_V \sim 0$

B_e = .9 slug/ft^2 $\quad \gamma_{Ie}$ = -20° $\quad V_{Ie}$ = 195586 fps

$\frac{m_a}{m_e}$ = .2 $\quad t_u$ = 57.5 after .1 g

Launch Vehicle

The launch vehicle is initially selected to be the 7 Segment TITI D/Centaur/Burner II with 970 pounds of payload capability in excess of 1450 pounds TOPS spacecraft weight. This selection maximizes the mission capabilities. Chapter V discusses the other potential choices in the area of payload, launch vehicle and probe survival depth.

B. Engineering Concept Evolution

This section describes the rationale leading to the evolution of the engineering concepts at the system level. Although the environmental models and the science mission objectives provide the basis for much of the engineering design criteria, the dominating problem throughout the study was the system integration and engineering design of the communications data link. The data return mode interfaces with every major system and operation, and the successful integration of its requirements into the mission design was the most difficult task of the study. The launch/arrival date selection, the interplanetary trajectory, the planet encounter and targeting geometries, the spacecraft flyby geometry, and the entry probe trajectory and mission duration all had a critical impact on the data return system design.

Section IVB-2, below, describes the system level interfaces involved in the selection of the candidate data return modes. Sections IVB-3 through -6 describe the system trades for the descent probe concepts, the entry probe concepts, the deflection system concepts, and the spacecraft adaptations.

1. Science Payload Criteria

The science criteria of Chapter III established the types of measurements, measurement interval, required ballistic coefficients, data rates, and descent profiles. Figure IVB1-1 shows the probe descent depth (pressure) with time for a single probe and a split probe concept. The split probe has the same types of science instruments as the single; however, they are distributed or duplicated on the upper and lower probe to provide complete science coverage with a much reduced descent mission time.

Chapter III describes in detail the science selection rationale.

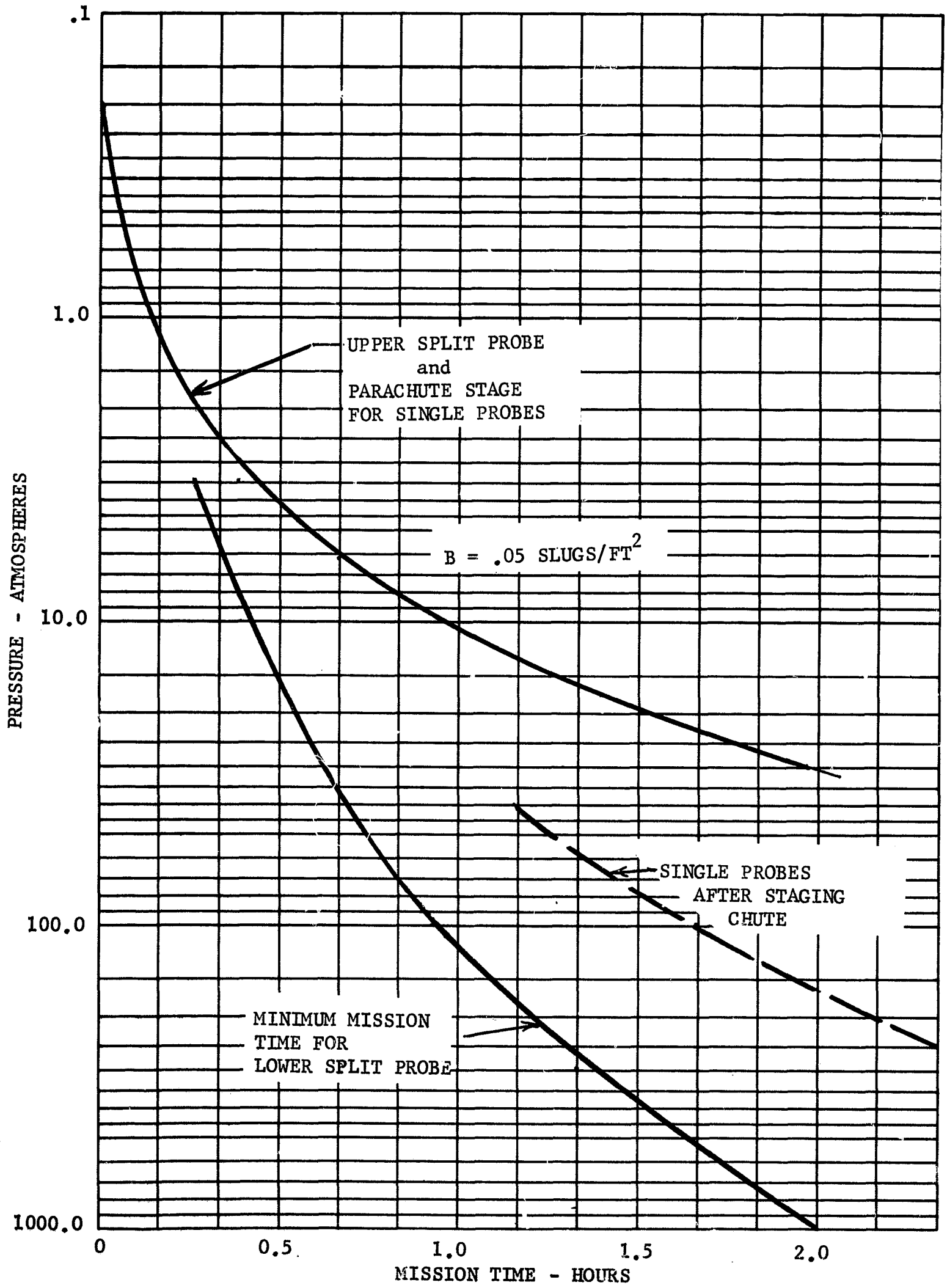


Figure IVB1-1 Mission Time with Dep[illegible]h

2. Data Return Modes

A. Major Factors

Several interrelated factors influence the selection of a mode for retrieving data from the descending probe and transmitting the data to earth. The exact nature of the interrelationships is also influenced by the mode selected.

The impact on the data return mode of the factors listed below are discussed in the following paragraphs.

Space loss (both from Jupiter to earth and from probe to spacecraft)
Atmospheric attenuation
Approach geometry
Entry weight vs entry angle
Probe protection vs penetration depth

B. Candidate Data Return Modes

The primary candidate data return modes are a direct link from probe to earth, and a relay link from probe to spacecraft to earth. A third mode which evolved during the study uses two probes descending to different depths in a probe to probe relay link. The split probe concept provides reasonable designs at depths from 200 to 1000 atmospheres, whereas the single probe concept requires excessive transmitter power and becomes very heavy at depths greater than 300 to 400 atmospheres. In the 10 to 300 atmosphere range the single probe is adequate.

The following paragraphs describe the concepts evolved for each of these candidate data return modes.

1. Direct Link

The direct link data return mode, with a line-of-sight requirement directly to earth, must have sufficient power and gain to overcome the Earth-Jupiter distance, the atmospheric attenuation, and the reduced antenna gain due to the wide variation in the probe aspect angle caused by planet rotation for missions of any useful duration, i.e., over one hour or 36^{o} of rotation.

The Earth-Jupiter communications range, Figure IVB2-1, is shown as a function of arrival date. The shaded areas are arrival restrictions due to sun interference. The variation in communications distances is from about 4.5 AU to 6.4 AU. Thirty-day launch periods and near minimum launch energies result in arrivals covering nearly the full range of possible communications distances as noted by the dashed lines; however, reduced launch periods result in somewhat reduced communications ranges. At these ranges, the depth into the atmosphere from which a probe can communicate with earth is limited.

The science descent time criteria, discussed in Section IV.B.1, established the relationship between probe descent time and descent depth into the atmosphere, Figure IVB1-1. Figure IVB2-2 depicts the corresponding atmospheric attenuation of the radio signals with depth and frequency. From this figure it is apparent that a signal at the DSN frequency of 2.3 GHz is highly attenuated in the atmosphere. At this frequency, a probe depth of about 20 atms, the 3 db attenuation would require doubling the already large transmitter power necessary to cover the range to earth. This situation suggests using the split relay probe with reduced frequency in the lower probe relay to overcome the atmospheric attenuation with depth. This concept is examined later in connection with the relay link discussion.

A major factor in the direct relay with earth is the increase in atmospheric absorption as the probe aspect angle changes with planet rotation. Antenna gain is also affected by aspect angle, but this factor can be accommodated by appropriate antenna design. Increased mission time, and consequent increased planet rotation, is required to reach greater depths as described in Figure IVB1-1. Therefore, for missions to any significant depth, the entry point must be targeted near the subearth point in the direct link concept.

COMMUNICATIONS RANGE

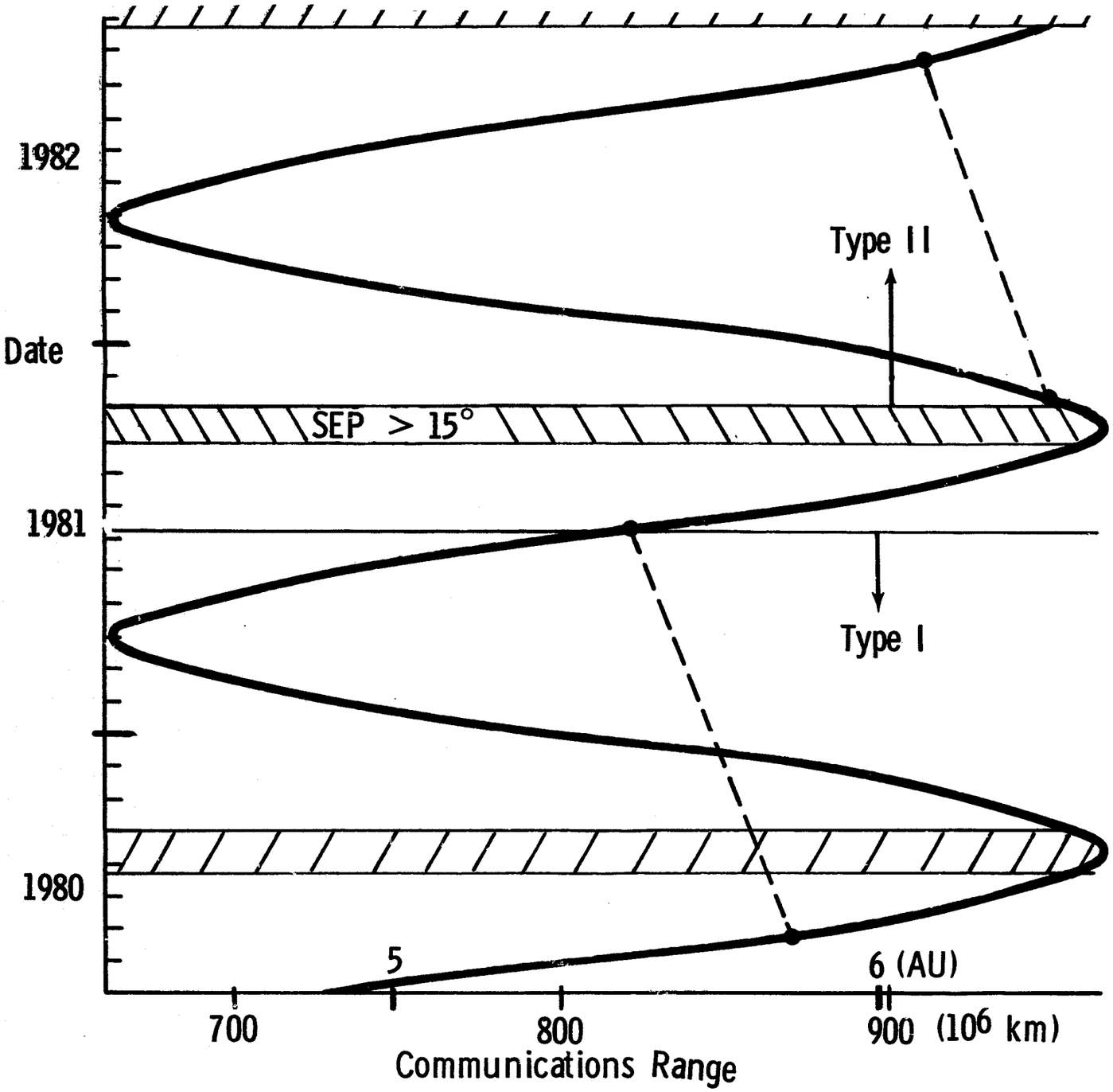


Figure IVB2-1

ZENITH ATTENUATION–NOMINAL ATMOS

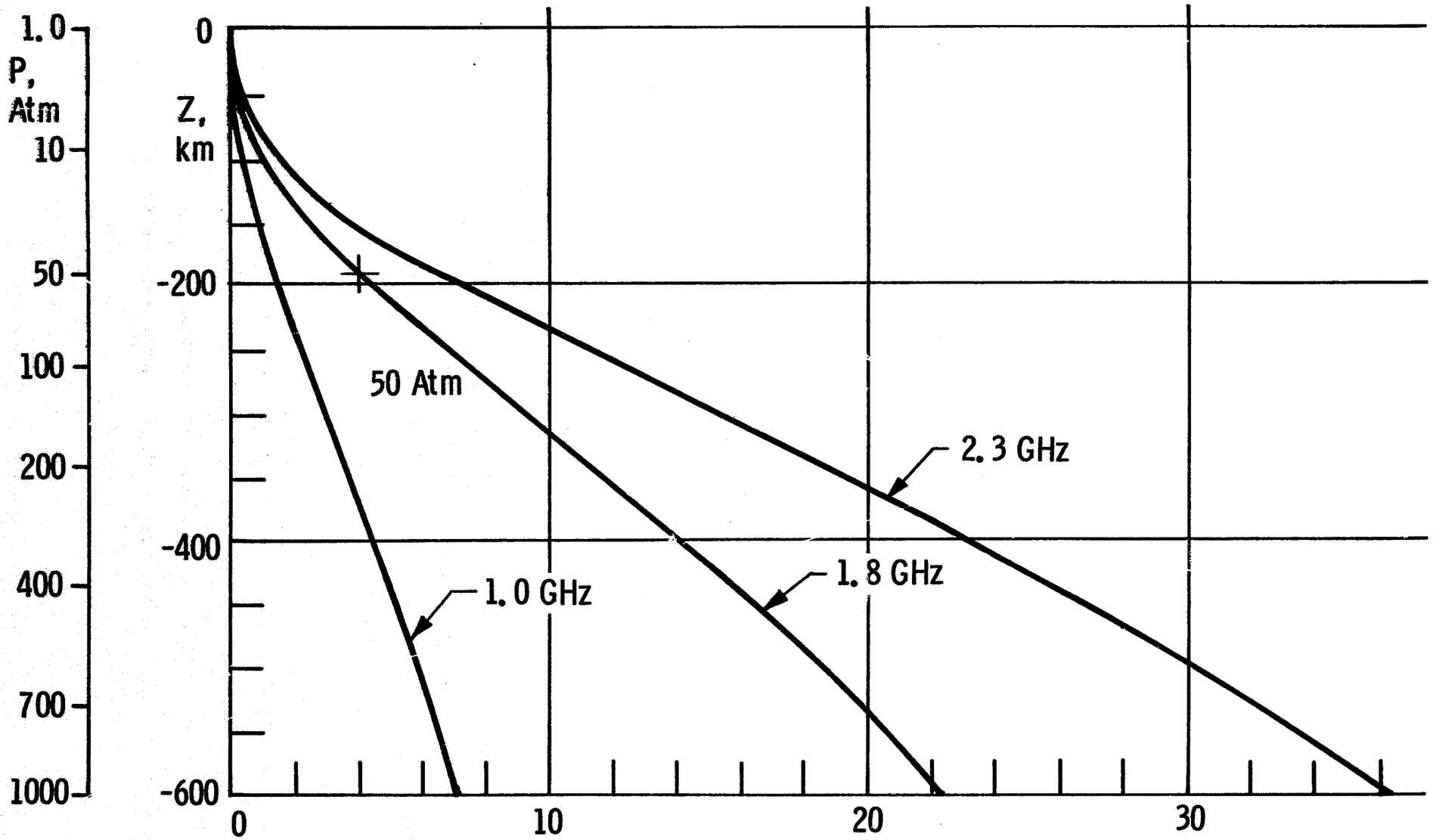


Figure IVB2-2

From Figure IVB2-3, the variation in probe aspect angle to earth with time from entry is shown as a function of entry angle for a typical arrival date. For example, at an entry angle, γ_E, of -40 degrees, the entry occurs at an aspect angle to earth of zero, i.e., entry is at subearth, but the angle builds up to 35 degrees at the end of a one hour mission. At a -50 degree entry angle, the aspect angle is minimized by balancing it about the subearth point. To achieve a zero aspect angle at the end of a one hour mission would require an entry angle of -60 degrees. The optimum apparently lies somewhere between these extremes since steeper entry angles result in weight penalties in the heat shield and aeroshell while shallower entry angles result in weight penalties in the data link due to the increased atmospheric absorption given by the higher aspect angles encountered at the deep end of the mission.

Because of the impact on both the spacecraft and the probe, a direct and a relay link system can only be compared on the basis of launch weights. A complete mission design was carried out for a direct link mission (Mission F). This mission was designed to give the same science return as Mission D, the mini-probe mission. The resulting system weights are 260 lbs, Mission D and 615 lbs, Mission F. Therefore, the relay link is preferable even for this modest mission. The differences would be more pronounced for more sophisticated missions. Figure IVB2-4 shows the direct link transmitter power requirements vs depth for two bit rates, calculated by extending the Mission F design.

2. Relay Link

The relay link concept, although it has the spacecraft as an added system, provides much more versatility in targeting and overall mission design and reduces the separate data link design requirements to more manageable levels. Whereas the probe in

DIRECT LINK COMMUNICATIONS

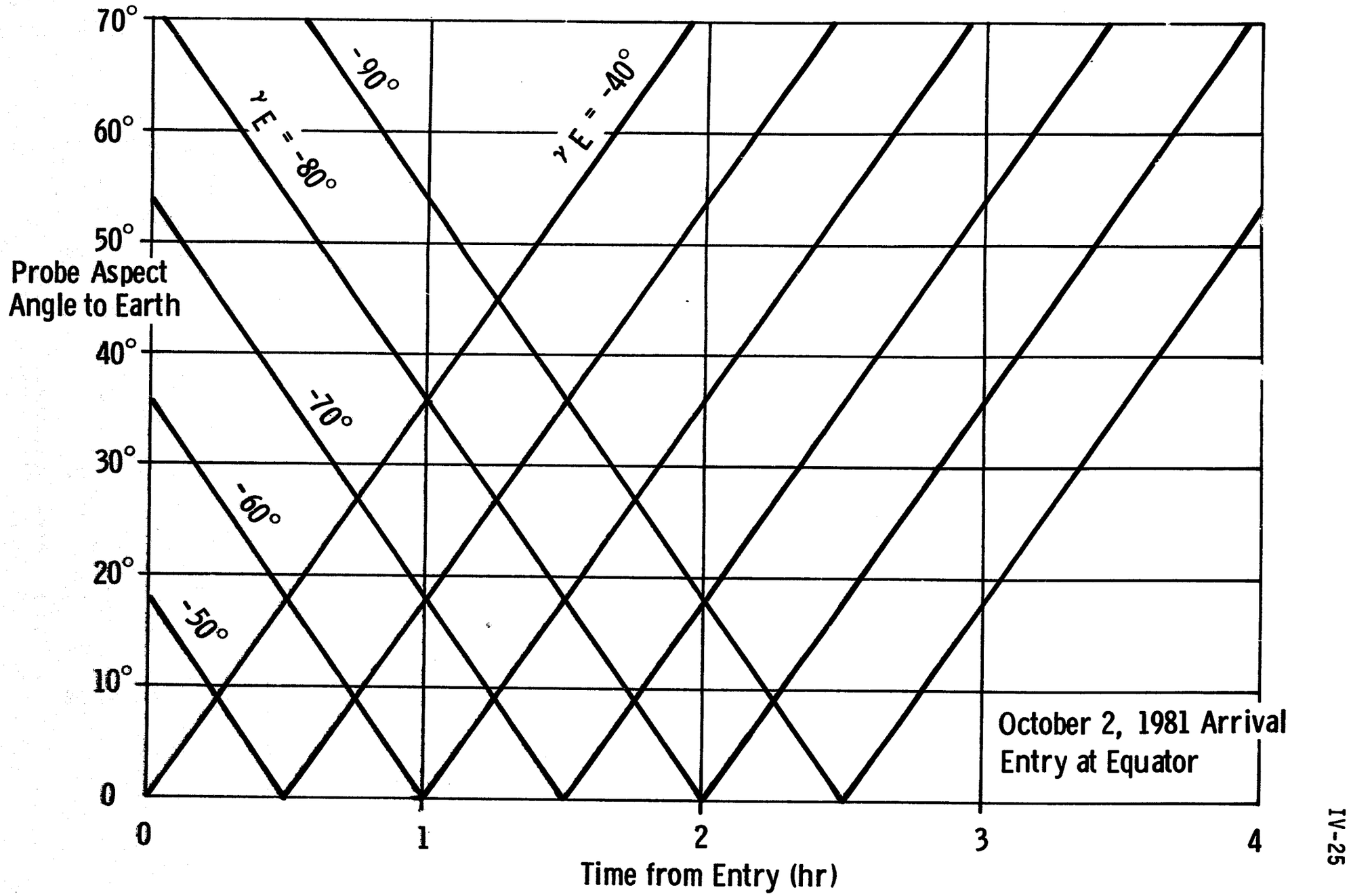


Figure IVB2-3

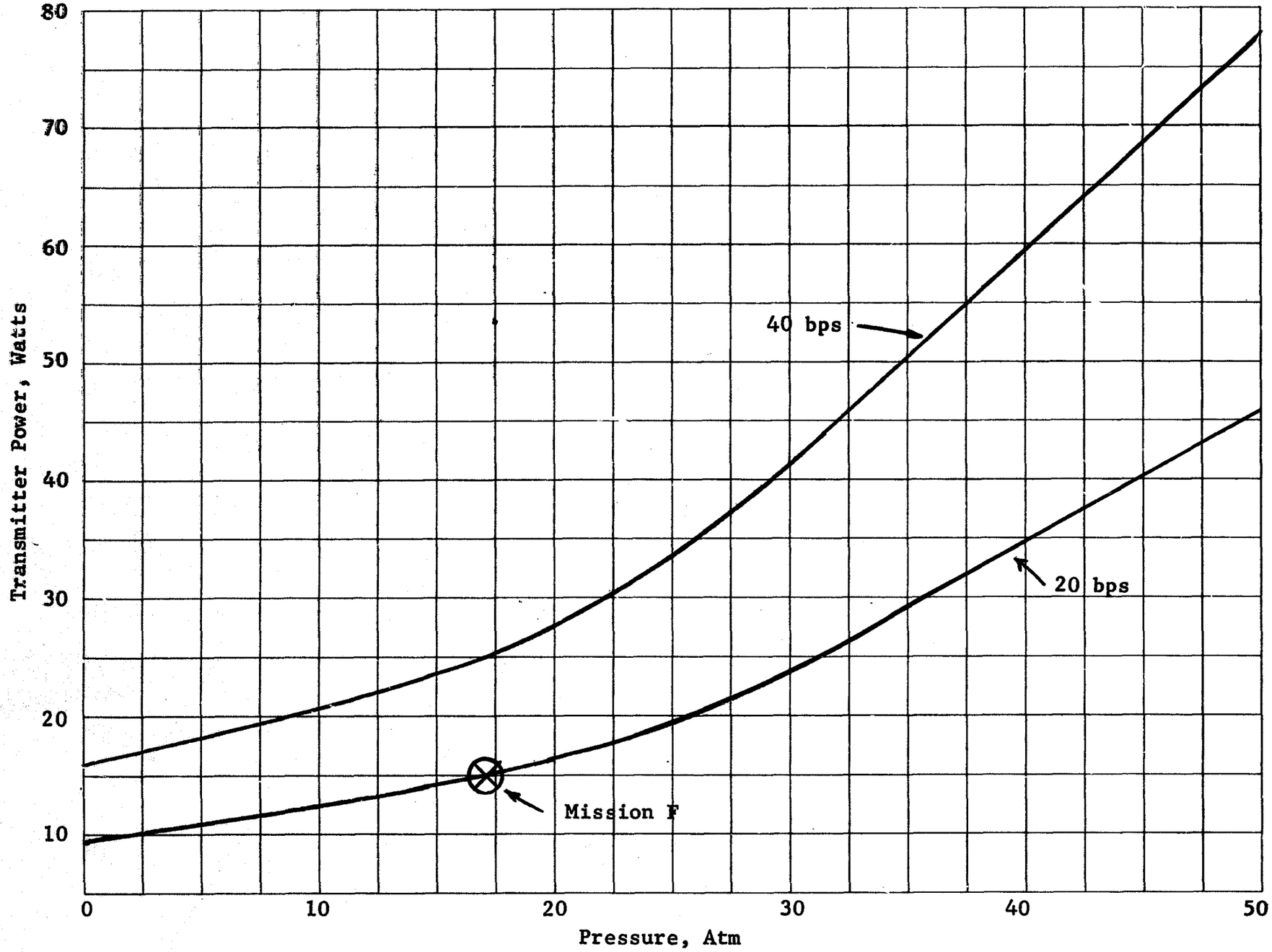


Figure IVB2-4 Transmitter Power vs Depth of Penetration, Direct Links

the direct link concept must use the DSN frequencies and line-of-sight to earth targeting constraint, the probe in the relay concept can use an optimized data link to the spacecraft with extended mission times and, therefore, extended depths. A significant portion of the descent mission may be conducted on the dark side if required. Using the spacecraft as a relay introduces the problem of designing the encounter and flyby trajectory such that the probe/spacecraft communications geometry interface and antenna aspect angles provide reasonable design requirements for the data link. By taking advantage of the planet's rotation rate and adjusting the spacecraft flyby periapsis radius, the spacecraft and probe trajectories can be nearly synchronized resulting in a minimum communications range and probe-S/C aspect angles. Figure IVB2-5 shows a near optimum relative geometry at an R_p of 2.0 R_J and Figure IVB2-6 shows the effect of varying the flyby periapsis radius on the resultant communication range. As flyby radius is reduced below about 2.0 R_J the data link doppler rates increase and acquisition of the probe after entry becomes increasingly difficult for the spacecraft.

With near minimum communications ranges obtained at a flyby radius of 2.0 R_J, the probe/spacecraft data link was optimized by trading system design factors such as spacecraft antenna size, probe transmitter power and frequency, and mission time and depth.

The spacecraft receiving antenna characteristics are shown in Figure IVB2-7 as a function of frequency and depth. Although lower frequencies are desirable to reduce atmospheric attenuation (Figure IVB2-2) they require a larger spacecraft antenna and result in higher spacecraft antenna noise temperatures with associated losses.

The descent probe weight is especially sensitive to depth, mission time, and transmitter power required for data return. The depth and mission time establish the combination of pressure and

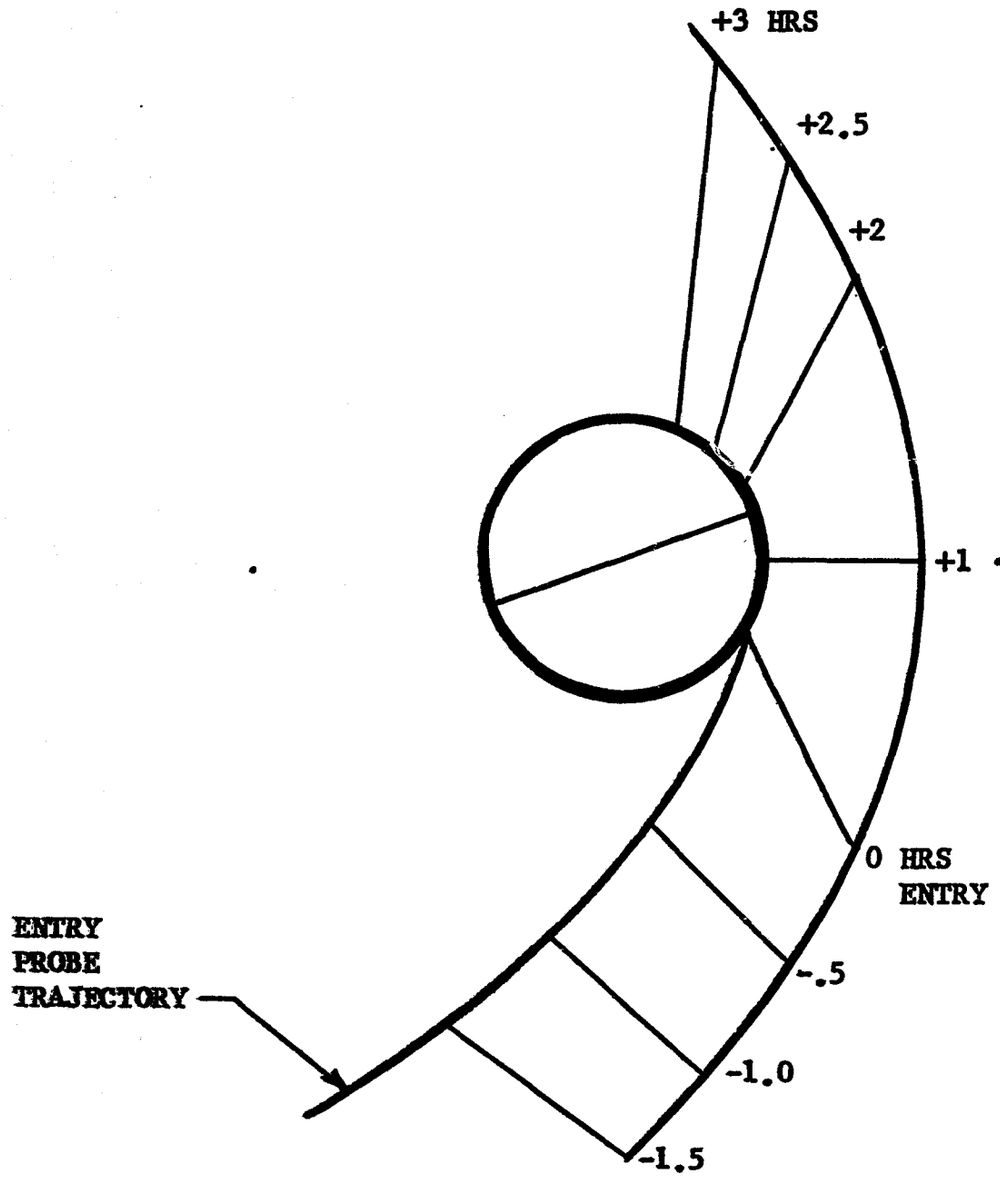
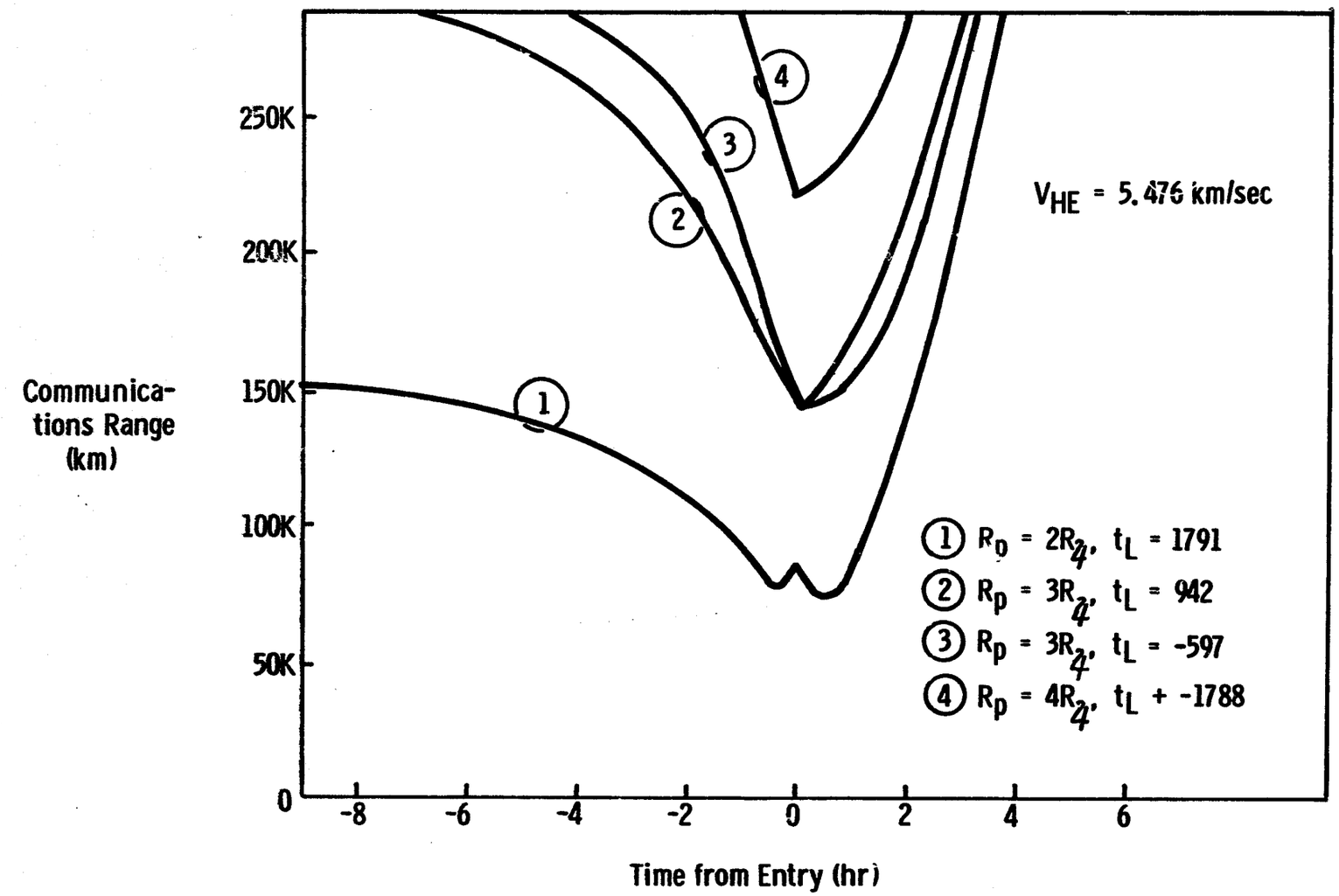


Figure IVB2-5 Typical Encounter Geometry

RELAY COMMUNICATIONS RANGE R_p= 2 TO 4



89

Figure IVB2-6

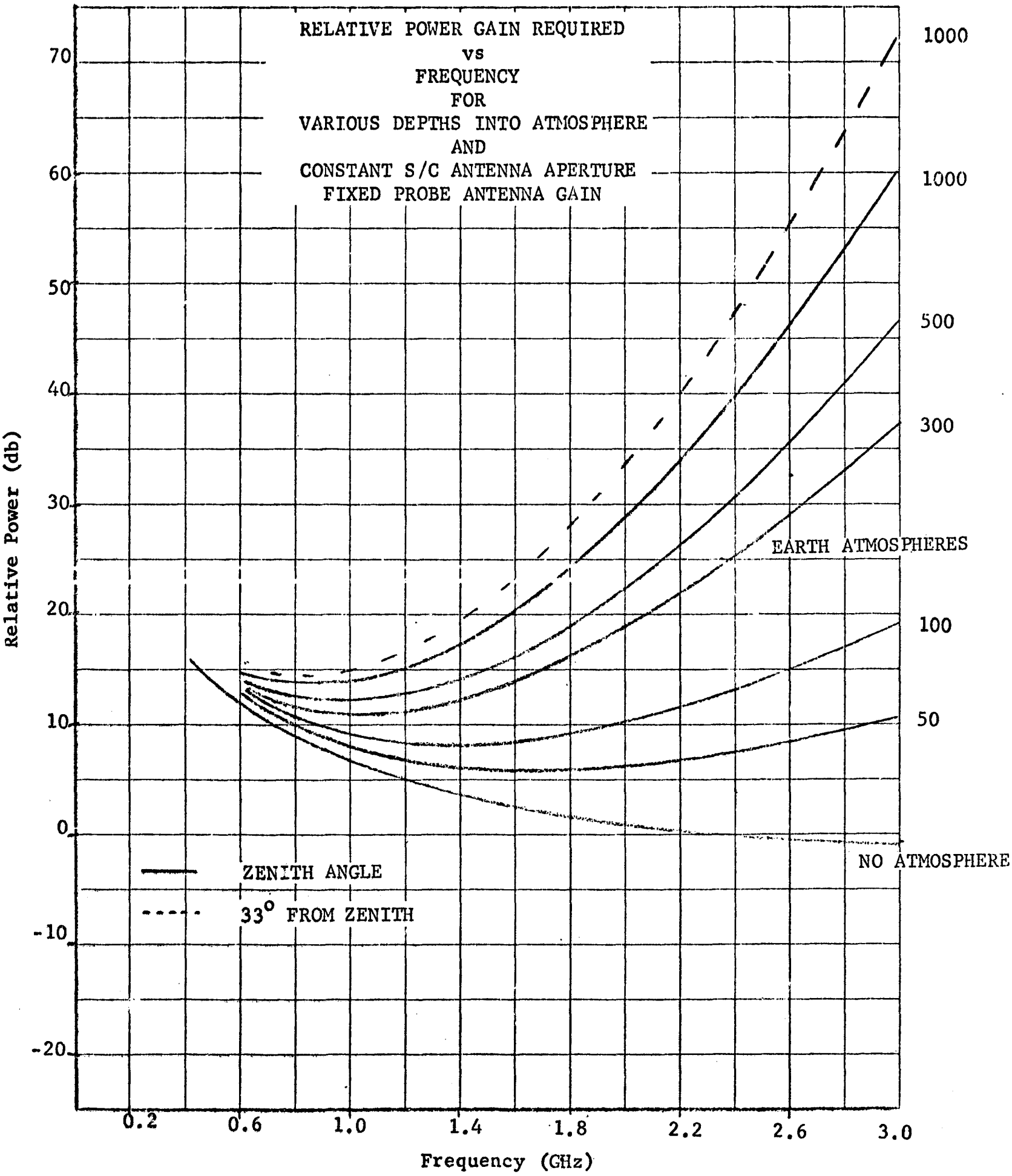


Figure IVB2-7 Relative Power Gain Required Versus Frequency for Various Depths into Atmosphere and Constant S/C Antenna Aperture Fixed Probe Antenna Gain

external heat load. The transmitter produces the dominant internal heat load. Therefore, these factors, in conjunction with the associated volumes, establish the probe design. For depth below about 300 to 400 atmospheres, the pressure shell and insulation become more than one half the weight in all descent probe designs. For a single probe concept descending to depths below about 300 atms, the mission time becomes large in order to meet the science criteria for measurement interval, and the atmospheric attenuation becomes significant. By utilizing the split probe concept in which the upper probe acts as an additional data link relay to the spacecraft, and the lower probe simultaneously measures the deeper atmosphere, the mission time and required transmitter power are both greatly reduced. A comparison of transmitter power required for the single and split probe concepts is shown in Figure IVB2-8. For the relatively short range between the split probes, the atmospheric attenuation effects are easily overcome by a small transmitter (2 watts) with optimized frequency. The upper relay probe is essentially above the depth where atmospheric attenuation is significant and its data link to the spacecraft is optimized for the space loss and spacecraft constraints. Figure IVB2-9 compares single and split probe concepts by weight with depth for typical conditions. The significant weight penalty for the single probe concept at greater depths is due to the extended mission time required and the large transmitter power required to communicate directly with the spacecraft through the atmosphere.

Both TOPS and Pioneer F/G spacecraft were considered in support of the atmospheric probe mission. A probe tracking and data link antenna is required on the relay spacecraft with accurate pointing capability. On the three-axis-stabilized TOPS spacecraft, a boom mounted antenna with a rotation angle of about 130^{o} provided the required coverage for most missions. For the spin-stabilized Pioneer F/G spacecraft, three antenna options were considered. The first is an electronically de-spun phased array; the second is a mechanic-

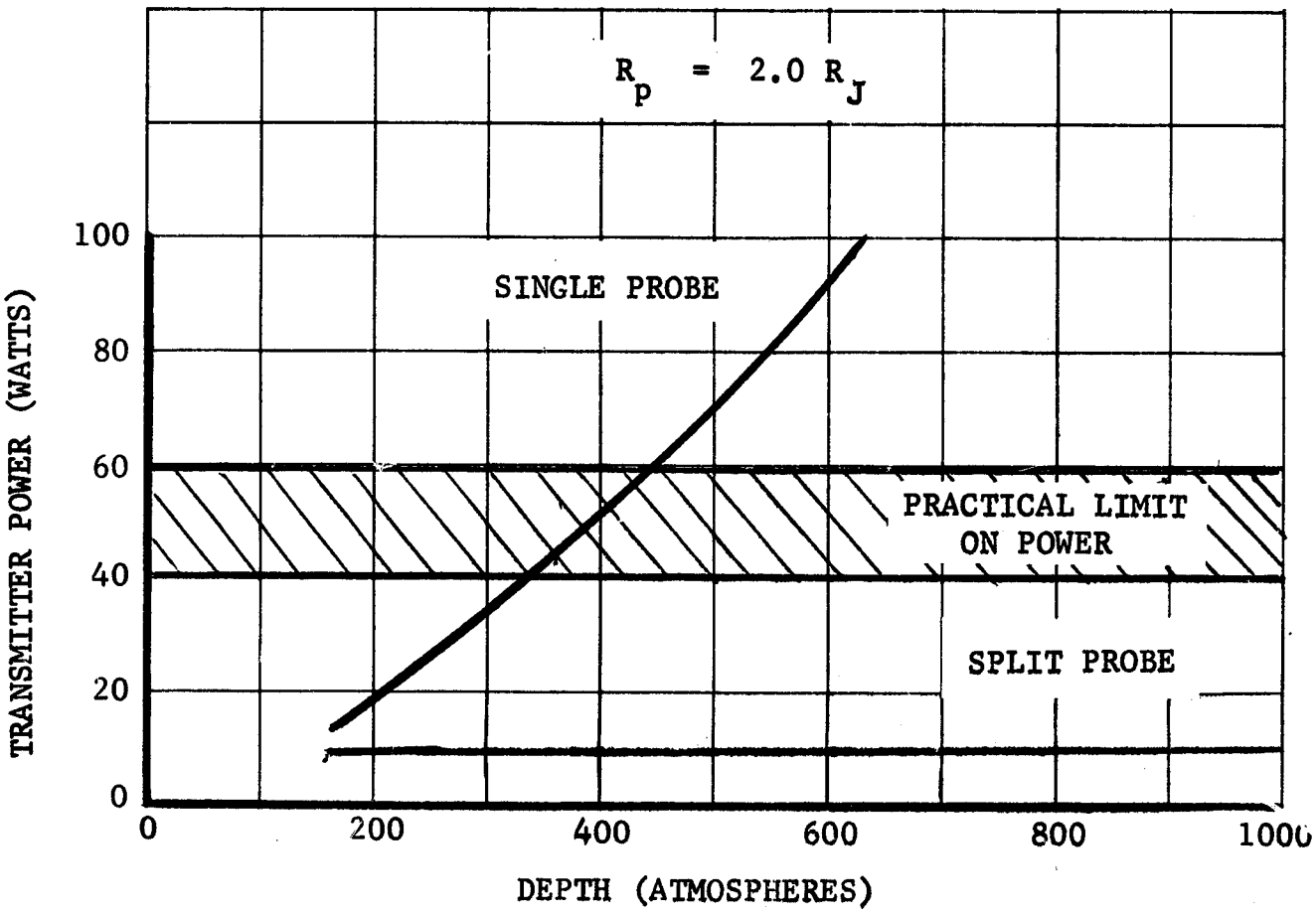


Figure IVB2-8 Transmitter Power Requirements

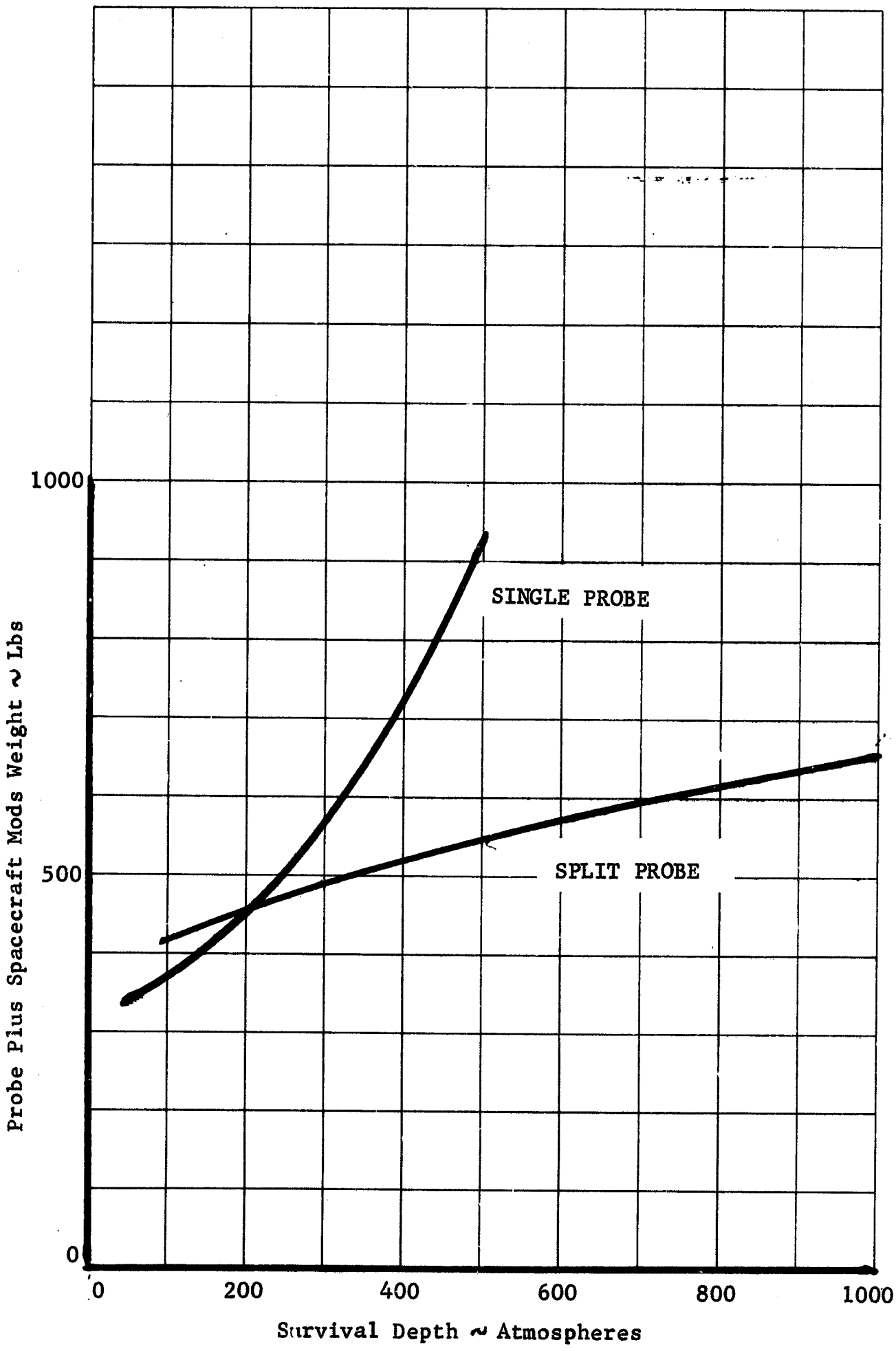
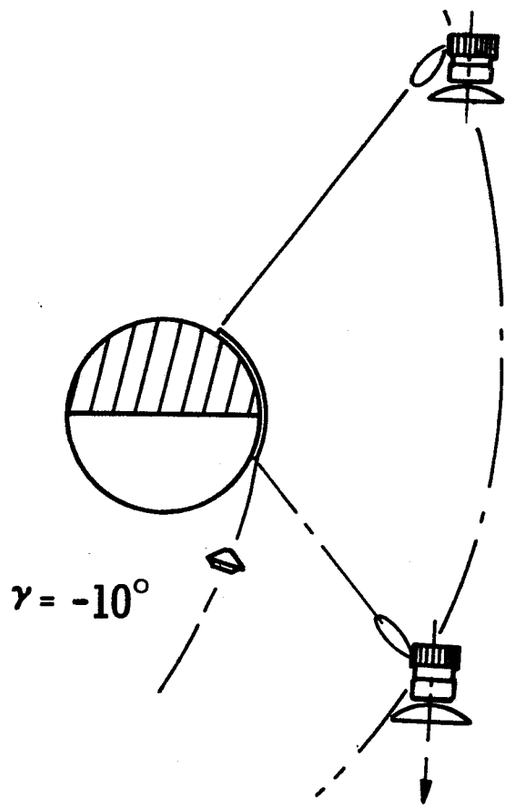


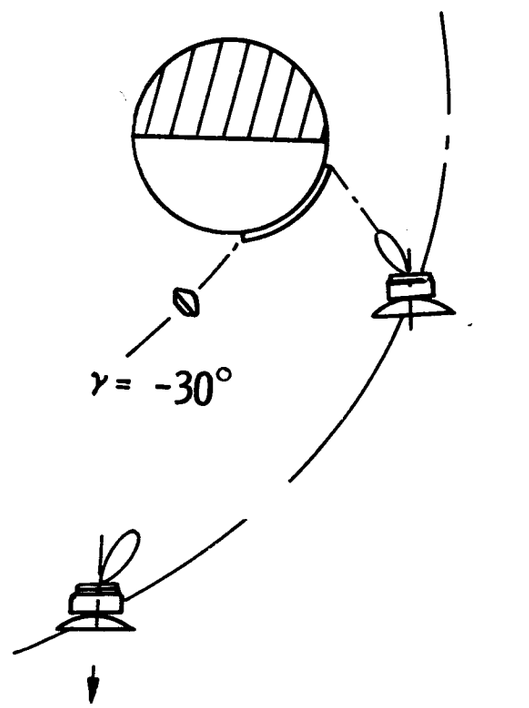
Figure IVB2-9 Typical Mission Single and Split Probe Weights

ally de-spun antenna mounted near the center line with limited rotation of about 40^{o}; and the third is a mechanically de-spun antenna mounted on a boom with counterweight and an aspect angle rotation of about 130^{o}, equal to that of the TOPS spacecraft. The third option antenna can perform similarly to the TOPS antenna and therefore no change in mission sequence is required. However, the first two Pioneer antenna options are restricted in pointing angle and require a modified flyby mission sequence. Figure IVB2-10 depicts the trajectory in which the atmospheric mission is conducted as the spacecraft approaches and then passes periapsis. The spacecraft mounted antenna must track through, typically, 130^{o}. The Pioneer "pre-periapsis" mission, also depicted, must be conducted prior to reaching periapsis because of the restricted angle of rotation of the de-spun antennas. A weight penalty results from the increased communications range for the Pioneer pre-periapsis mission and, even more significant, the allowable descent probe mission time is restricted by the limited antenna field of rotation constraint on the relay geometry.

The following sections discuss the detailed engineering evolution of the various subsystems involved in the direct and relay link mission concepts.



PERIAPSIS
RELAY



PRE-PERIAPSIS RELAY

Figure IVB.2-10 Comparison of Periapsis and Pre-periapsis Relay Missions

3. Entry Vehicle and Descent Probe Design Concepts

The environmental protection of the science and telecommunications package for Jupiter probes involves many of the same considerations as for previous Venus probe studies. Hence the entry vehicle structure and pressure vessel design approaches of those studies generally pertain, e.g., the concept of a separate pressure resistant instrument container which is mounted inside the entry aeroshell and extracted after entry to facilitate science measurements and descent rate control. Several aspects of the Jovian entry and descent environment are substantially different however:

a) The small H_2 molecules, and the higher ambient pressures and temperatures encountered during the post entry descent phase result in a reduction in the performance of porous external insulations. Thus for a given payload volume, probes using the external insulation concept become larger. On the other hand the higher temperatures dictate that at least some external insulation be used to keep structural temperatures below the knee in the strength vs temperature curves $\sim$ 1100°F.

b) Large heat shield unit-weights dictate that surface area of the entry aeroshell be kept as small as possible which in turn puts a premium on the size as well as the weight of the descent probes housed within the entry aeroshells.

c) Half-cone angles for the aeroshell are limited to 55° to 60° due to heat shield requirements.

d) The generally higher entry G forces require more consideration in supporting the concentrated masses of the descent probes within the entry aeroshell.

e) The maximum entry ballistic coefficient is determined by the requirement to decelerate to subsonic velocities by .1 atm to .2 atm. The critical value varies with entry angle and ranges from 1.6 slugs/ft^2 at $\gamma = -20°$ down to .8 slugs/ft^2 at $\gamma = -50°$. To achieve ballistic coefficients below about 1.0 slugs/ft^2 requires a larger, and thus a heavier aeroshell than one sized only to be adequate to contain the descent probe.

f) Use of the relay mode, and the relatively broad beam probe antennas it permits, relieves the problem of configuring the probes to strict aerodynamic requirements to minimize turbulence induced oscillations.

g) At the high end of the range of interest the pressures dictate thick walled pressure vessels if the low-density structural alloys, aluminum and beryllium are used. The bending effect introduced by the thick walled vessels raises the stress levels over the normal hoop compression values and results in these normally efficient materials not providing the minimum weight systems.

h) Packaging two descent probes within the same aeroshell, for the split probe concept, requires deviating from optimum structural shapes and/or using several modules for the upper probe equipment due to the requirement to minimize the axial aeroshell dimensions because of dynamic stability considerations and weight penalties.

These considerations and others have led to the adoption of configurations for split and single probes shown in Figure IVB3-1. The combined inside/outside insulation arrangement shown in Figure IVB3-2 is being used for deeply penetrating probes while for shallower probes the external insulation is omitted. Weight

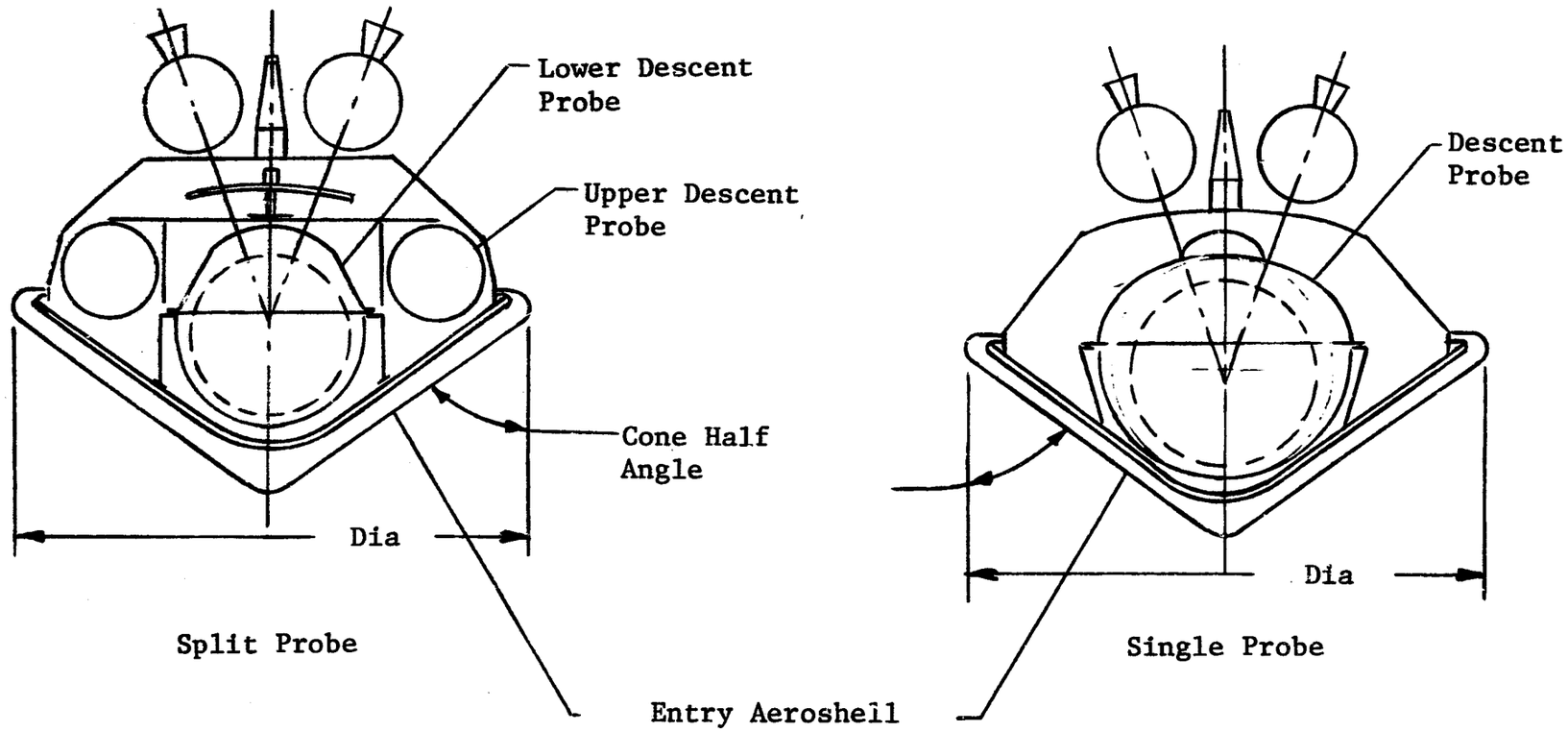
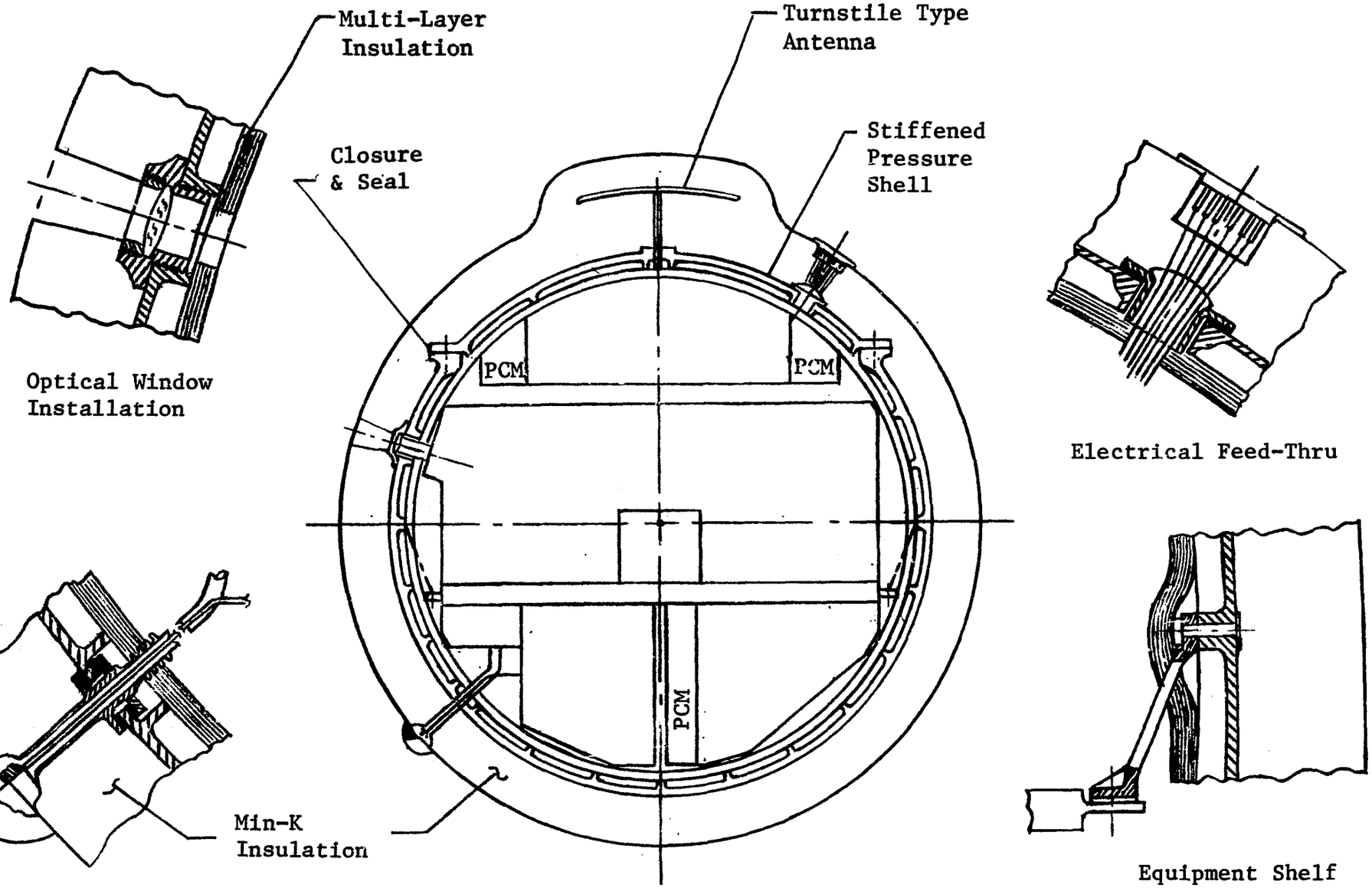


Figure IVB3-1 Parametric Probe Configurations



Optical Window Installation

Electrical Feed-Thru

Atmospheric Sample Inlet Duct

Equipment Shelf Hanger

Figure IVB3-2 Design Example Descent Probe Structural/Thermal Concept

and size tradeoffs are discussed in Volume III Chapter V. Also discussed in that chapter are alternative design concepts involving partial admittance of the ambient pressure into the payload or partially balancing the ambient pressure with internal pressure. These were found not to offer any significant weight advantage although seal problems are alleviated in the first of these.

4. Deflection Concepts

Very simple probe deflection maneuvers were found to suffice (based on analyses) in the case of the Venus probes of previous studies, consequently this approach was examined initially for application to the Jupiter probe missions. The procedure (for the Venus case) was the following. The probes were oriented to the proper ΔV angle by the spacecraft, released, spun up for stability during a fixed duration solid rocket motor firing, and then allowed to enter (after despinning) at whatever angle of attack resulted, provided it did not exceed about 50 degrees. Dispersions in arrival leadtime and angle were not significant due to use of direct link communications and the acceptability of steeper angles from a targeting and entry severity standpoint.

For Jupiter, the use of the relay mode and the desire for shallow entry has imposed much stricter requirements on ΔV implementation. Consequently several versions of an active guidance and control system onboard the probe have evolved; a 3-axis strapdown system for use with TOPS and a probe precession technique for use with Pioneer. These are described in subsequent chapters. In addition some consideration was given to deflecting the spacecraft instead of the probes so as to use the spacecraft G&C systems to induce an accurate probe trajectory. Although this approach has the potential for greater accuracy in the case

of the pioneer spacecraft than is achievable with the probe G&C system, it has the disadvantages of requiring one or more additional post probe separation course corrections and requires targeting the spacecraft initially on an impacting trajectory. For the purposes of this study the deflection maneuvers were limited to probe deflection.

Probe attitude at entry (initial angle of attack) is considered also to be much more critical for the Jupiter Probes due to the greater severity of the entry and the probability of significant heating before aerodynamic convergence can take place. This leads to the requirement for an onboard system to orient the probe after the ΔV implementation. Weights are included for this function in the probe designs.

5. Spacecraft Adaptation

Large probes, weighing up to 50 or 60% of the spacecraft weight, in the case of TOPS, and over 100% of the spacecraft weight in the case of Pioneer, have been found to have significant impact on these vehicles. However, in the medium range of probes, 300 to 450 lb, the provisions for adapting the probes appear quite reasonable.

The TOPS probes are nestled up against the propulsion compartment to minimize CG shift and minimize support structure weight. The natural hard points on both bodies are utilized to the fullest degree possible. A less important consideration is choosing the probe location which minimizes the reorientation required of the spacecraft at probe separation.

The tracking antenna is located on the scan platform truss and deploys with that system. Two degrees of freedom are provided for the antenna.

The Pioneer Probes are mounted on the axis which is the spin axis during flight, which offsets them somewhat from the vehicle centerline at launch. The main concern, however, in the Pioneer probe mounting is maintaining the spin axis as the maximum inertia axis. This becomes more difficult with large probes since their contribution to transverse inertia increases faster than does their contribution to spin axis inertia.

Probe installations are shown in Chapters VI and VII.

C. Engineering Experiment

Engineering payloads for a first Jupiter mission can be considered to fall into two categories: measurements made for performance evaluation or diagnostic purposes and measurements made to investigate the effects, on system performance, of specific characteristics of the Jupiter environment.

1. Engineering Payloads

The function of the performance evaluation and diagnostic instrumentation is to provide data by which the technological success (or probability of success) of the mission can be evaluated, irrespective of the degree to which the science objectives are achieved. The engineering payload is not a separate subsystem but is related to all subsystems with closest association to the instrumentation system. During prelaunch testing of probe systems the engineering payload will be used to assure maintenance of operability and integrity. It will also be used to verify probe systems status during launch operations, launch and interplanetary cruise. However, it is during the final mission phases of probe separation, coast, entry, and descent that the engineering payl will serve its most important functions for the probe subsystems ese functions are described in the following subparagraphs.

a. Structural/Mechanical Subsystems

The structural/mechanical subsystem designs are based upon the anticipated environments due to entry and descent through the Jupiter atmosphere. The important considerations are design integrity and an assessment of the degree to which the design is conservative. It must also be recognized that it is not likely that the complete simulation of Jupiter entry will be accomplished prior to the mission. These measurements will therefore have great importance for the design of follow on missions. The following instrumentation will be required:

1. Internal pressure of the probe pressure vessel.
2. Internal temperature of the probe at the center

3. Temperature of the probe interior wall.
4. Temperature distribution through the exterior insulation of the probe.
5. Subsurface temperature of the heat shield.
6. Exterior surface temperature of the aeroshell.
7. Rate of heat shield recession during entry.

b. Electrical Power Subsystem

The power subsystem measurements can be limited to battery voltage and current and battery temperature because this system can be qualified in all anticipated environments prior to the mission.

c. Communications Subsystem

Measurements of supply voltages and operating voltages of transmitters and receivers will be required for engineering diagnostic purposes. Measurements of received signal strength will provide information on actual attenuation through the Jupiter atmosphere as well as on system operation. If a split probe relay link is used the signal strength measurements will have more significance because of the increased ability to distinguish the effects of attenuating layers in the atmosphere. The receiving equipment aboard the spacecraft will require measurements of temperature of the receiving antenna preamplifier and of the antenna positioning assembly. The direction of antenna pointing will also be measured.

d. Programmer Sequencer Subsystem

Sequencer operating voltages will be measured as will be the sequenced functions. Measurements of function accomplishment will be given preference to command-to-accomplish wherever this does not cause undue complexity. Verification of commands and updates received from the spacecraft prior to separation will also be measured.

e. Attitude Control

The attitude control system will be operative during the period of probe separation, deflection, and orientation for entry. Measurements of operating voltages and outputs of gyros or accelerometers will be required.

f. Data transfer subsystem operating voltages of coders and decoders and verification of commutator operation will be measured. A time base for correlation of mission events will be available as part of the data stream.

2. Engineering Experiments

Engineering experiments on specific characteristics of the Jpiter environment were not given detailed consideration during this study of a first Jupiter atmospheric entry mission. However, a few items were given some attention to provide a first assessment of importance to engineering design. These included:

Decameter radiation
Entry heating rate peaks
Wind and turbulence measurements
Radiation belt energy distribution

a. Decameter Radiation

With regard to the decameter radiation experiment, measurements might be made in the magnetosphere, the ionosphere, and the atmosphere. The magnetosphere can be probed by the spacecraft and these measurements can be compared with ionospheric and atmospheric measurements made by a probe. The frequency range of interest extends from 43 Mhz, with a peak near 18 Mhz down to at least 4.8 MHz where the ionosphere of Earth limits earth based observations. Observed flux densities are of the order of 10^{-18} watt m^{-2} $(cps)^{-1}$ with bandwidths of the order of 10^6 cps ([1], pp. 73-75, 82). The size of the regions in which the emissions originate seems to be very small in comparison with the radius of the planet, since terrestrial observations of the same event from different locations show strong ionospheric scintillation effects. At distances of 10^8 m $(\sim 1\ R_{21})$ from the origin, it is justified to use the simple inverse square law for the radiation from a point source to obtain a first estimate. This gives a

---

1. A. Smith and Th. Carr: Radio Exploration of the Planetary System. Van Nostrand Co., Inc., Publ, Princeton, N. J., 1964.

first estimate of the order of 10^{-4} watts/m^2. This is many orders of magnitude lower than levels at which spacecraft systems have been routinely tested for electromagnetic compatibility and, in the case of ordnance devices, for compliance with the range safety requirements of the Eastern Test Range. There appears to be no requirement for this measurement for the probes of this study. If a future requirement is identified, small receivers, possibly with logarithmic response, with small stub monopole antennas should be considered. Separate antennas on the probe would probable be used for ionospheric (pre-entry) and atmospheric (post entry) phases of the mission.

b. Entry Heating Rate Peaks

The measurement of entry heating rate peaks is not within the capability of any known instrumentation. A radiometer might provide some information provided that an adequate viewing aperture could be incorporated without degrading the performance of the heat shield which is most unlikely. Aside from this, the interaction of the carbon vapor with the incident radiation would make interpretation of the radiometer data quite difficult. Some information can of course be inferred from heat shield and insulation performance measurements discussed under engineering payloads. It should be noted that any heating rate radiometer measurements during entry would significantly increase the data storage requirements, possibly placing these measurements in competition with the science objectives.

c. Winds and Turbulence Measurements

Very limited information on wind and turbulence in the Jupiter atmosphere can be inferred from the accelerometers carried in the science payloads considered during the study. For the design example mission these are active down to 30 atmospheres with a data capability of 30 bits every 10 seconds. The principal implication to probe system design is associated with degradation (or loss) of the communications link due to disorientation of the probe antenna. This is likely to be most severe for direct link missions, somewhat less for single probes using relay communications and going to significant (∿500 atm) depths. Least sensitive of the missions considered is the probe-to-probe relay link in the split probe concepts.

d. Radiation Belt Energy Distribution

The energy distribution and instantaneous magnitude of the Jupiter radiation belt can be monitored by the spacecraft at large distances from the planet. It may also be possible to make some determination of the conductivity of the Jupiter atmosphere by including a "conductivity meter" to sample the atmosphere in this respect during probe descent. The desirability of these measurements is greatly influenced by the radiation belt models. It is noted in Section IIB that, for the nominal model, local protection would probably be required around individual modules.

D. Mission Effectiveness Studies

Studies of mission effectiveness were based on a mathematical model developed for comparing different missions. The basis for comparison was the degree to which measurements were provided consistent with achievement of the science objectives. Basic outputs of the study were total science value and total science value per pound of probe system weight. In addition, a number of probe designs were evaluated in support of the parametric studies.

1. Mission Effectiveness of the Design Example and Sample Missions

The mission science objectives were given in the form of seven science questions, (Table III.B-1, Chapter III) concerning Jupiter's atmosphere. These questions were translated into sixteen observables shown in Chapter III, Table III.B-2. It was assumed that the observables were equally important in value. A science value of 1.0 was assigned when the observable was perfectly achieved by the mission. Lower science values were assigned when the observable was only partially achieved. The schemes for assignment of the science values included consideration of the following:

a. Existence and capability of instrument sets to make the necessary measurements.
b. Location of probe with respect to latitude and distance from subsolar point when measurement is made.
c. Location of probe with respect to pressure-depth when measurement is made.
d. The separation (in atmospheres) between successive measurements.

The science payload requirements defined in Chapter III for the Design Example and Sample Missions were combined in the mathematical model with representations of mission targeting, descent profiles, and data return. A generalized picture of the relationships is shown in Figure IVD-1. A detailed description of the model, its operation, and value assignment methods is given in Chapter VI of Volume III.

Table IVD-1 gives the science evaluations of the Design Example and Sample Missions.

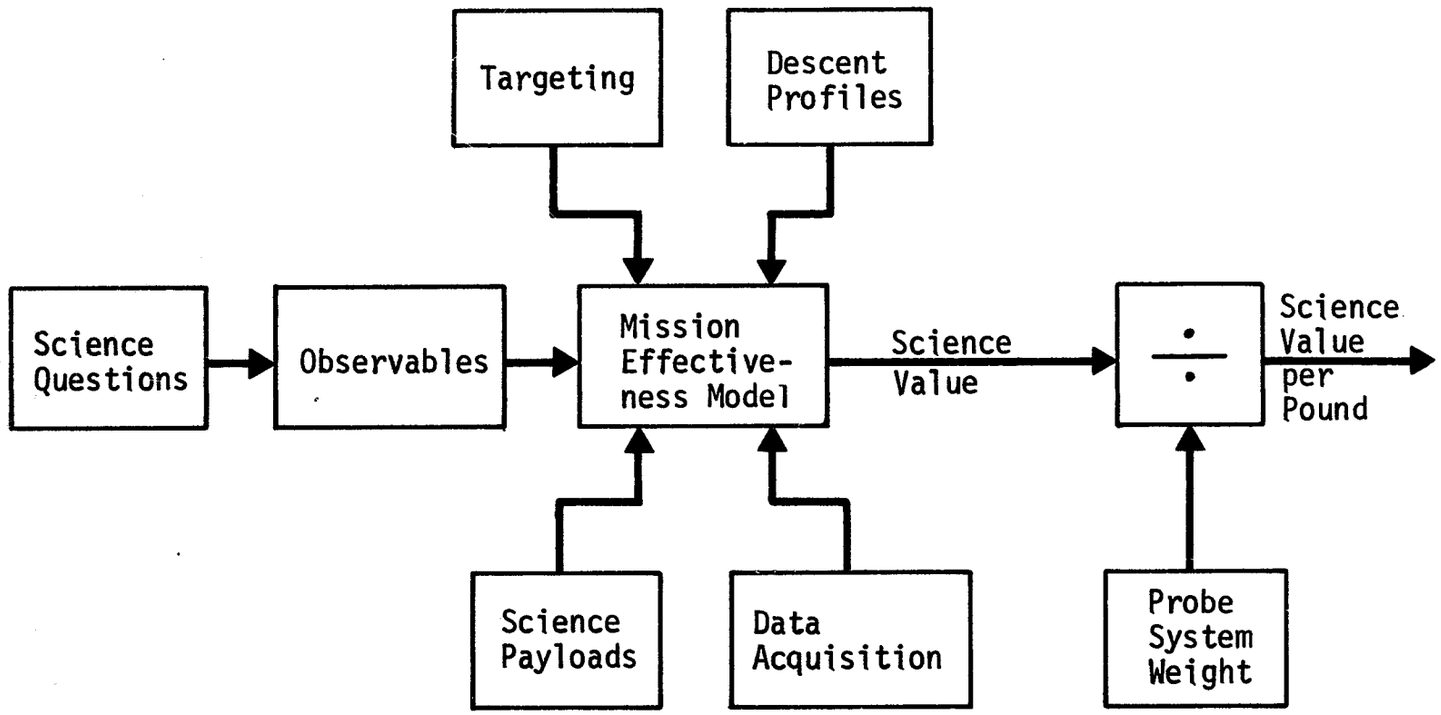


Figure IVD-1 Diagram of Mission Effectiveness Relationships

Missions B and C are grouped together, since the only difference is the orbiting of the spacecraft around Jupiter subsequent to probe release, in the case of Mission C.

TABLE IV, D-1

SCIENCE EVALUATIONS OF SAMPLE MISSIONS

Mission	Science Value	Total System Weight	Value Per Pound	Comment
DE	6.187	561	.0110	Lightside entry-science to 300 ATM.
A_1	4.522	404	.0112	Dark side entry-science to 10 ATM.
A_2	5.948	558	.0107	Dark side entry-split probe - science to 100 ATM.
B&C	8.097	600	.0135	Enter close to subsolar, expanded science payload - science to 72.4 ATM.
D	3.335	226	.0148	Darkside entry - science to 18 ATM - min. payload.
E	5.898	493	.0120	Dark side entry - science to 72.4 ATM.
F	3.335	617	.0054	Light side entry - science as in Mission D.

The science values of Table IVD-1 are the numerical outputs of the computer using the mathematical model and the mission descriptions as outlined above. These numbers have no meaning individually but they do provide a way to rank the missions in order of total achievement with at least a good estimate of ratios of total achievement between missions.

The Total System Weight listed in the table represents the launch weight of the probe systems including modifications to the spacecraft. The system weight of Mission C is partly an exception because the spacecraft modifications required for orbit insertion were not included.

Most of these numbers are slightly different than the final weights reported elsewhere in this document. The value per pound and comment columns are self-explanatory.

Inferences that can be drawn from the valuations of Table IVD-1 include:

a. For a given science payload, the deeper the probe descends the greater is the resulting value.

b. For a given designed pressure depth, the greater the science payload, the greater is the resulting value.

4. Evaluation of Parametric Probe Study

The effectiveness of a number of probe designs was evaluated, each having a -20° entry angle. One half of these designs employed a split-probe concept where the lower probe carried a pressure sensor, temperature sensor and a gas chromatograph/mass spectrometer. The upper probe carried the nominal science payload as did the other half of the designs consisting of a single probe. The variations among the designs resulted from the different design pressure-depths. Table IVD-2 tabulates some results of these evaluations.

TABLE IVD-2

EFFECT OF DESIGN DEPTH ON SCIENCE VALUE

Probe Type	Design Pressure-Depth (ATM)	Science Value	Total Probe System Weight	Value Per Pound
Single Probe	50	5.177	341	.0157
	100	5.516	372	.0148
	300	6.187	561	.0110
	500	6.488	936	.0068
Split Probe	10/100	5.825	416	.0140
	17/300	6.085	486	.0125
	22/500	6.341	543	.0117
	31/1000	6.602	653	.0101

Several inferences can be drawn from this group of evaluations, as an aid in mission design.

a. Science value increases with increased design depth but with diminishing returns.

b. Value per pound decreases with increased design depth for depths greater than 50 atmospheres in the nominal atmosphere model.

c. Since the science value is low right after staging, a maximum value per pound can be expected somewhere between staging and 50 atmospheres for the nominal atmosphere, and somewhere between staging and 300 atmospheres in the super cool atmosphere model.

d. A tradeoff of weight between an increased pressure-depth or an increased science instrumentation can now be drawn between the results of Tables IVD-1 and IVD-2. Starting with the 100 ATM single probe on Table IVD-2, 189 pounds can be added to allow the probe to descend to 300 ATM with an increase in mission value of 0.671. As an alternative, the science instrumentation can be increased resulting in an increase in system weight of 228 pounds to produce a Mission B with an increase of science value of 2.581. In other words, increasing the science instrumentation increases the resulting science value three times as fast as increasing the design depth, for these two very similar examples.

e. The requirement to penetrate well below the clouds represents a level of about 150 atmospheres in the Cool-Dense model. The probe design pressure-depth should be at least that deep, regardless of other considerations, as long as there is a chance that the Cool-Dense model could approximate the Jupiter atmosphere.

Figure IV-2 is a composite plot of the degree to which the science questions (observables) are answered by two probe configurations. The first is a split probe descending to 1000 atmospheres and the second is a single probe descending to 300 atmospheres. It is apparent that significant value differences exist only with respect to questions

1, 2, 4 and 5. This detailed comparison is also borne out by Table IVD-2 where the science values increase with increasing system weights while the science values per pound are inversely related to the weights.

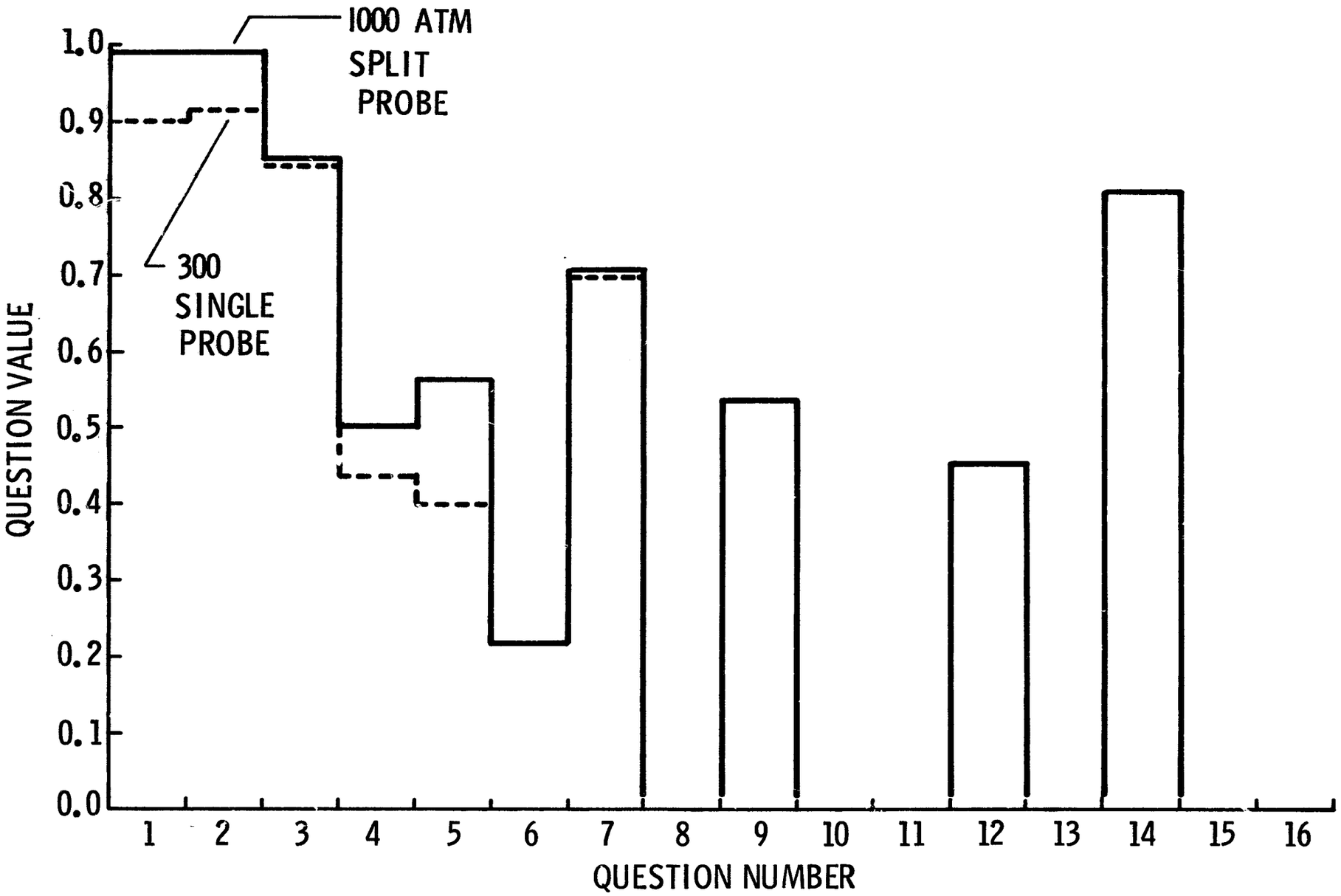


Figure IVD-2 Science Value Versus Question Number for Two Configurations

V. BASELINE PARAMETRIC PROBE SYSTEM IMPLEMENTATION STUDY

A. Introduction

The primary objective of the Jupiter Probe Study is to examine the feasibility of obtaining science data at increasing depths in the atmosphere and the penalties in subsystem design associated with increasing depth. In this chapter, the science requirements and probe engineering concepts defined in previous chapters are applied to the determination of system weight and power requirements for a range of survival depths. The spacecraft relay mode is selected since as noted previously it affords much greater flexibility and data return potential than does the direct link mode.

In performing this study, a flyby radius at periapsis, R_p, of 2.0 Jupiter Radii, which is optimum for probe communications, is used as the basis but the influence of larger values is also examined. The larger values are of interest when considering combining probes with multi-planet missions where R_p is constrained by the swingby requirements. Entry angle, γ_E, variations are included since targeting for areas well into the light side involves steep entry angles, γ_E. Finally; the influence of science payload weight and bit rate; the impact of a cool dense atmosphere; the influence of launch opportunities other than 1978; and the influence of heat shield weight fraction variation are also examined.

The intent of this study is to provide design information parametrically so that it can be used to estimate probe and total system weights and power requirements for a sufficiently broad range of conditions to be of value in future mission planning. The following paragraphs contain a discussion and definition of the descent profiles and ground rules used in the parametric study as well as the size, weight and power-required data obtained. From these, bounds on probe mission operation are identified.

In Chapter VI, system design and mission operations are detailed for one of the probes analyzed in the parametric matrix of this chapter.

B. Science Payload and Descent Profiles

Payload

The nominal payload defined in Chapter III constitutes the basis for the parametric study. Weight and power requirements are as follows:

Descent Phase	Weight (lbs.)	Power (w)	Volume ($in.^3$)
Temperature (2)	3.0	.2	15
Pressure (5)		.1	10
Accelerometer Triad (at cg)	3.0	3.0	18
Single Accelerometer off (off cg)	1.0	1.0	6
Gas Chromatograph/Neutral Mass Spectrometer	7.0	12.0	320
Photometers (3)	2.0	1.0	36
	16.0	17.3	405
Pre Entry			
Ion Mass Spectrometer	3	1	80

Single Probe Descent Profiles

The desired sampling interval (No. of samples/scale height) and the sample processing time for each of the instruments in the nominal payload was established in Chapter III. These quantities establish the allowable descent velocity of the probe. The shortest duration descent profile, and therefore the one yielding the lightest system weight, would be one with a variable Ballistic Coefficient, ie, a

ballistic coefficient increasing in a fashion such that the velocity stays at the maximum allowable value. Since such a continuously varying coefficient is not practical to achieve, a two stage ballistic coefficient descent profile was adopted. The first stage, which begins when the entry aeroshell is jettisoned, uses a parachute to achieve the required drag and the second stage achieves it through aerodynamic modifications to the pressure vessel. The staging times are selected to obtain the minimum descent time. (The slight decrease in time which would be achievable with a three or four stage descent does not appear to justify the added complexity.)

Five altitudes were chosen to cover the range to 1000 atm: 50, 100, 300, 500 and 1000 atm. A 2-stage profile was then calculated for each altitude as described above and the resulting profiles are plotted in Figure VB-1. Resulting descent times are respectively 1.30, 1.65, 2.47, 3.03 and 3.75 hours. The first stage in each requires a ballistic coefficient of 0.05 slugs/ft^2 which is established by the velocity requirement at 1.0 atm, i.e., although initial sampling is started at 0.2 bars (the altitude of chute deployment) the sample interval criteria is not adhered to above 1.0 bar since an excessively large parachute and extremely long descent times would result.

Bit rates consistent with the sampling criteria of Chapter III require 40 B/S at start of descent with a switch to 10 B/S near the end of the longer missions.

Split Probe Descent Profiles

As discussed in Chapter IV the dual relay or "split" probe concept is attractive for achieving data return from deeply penetrating probes or from probes associated with flyby spacecraft operating at

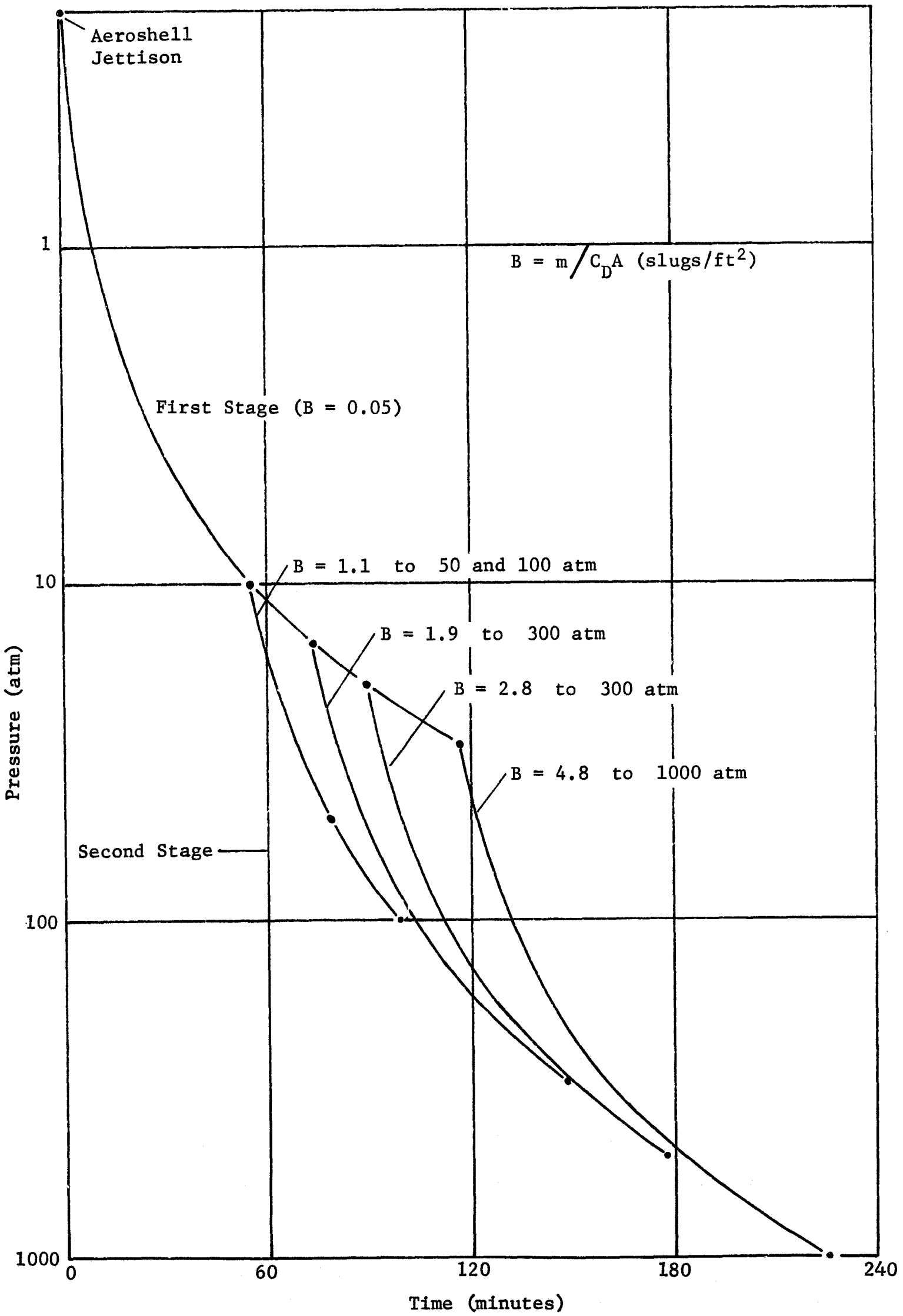


Figure VB-1 Single Probe Descent Profiles

large periapsis radii, e.g., 1979 Grand Tour spacecraft. Consequently a set of split probe descent profiles was also developed for the same altitude levels, 50, 100, 300, 500 and 1000 bars. The depth of the upper, or relay, probe and the ballistic coefficients of the lower probes were again selected to yield the shortest duration mission possible within the sampling interval criteria. The resulting time and bit rate profiles are shown in Figure VB-2. The descent times are 0.73, 0.93, 1.33, 1.58 and 2.0 hours respectively or about 55% of the single probe times.

Pre-entry Science Profiles

A pre-entry bit rate of 100 B/S has been defined as the desired minimum, however, probe power requirements in this parametric study are based only on the descent phase bit rate requirements to emphasize the sensitivity of probe systems to survival depth. For several cases where the resulting system does not provide the minimum pre-entry bit rate, the required modifications to the system are identified.

C. Selection of Parameter Ranges

1. Periapsis Radius, R_p: as determined from trade studies conducted for the trial mission (Chapter VII, Vol III), a value of R_p = 2.0 R_{2l} was found to be near-optimum for the probe/spacecraft communications link for mission times in the range of 1 to 3 hours. This value was therefore used for the major portion of the parametric study. However, since R_p's as large as 6.8 R_{2l} are required for Grand Tour missions, it was decided to examine the influence on the probe systems of an R_p that large. An intermediate value, R_p = 4.0 R_{2l} was included.

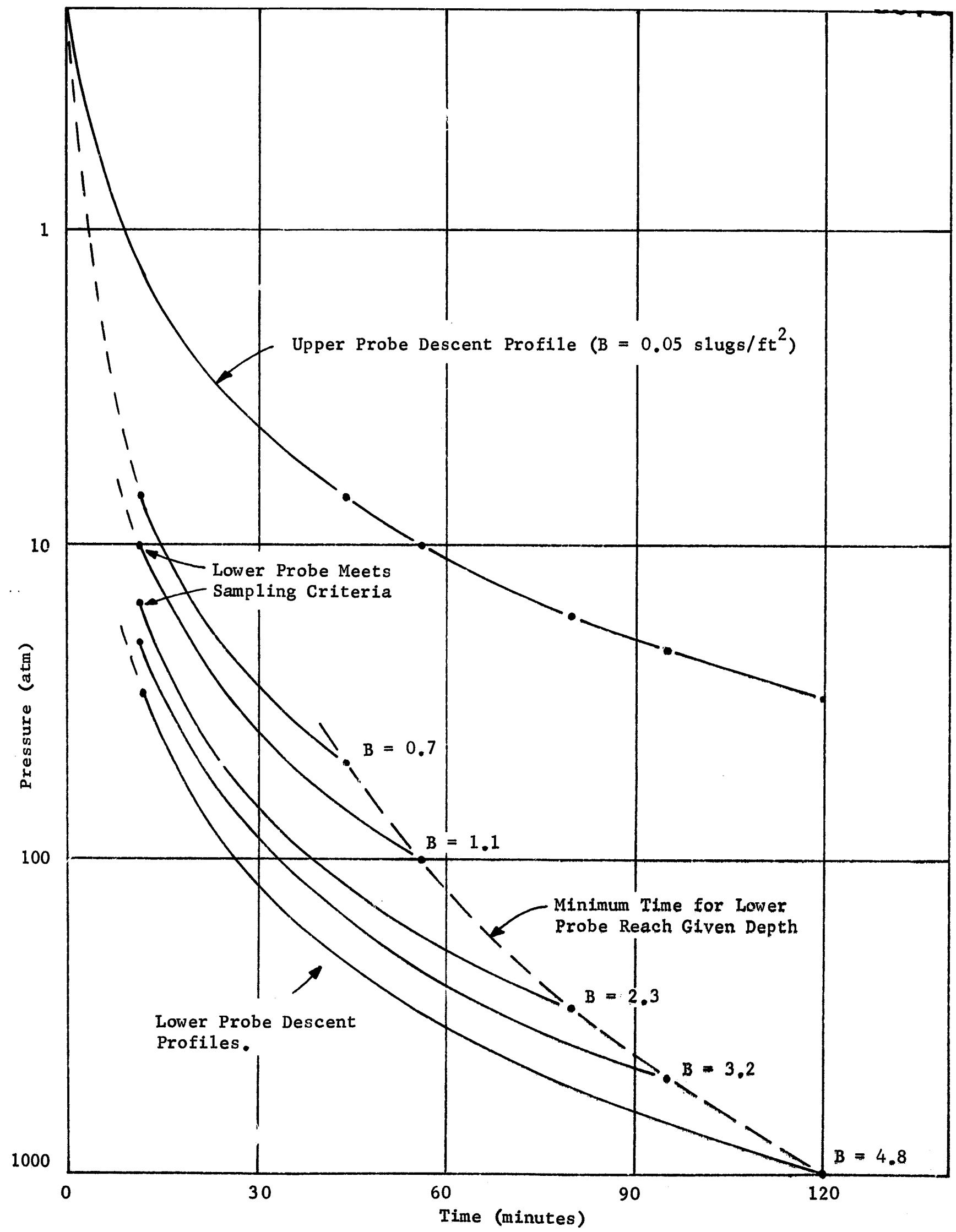


Figure VB-2 Split Probe Descent Profiles

2. Entry Angle, γ_E: With an $R_P = 2.0$, and with a Probe Ejection Range of 10×10^6 km, the minimum entry angle which precludes skip-out is $\sim$-8° based on 3σ ΔV implementation errors of 1% in magnitude and 1° in application angle (Skip-out occurs at -4.0 degrees). The angle to preclude skip-out increases to $\sim$-20° for larger ejection ranges and larger implementation errors. A value of $\gamma_E = -10°$ was selected as the lower bound for purposes of the study.

For the upper bound, a $\gamma_E = -50$ was selected, since this angle permits targeting such that the subsolar point can be bracketed in the probe descent phase. Steeper angles do not appear to afford any particular increase in science return and do result in severe weight penalties in the probe aeroshell design.

3. Science Weight and Bit Rate

Payload weights of ½ and twice the nominal value were examined, with a fixed bit rate; and bit rates of ½ and twice the nominal were considered with a fixed science payload weight.

4. Atmosphere Model

The Cool Dense model was evaluated for a 300-bar single probe and a 1000-bar split probe to determine probe weight and power requirements relative to the Nominal model.

5. Heat Shield

Heat Shield Weight Fractions of 50% greater and 50% less than the nominal values were evaluated.

D. Ground Rule and Assumptions Summary

1. General

Range at Probe Deflection - 2.6×10^7 km for TOPS; 1.0×10^7 for Pioneer.

1978 Launch opportunity - Type II trajectory.*

Nominal atmosphere model.

Nominal science payload.

Bit rate - Initial/Final = 40/10 B/S.

Single probes to have a maximum of two (2) ballistic coefficient stages after aeroshell jettison with only one of these making use of a parachute.

Descent instrument deployment must occur at or above 0.2 ATM at which time the entry vehicle velocity must have been reduced to at least M.8 to facilitate chute deployment. This fixes the minimum allowable entry ballistic coefficient for any entry angle.

2. Spacecraft

The parametric study is primarily based on the TOPS Vehicle since the probe tracking antenna scan angle range was initially considered to be too large, $\sim 150°$ to cover the full descent depth range, to use the Pioneer spacecraft. However, the concept of a boom-mounted, mechanically despun and gimballed antenna, discussed in Chapter V, Vol III makes it possible to consider the Pioneer spacecraft for these probes also. Reduced accuracy of ΔV implementation, due to the spinning spacecraft, may still constrain the Pioneer applicability, see Section G and H.

---

* Probe system results can be applied also to Type I trajectories since the V_{HP} differences do not significantly alter the communications geometry which can be achieved.

The Spacecraft Modification Weights are based on the JPL Probe on TOPS Study,** as modified for differences in the MMC probe antenna concepts, etc. Table VB-1 of Vol III shows the breakdown of these weights.

Pioneer spacecraft modification weights are estimated based on the mechanically despun probe antenna concept and are shown in Table VB-2 of Volume III.

**NASA Briefing on TOPS by JPL 6/29/70.

3. Communications Ground Rules

It was necessary to establish the following ground rules for treating the telecommunications and data handling subsystem for the baseline parametric portion of the study in order to provide an equal degree of optimization of the systems for the various entry and trajectory conditions:

a. Select frequency, transmitter power and antenna parameters to meet the communications relay link requirements for the post entry phase of each probe mission.

b. Determine what bit rate if any results during the pre-entry phase.

c. In determining transmitter and antenna requirements for the probe to S/C link, begin with a reference system of a 10 watt probe transmitter output power, a 7 db-100° half power beamwidth probe antenna, and a 3.4 ft diameter spacecraft relay antenna. Increase power in steps of 10 watts as required until 40 watts is reached. If more signal is required increase spacecraft antenna diameter until a maximum diameter of 4.9 ft is reached. If still more signal is required increase transmitter power in steps of 10 watts until 60 watts output is reached. Do not consider requirements beyond 60 watts and 4.9 ft diameter spacecraft antenna.

d. Modulation for all missions for the probe to S/C link was to be coherent PCM/PSK/PM using a single square wave subcarrier biphase modulated by a 1/3 rate constraint length 4 and convolutional encoded bit stream. Bit error rate probability requirement was set at 5 parts in 10^4. (See the Design Control Table for the Design Example Mission, Chapter VI.)

e. Initial bit rates for post entry were set at 40 bps. This rate was lowered to 20 bps for the upper probe of a split probe mission when the upper probe reached a depth of 17 atmospheres. For single probe missions the rate was lowered from 40 to 10 bps when the probe reached a depth of 30 atmospheres except for a 50 atmosphere terminal descent profile where the target depth for the mission

was only 50 atmospheres. The lower probe data rate for a split probe was 9.85 bps. Wide band noncoherent FSK modulation is used for the probe to probe link. An example communications design control table for a split probe for a 1000 Earth atmospheres depth is given in Table VD-1.

f. For pre-entry communications the probe transmitter was to be used in conjunction with a relay antenna mounted on the rear of the entry vehicle. This antenna pattern is either of the butterfly type or similar to the entry probe antenna depending upon the pre-entry antenna aspect angles. The post entry probe relay antenna is not exposed at this time and cannot be used until after the probe is staged from the aeroshell.

g. Acquisition and storage (in the probe) of entry data as well as the first 3 minutes of post entry data is assumed. This data is multiplexed with real time data in the post entry data transmission mode.

h. The TOPS S/C subsystem for the baseline parametric study required the adding of an automatic frequency acquisition and auto track relay antenna system, data receiver, demodulator, decoder, bit synchronizer, data storage interface and control as well as programmer control for signal acquisition. Weight of these subsystems was assumed fixed except for the antenna which for some uses varied in size depending upon the communications geometry for a particular entry flight path angle and R_p.

i. Weight of the entry vehicle data handling system including the probe subsystems was fixed depending upon whether it was a single or split probe mission.

j. The lower probe telecommunications and data handling subsystems were held constant for all depths since the weight change would have been insignificant.

k. For purposes of determining transmitter power and antenna requirements a total signal to noise power density ratio as shown in Figure VD-1 would be used.

l. Transmitter weight and input power for a given output power is shown in Figure VD-2 for transmitter output up to 70 watts. Serious consideration was not given to use of transmitters having outputs higher than 40 watts.

TABLE VD-1

PROBE TO PROBE COMMUNICATION LINK CALCULATIONS
(NOMINAL ATMOSPHERE)

WIDE BAND FSK

		Adverse (db)
Transmitter Power (2 W, 1 GHz)	+33 dbm	0
Transmit Antenna Gain (Max)	+5.0 db	0
Transmit Antenna Pointing Loss (@ 45°)	-1.5 db	5.2*
Receive Antenna Gain	+5.0 db	0
Receive Antenna Pointing Loss (@ 45°)	-1.5 db	2.5*
Transmit Circuit Loss	-0.5 db	0.5
Receive Circuit Loss	-0.2 db	0.2
Atmospheric Losses	-8.9 db	0
Polarizaton and Miscellaneous	-1.0 db	0.3
Space Loss (595 km, 1.0 GHz)	-147.9 db	1.0
Total Gains and Losses	-151.5 db	9.7
Received Signal Power	-118.5 dbm	9.7
Receive Noise Power Density (System Temp = 2130°k)	-165.3 dbm	1.0
Filter Bandwidth (13 kHz)	+41.1 db	0
Required Input SNR (Bit Error Probability 1×10^{-5})	-5.0 db	0
Required Input Signal Power	-129.2 dbm	10.7
Margin	+10.7 db	10.7 db

NOTES:

*Allowance for turbulence.

1. Upper probe at 31 Earth atmospheres.
2. Lower probe at 1000 Earth atmospheres.

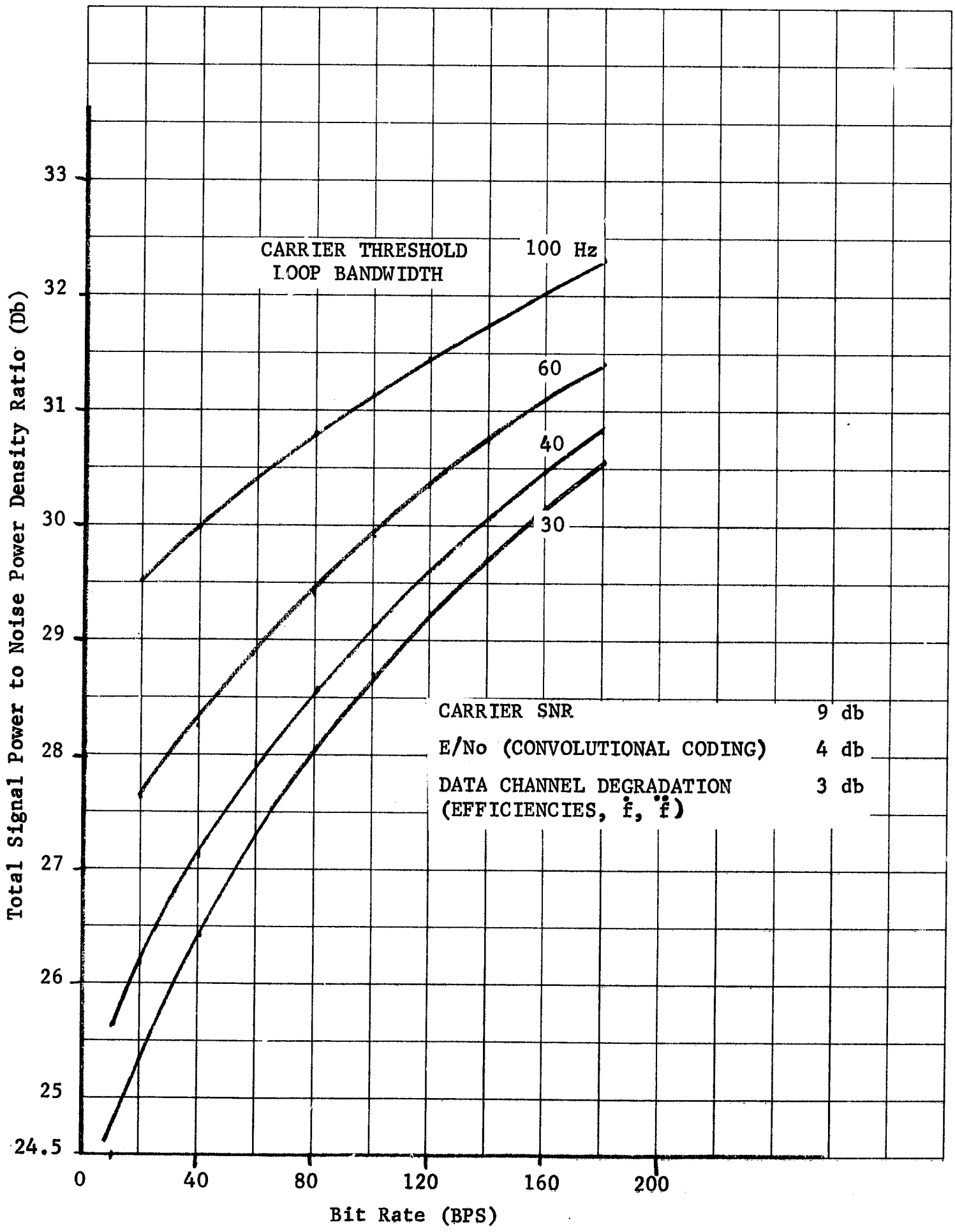


Figure VD-1 Total Signal Power to Noise Spectral Density, Probe to Spacecraft Relay Link, Baseline Parametric Mission

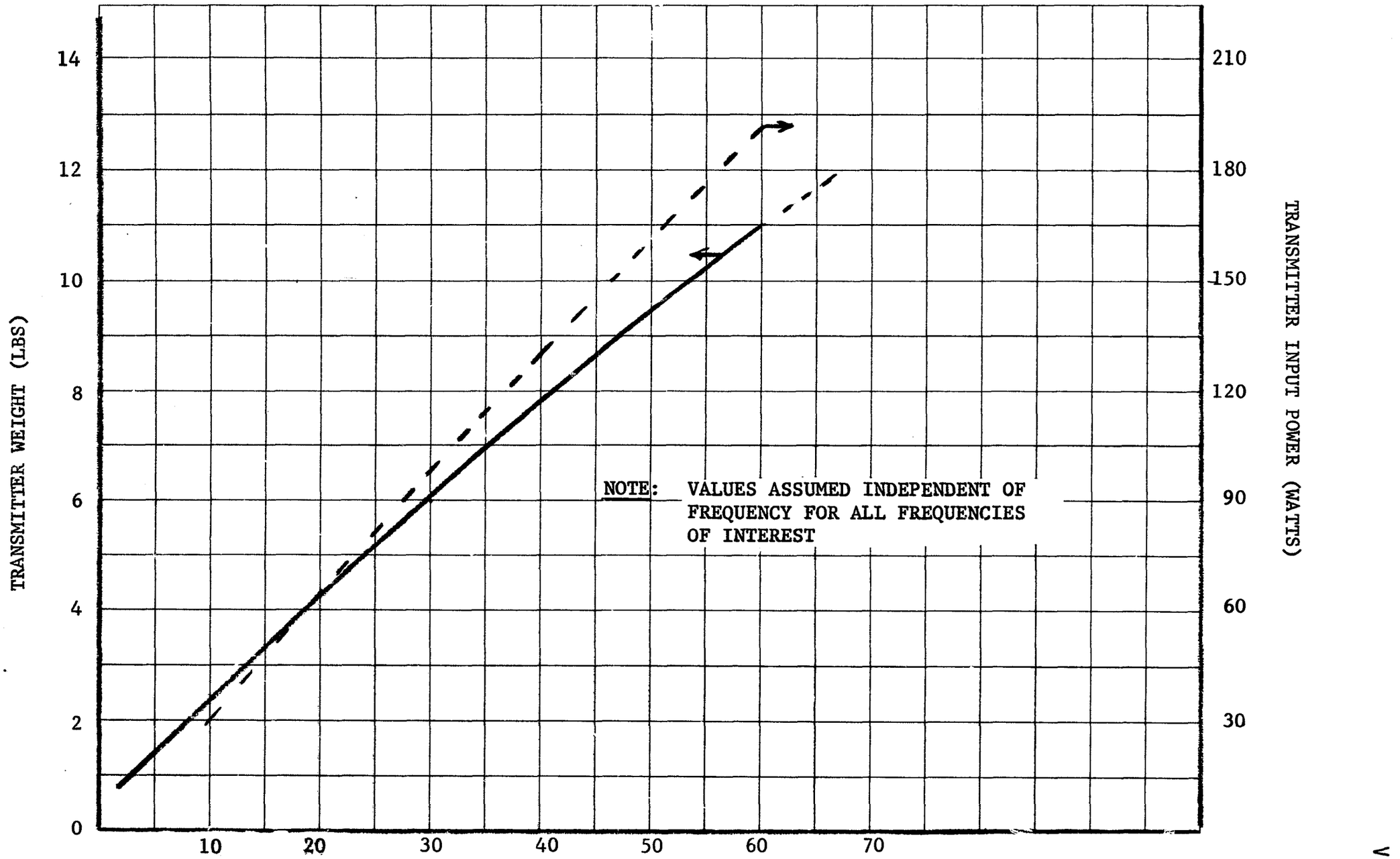


Figure VD-2 Baseline Parametric Study Transmitter Weight & Input Power vs Power Output

4. Thermal/Structural/Mechanical Ground Rules

The concepts and configurations described in Chapter IV form the basis for the parametric study. Specifically:

Entry and Descent Probe Configurations - Figure IVB3-1 shows the arrangement for the single and split probes. The methods of obtaining weight estimations for the subsystems, e.g., heat shield, aeroshell structure, pressure vessel, insulation aerodynamic stability, etc., are given in Chapter V, Volume III. The effect of increasing γ_E is accounted for both in aeroshell weight, due to the higher dynamic pressures on the support structure and insulation weights due to the higher G. Component weights (electronics) are not increased to account for the higher G at steep gammas since the appropriate data is not available.

Deflection Method of Operation - Method 1 (3-axis guidance and control system on the probe) is used for subsystem weight estimations for TOPS missions - see Chapter V, Volume III. The deflection system is jettisoned prior to entry. Also jettisoned is the thermal control insulation blanket and the Ion Mass Spectrometer. For Pioneer, Method 2 (spin stabilization and precession) is the basis, see Chapter V, Volume III.

E. Results and General Observations - Probe System Parametric Study

1. Tabulations of Results

Table VE-1 contains a summary of the probe system weights and power requirements obtained for all the combinations of descent survival depth, γ, R_p, and model atmosphere analyzed. More detailed breakdowns of the subsystem contributions for a number of the probes can be found in Table VE-2. Each data point represents a specific design.

2. General Observations and Trends

Several observations are made below and a more detailed discussion follows in Sections F through J.

a. Entry Aeroshell and Total Probe Systems weights vary significantly with γ due to the strong influence of dynamic pressure on aeroshell structure weight. The Descent Probe (portion of total probe system which remains after the aeroshell is jettisoned) weight does not vary significantly with entry angle because the tendency for increased insulation and internal support structure weight due to the higher entry G loads is offset (in most cases) by improved communications geometry.

b. Although total probe system weight increases steeply with increasing depth, probe power requirements become critical before weight becomes critical for single probes going to significant depths or associated with large Periapsis Radii. Split probes are not so constrained.

c. For a single probe to 300 bars, designing for both the Cool Dense atmosphere model and the nominal atmosphere model results in a 30% increase in total system weight over that required for the nominal atmosphere. Designing the same 300 bar probe just for the Cool-Dense model can be accomplished for essentially the same weight as the nominal model probe, as the reduced descent time and lower temperature in the cool model more than offset the increased transmitter power required to deal with the greater atmospheric attenuation but the entry dynamic pressures are more severe.

TABLE VE-1

SUMMARY OF PARAMETRIC STUDY PROBE SY

No.	R_P	γ (DEG)	Survival Depth Single (Atm)	Survival Depth Split (Atm)	ΔV (M/S)	Probe RF Power Req'd (Watts)	Frequency (GHz)	Trac Ante Dia (f
1			50			10	1.6	3.4
2			100			20	1.6	3.4
3		-10	300		75	40	1.2	4.9
4			500			70	1.2	4.9
6				300		10*	2.3	3.4
7				500		10*	2.3	3.4
8				1000		20*	2.3	3.4
9			50			10/20	1.8/2.3	3.4/
10			100			20/30	1.6/2.0	3.4/
11 (11 COOL**)			300			40 (60)	1.2 (.85)	4.2
12	2.0	-20	500		80	70		4.9
13A				100		10*	2.3	3.4
14				300		10*	2.3	3.4
15				500		10*	2.3	3.4
16				1000		10*	2.3	3.4
17		-30	50		90	10	2.0	3.4
19			300			40	1.2	3.6
25			50			20	1.6	3.4
27		-50	300		125	30	1.6	3.4
31				500		20*	2.3	3.4
32				1000		20*	2.3	3.4
33			50			40	1.8	4.2
34		-20	100		200	50	1.4	4.9
35	4.0		300			152	1.0	4.9
37				300		30*	2.3	3.4
38				500		40*	2.3	3.4
40			50			113	1.8	4.9
43	6.8	-20		300	331	50*	2.3	4.9
44				500		50*	2.3	4.9

(*) Upper Probe - Lower Probes are all 2 watts

(**) Designed for both Nominal and Cool Atmosphere Models

FOLDOUT FRAME

TABLE VE-1

V-19 and V-20

STUDY PROBE SYSTEM CHARACTERISTICS

quency GHz)	Tracking Antenna Diam. (ft)	Pre-Entry Bit Rate (B/S)	Science + Comm & Power Weight (lbs)	Descent Probe Wt. (lbs)	Entry Weight (lbs)	Probe Installed on S/C (lbs)	TOTAL PROBE SYSTEM WEIGHT (lbs)
	3.4	22	45.9	69.4	228	248	320
	3.4	78	50.3	82.0	249	270	344
	4.9	200	63.6	149.7	370	399	492
	4.9	200	83.5	258.6	601	638	755
	3.4	50	68.5	130.5	337	363	446
	3.4	60	69.4	157.2	388	417	514
	3.4	200	74.7	216.5	497	534	642
/2.3	3.4/3.4	0/120	45.9/49	70.7	246	267	341
/2.0	3.4/3.4	20/120	50.3/53	84.5	273	296	372
(.85)	4.2 (4.9)	180 (180)	63.6 (73)	156.6 (180)	427 (56 2)	461 (605)	557 (718)
	4.9	120	86.0	272.0	750	803	936
	3.4	0	67.4	115.0	310	335	416
	3.4	0	68.5	135.0	370	399	486
	3.4	0	69.4	160.0	418	451	543
	3.4	100	70.6	210.0	514	552	654
	3.4	0	45.9	75.0	312	341	422
	3.6	50	63.6	162.7	573	578	683
	3.4	20	49.0	83.4	478	533	633
	3.4	0	58.3	158.5	805	881	1016
	3.4	0	72.9	180.3	810	886	1022
	3.4	0	74.7	236.9	1032	1122	1283
	4.2	0	56.4	89.5	298	352	437
	4.9	10	62.1	108.9	342	402	495
	4.9	-	-	-	-	-	-
	3.4	0	74.9	142.0	389	450	552
	3.4	0	76.9	172.8	474	547	649
	4.9	-	80.5	123.0	410	508	611
	4.9	-	82.3	152.0	404	502	606
	4.9	-	84.5	183.9	489	600	713

FOLDOUT FRAME

TABLE VE-2a

PARAMETRIC STUDY - SINGLE PROBE WE

Item	Probe Number from Parametric 1	2	3	4	9	11
Entry Angle, γ , (Deg.)	-10	-10	-10	-10	-20	-20
Descent Probe B ($Slugs/Ft^2$)	.05 1.1	.05 1.1	.05 1.9	.05 2.8	.05 1.1	.05 1.9
Maximum Ambient Presssure (ATM)	50	100	300	500	50	300
Maximum Ambient Temperature (°F)	584	833	1335	1630	584	1335
Descent Probe Shell Temp. (°F)	584	833	1100	1100	584	1100
Shell Material	Titanium	Titanium	Inconel	Inconel	Titanium	Inconel
SYSTEM WEIGHTS (LBS)						
Science Plus Comm/Power	45.9	50.3	63.6	83.5	45.9	63.6
Structure	15.7	22.6	55.9	118.8	17.0	58.2
Thermal Control	.3	.6	19.2	35.8	.3	20.3
Antenna	1.5	1.5	1.5	1.5	1.5	1.5
Misc. Struct. and Mech.	6.0	7.0	9.5	19.0	6.0	10.3
Descent Probe Total	(69.4)	(82.0)	(149.7)	(258.6)	(70.7)	(153.9)
E.V. Auxil. Struc and Mech.	(13.5)	(14.0)	(16.0)	(20.5)	(13.5)	(19.7)
E.V., ACS/Comm/Power	(42.0)	(42.0)	(42.0)	(42.0)	(42.0)	(42.0)
Entry A/S Struct.	(28.0)	(29.0)	(38.0)	(70.0)	(39.0)	(66.0)
Heat Shield	(75.0)	(82.0)	(124.3)	(210.0)	(81.2)	(145.4)
Entry Vehicle Total	227.9	249.0	370.0	601.0	246.0	427.0
Aeroshell Dia (Ft)	3.0	3.0	3.5	4.5	3.0	3.5
Entry Ballistic Coefficient	.74	.81	.89	.88	.80	1.02
Deflection Propulsion System (lbs)	(13.0)	(14.0)	(21.0)	(34.0)	(14.0)	(26.0)
ACS/TCS (Expended) (lbs)	(7.0)	(7.0)	(7.0)	(8.0)	(7.0)	(8.0)
Probe at Separation (lbs)	248.0	270.0	399.0	638.0	267.0	461
Spacecraft Mods (lbs)	(72.0)	(74.0)	(93.0)	(117.0)	(74.0)	(96)
Total (lbs)	320.0	344.0	492.0	755.0	341.0	557

FOLDOUT FRAME

ABLE VE-2a

SINGLE PROBE WEIGHT BREAKDOWN

from Parametric Matrix

	11	11* (COOL & NOM)	11** (COOL ONLY)	17	19	25	27	33	34
	-20	-20	-20	-30	-30	-50	-50	-20	-20
.1	.05 1.9	.05 1.9	0.5 1.9	.05 1.1	.05 1.9	.05 1.1	.05 1.1	.05 1.1	.05 1.1
	300	300	300	50	300	50	300	50	100
	1335	1335	375	584	1335	584	1335	584	833
	1100	1100	375	584	1100	584	1100	584	833
um	Inconel	Inconel	Titanium	Titanium	Inconel	Titanium	Inconel	Titanium	Titanium
	63.6	73.0	65.1	45.9	63.6	49.0	58.3	56.4	62.1
	58.2	67.5	41.8	18.3	58.9	22.5	60.7	20.6	30.6
	20.3	23.3	.3	.3	20.7	0.4	20.5	0.3	2.2
	1.5	1.5	1.5	1.5	1.5	1.5	1.5	1.5	1.5
	10.3	14.5	11.0	9.0	18.0	10.0	17.5	10.7	12.5
	(153.9)	(179.8)	(119.7)	(75.0)	(162.7)	(83.4)	(158.5)	(89.5)	(108.9)
	(19.7)	(19.0)	(19.7)	(18.5)	(22.5)	(21.0)	(28.5)	(18.0)	(19.5)
	(42.0)	(42.0)	(42.0)	(42.0)	(42.0)	(42.0)	(42.0)	(42.0)	(42.0)
	(66.0)	(123.0)	(90.0)	(63.0)	(120.0_	(161.0)	(293.0)	(47.0)	(54.0)
	(145.4)	(196.0)	(141.0)	(112.0)	(186.0)	(170.6)	(285.0)	(101.5)	(117.6)
	427.0	562.0	412.0	312.0	533.0	478.0	805.0	298.0	342.0
	3.5	4.0	3.5	3.0	4.0	4.0	5.0	3.0	3.25
	1.02	1.02	1.0	1.0	.97	.874	.94	.98	.95
	(26.0)	(35.0)	(26.0)	(22.0)	(37.0)	(47.0)	(67.0)	(47.0)	(53.0)
	(8.0)	(8.0)	(8.0)	(7.0)	(8.0)	(8.0)	(9.0)	(7.0)	(7.0)
	461	605.0	446.5	341.0	578.0	533.0	881.0	352.0	402.0
	(96)	(113.0)	(98.0)	(81.0)	(105.0)	(100.0)	(135.0)	(85.0)	(93.0)
	557	718.0	544.5	422.0	683	633.0	1016.0	437.0	495.0

FOLDOUT FRAME 2

Table VE-2b Parametric Study - Spli

Probe Number from Param

	6		7		8	
Entry Angle, (Deg)	-10		-10		-10	
	U	L	U	L	U	L
Descent Probe B ($Slugs/ft^2$)	.05	2.3	.05	3.2	.05	4.8
Maximum Ambient Press. (Atm)	17	300	22	500	31	1000
Maximum Ambient Temp. (°F)	293	1335	354	1630	444	2098
Descent Probe Shell Temp. (°F)	293	1100	354	1100	444	1100
Shell Material	Titanium	Inconel	Titanium	Inconel	Titanium	Inconel
SYSTEM WEIGHTS (Lbs)						
Science Plus Comm/Power	41.0	27.5	41.6	27.8	46.6	28.1
Structure	9.5	22.7	10.6	37.6	13.2	78.1
Thermal Control	.2	9.7	.3	18.4	.6	27.
Antennas	2.5	1.4	2.5	1.4	2.5	1.4
Misc. Struct. and Mech.	11.0	5.0	12.0	5.0	14.0	5.0
Descent Probe Total	(130.5)		(157.2)		(216.5)	
E.V. Aux. Struct and Mech	(15.5)		(16.5)		(19.5)	
E.V. ACS/Comm/Power	(42.0)		(42.0)		(42.0)	
Entry A/S Struct.	(36.0)		42.0)		(55.0)	
Heatshield	(112.0)		(130.0)		(164.0)	
Entry Vehicle Total	337.0		388.0		497.0	
A/S Dia. (Ft.)	3.25		3.5		4.0	
Entry Ballistic Coef. ($slugs/ft^2$)	.94		.93		.91	
Deflection Propulsion System (lbs)	(19.0)		(22.0)		(29.0)	
ACS/TCS (Expended) (lbs)	(7.0)		(7.0)		(8.0)	
Probe at Separation (lbs)	363.0		417.0		534.0	
Spacecraft Mods (lbs)	(83.0)		(97.0)		(108.0)	
Total (lbs)	446.0		514.0		642.0	

FOLDOUT FRAME

c Study - Split Probe Weight Breakdown

er from Parametric Matrix

8		32		31		38		44	
-10		-50		-50		-20		-20	
	L	U	L	U	L	U	L	U	L
	4.8	.05	4.8	.05	3.2	.05	3.2	.05	3.2
	1000	31	1000	22	500	22	500	22	500
	2098	444	2098	354	1630	354	1630	354	1630
	1100	444	1100	354	1100	354	1100	354	1100
um	Inconel	Titanium	Inconel	Titanium	Inconel	Titanium	Inconel	Titanium	Inconel
	28.1	46.6	28.1	45.1	27.8	49.1	27.8	56.7	27.8
	78.1	18.7	89.6	16.8	44.0	13.9	39.1	16.2	39.1
	27.	.7	29.3	.4	19.7	.3	18.7	1.5	18.7
	1.4	2.5	1.4	2.5	1.4	2.5	1.4	2.5	1.4
	5.0	15.0	5.0	15.5	7.0	15.0	5.0	15.0	5.0
216.5)		(236.9)		(180.2)		(172.8)		(183.9)	
(19.5)		(29.0)		(22.0)		(22.0)		(22.0)	
(42.0)		(42.0)		(42.0)		(42.0)		(42.0)	
(55.0)		(365.0)		(294.0)		(77.0)		(77.0)	
164.0)		(359.0)		(272.0)		(160.0)		(164.0)	
497.0		(1032.0)		810.0		474.0		489.0	
4.0		5.5		5.0		3.75		3.75	
.91		1.0		.95		.99		1.02	
(29.0)		(80.0)		(67.0)		(65.0)		(103.0)	
(8.0)		(10.0)		(9.0)		(8.0)		(8.0)	
534.0		1122.0		886.0		547.0		600.0	
108.0)		(161.0)		(136.0)		(102.0)		(113.0)	
642.0		(1283.0)		1022.0		649.0		713.0	

FOLDOUT FRAME

2

F. Influence of Mission Parameters on Survival Depth, Probe System Weight and Power Requirements.

1. Survival Depth

The sensitivity to survival depth of the Total Probe System Weight (probe weight plus spacecraft modifications) is given in Figure VF-1 for the conditions of $\gamma_E = -20°$ and $R_P = 2.0$. These conditions are defined as the Reference conditions in the discussions that follow. Launch vehicle capabilities for delivering probes are also shown on the Figure. These are derived by subtracting the basic weight of the TOPS spacecraft, 1450 lbs, from the total L.V. capability. Thus the survival depth that can be achieved with any particular L.V. system and TOPS can be determined from the Figure (for the Reference conditions). The Pioneer Spacecraft situation is discussed in Section G.

From Figure VF-1 it is apparent that as far as L.V. payload capability is concerned, either the 7 segment TIIID Centaur with Burner II or the 5 segment TIIID stretched Centaur with Burner II, would be capable of delivering a single probe designed for survival to a depth of 500 atmospheres or greater. However, practical limits on probe transmitter power, 40 to 50 watts, are seen to limit the penetration to about 300 ATM. At this depth, the 5 segment TIIID Centaur with Burner II will just provide the required capability, with a Type II trajectory. For Type I trajectories, shallower survival depths result for any given launch vehicle, e.g., 250 ATM is the maximum for the 7 segment TIIID and 150 ATM for the 5 segment TIIID with the stretched Centaur.

For any specific mission it should be noted that mission-peculiar constraints may reduce the available payload by 100-200 lbs and hence reduce the achievable survival depth.

The split probe concept is seen to afford much greater depth potential, with 1000 ATM achievable for Type II trajectories and 340 ATM for Type I. The reason for only a moderate total-system-weight increase with depth for the split probes can be understood from Figure VF-2. The single probe science and data system weights are seen to remain almost unchanged with increasing depth and thus the descent probe weight build-up with depth only reflects the higher pressure and temperatures experienced. Contrasted with this in the case of the single

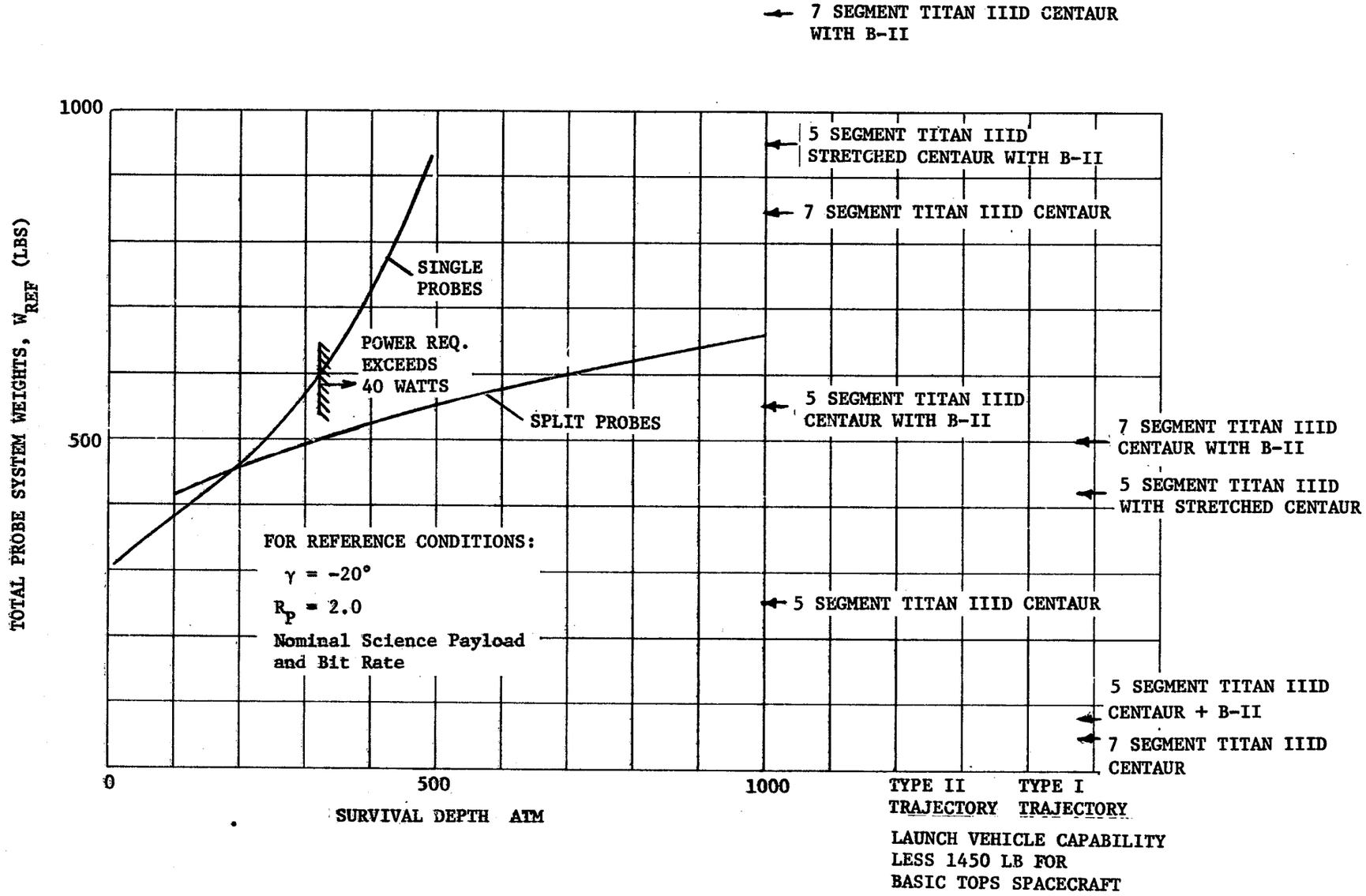


Figure VF-1 Survival Depth Achievable With Various Launch Vehicles

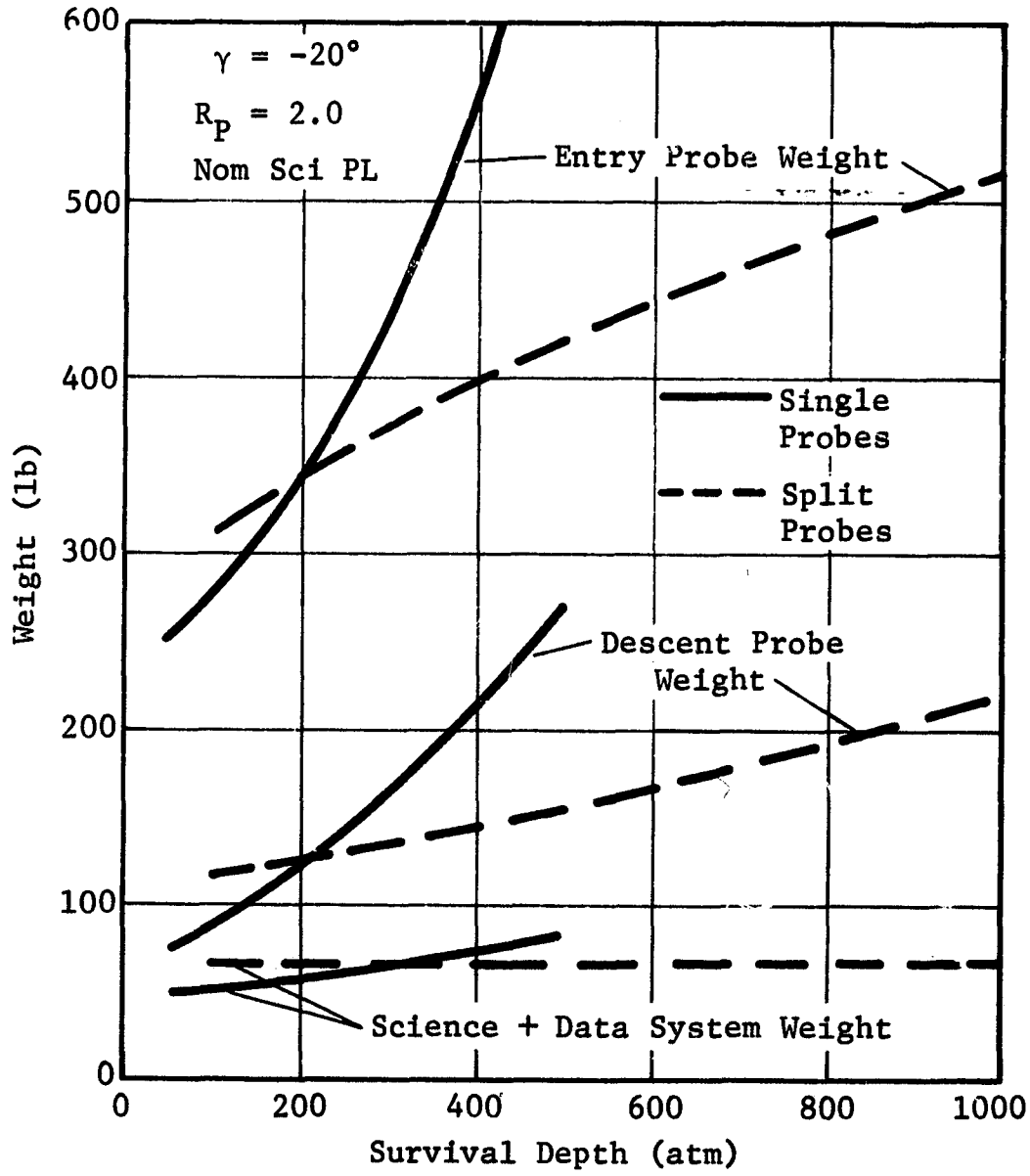


Figure VF-2 Reference Condition Probe Systems Weight Sensitivity to Survival Depth

probes is a significant data system weight (and volume) increase with depth which significantly magnifies the Descent probe weight build-up at higher pressures and temperatures.

2. Entry Angle Influence on System Weight

The total probe system weights for the various γ's analyzed for the $R_p = 2.0$ cases (Table VE-1) were normalized by dividing by the weights for the $\gamma = -20°$ (Reference) condition. Plots of the resulting weight fractions, $W/W_{(\gamma = -20°)}$, are shown in Figure VF-3.

From Figure VF-3 it is seen that a 30° increase in γ results in about a factor of 2 weight increase. Relatively small differences are seen in the sensitivity to γ between single and split probes designed for vastly different depths.

3. Radius of Periapsis, R_p, Influence on System Weight and Power

A plot of total probe system weights normalized by the Reference weight for the $R_p = 2.0$ case is shown in Figure VF-4a. Probe weights from Table VE-1 for various R_p's were divided by the Reference value weights ($R_p = 2.0$ and $\gamma = -20°$). From the resulting fractions, $W/W_{(R_p = 2.0)}$, a substantial difference is seen to exist in the R_p sensitivities of single vs split probes. This is due primarily to the marked differences in transmitter power requirements between single and split probes seen in Figure VF-4b. The lower power requirements for split probes are accounted for by the fact that the upper (relay) probe stays above 30 ATM even for the 1000 ATM survival depth cases.

Figure VF-4b shows that single probes are limited to $\sim$ 10 atm by transmitter power limits at a periapsis radius of 6.8.

4. Influence of Science Payload and Bit Rate

Science weight and bit rate variations have a relatively mild influence on total system weights compared to the influence of survival depth or entry angle, see Figure VF-5. Bit rate increases are more significant in terms of their influence on the depth at which an excessive power requirement is reached, e.g., a factor of two increase in bit rate increases the 300 ATM probe power requirement from 40 to almost 50 watts creating a marginal situation.

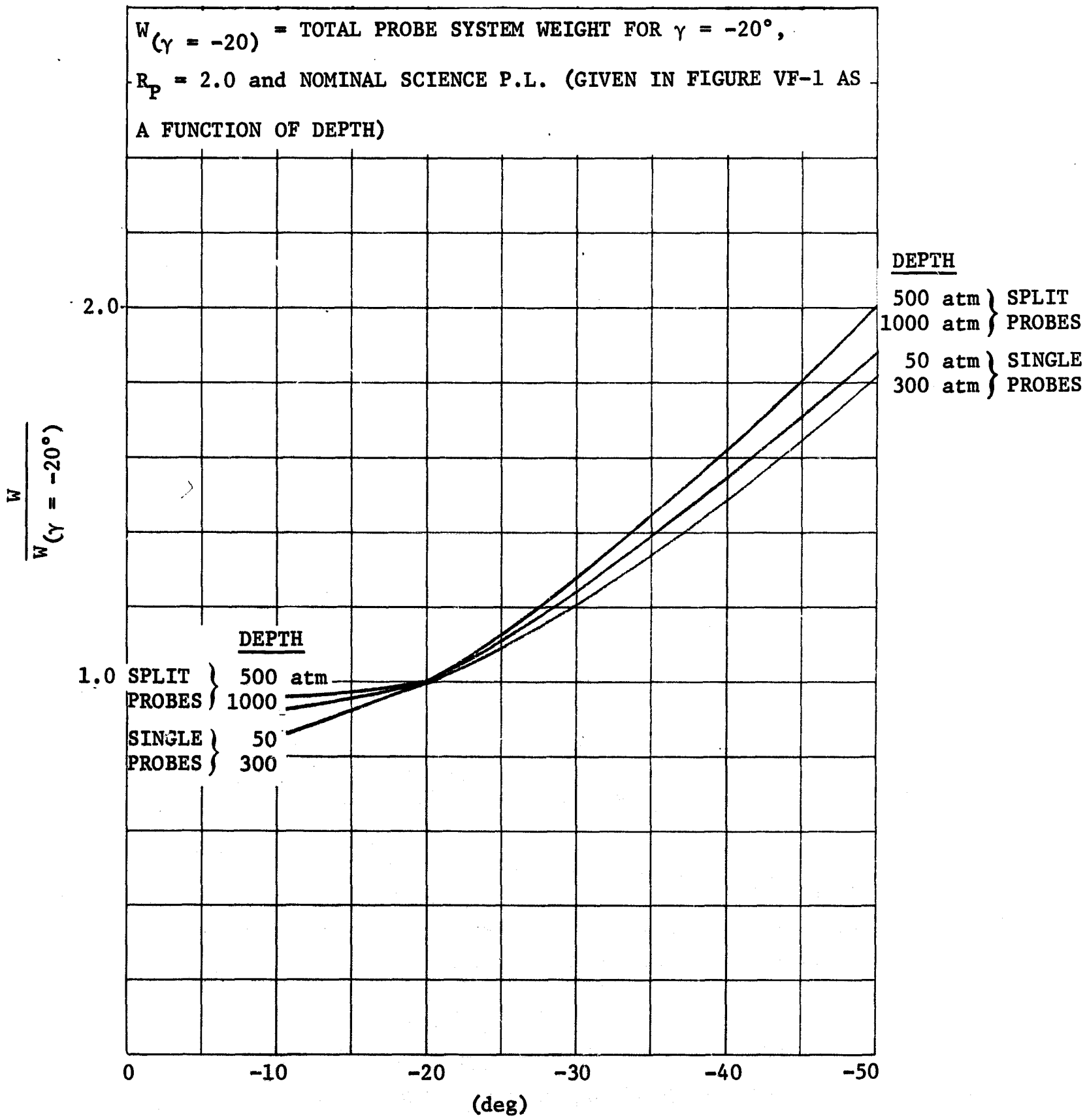
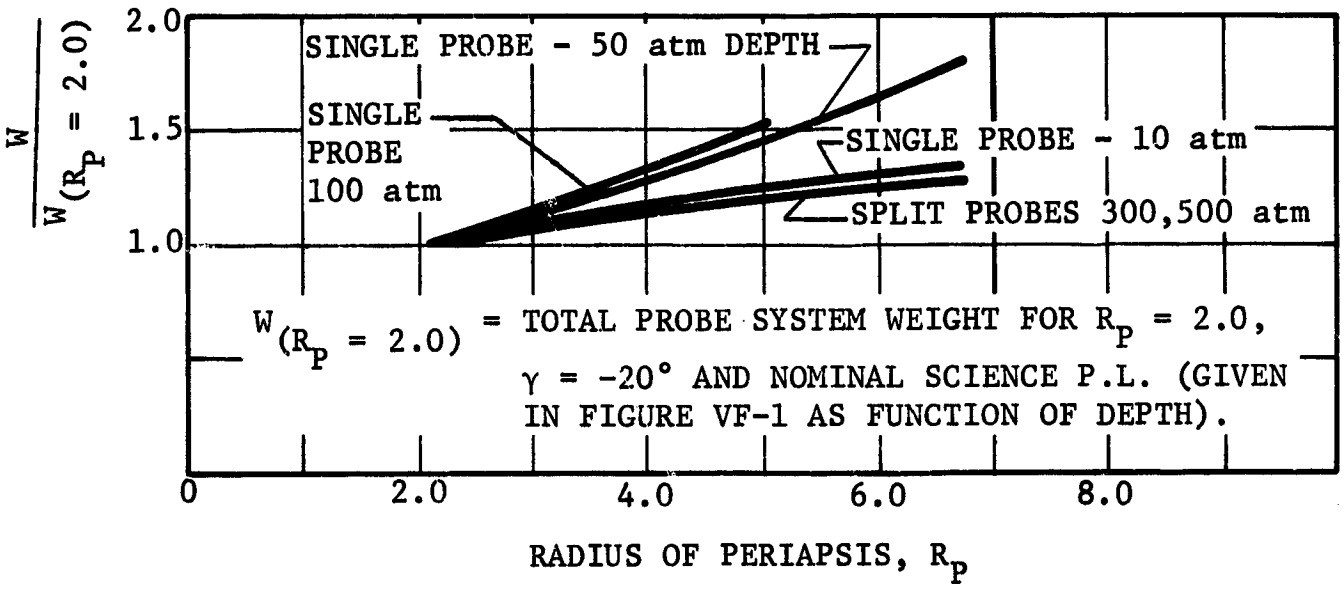
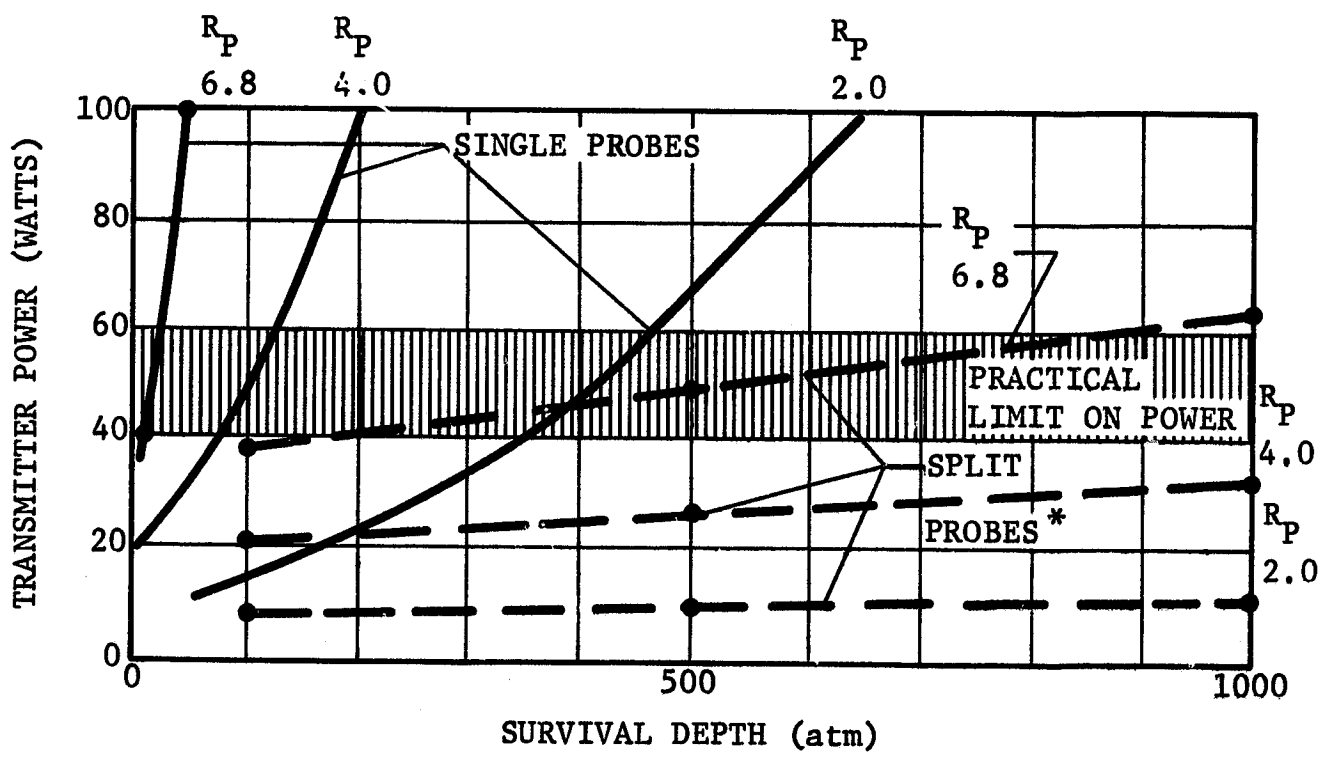


Figure VF-3 Total Probe System Weight Sensitivity to Entry Angle



a) TOTAL PROBE SYSTEM WEIGHT SENSITIVITY TO R_P



*Power required for relay link in upper probe.

b) DEPTH AND R_P CONSTRAINTS DUE TO POWER REQUIREMENTS

Figure VF-4 Effect of Radius of Periapsis R_P on Total Probe System Weight and Power Required

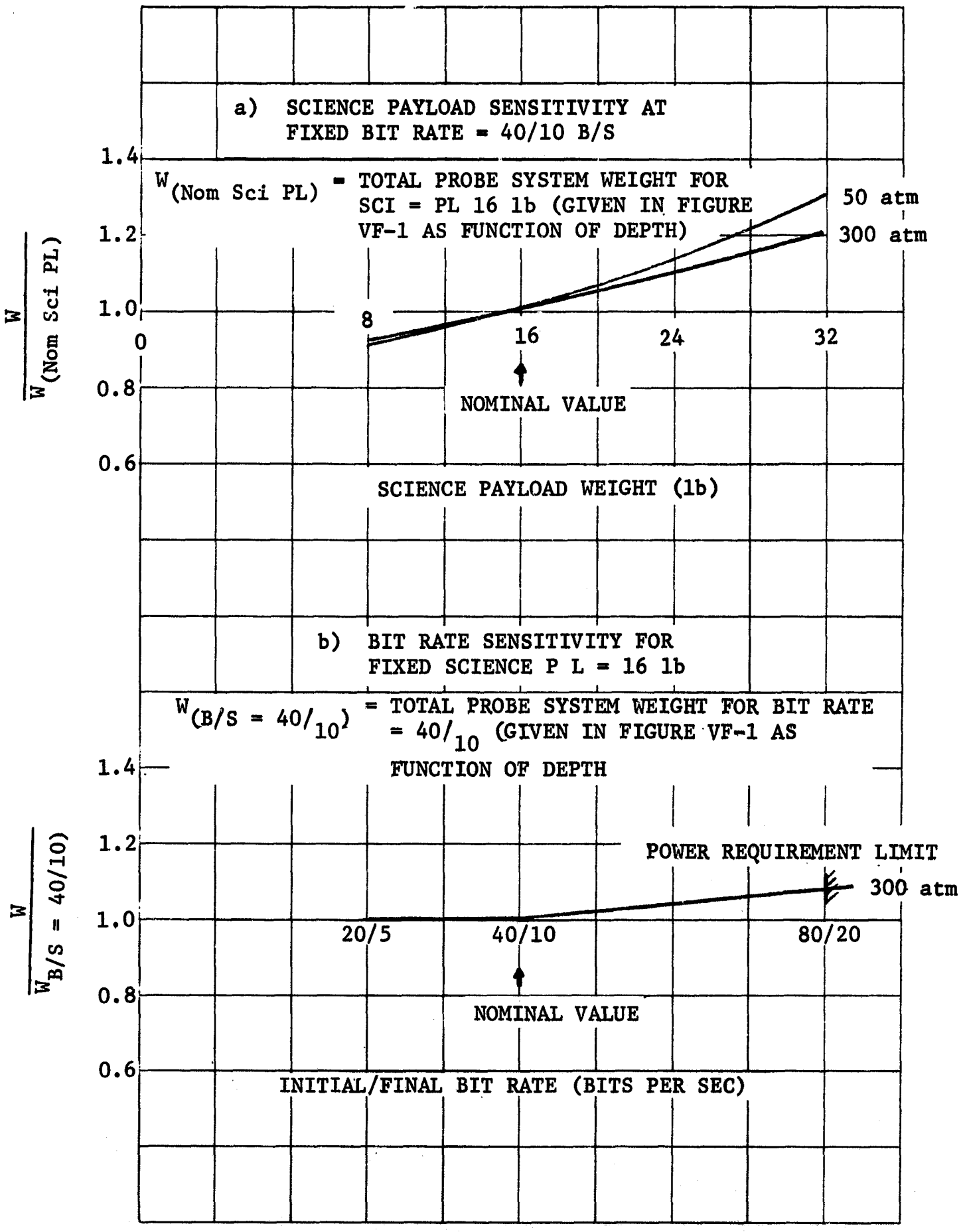


Figure VF-5 Sensitivity of Total Probe System Weight to Science Payload and Bit Rate - Single Probe Concept

5. Use of Sensitivity Plots for Estimating System Weights

To obtain the approximate Total Probe System Weight for any desired combination of the parameters evaluated (gamma, R_p, Science Payload, and Bit Rate) the weight factors of Figures VF-3 through VF-5 can be multiplied together and by the Reference Weight values from Figure VF-1 (at the desired survival depth). This process is illustrated in the following examples:

a) Performing lightside entries with Type I trajectories

If a Type I, lightside entry is desired having a minimum mission duration of 1 hour within 70° of the subsolar point, a steeper entry angle is required than the -20° used in establishing the Reference weights of Figure VF-1. This, in conjunction with the lower weight capability of the Type I trajectory, dictates that either the probe survival depth or the science payload, or both, be reduced. The amount can be determined from the sensitivity plots as illustrated below:

Lightside, Type I Entry - 1978

Time-in-Sun:

One hour within 70° of subsun.

γ_E Requirements:

γ_E = -48° due to above time-in-Sun requirement. (-48° is the steepest entry required during the arrival-date span associated with a 30 day launch window).

Normalized Entry Angle Weight Factor, $W_{(-48°)}/W_{(-20°)}$ = 1.8

(From Figure VF-3)

Normalized Science P.L. Weight Factor, $W_{.5NOM}/W_{NOM}$ = 0.9

(From Figure VF-5)

Product of Weight Factors = 1.8 x .9 = 1.62 = W/W_{REF}

Maximum Probe System Weight Capability - Type I = 500 lb

(From Table VF-1)

W_{REF} = Equivalent Weight for Reference Conditions = $\frac{500}{1.62}$ lb = 309 lb

Survival Depth for 309 lb = 10 atm (From Figure VF-1)

Conclusions: A 1-hr lightside, Type I, mission designed to a depth of 10 bars and containing a science payload 50% smaller than the nominal payload can be performed using the maximum capability of the 7 segment Titan IIID Centaur B II launch vehicle (500 lb).

Designating a time of one-half hour in the Sun instead of 1 hour changes the entry angle to -36° (weight factor, $\frac{W_{(-36°)}}{W_{(-20°)}}$, = 1.4) and the Equivalent weight for Reference conditions to $\frac{500}{1.4}$ or 357 lb, which corresponds to a survival depth of 70 atmospheres.

b. Use of "Excess" Launch Vehicle Capability to Improve Probe Performance at a Given Survival Depth.

Since for Type II trajectories and single probes, the 300 atm depth limit is dictated by power requirements and not by launch vehicle weight capability limits, the "excess" weight can be utilized to increase the entry angle capability (hence the lightside mission duration) or the science payload capability. For example, the 950 lb available with the 5 segment TIIID stretched Centaur with Burner II is a factor of 950/557 or 1.7 over the 300 atm Reference condition probe. Referring again to Figure VF-3, this is seen to permit a -47° entry which would let the probe enter close to the subsolar point.

An alternative way to benefit from the payload capability can be seen from Figure VF-5, i.e., doubling the science payload and the bit rate is seen to result in a total increase of 1.2 x 1.08 or 1.3. Thus the 300 atm probe total system weight, with such a payload would be 1.3 (557) or 725 lb, still well within capability of the 3 larger launch vehicles. The 725-lb expanded-payload probe would be equivalent in weight to a nominal-science probe designed for 400 atm (Figure VF-1). Other comparisons can be performed in a similar manner.

A precaution should be noted; for total system weights greater than about that of the reference 300 atm probe (557 lb), the modifications to the TOPS trajectory correction system become significant, see Chapter V, Volume III.

4. Launch Opportunities Other Than 1978

Launch Vehicle capabilities for the 1979 and 1980-81 opportunities are shown in Table VF-1, (with the 1450 basic TOPS weight subtracted out). Achievable probe depths for the reference conditions can be determined by comparing the tabular values with the Total Probe System Weight versus depth curves of Figure VF-1.

For the Single Probe Concept, and for Type I trajectories, the maximum survival depth for the Reference conditions (γ = -20, R_p = 2.0, P.L. = Nominal Science) increased from 250 ATM in 1978 to 300 atm in 1979 and 1980-81.

For Type II trajectories no increases are found in maximum probe survival depths in 1979-81 due to power-requirement constraints overriding weight limitations; still, the increased launch vehicle capability of 1979 and 80 can be utilized to achieve increased performance at survival depths within the power constraints. The increased performance is determined as described in a previous paragraph.

5. Multiplanet Missions

Table VF-1 shows Launch Vehicle capabilities for Jupiter-Uranus/Neptune Grand Tour missions for 1978 and 1979. Values are seen to be somewhat less than Jupiter-only missions due to the influence on C_3 of Radius-of-Periapsis constraints. To illustrate: an R_p of 6.8 is currently associated with the JUN 1979 mission by JPL, this results in a gross lift-off capability (with 7 seg TIIID Centaur, Burner II) of 1900 lbs -- only 450 lbs over the basic TOPS weight. Also the large R_p value was seen to be a constraint on survival depth, 10 ATM for R_p = 6.8, through its influence on power requirements. Some leeway is presumed possible in the selection of R_p, but reducing it increases the C_3 and at $R_p = \sim 4.8$, the gross lift-off weight capability drops to 1450 lb and thus the net weight available for probe systems goes to zero (See Figure VF-6). Consequently, reducing the R_p below 6.8 does not appear to be advantageous.

Table VF-1

Net Launch Vehicle Capabilities (TOPS Weight of 1450 lb is Subtracted from Total)

Launch Window	Launch Vehicle	1978		1979		1980-81		JUN* 1978	JUN* 1979
		Type I	Type II	Type I	Type II	Type I	Type II	Type I	Type I
30 Day	7 Seg Titan IIID Centaur w Burner II	500	1150	600	1100	900	1400	450	450
	7 Seg Titan III D Centaur w/o Burner II	50	850	150	1220	570	1220	-50	-50
20 Day	5 Seg Titan III D Centaur w Burner II	80	550	230	700	600	870	-330	-330
	5 Seg Titan III D Centaur w/o Burner II	-380	260	-150	460	340	670	-930	-930
	5 Seg Titan III D Stretched Centaur with Burner II	420	950	560	1400	1000	1270	-50	-50

*Grand Tour Missions - C_3 set at 112 km^2/sec^2

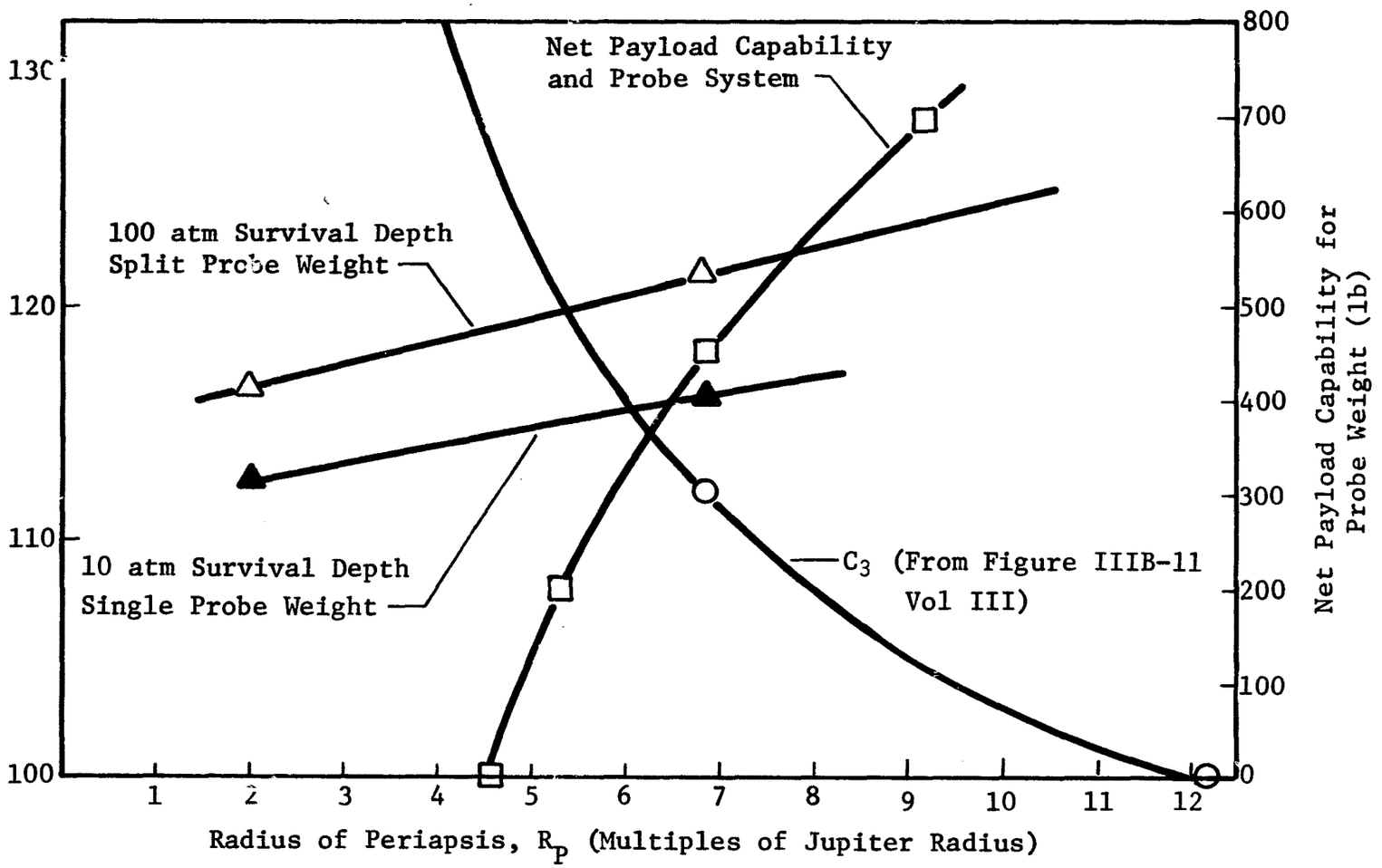


Figure VF-6 Variation of Launch Vehicle Payload Capability and Probe Weight with Radius of Periapsis - 1979 JUN Grand Tour Mission

The R_p = 6.8 and a probe depth of 10 atm corresponds to a probe system weight of about 400 lb (1.31 from Figure VF-4 times the 308 lb Reference weight from Figure VF-1 at 10 atm) which is within the 450 lb available.

In contrast to the single probe situation, with the split probe concept at R_p = 6.8 a depth capability of 100 atm is possible within the 40 w limit on probe power. The weight for such a probe is ∿ 533 lb, based on multiplying 1.28 (from Figure VF-2) times the 415 lb weight for R_p = 2.0 (from VF-1), and this exceeds the 450 lb available. However, the relatively mild slope of the probe weight versus R_p suggests that at an R_p somewhat larger than 6.8, a condition will exist where the increase in launch vehicle payload capability will match the increase in probe system weight. This situation is also depicted in Figure VF-6 from which the crossover point is seen to occur at R_p = 7.8 with a total probe system weight of ∿ 560 lb. Such a mission would thus appear to be feasible, although due to the increased communications range at the 7.8 periapsis radius, the 100 atm probe depth would have to be decreased slightly if the 40 watt transmitter power is to be maintained.

Probe missions combined with Grand Tour missions are further examined in Chapter VII in the discussions of Missions A-1, A-2.

G. Use of the Pioneer Spacecraft with the Probes of the Parametric Study

The Pioneer spacecraft was not originally considered in connection with the full range of probes examined in the Parametric Study due to the difficulty of providing a tracking antenna on the spinning spacecraft that could cover the range in spacecraft-probe aspect angle required, ∿ 150°. However, pursuant to the mechanically despun antenna work conducted for Mission B (a mission designed for Pioneer by establishing a limited aspect angle coverage, ±45°) it was concluded that the mechanically despun concept could probably be extended to obtain full probe tracking capability. This approach is discussed in Chapter V of Volume III. It involves use of a boom-mounted, gimballed antenna.

Assuming that such a configuration is feasible, and also that the potentially greater lead-time and entry-angle dispersions (due to Pioneer's large tolerance on commanded turn accuracy) are acceptable, the various probe missions of this chapter can also be delivered by a Pioneer spacecraft and smaller launch vehicles can be used.

Table VG-1 shows the revised probe system weights to account for the differences in the method of operation and spacecraft modifications with Pioneer. Primary differences are:

a. Smaller Probe Ejection Range, 10×10^6 km vs 26×10^6 km (to reduce dispersions due to probe ΔV implementation errors and reduce thermal control requirements).

b. Active Thermal Control System on board probe (due to lack of power availability on Pioneer to preheat probe prior to probe ejection).

c. Different Guidance and Control System on Probe (cannot use spacecraft to orient for ΔV, due to commanded turn inaccuracy, thus need precession system on probe).

d. Increased probe ΔV propulsion system weight (due to decreased ejection range).

e. Despun Probe Tracking Antenna.

f. Larger Structural Modification Weights.

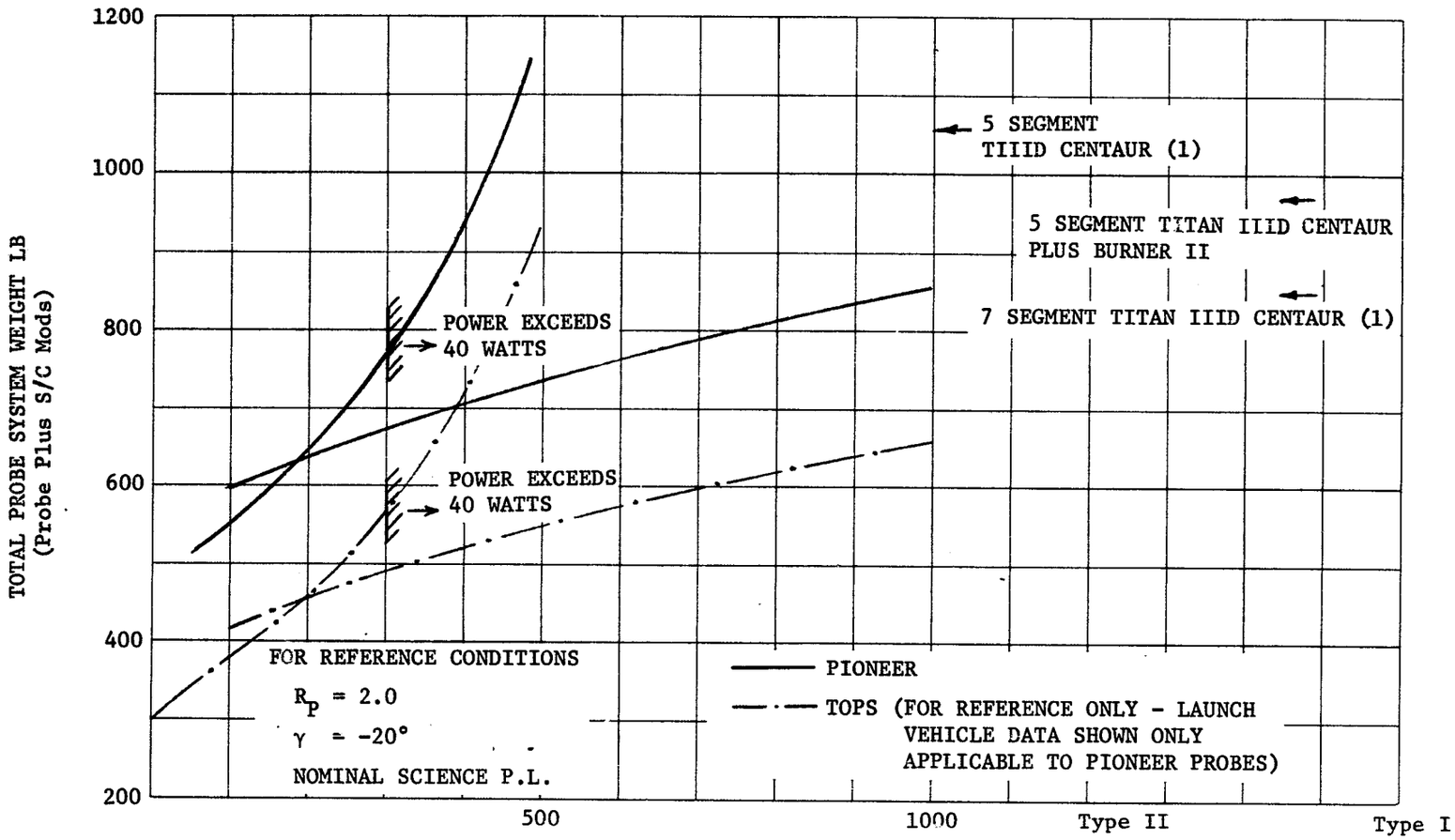
g. Data Storage System addition.

h. Increases in midcourse ΔV propellant, except that when Burner II is used the increased accuracy of insertion into the Jupiter trajectory more than offsets the effect of the added probe mass.

Total Probe System Weights from the table are plotted in Figure VG-1 along with the comparable values for the TOPS probes. Also shown on the figures are the launch vehicle capability values based on lift-off weight less the basic Pioneer weight, 557 lb.

Table VG-1 Total Probe System Weights Based on Pioneer S/C

No.	R_{EJ} (km)	R_P	γ (deg)	Depth		W_{Entry} [TOPS] (lb)	Δ T/C Sys Batt/ Heater [Fixed] (lb)	Δ G & C System [Fixed] (lb)	Δ Heatshield for TCS/G&S (lb)	New W_{Entry} (lb)	ACS/ICS Expended (lb)	ΔV M/S	W_{Probe} Installed (lb)	W_{Total} (lb)
				Single (atm)	Double (atm)									
9	10^7	2.0	-20	50		246	33	-5	+16	290	7	47	344	513
10		2.0	-20	100		273	33	-5	+16	317	7	50	374	636
11		2.0	-20	300		431	33	-5	+16	475	8	66	549	751
12		2.0	-20	500		750	33	-5	+16	794	9	100	903	1165
13A		2.0	-20		100	310	33	-5	+16	354	7	53	414	596
14		2.0	-20		300	370	33	-5	+16	414	8	61	483	678
15		2.0	-20		500	418	33	-5	+16	462	8	65	535	734
16		2.0	-20		1000	514	33	-5	+16	558	8	75	641	859



(1) 100 LB PROPELLANT FOR MIDCOURSE CORRECTIONS SUBTRACTED FROM CAPABILITY OF LAUNCH VEHICLES, EXCEPT THOSE UTILIZING BURNER II. (100 lb CORRESPONDS TO ADDED PROPELLANT NEEDED TO MAINTAIN 200 M/S ΔV WITH AN 800-lb PROBE SYSTEM ON BOARD)

Figure VG-1 Survival Depth With Pioneer Probes

From Figure VG-1 it is seen that as far as launch vehicle capability is concerned, essentially no constraints are imposed on probe depth for the reference conditions, $R_p = 2.0$; $\gamma = -20$, for either Type I or Type II missions. Probe power vs depth constraints discussed previously remain in effect.

Another consideration is the planetary vehicle dynamic stability when probes larger than the 500 lb class (700 lb Total Probe System weight class) are considered. Roll to transverse inertia ratios are reduced with increasing probe mass and a point can be reached where larger-diameter probes than optimum must be used or balance weights added to offset this effect.

H. Deflection Implementation Accuracy Impact on Probe Parametric Study Results.

Probe lead-time dispersions, and hence probe/spacecraft aspect angle dispersions, vary with ΔV implementation accuracy and with probe ejection range. Sensitivity curves relating these parameters are not available, however, as an example the probe transmitter power required to handle the aspect angle dispersions for the situations listed below was found to differ by a factor of two.

	Ejection Range, R_{eJ}	ΔV Application Angle Error Assumed. (3σ)	ΔV Magnitude Error Assumed (3σ)
a.	10×10^6 km	1°	1%
b.	26×10^6	1.5°	1%

The effect of differences in probe power on total probe system weight can be inferred from the results of the parametric study presented in Table VE-1. Data from that table plotted in Figure VH-1 shows the relative weights for probes designed to give depths with different power transmitters. This data can be applied to assess the impact of accuracy assumptions on probe weight and survival depth, when the accuracy influence on power is known.

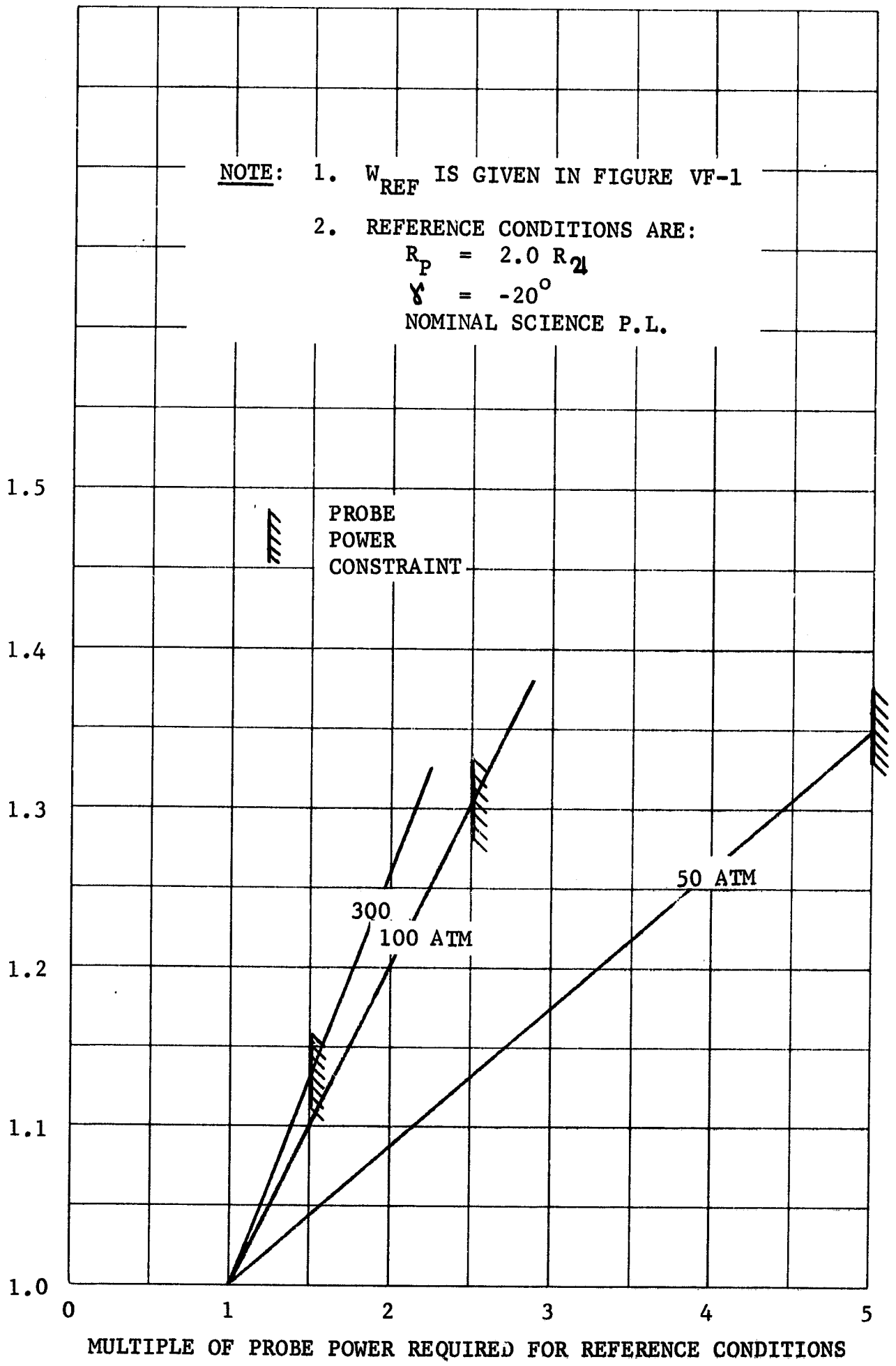


Figure VH-1 Sensitivity of Single Probe System Weights to Increased Power Requirements

I. Impact of Heat Shield Weight Fraction Uncertainties on Parametric Study Results.

The probe weights of this chapter are based on the heat shield weight fraction data provided by JPL. Since considerable uncertainty necessarily exists at this time in the heating and ablation analysis procedures, the impact of heat shield weight fraction variations on probe systems weight, and hence survival depth, has been examined. The results are shown in Table VI-1 and Figure VI-1.

It can be seen that the survival depth of 300 atm achievable with the 5 segment TIIIC Centaur with Burner II is altered to 170 Atm and 390 Atm respectively if 50% greater or lesser heat shield weights are found to be appropriate.

TABLE VI-1

EFFECT ON TOTAL SYSTEM WEIGHT OF HEAT SHIELD WEIGHT FRACTION UNCERTAINTY

		Nominal H/S Wt Fraction			1.5 x Nominal H/S Wt Fraction			0.5 x Nominal H/S Wt Fraction		
No.	Depth	Weight Fraction	W_{E}*	Total Probe System Weight*	Weight Fraction	W_{E}*	Total Probe System Weight*	Weight Fraction	W_{E}*	Total Probe System Weight*
	(atm)		(lb)	(lb)		(lb)	(lb)		(lb)	(lb)
9	50	0.33	246	341	0.495	326	434	0.165	185	271
11	300	0.34	427	557	0.51	575	740	0.17	340	456
8	1000Δ	0.35	506	642	0.525	692	863	0.175	398	522

*This includes the change in structural weight to account for the changed heat shield mass during entry.

ΔSplit probe

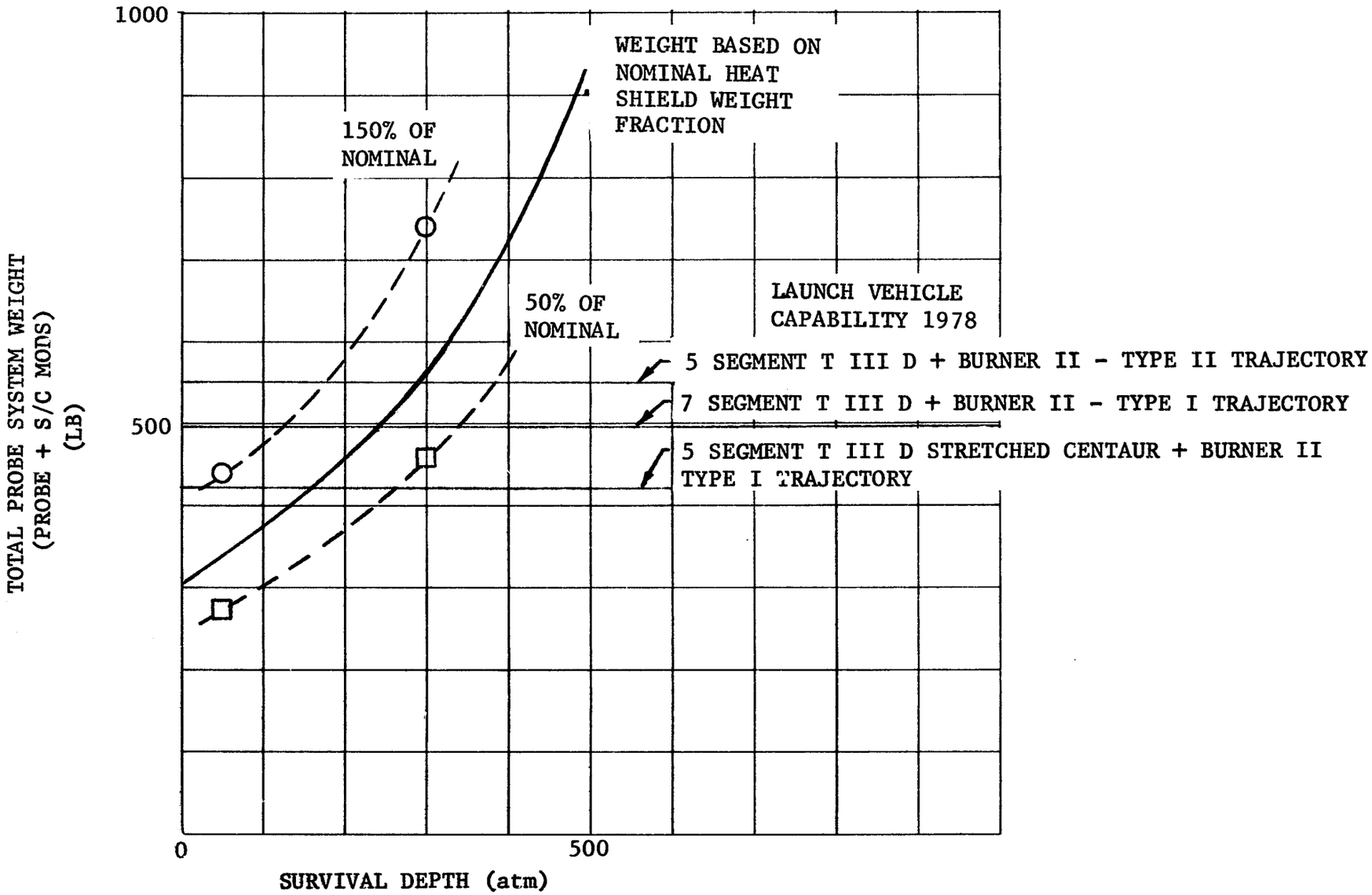


Figure VI-1 Sensitivity of Survival Depth to Heat Shield Weight Fraction - TOPS Probes

J. Impact of the Cool Dense Model Atmosphere on Communications Parameters for the Baseline Parametric Study.

Consideration of the effects of using the cool dense atmospheric model as opposed to the nominal model was given for a single probe to depths of 300 atmospheres and a split probe to depths of 31 atmospheres for the upper probe and 1000 atmospheres for the lower probe. Each was for a γ_E Of -20° and a R_p of 2 R_J.

For the single probe case the details of which are given in Chapter IV under the Design Example Mission it was found that the probe to spacecraft link margin was exceeded at a depth of 30 atmospheres in the cool dense atmosphere. This is due to the greater absorption in loss given by this model atmosphere. At 300 atmospheres in the cool dense atmosphere the link margin was 6 db below the sum of adverse tolerances. If one were to design for the cool dense atmosphere for the above case (300 atmospheres for the cool dense) one would reduce the frequency of the probe to spacecraft link from a value of 1.2 GHz to a value of 0.85 GHz and, further, increase the link gain by 3 db. Once having done this the link would also accommodate the nominal atmosphere model to at least 300 atmospheres provided the probe's thermal/structural system is designed to withstand the additional transmitter size and battery energy. (See Chapter IV.)

For the split probe case in the cool dense atmosphere it was found that at 1.1 hours after entry the lower probe had reached 1000 atmospheres and at 1.25 hours the upper probe had reached 31 atmospheres as opposed to a required time of 2 hours for the same events to occur in the nominal atmosphere.

The probe to probe link in the cool dense atmosphere suffers an additional loss of 14.8 db due to atmospheric attenuation. However, the space loss improves by 7.8 db due to the shorter range. The net result is a deficiency of 7 db in the probe to probe link at the nominal frequency of 1.0 GHz. It was found that by reducing the probe to probe link frequency to 0.85 GHz a 7.2 db improvement would result from the difference between the increase due to system temperature and reductions

in space loss and atmospheric attenuation. Thus the 7.2 db improvement at 0.85 GHz more than restores the 7.0 db deficiency found at 1.0 GHz in the cool dense model. This change in frequency requires scaling up the probe to probe relay antennas by a factor of approximately 1.18 in size. Comparisons of the probe to probe link parameters for the 3 cases are shown in Table VJ-1.

The probe to spacecraft radio link also suffers a degradation due to the cool dense atmosphere as shown in Figure VJ-1 which illustrates the difference in relay link losses as a function of time for both the nominal and cool dense atmospheres. To accommodate the cool dense atmosphere for probe to spacecraft communications a reduction in radiofrequency from a value of 2.3 to a value of 2.0 GHz will give the required improvement of 2.0 db in link margin at the end of the mission at a cost of reducing pre-entry and entry margin by one db. The 10 watt probe transmitter and 3.4 ft diameter spacecraft antenna operating at the new frequency of 2.0 GHz will provide the necessary margin for the post entry communications and sustain a pre entry bit rate of 65 bps as opposed to a 100 bps preentry rate in the nominal atmosphere.

Margin vs time for the spacecraft to probe link is shown in Figure VJ-2 for the two atmospheres and two radio frequencies.

TABLE VJ-1

PROBE TO PROBE COMMUNICATION LINK CALCULATIONS

WIDE BAND FSK

Atmosphere Model	Nominal	Cool - Dense		
Radio Frequency	1.0 GHz	1.0 GHz	0.85 GHz	
Range	595 km	240 km	240 km	Adverse (db)
Transmitter Power (2 W)	+ 33 dbm	+ 33 dbm	+ 33 dbm	0
Transmit Antenna Gain (Max)	+ 5 db	+ 5.0 db	+ 5.0 db	0
Transmit Antenna Pointing Loss (@ 45°)	- 1.5 db	- 1.5 db	- 1.5 db	5.2
Receive Antenna Gain	+ 5.0 db	+ 5.0 db	+ 5.0 db	0
Receive Antenna Pointing Loss (@ 45°)	- 1.5 db	- 1.5 db	- 1.5 db	2.5
Transmit Circuit Loss	- 0.5 db	- 0.5 db	- 0.5 db	0.5
Receive Circuit Loss	- 0.2 db	- 0.2 db	- 0.2 db	0.2
Atmospheric Losses	- 8.9 db	- 23.7 db	- 17.2 db	0
Polarization and Miscellaneous	- 1.0 db	- 1.0 db	- 1.0 db	0.3
Space Loss	-147.9 db	-140.1 db	-138.7 db	1.0
Total Gains and Losses	-151.5 db	-158.5 db	-150.6 db	9.7
Received Signal Power	-118.5 dbm	-125.5 dbm	-117.6 dbm	9.7
Receive Noise Power Density	-165.3 dbm	-165.3 dbm	-164.6 dbm	1.0
Filter Bandwidth (13 kHz)	+ 41.1 db	+ 41.1 db	+ 41.1 db	0
Required Input SNR (Bit Error Probability 1 x 10^{-5})	- 5.0 db	- 5.0 db	- 5.0 db	0
Required Input Signal Power	-129.2 dbm	-129.2 dbm	-128.5 dbm	10.7
Margin	+ 10.7	+ 3.7	+ 10.9	10.7 db

NOTE: For upper probe at 31 atmospheres and lower probe at 1000 atmospheres.

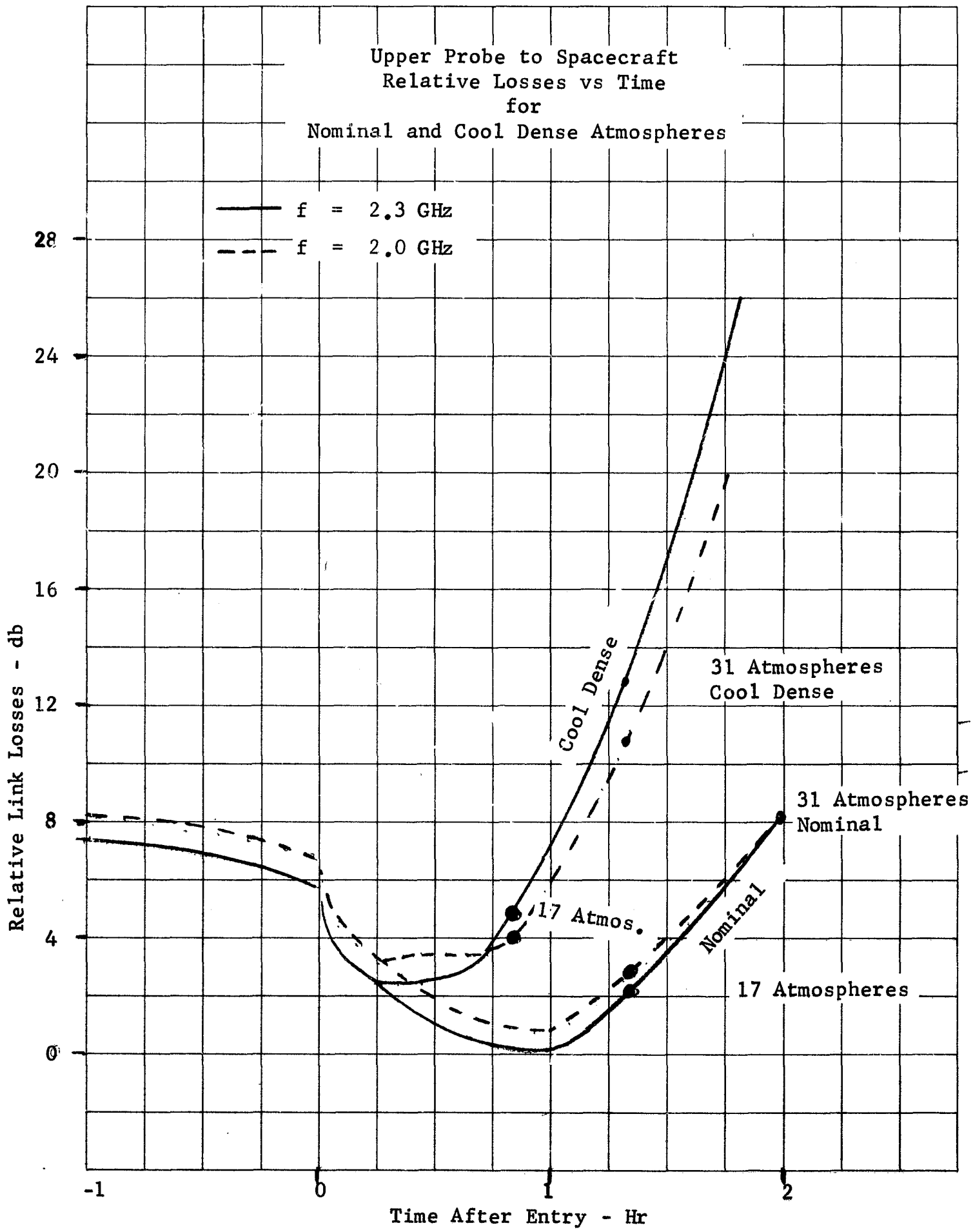


Figure VJ-1 Relative Losses for Upper Probe to Spacecraft Link for Two Atmospheric Models.

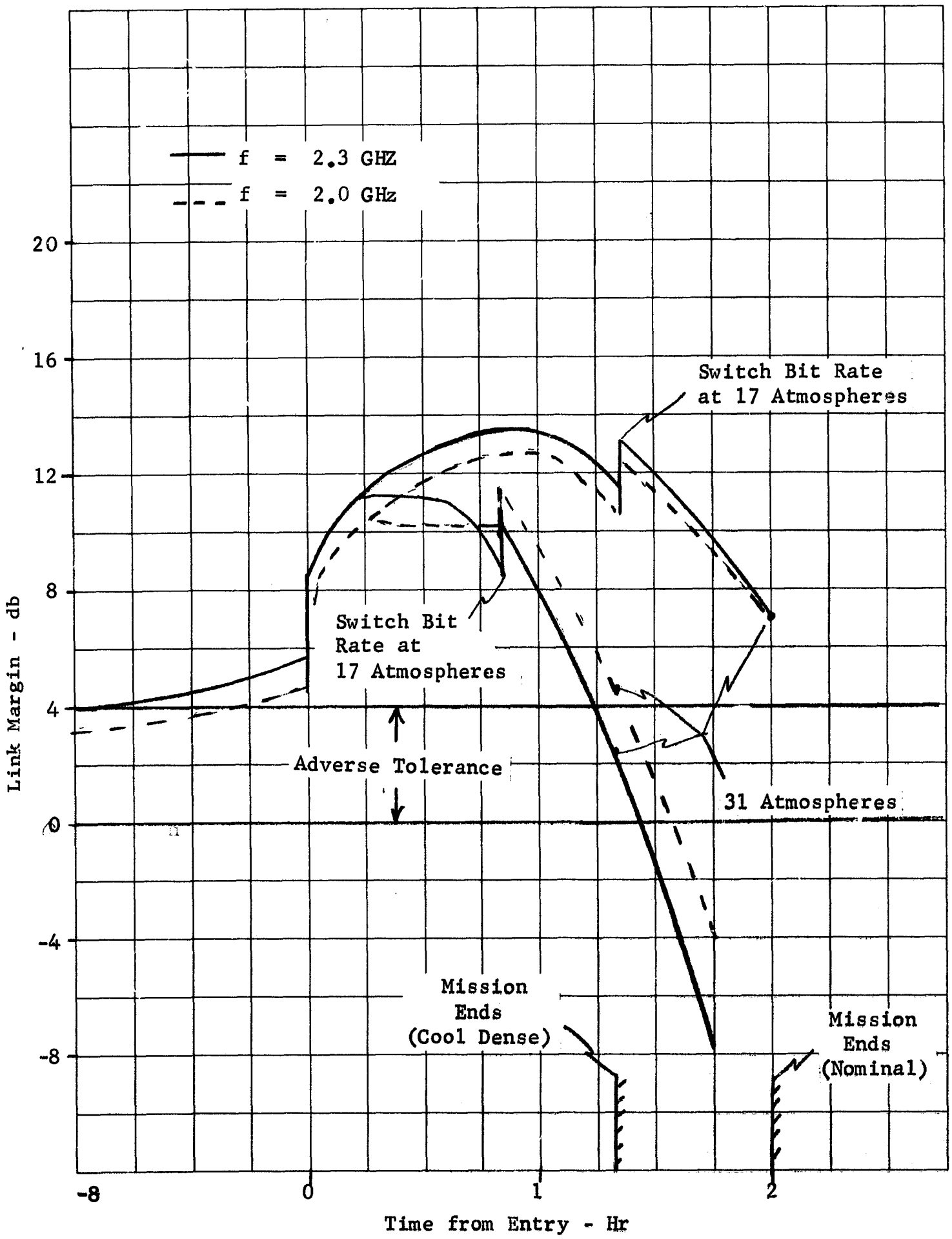


Figure VJ-2 Margin vs Time for Upper Probe to Spacecraft Communications Link for 2 Atmospheric Models.

K. Impact of Cool Dense Model Atmosphere on Probe System Weights

In the previous section the requirement for a 3 db increase in communications link gain was identified for the 300 atm single probe for the case of the cool dense atmosphere model. This can be achieved by increasing the transmitter power by 50% and enlarging the tracking antenna dish diameter (on the spacecraft) by 20%. The consequence of this in terms of probe systems weights is summarized in Table VE-2 under the headings for probes 11, 11 (cool + nominal) and 11 (cool only).

For the "11 (cool + nominal)" case, the thermal/structural system is modified to protect the enlarged-transmitter version of the descent probe (required by the cool atm model) to the 300 atm depth in the hotter, longer-descent-time, nominal atmosphere. This modification increases the descent probe weight by 17%. Next, the entry aeroshell is modified to withstand the higher peak dynamic pressure of the cool model entry. The result of the increases in aeroshell and descent probe weights is a total entry weight 30% greater than that for the Nominal atmosphere probe.

For the "11 (cool only)" case, only the cool atmosphere is considered in the design of the descent thermal/structural protection. Since at the maximum depth 300 atm, the temperature is only 346°F, and since battery weight is reduced by the 1.5-hr vs 2.5-hr descent time (even though the transmitter power was increased) the result is a 27% reduction in descent probe weight. This is almost exactly offset by the increased entry aeroshell weight for the higher, cool-model, dynamic pressures. The total cool-model entry probe weight is thus within a few pounds of the nominal-model probe weight.

If this 300 atm cool-model probe were to encounter the nominal atmosphere it would fail due to exceeding the design temperatures at a depth of 20 atm.

The impact of the cool-model atmosphere on the split probe design concept is much less pronounced. With the frequency modifications identified in the previous section, the 1000 atm split probe can be designed to function in either or both models without affecting the system weights.

VI. DESIGN EXAMPLE MISSION

A. Design Example Selection Rationale

From the range of probe systems evaluated in the parametric study of the previous chapter, a single, staged, probe to 300 atm was selected to illustrate probe system implementation in some detail. The 300 atm probe represents about the maximum practical depth for the single probe concept due to the increasing probe transmitter power requirements and the sharply increasing system weight. The -20° entry angle selected permits 1 hour of the probe descent to occur within 70° of the subsolar point; is large enough to assure no skip out - even with less than ideal ΔV implementation accuracy, and is small enough not to impose large entry aeroshell weight penalties. The Radius of Periapsis of 2.0 R_{2l} favors the relay link communications geometry. Launch occurs on September 25, 1978 with Jupiter arrival on November 4, 1981.

B. Profile of the Design Example Mission

1. Prelaunch

The TITAN III D Launch Vehicle including the seven segment solid rocket motors will be integrated with the CENTAUR and the BURNER II upper stages on the Launch Stand at the Eastern Test Range (ETR). The Entry Probe will be integrated with the TOPS spacecraft and delivered to the launch stand as a checked out Planetary vehicle after systems demonstration testing of the probe and spacecraft in all operating configurations. The payload fairing may be used for protection of the Planetary Vehicle during transport to the launch pad, or another protective cover may be required. The systems will be brought to a state of readiness for launch within a 30 day period. Monitoring requirements for the entry probe during launch preparations will be limited to status checks from the science and engineering payloads of the probe as telemetered through the TOPS spacecraft.

2. Launch

The launch weight of the payload, not including the payload fairing, will be within 2400 lbs, to achieve an injection energy, C_3, of 99.0 km^2/sec^2. The launch phase will include separation of the payload fairing after passing through high aerodynamic pressures, followed by insertion into a parking orbit of 100 nm. The planetary vehicle will then be placed on the Type II interplanetary trajectory and separated from the BURNER II stage. The TOPS spacecraft attitude control system (three axis momentum wheels augmented by hydrazine thrusters) will stabilize the planetary vehicle and acquire the Sun-Canopus celestial references. Booms supporting the RTG's and spacecraft science will be deployed. No deployment of booms will be required for probe systems for this mission.

3. Interplanetary Cruise

Interplanetary cruise to Jupiter will include the collection of interplanetary science data by the spacecraft. Midcourse corrections will be applied to the trajectory to achieve a Jupiter

flyby with a periapsis radius of 2.0 Jupiter radii. Probe systems will be monitored over the spacecraft communications links during this period. The spacecraft will provide power (~50 watts) for heating of entry probe systems and the electronics and drive assembly of the antenna for receiving entry probe signals. Spacecraft mounted probe support equipment including the receiver and decoder will be mounted with spacecraft electronics and will be thermally controlled by the spacecraft thermal control system.

4. Jupiter Encounter

As the planetary vehicle enters the Jupiter sphere of influence (4.8×10^7 km), final trajectory corrections will be made based on range and doppler data from the Deep Space Net.

The spacecraft planetary science instruments will be activated and the probe attitude control and sequencing systems will be turned on and checked out. Update commands including reference time and attitude orientation will be transmitted from the spacecraft to the probe. During the latter part of this period entry probe systems will be heated to $115^{\circ}F$ to assure that lower limits will not be exceeded during the period of coast to the planet. This will require approximately 100 watts from the spacecraft for a period of three days.

5. Probe Separation and Deflection

The deflection radius for the design example mission was chosen at 2.6×10^7 km to assure an angle of at least 15 degrees between the spacecraft earth line and the earth sun line. See Sec IVA for a detailed discussion.

At a distance of 2.6×10^7 km the spacecraft will maneuver to the proper attitude orientation for probe separation and deflection to the entry trajectory. The probe attitude control sensors will be operating but ACS thrusters will be inhibited until final attitude reference data has been transferred from the spacecraft to the probe. The probe will then be separated with a relative velocity of approximately 0.3 meters/sec to minimize disturbing

torques on both the spacecraft and the probe. At separation, the probe attitude control thrusters will be activated and will maintain attituae control for a period of approximately twenty minutes while the probe drifts away from the spacecraft. The probe solid rocket motor deflection system will then be activated to impart a velocity increment of 81 meters per second at an angle of -106.5°. The deflection acceleration will be monitored by the probe attitude control system which will terminate propulsion when the proper velocity is attained. The velocity increment will be selected to provide a probe entry angle of, γ_E, of -20°, and to cause the spacecraft to be directly over the probe at spacecraft periapsis passage. Following probe deflection, the attitude control system will orient the probe for zero angle of attack at entry, and will then spin the probe about the longitudinal axis at a rate of approximately three radians per second. The attitude control system will then be shutdown. The period of coast to the planet will be 40 days and during this period probe systems will be dormant except for a timer. The passive probe thermal control system will limit the temperature at the probe interior to 50°F.

6. Coast to the Planet

The spinning probe will coast to the planet for a period of 40 days oriented to achieve an entry angle of -20° and a zero angle of attack. 1.2 hours prior to entry, at a distance of 3 Jupiter radii, the ion mass spectrometer will be turned on and the radio link from the probe to the spacecraft will be activated for transmission of science data at 180 bps. Seventeen minutes prior to entry as determined by updated ephemeris data and reference timing from the spacecraft prior to separation the probe will be despun to approximately 0.5 radian per second. This will be accomplished by a system of despin weights that will be jettisoned after use.

7. Probe Entry

Entry is assumed to occur at an altitude of 487.7 km above the reference radius of 71420 km where the atmospheric pressure is assumed to be one atmosphere. The relative velocity between the

probe and the Jupiter atmosphere will be 47.8 km/sec. The entry ballistic coefficient will be 1.02 sl/ft^2. Entry of the probe will occur 57 minutes prior to the time of spacecraft periapsis passage. The 4.15 foot diameter antenna mounted on the spacecraft for receiving probe data will be programmed to reacquire the probe signal which is expected to be lost during entry.

The entry deceleration will be sensed and, at E + 10 sec when a value of 0.1 g is reached, the probe timer will be reset to establish an updated value for aeroshell staging.

Entry data from the science and engineering payloads will be placed in storage.

8. Probe Deceleration and Descent

A decelerator will be deployed 62 seconds after entry when the atmospheric pressure is 200 mb, and Mach number is 0.55. The probe transmitter will be turned on and real time data will be transmitted to the spacecraft at a rate of 40 bps. At the end of three minutes the data transmission mode will be changed to combine the transmission of real time data and the stored entry data. The stored data transmission will be completed at the end of 89 minutes.

The probe will descend with a ballistic coefficient of 0.050 sl/ft^2 to a depth of 15 atmospheres ($\sim$72 minutes) when the decelerator will be staged by pressure sensing to provide a ballistic coefficient of 1.9 sl/ft^2.

At 30 atmospheres, also by pressure sensing, the accelerometer and photometer data collection will be discontinued and pressure, temperature and GC/MS data will be transmitted at 40 bps. This mode will continue to a depth of 105 atmospheres when the bit rate will be decreased to 10 bps. The mission will be completed when the probe design depth of 300 atmospheres is reached approximately 2.5 hours after entry.

The approach geometry for the Design Example Mission is shown in Figure VI-B-1. The probe descent profile is shown in Figure VI-B-2.

C. Sequence of Events

Major sequenced events and design parameters for the Design Example mission are shown in Table VI-C-1. A detailed sequence from probe separation is shown in Table VI-C-2.

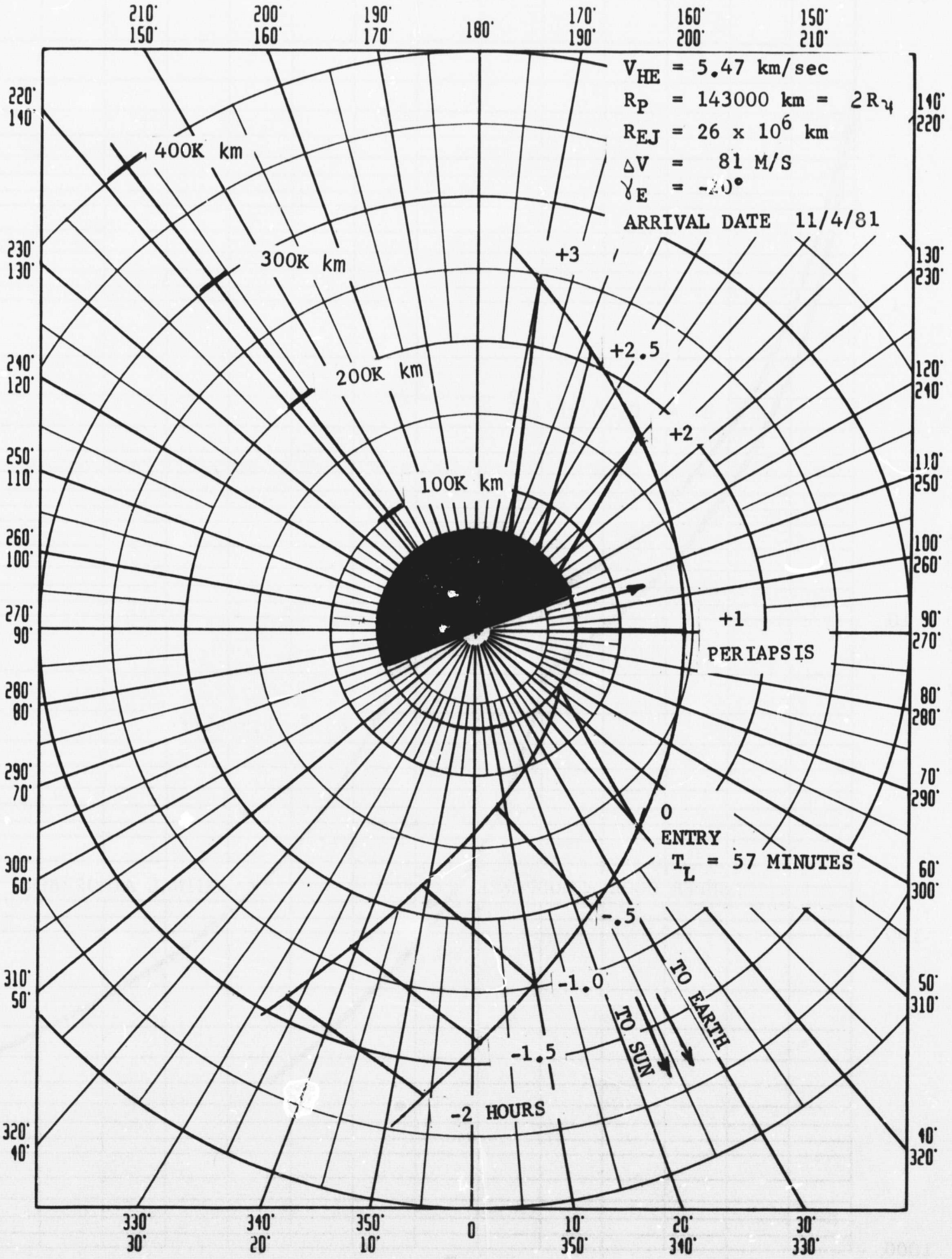


FIGURE VIB-1
APPROACH GEOMETRY
DESIGN EXAMPLE MISSION

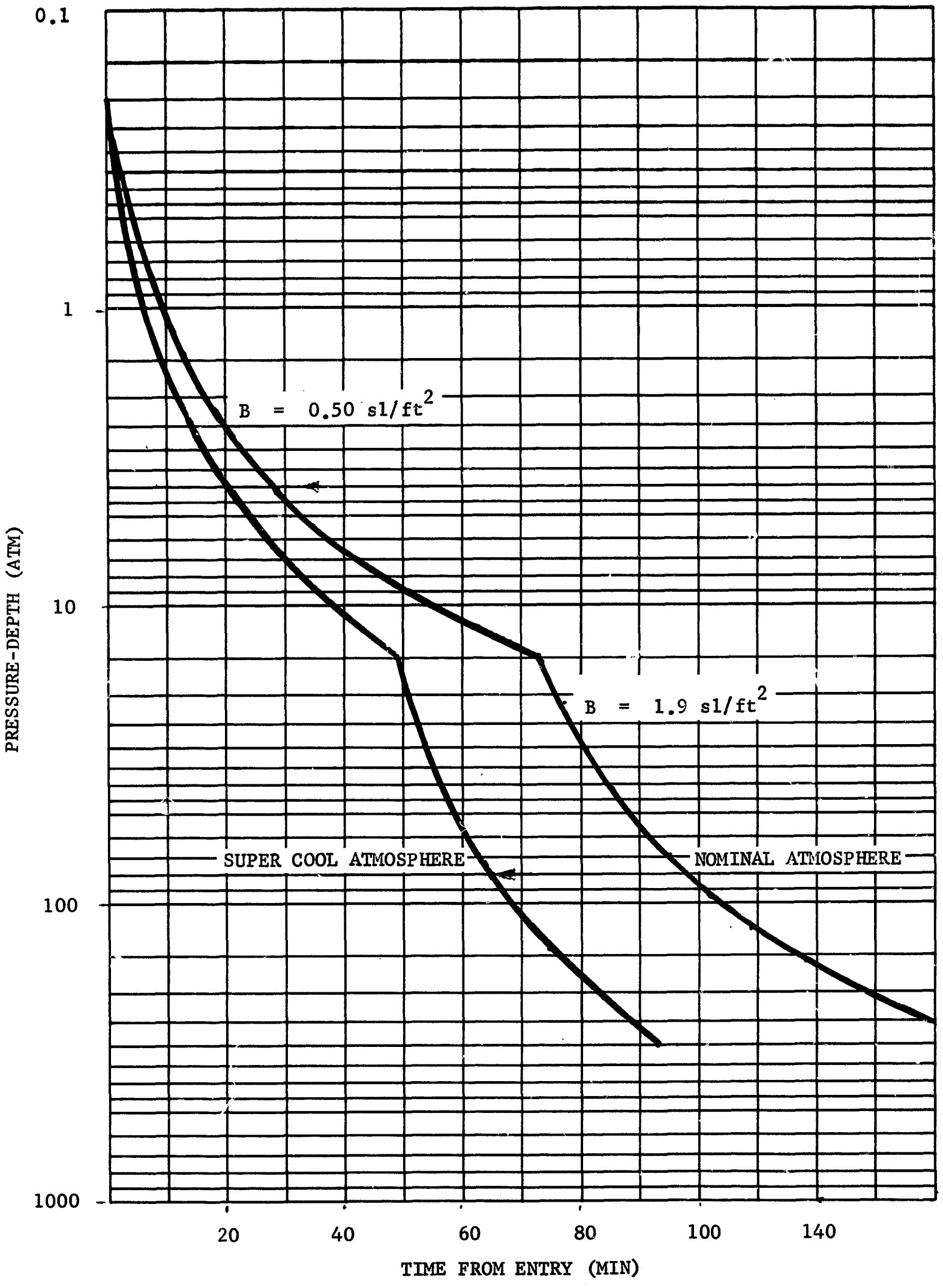


Figure VIB-2 Descent Profiles Design Example Mission Nominal and Supercool Atmospheres.

LAUNCH, INTERPLANETARY CRUISE, AND ENCOUNTER PARAMETERS
FOR JUPITER
DESIGN EXAMPLE

TABLE VIC-1

LAUNCH PARAMETERS	
LAUNCH DATE (NOMINAL)	9/25/78
LAUNCH VEHICLE	TITAN III D CENTAUR (7 SEG WITH BURNER II)
LAUNCH PERIOD	30 DAYS
PARKING ORBIT ALTITUDE	100 NAUTICAL MILES
SPACECRAFT	TOPS
SPACECRAFT WEIGHT	1450. LBS
PAYLOAD WEIGHT (INCL S/C)	2420 LBS
FAIRING SEPARATION	CORE 2 IGNITION PLUS 10 SEC
MAX LAUNCH AZIMUTH	115 DEG
INTERPLANETARY CRUISE PARAMETERS	
TRAJECTORY	TYPE II
DECLINATION OF LAUNCH ASYMPTOTE	
DLA	6.6 DEGREES
RIGHT ASCENSION	118.4 DEGREES
INJECTION ENERGY, C3	99.0 KM2/SEC2
FLIGHT TIME	1136 DAYS (NOMINAL)
SEMI-MAJOR AXIS	3.22 A.U.
RADIUS OF APHELION	5.5 A. U.
ECCENTRICITY	0.695
INCLINATION TO ECLIPTIC	3.6 DEGREES
CENTRAL ANGLE OF TRAVEL	200.7 DEGREES
TRUE ANOMALY AT DEPARTURE	342.0 DEGREES
ENCOUNTER PARAMETERS	
JUPITER ARRIVAL DATE	11/4/81 (NOMINAL)
TRUE ANOMALY AT ARRIVAL	182.8 DEGREES
EXCESS VELOCITY, VHP	5.47 KM/SEC
DEC OF VHP VECTOR	27.4 DEGREES
RIGHT ASC OF VHP VECTOR	106.8 DEGREES
(WITH RESPECT TO VERNAL EQUINOX, EARTH EQUATORIAL SYSTEM)	
DEC OF VHP VECTOR	3.2 DEGREES
(WITH RESPECT TO EQUATOR OF JUPITER)	
COMMUNICATION RANGE	6.4 A.U.
DEFLECTION PARAMETERS	
BUS TRAJECTORY	FLYBY
PERIAPSIS RADIUS OF BUS	143000. KM = 2 JUPITER RADII
DEFLECTION RADIUS	26,000,000. KM
INCLINATION OF TRAJECTORY	7.5 DEGREES
(WITH RESPECT TO EQUATOR OF JUPITER)	
DEFLECTION VELOCITY	81 METERS/SEC
DEFLECTION ANGLE	-106.5 DEGREES
CAPSULE COAST TIME	40 DAYS
LEAD TIME	57 MINUTES
LEAD ANGLE	-16.51 DEGREES

* * * * ENTRY PROBE DESIGN DATA * * * *

RELATIVE ENTRY VELOCITY	47.8 KM/SEC = 156789 FT/SEC
ENTRY ANGLE	-20. DEGREES (SKIPOUT AT -3.97 DEG)
ENTRY ALTITUDE (TIME=0)	487.7 KM = 1,600,000. FEET
ENTRY RADIUS	71907.7 KM
ENTRY LATITUDE	6 DEGREES
ENTRY LONGITUDE	34 DEGREES
(RELATIVE TO MERIDIAN OF SUN)	

* *

* * * * AEROSHELL DATA * * * *

ENTRY BALLISTIC COEFFICIENT	1.02 SLUGS/FT2
TIME TO .1 G POINT	10.0 SECONDS
TIME OF MAXIMUM DECELERATION AND MAX DYNAMIC PRESSURE	21.0 SECONDS
MAXIMUM DECELERATION	996. G
MAXIMUM DYNAMIC PRESSURE	26.329 LB/FT2
TIME OF MACH 1 OCCURRENCE	39.0 SECONDS
AEROSHELL STARTING	
ALTITUDE	33 KM=200 MB
MACH NUMBER	.55
DYNAMIC PRESSURE	92.3 LB/FT2
TEMPERATURE	203.4 DEG R
DENSITY	.00009726 SLUG/FT3
TIME (TS)	62.0 SECONDS

TABLE VI-C-2

SEQUENCE OF EVENTS

DESIGN EXAMPLE MISSION

TIME	EVENT	NOTES
E-(40 +) days	Final trajectory observations with DSN. Final determination of deflection velocity, an le, and time of application. Turn on probe systems, checkout, and update. Begin attitude maneuver for probe separation.	Spacecraft downlink to earth through the high gain antenna. Uplink commands are through the forward low gain antenna until attitude maneuvers begin, when the low gain antennas are used.
E-40 days	Complete separation attitude maneuver. Transmit reference timing to the entry vehicle. Separate entry vehicle. Return spacecraft to earth orientation with high gain antenna. Probe attitude control system operating.	Separation velocity of 1 foot per second. $R = 2.6 \times 10^7$ km. $V_{HP} = 5.476$ km/sec $\gamma_E = -20°$
(Separation plus 20 mins)	Initiate deflection impulse. Sense acceleration and shut down. Orient to zero entry angle of attack. Spin up probe. Shutdown ACS.	$\Delta V = 81$ mps, ($\gamma = -106.5°$) $\omega = 3$ rads/sec
E-1.2 hrs	Activate mass spectrometer and RF link to spacecraft. Transmit pre-entry science.	$R = 3 R_J$ Probe support system aboard the spacecraft acquires probe signal in both frequency and direction. Position tracking is programmed at $\approx$ 0.5 deg/second. Data rate from entry vehicle to spacecraft is 180 bps.
E-17 mins	Despin entry vehicle, jettison weights Prepare to store entry data.	$W = 0.5$ rads/sec
E = 0	Beginning of Entry. Collect entry data and store.	$B_E = 0.90$ sl/ft^2 (488 km above 1 atm) Lead Time = 57 mins
E + 10 sec	Sense 0.1 g.	Reference Time: Reset timer.

Sequence of Events Design Example Mission - Continued

TIME	EVENT	NOTES
E + 62 sec T_s = 0	Deploy decelerator. Stage Aeroshell/Heat shield. Reacquire probe signal to spacecraft. Transmit stored data at 40 bps.	P = 200 mb M = 0.55 B = 0.05 sl/ft^2
T_s + 72 mins	Sense 15 atm; Stage decelerator	B = 1.9 sl/ft^2
T_s + 79 mins	Sense 30 atm; Change data mode.	(Omit photometer and accelerometer data).
T_s + 89 mins	Stored entry data readout complete.	
T_s + 104 mins	Sense 105 atm	Change data rate to 10 bps
T_s + 147 mins	300 atm mission complete	H = -395 km Nominal atmosphere

D. Configuration Summary - Design Example Case

The inboard profile of the Design Example Probe is shown in Figure VID-1. Major characteristics are summarized in Table VID-1 and the system weight breakdown in Table VID-2.

Descriptions of these systems are provided in the following sections.

E. Mechanical and Support Systems

1. Descent Probe Description

The descent probe is an integrated system that provides the science instruments and communication equipment with a controlled environment during science data gathering and transmission. The probe descends ballistically into an increasingly higher ambient pressure and temperature environment during its mission lifetime. The ambient conditions at the terminal point are 300 earth atmospheres and 1335°F.

The equipment is protected from the environment by a structural/thermal concept consisting of an evacuated pressure vessel with a combination of 1.1 inch thickness of Min-K external insulation to reduce the temperature to the pressure shell to 1100°F, and an internal layer of multi-layer insulation .30 inch thick to prevent the temperature of the internal equipment from rising above 125°F during mission lifetime. Local heat from operating equipment sources is absorbed by phase change material. Figure VID-2 shows the descent probe thermal/structural design.

The pressure vessel is a monocoque spherical shell of Inconel 718 superalloy with a wall thickness of .19 inch. Limiting it to 1100°F by external insulation and controlling the internal temperature with the multilayer insulation and PCM results in the lowest weight and a near minimum size envelope for aeroshell packaging.

The pressure vessel closure is concentric with the antenna and is above the maximum breadth point to minimize weight and avoid interference with science instrument mounting. The mass spectrometer and pressure transducers are provided with a duct system to enable

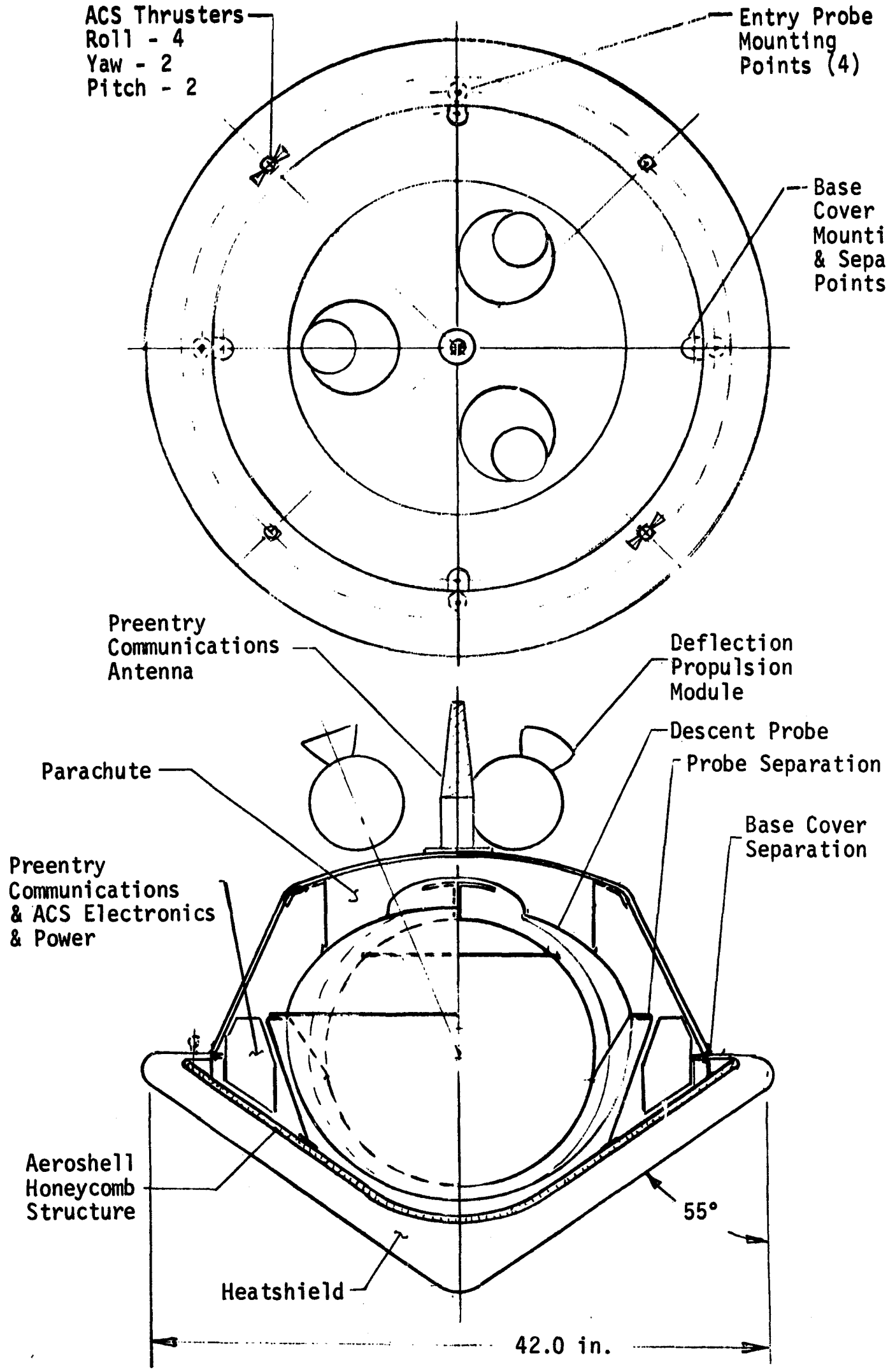


Fig. VI-D-1 Entry Probe Inboard Profile, Design Example

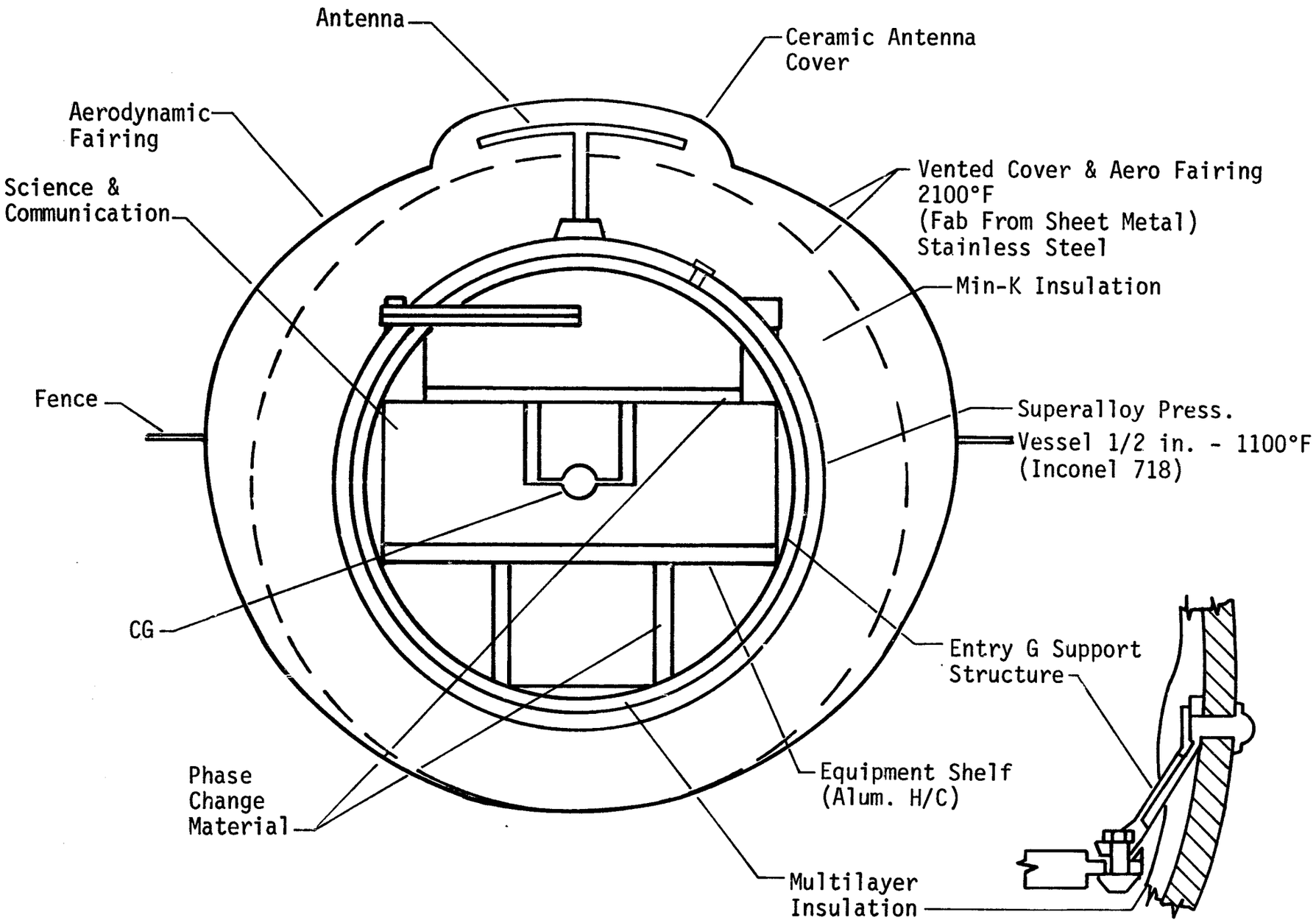


Figure VID-2

Thermal Structural Design
Design Example Descent Probe

TABLE VI-D-1

DESIGN EXAMPLE PROBE CHARACTERISTICS SUMMARY

Type Probe:	Single (Staged)
Entry Angle:	-20^{o}
Data Return Mode:	Relay
S/C Radius of Periapsis	2.0 $R_{\mathcal{4}}$
Science Payload:	16 lbs. Descent Phase 3 lbs. Pre entry
Bit Rate:	40/10 B/S Descent Phase 180 B/S Pre entry
Transmitter Power:	40 Watts
Descent Time:	2.47 Hrs.
Entry Ballistic Coefficient:	1.03 Slugs/ft^2
Probe Diameter:	3.5 Feet
Entry Weight:	427 lbs.
Probe vs Installed on TOPS S/C	467 lbs.
Total Probe System Weight (incl S/C Mods):	569 lbs.
Liftoff Weight	2019 lbs
Launch Vehicle Capability (7 segment TIIID Centaur with Burner II)	2420 lbs

TABLE VID-2

DESIGN EXAMPLE PROBE WEIGHT SUMMARY

Item	Wt. (lbs)	
Descent Probe		
Science	16.0	
Communications and Power	47.6	
Structure	58.2	
Thermal Control	20.3	
Mechanical and Aero Systems	11.5	
		(153.6)
Parachute	7.2	
Parachute Canister	1.5	
De-Spin System (Fixed)	1.0	
Separation Mechanisms	3.0	
Delta Structure in A/S Mountings for High G	3.0	
		(15.7)
Entry Vehicle ACS	25.0	
Pre-entry Commun. Electronics, Power and Antenna)	17.0	
Equipment Inst'l Structure	4.3	
		(46.3)
Aeroshell Structure		(66.0)
Heatshield		(145.4)
Entry Weight		(427.00)
Deflection Propulsion System	26.0	
De-Spin & APS (Spent)	3.00	
Ion Mass Spectrometer (Jettisons)	3.00	
Thermal Blanket; Mounting and Separation	8.00	
		(40.0)
Probe Installed Weight		(467.00)
Spacecraft Modifications		(102.0)
		(569.0)
Basic TOPS Spacecraft		(1450.0)
TOTAL		2019.0

the atmospheric sample acquisition and transport. Optical windows are provided for the science instruments such as the photometers. All penetrations of the pressure shell must provide a hermetic seal to ensure a vacuum in the vessel during the descent mode.

The phase change material is contained in metallic jackets configured to utilize avialable free volume and attached directly to local heat sources or with a conductive lead for a heat path. The primary source of heat is the transmitter.

The equipment is supported within the pressure shell on a shelf of structural sandwich connected to the vessel walls by tension hangers for high g-loads in the entry vehicle axial direction when mounted in the entry aeroshell. The tension hangers of titanium minimize the heat short of the pressure shell to the mounted equipment.

A vacuum environment is required in the pressure shell during the final descent mode to ensure the performance of the multi-layer insulation. Due to the out-gassing of some of the materials of the internal equipment during the cruise, a pressure sufficient to seriously degrade the insulation preformance would be built up. Consequently the pressure vessel is vented to the local ambient pressure for the cruise phase and then resealed prior to entry. This is accomplished by opening the vent after the final pressure-integrity checkout in the prelaunch phase and then closing it just prior to entry by firing a squib- operated pyrotechnic valve. The charge, which is contained to prevent damage to the external insulation, thrusts a tapered plug into a mating sleeve that has theretofore served as the vent passage. The wedging action of the driven plug provides the closure of the vent with the external pressure acting to engage the plug further.

The reliability of pyrotechnic squibs is high and two pyrotechnic valves could be arranged in series such that either one would effect the vessel closure.

The external insulation is protected with a metal cover that also provides aerodynamic smoothness. In the area of the antenna, a curved turnstile design, the cover is formed of glass polymide to provide RF transparency. This cover provides protection for the antenna from parachute harness and reef lines at parachute deployment.

The required subsonic descent ballistic coefficient is 1.9 for this probe. The ballistic coefficient of the spherical body with no auxiliary drag devices is too high. To provide the desired ballistic coefficient of 1.9 within the packaging limits of the aeroshell and at minimum weight, the aerodynamic cover/shroud is expanded to a larger external radius where the center of its radii is above the c.g. of the descent probe approximately 3.0 inches. At this level a circumferential external flange around the periphery of the shell serves to spoil the aerodynamic flow, consequently increasing the drag. This arrangement, shown in Figure VID-1, yields the required m/C_DA.

The descent probe weight breakdown is given below:

Descent Probe Weight Breakdown

Item	Wt. (lbs)
Science Equipment Communications and Power	63.6
Internal Structure	8.7
Pressure Shell	49.5
Min-K Insulation	15.3
Multi-Layer Insulation	1.0
Phase Change Material	4.0
Antenna	1.5
Insulation Cover/Aero Shovel	5.0
Aerodynamic Trip and Delta For High Gr.	3.5
Pyrotechnic Vent Valve and Installation	1.5
TOTAL DESCENT PROBE WT.	153.6

2. Entry Vehicle

The aeroshell configuration shown in Figure VID-1, is typical of all the single probes of this study. Because of the extensive thickness of heatshield necessary on the frontal body of the aeroshell structure and the relatively small aeroshell diameter, the

axial depth begins to impact the problem of overall packaging and the static margin. Since the probes packaged are large in proportion to the aeroshell within which they are packaged, it is desirable to take advantage of every opportunity to minimize depth in the entry vehicle configuration or to nest the payload deeper into the aeroshell. From studies discussed in Volume III, sandwich aeroshells were found to be as light as ring-stiffened monocoque shells. Consequently a titanium sandwich structure was selected since it results in a thinner and more uniform structural envelope for packaging.

The general stability of the cone shell is provided by a ring frame at the major diameter. The base structure is normal to the probe centerline at the major diameter so that a minimum edge radius may be achieved around the rim of the probe. A direct blend from the forebody into a base cone, along the 40° breakaway angle normally used would result in excessive heatshielding around the rim because of the excessive thickness to be blended. This would increase the rim area exposed to the heating as well as add unnecessary weight.

The base cover cone interfaces with the major ring at the frame's inner chord. The depth of the base cover is as required to package the descent probe and its parachute. The base cover mounts the preentry probe tracking antenna and the deflection propulsion module. It also provides the canister compartment to contain the parachute until probe extraction is desired when the cover is jettisoned exposing the parachute for deployment. The cover mounts to the aeroshell forward cone through pyrotechnic tension bolts integral with a thruster. The cover separates and jettisons by firing the thrusters that impart a cover separation impulse aft to free and jettison it.

The descent probe mounts to the entry aeroshell at the probe's aerodynamic fence by pyrotechnic separation nuts. The descent probe loads at entry are transmitted to the aeroshell through a ring beam interfacing at the fence.

The portions of the deflection phase attitude propulsion system that are external to the aeroshell, i.e., the cold gas jets, are mounted to the aft face of the ring frame at the probe maximum diameter. A de-spin yo-yo system is provided since it will remove a fixed fraction of the actual spin momentum (using the ACS Jets would change the spin rate by a precalculated amount and thus could result in a higher rate than desired unless a roll reference system is added). The probe mounts to the spacecraft through pyrotechnic attachments at the major ring. The Guidance and Control gyro package, electronics, APS gas supply, and the pre-entry electronics mount internally, distributed circumferentially at the major ring. This location is optimum for mounting of these systems and the probe support since the major ring frame is a rigid integral part of the bulk of the aeroshell mass and is essentially in the plane of the entry vehicle c.g. Distribution of the masses here augments the desired inertia proportions for spin stability.

The aerodecelerator design for the probe's withdrawal out of the aeroshell is based on a ballistic coefficient requirement for descent velocity control of .05 slug/ft^2. For the 154 lb descent probe a 20 foot diameter parachute is required based on the design data of Volume III. The parachute is of the disk-gap-band type fabricated of polyester fabric.

3. Deflection and Approach

The probe deflection maneuver is accomplished by first orienting the TOPS spacecraft to the attitude which aligns the probe axis with the ΔV vector. This reference is transferred to a 3-axis strapdown inertial guidance system on board the probe. A spring system then eases the probe away from the spacecraft and a rocket motor system imparts the 81 m/s velocity increment. Three small motors make up the ΔV system as indicated in Figure VID-1 in order to maintain symmetry while leaving the centerline location for the preentry antenna. Use of a single motor on the ℄ would preclude any torques induced by unequal thrust termination. However, in addition to the antenna location interference, it would result in a greater overall probe length which in turn would aggravate the c.g. offset problem in mounting the probe on the spacecraft. These problems with the single motor configuration could be overcome if the thrust termination problem with 3 motors is found to be a dominant factor. A 3-axis cold gas attitude propulsion system and the 3-axis strapdown G&C system maintain the reference orientation during ΔV burn; control ΔV magnitude (by initiating blowing of the nozzles in the case of the solid system); and subsequently reorient the probe to the attitude corresponding to zero angle of attack at entry. This attitude is maintained for the ∿ 40-day approach period by spinning-up the probe so that the 3-axis system does not have to be kept in operation.

Despinning prior to entry to a near zero (∿ 1/2 rad/sec) rate is achieved by yo-yo's but the roll jets could be reactivated for this function and could possibly be used to trim out all roll if a sun sensor system were added to establish a roll reference.

The 3-axis strapdown system is similar to that used by Viking for deorbit control and is discussed further in Volume III, Chapter V. Overall accuracies with this method are within 1° to 1 1/2° in ΔV application angle and 1% in ΔV magnitude.

An alternative to the solid rocket motor ΔV system and the cold gas attitude propulsion system is a combined ΔV/APS system using hydrazine monopropellant. For providing the ΔV, the monopropellant was found to be heavier, See Chapter V Volume III, but the advantages of combining the systems might well offset the weight differences.

Thermal control during the approach phase is achieved by preheating the probe to the maximum non-operating temperature of its equipment, 125°F, prior to its release from the spacecraft and encasing the entire probe with a 3/4 inch thick multilayer blanket. With this arrangement, the probe temperature does not cool to below its allowable temperature prior to entry.

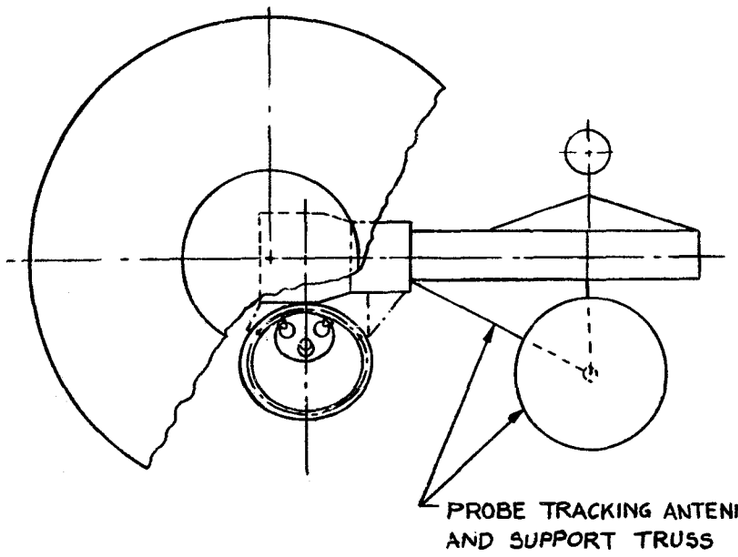
4. Spacecraft/Probe Integration

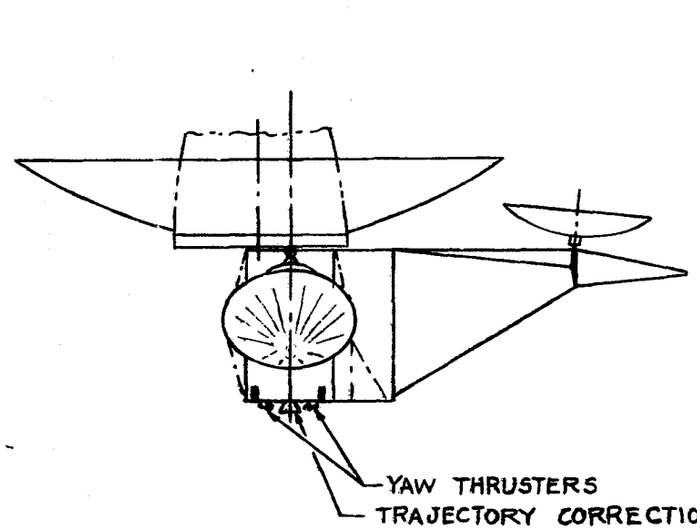
The probe is mounted to the -Y side of the equipment compartment in the Y-Y plane at an angle of 40 degrees with the planetary vehicle roll axis. The tilted position results in a c.g. offset from TOPS spacecraft c.g. of approximately 7.0 inches. The planetary vehicle configuration is shown in Figure VIE-1.

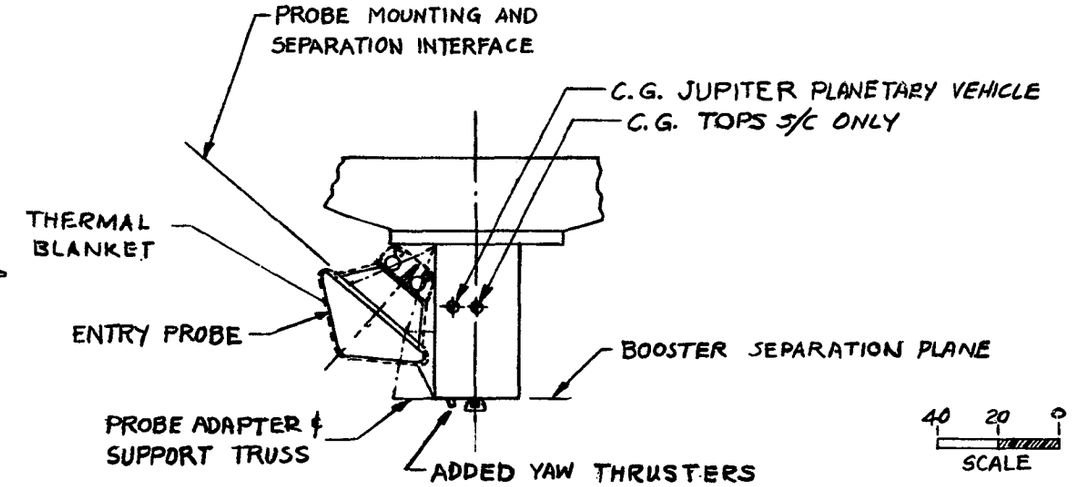
The probe mounts on the spacecraft through a truss structure that attaches to the equipment compartment at the corners and edges where framing structure exists. This position of the probe does not directly block off the roll jets on the compartment although some impingement occurs. The truss extends down

to the booster interface plane and provides a mount point to the booster adapter. Relocation of the plasma wave detector and magnetometer booms to the RTG boom is also required.

Two additional yaw thrusters are required as shown in Figure VIE-1 to prevent cross coupling due to the CG offset caused by the probe. An additional effect of the CG offset is to require that the thrust line of the trajectory correction propulsion system be capable of being directed 13 1/2 degrees off the existing TOPS Z axis.







PLANETARY VEHICLE CONFIGURATION
(TOPS SPACECRAFT)

FIGURE: VI E-1

The trajectory correction system and attitude propulsion must also provide more total impulse for each midcourse due to the increased mass and inertias (approximately a 30% increase). However, no additional propellant is required for Jupiter-only probe missions since only ∿ 25% of the existing system's capability is used to provide for corrections occurring prior to Jupiter. For probe missions combined with Grand Tour missions JPL* has found a maximum of 12 lbs additional propellant is required with a 400 lb probe.

The thermal control system of the TOPS spacecraft must be modified to allow for the presence of the probe. The probe is located in a position which partially blocks the louver panel's view to space. Varying amounts of sunlight (depending on the cone angle) are also reflected into the louver panels by the probe. The TOPS spacecraft has louver panels on both +Y and -Y sides of the electronic equipment compartment. The probe is mounted on the +Y axis in front of the +Y louver panel thus reducing its heat rejection capability. This situation can be corrected by incorporating one or more of the following modifications: increasing the size of the +Y louver panel and have the louver blades open in the +Z direction away from the sun; rearranging the equipment so that only low heat dissipation components are located on the +Y side; using heat pipes to transfer heat from the +Y side to the -Y side of the equipment compartment; or relocating the louvers to other surfaces of the compartment.

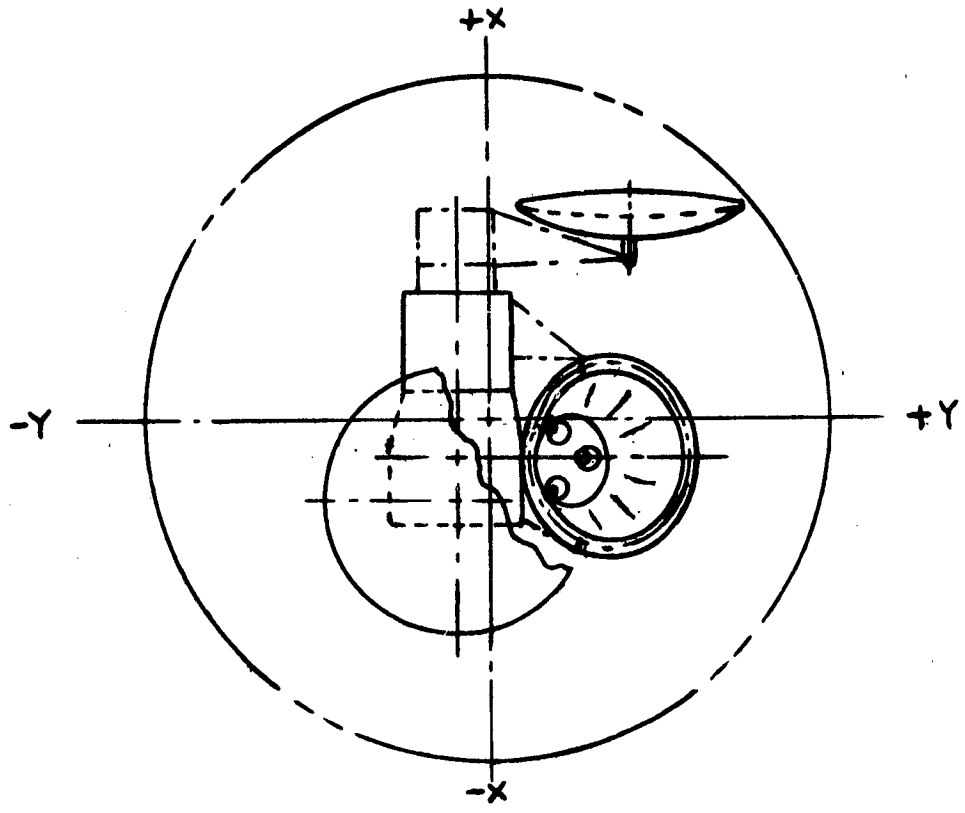
The weight breakdown for the modifications to TOPS are shown in Table VIE-1.

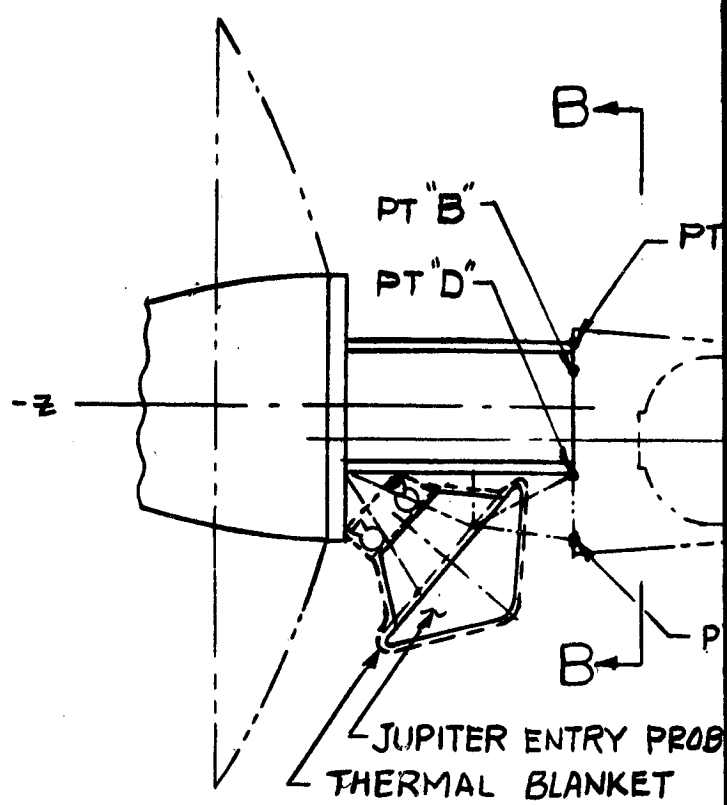
5. Launch Vehicle/Planetary Vehicle Integration

The planetary vehicle with all systems stored mounts within the Titan III/Centaur/Viking payload fairing as shown in Figure VIE-2. The probe tracking antenna mounts to the inboard segment of the scan platform truss and folds within the fairing envelope as shown. No antenna deployment is necessary beyond normal deployment of the science scan platform which also deploys the antenna.

---

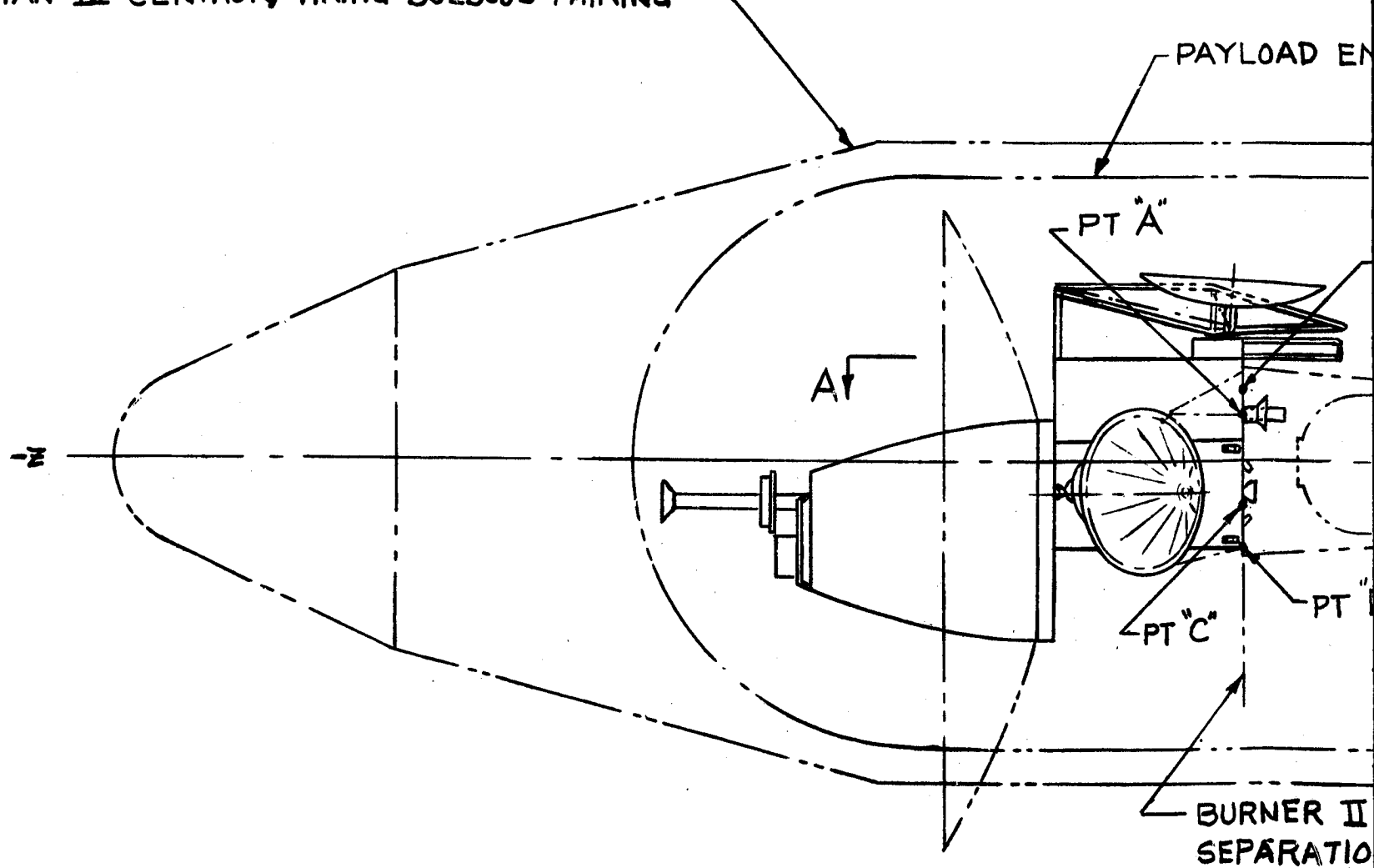
*NASA Briefing on Grand Tour missions with Probes by JPL 6-29-70.



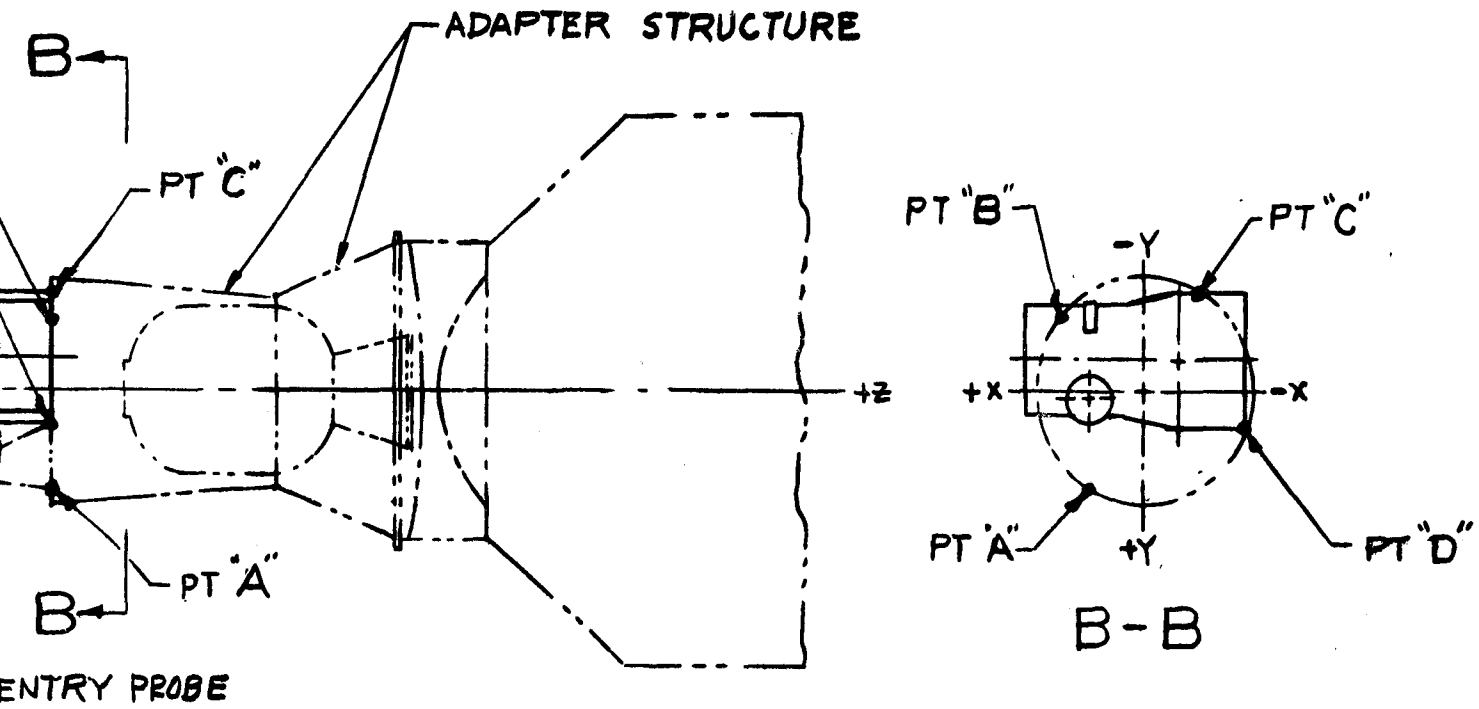


A – A

TITAN III CENTAUR/VIKING BULBOUS FAIRING



FOLDOUT FRAME

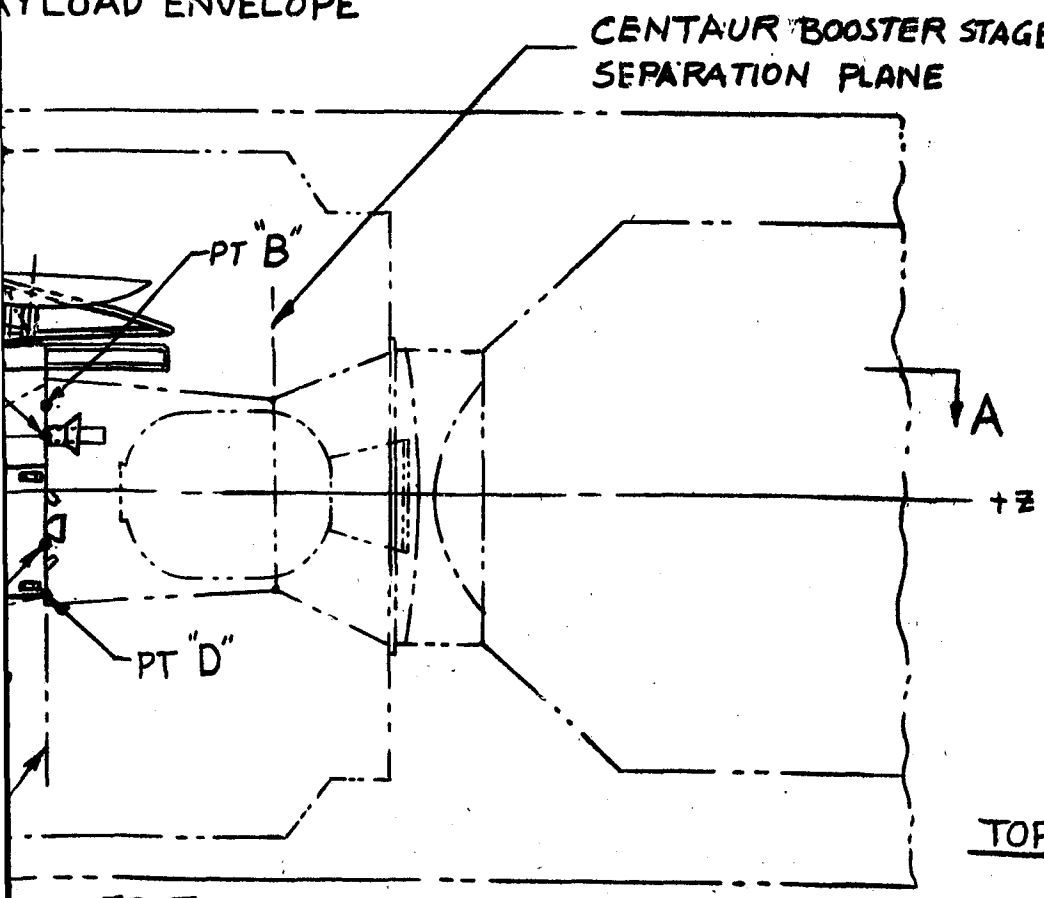


B-B

ENTRY PROBE
BLANKET

A—A

YLOAD ENVELOPE



URNER II STAGE
EPARATION PLANE

40 20 0
SCALE

TOPS PLANETARY VEHICLE/BOOSTER INSTALLATION

FIGURE: VI E-2

FOLDOUT FRAME

2

TABLE VIE-1

WEIGHT SUMMARY FOR MODIFICATIONS TO TOPS S/C

FOR

THE DESIGN EXAMPLE PROBE

ITEM		WEIGHT
Structure		46.0
Beefup Adaptor	6	
Beefup S/C	12	
Probe Support	28	
Boom Relocation		2.5
Antenna (Probe Tracking)		21.0
Attitude Propulsion System		2.0
Mechanical Devices		2.0
Temperature Control		5.0
Electronics for Probe Comm.		11.0
Data System		5.0
Power System Switching and Control		3.0
Cabling		5.0
		102.5

An adapter structure of stiffened skin construction from the centaur stage attachment to the planetary vehicle interface yields the lowest weight by minimizing transitional structure. Stiffening with longerons provides the compatibility with pyrotechnic nut/bolts for staging and attachment at the planetary vehicle interface.

The total liftoff weight of 2019 lbs (Table VID-2) is well within the launch vehicle capability of the 7 segment TIIID Centaur with Burner II, 2420 lbs, and also that for the 5 segment TIIID with the stretched Centaur.

The impact of designing the Design Example Mission Probe Mechanical Systems for the cool dense Atmosphere Model is covered in the discussion on Probe No. 11 of the parametric probe study, Chapter V, Section K.

F. Telecommunications, Data Handling and Power - (Design Example Mission)

1. Telecommunications

a. General

The basic approach to telecommunications for this mission is an extension of the approach taken for the baseline parametric study in that a relay communications link between the entry vehicle and the spacecraft is used for data transfer during the periods from 1 hour prior to probe entry ending at 0.1 g increasing and again from when staging of the probe from the aeroshell occurs until the communications link limit is reached after 2½ hours or more. Accelerometer and critical engineering data are stored in a memory during the period from 0.1g to staging. A single biphase modulated square wave subcarrier is used to modulate a 40 watt probe transmitter to provide bit rates of 180, 40, and 10 BPS for preentry, initial post entry, and the final mission phase respectively. Convolutional coding (rate 1/3, constraint length 4) is used to improve the undetected error rate. Decoding at the spacecraft is by means of a Viterbi algorithm decoder using soft decision by quantizing to 3 bits. Acquisition of the 1.2 GHz probe radio signal by the spacecraft receive system is required both prior to entry and following staging of the probe from the aeroshell. This function is accomplished by a frequency search and acquisition receiving system in conjunction with a 2-gimbal, simultaneous lobing auto track antenna having a 4.15 ft diameter reflector.

All relay data are stored in the TOPS data storage subsystem for subsequent transfer to Earth via either the spacecraft X or S band communications link.

Two dimensional communications geometry for the relay link, and antenna aspect angles and range for the mission all as a function of time are given in figures VIB-1 and VIF-2. A design control table showing relay communications link parameters at 2.5 hours after staging the Probe from the aeroshell is provided as Table VIF-1. Figure VIF-3 shows relative link losses as a function of time for the nominal atmosphere and for the cool-dense atmosphere. Figure VIF-4 shows margin as a function of time for both the nominal

FIGURE VIF-2

DESIGN EXAMPLE - ASPECT ANGLE AND RANGE VS. TIME

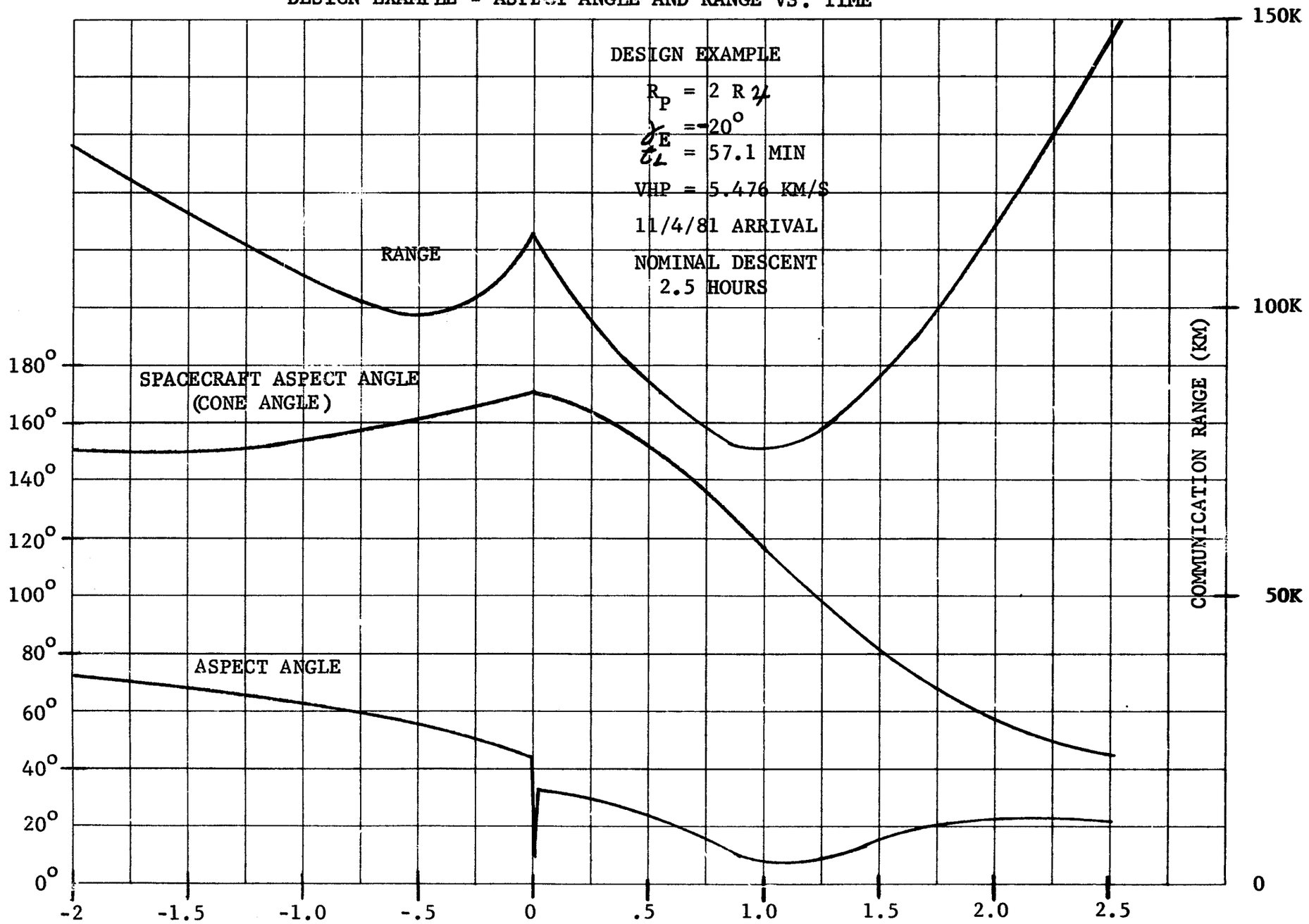


TABLE VIF-1

RELAY COMMUNICATIONS LINK DESIGN CONTROL TABLE

Parameters	Value db (w)	Comments
Transmitter Power	+ 16.0 dbw	40 watts
Transmitter Antenna Maximum Gain	+ 7.0	
Transmit Antenna Pointing Loss	- 0.3	16.58°
Polarization Loss	- 0.5	
Transmit Circuit Loss	- 0.7	
Atmospheric Attenuation and Defocusing Loss	- 6.5	300 Atmos
Receive Antenna Maximum Gain	+ 21.4	4.15 ft dia
Receive Antenna Pointing Loss	- 0.3	
Receive Circuit Loss	- 0.2	
Space Loss	-197.4	146,930 km
Total Received Power	-161.5 dbw	
System Noise Spectral Density	-192.4 dbw	
Carrier Channel		
Loop Noise Bandwidth	14.8	30 Hz
Threshold S/N	9.0	
Required Threshold Power	-168.6 dbw	
Modulation Loss	- 0.8	
Received Power	-162.3 dbw	
Margin	+ 6.3	
Data Channel ϕ = 24.6° = 0.464 rad		
Data Bit Rate	+ 10.0	10 bps
E_b/N_o (coded) $P_e^b = 5 \times 10^{-4}$	+ 4.0	K = 4; V = 3, $\frac{1}{3}$ rate
Subcarrier Reference Loss	- 0.9	
Carrier Noise Degradation	- 2.1	
Required Data Channel Power	-175.4 dbw	
Modulation Loss	- 7.6	
Received Power	-169.1 dbw	
Margin	6.3	
Adverse Tolerances		
Misc. Circuit Losses	0.4	
Transmit Antenna Pointing Loss	2.6	±30°
Spacecraft Antenna Pointing Loss	0.1	
System Temperature	0.0	
Modulation Index	0.4	
Range	0.5	
Atmospheric Attenuation	1.0	
	- 5.0	

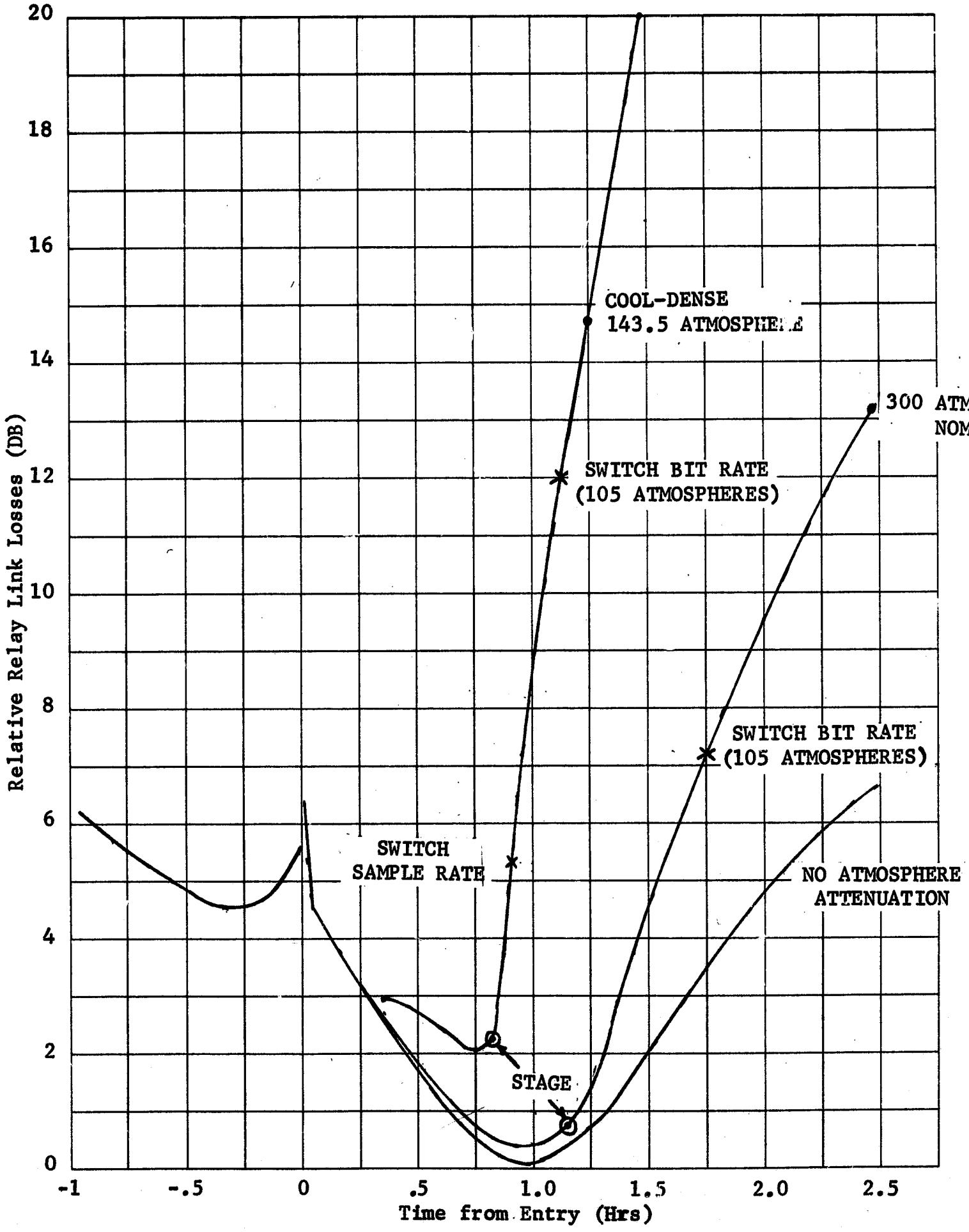


Figure VIF-3. Relative Relay Link Losses Versus Time, Design Example Mission

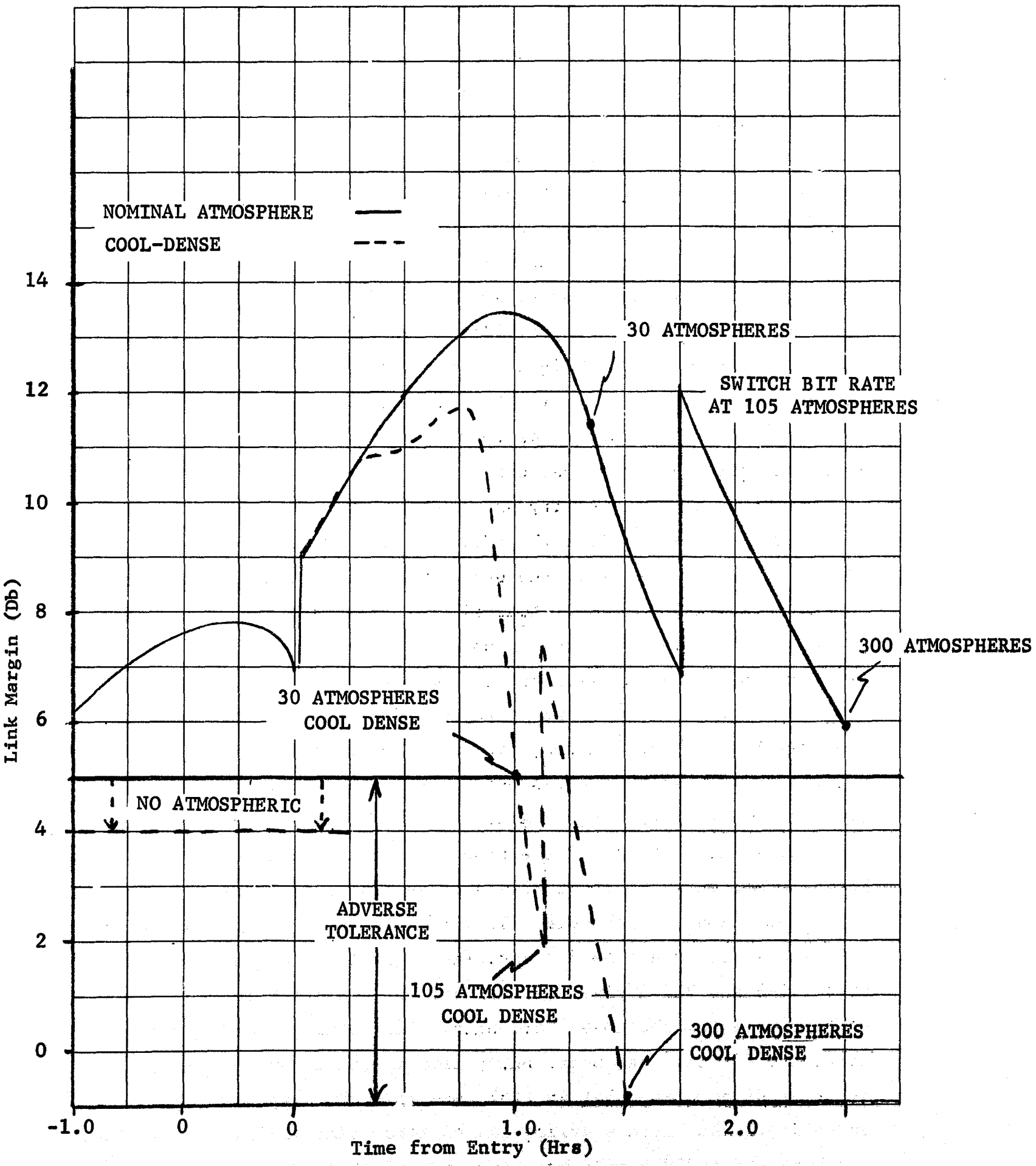


Figure VIF-4. Relay Communications Link Margin Versus Time, Design Example Mission

and cool-dense atmospheres. Increase in link gain of 6 db is required to communicate to a depth of 300 atmospheres in the cool-dense atmosphere at the nominal radio frequency. If one were to design for the cool dense atmosphere and a depth of 300 Earth Atmospheres he would lower the radio frequency to 0.85 GHz and increase link power gain by 3 db to compensate for the additional atmopsheric radio attenuation. This would accommodate both atmospheres to at least 300 Earth atmospheres depth.

b. The Descent Probe Telecommunications

The descent probe telecommunications system consists of a 1/3 rate, constraint length 4, convolutional encoder; square wave subcarrier oscillator and biphase modulator; 40 watt solid state phase modulated transmitter; output filter; transmission line; electronic RF switch and antenna. Weight and power allocations for these components are given in Table VIF-2. See also Volume III Chapter IV for discussion of selection of components.

c. Entry Vehicle Telecommunications

Transmission of telemetry data for 1 hour prior to entry of the entry vehicle requires the addition of an antenna on the rear of the entry vehicle since the descent probe antenna is not exposed during this mission phase. Nominal antenna aspect angles vary from 42 to 62° thus requiring use of an antenna having a "butterfly" pattern, giving a maximum gain of 4.5 db at 60 degrees off the spin axis. A typical antenna and pattern is discussed in Volume III, Chapter IV. The transmitter, modulator and convolutional coder physically located in the descent probe are also used at this time to save duplication of equipment.

Initial acquisition of the probe signal by the spacecraft 1.2 hours before entry is accomplished by searching in frequency through 3 beam positions in sequence. This requires 2.5 minutes for one complete search over the 3 σ uncertainty pointing dispersion. Figures VIF-5 and VIF-6 give the mean and uncertainties in Doppler and Doppler rate for the case where entry time is not sensed by the spacecraft and for the case where entry time is sensed by the spacecraft by means of assuming that initial loss of probe signal signifies entry if it also occurs during the expected time window. These data are based on a 250 sample Monte-Carlo navigation and accuracy analysis reported in Volume III Chapter IIIE. Figure VIF-7

TABLE VIF-2

TELECOMMUNICATIONS DATA HANDLING AND POWER
ENTRY VEHICLE

Aeroshell Mounted Equipment

	Wt (lb)	Power (Watts)
Telecommunications		
Relay Antenna	1.5	-
Data Handling		
Engineering Sensors	3.0	2
Electrical Power		
Power Conditioning	2.8	15 Peak
Battery	6.0	-
	(39.0)	
	Note 1	
Other		
Ion Mass Spectrometer	Note 2	1.0
ACS System	Note 2	10.0
Cabling	Note 2	
	13.3 lb	
	(46.3 lb)	
	Note 1	

Descent Probe Mounted Equipment

	Wt (lb)	Power (Watts)
Telecommunications		
Encoder/Modulator	1.5	3.0
Transmitter 1.2 GHz	8.0	130.0
Antenna and Relay	0.5	-
Data Handling		
Multiplexer and ADC	3.0	4.0
Format Generator and Control	6.0	5.5
Time and Sequencer	3.0	1.5
Power		
Power Conditioning	4.0	18.0
Battery	17.0	-
Subtotal	42.1	162.0
Other		
Science	Note 2	18.0
Cabling	Note 2	-
Total	42.1	180.0

NOTES:

1. When active thermal control is required - PIONEER spacecraft.
2. Weight included elsewhere.

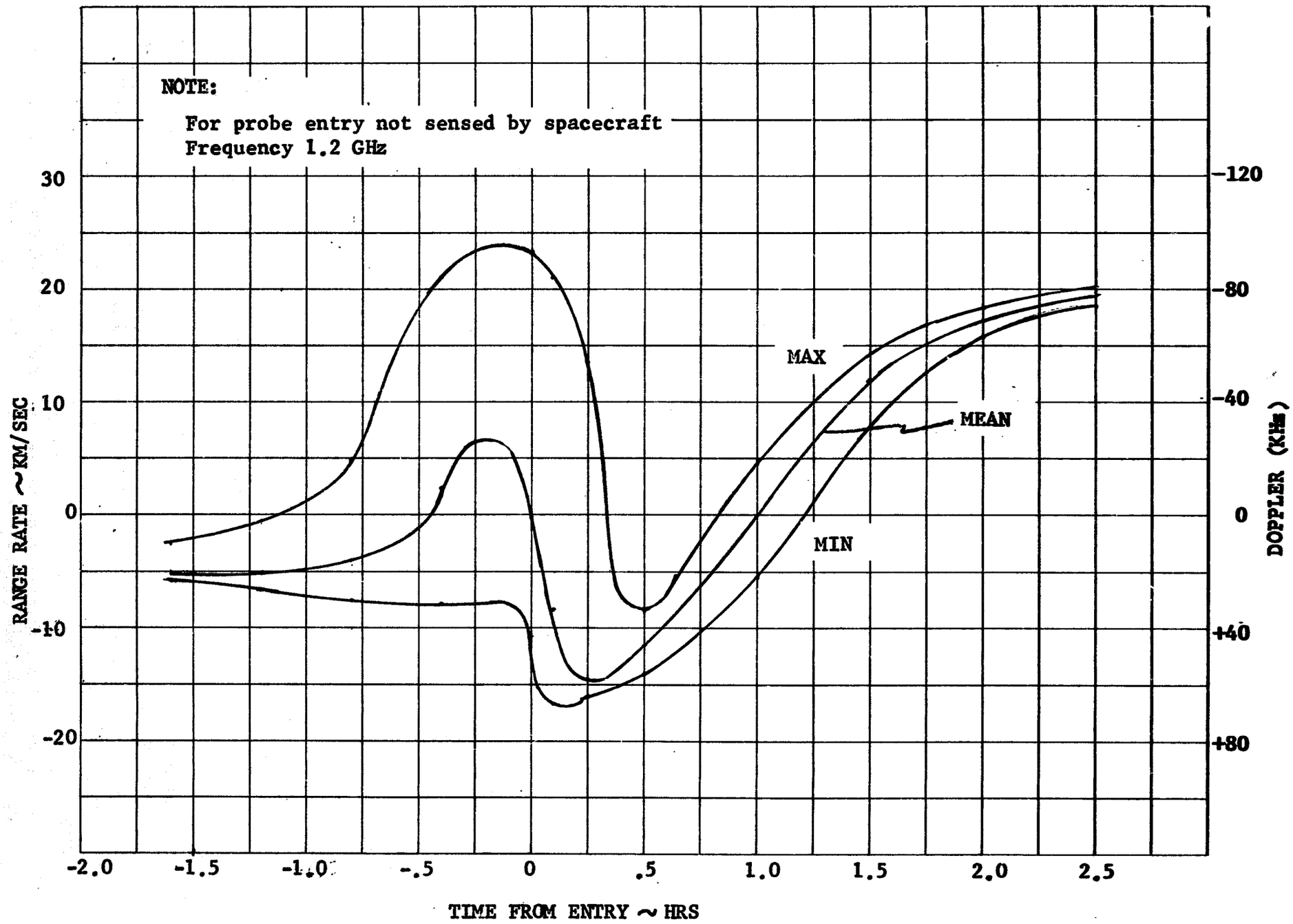


Figure VIF-5A Design Example Mission Range Rate and Doppler vs Time

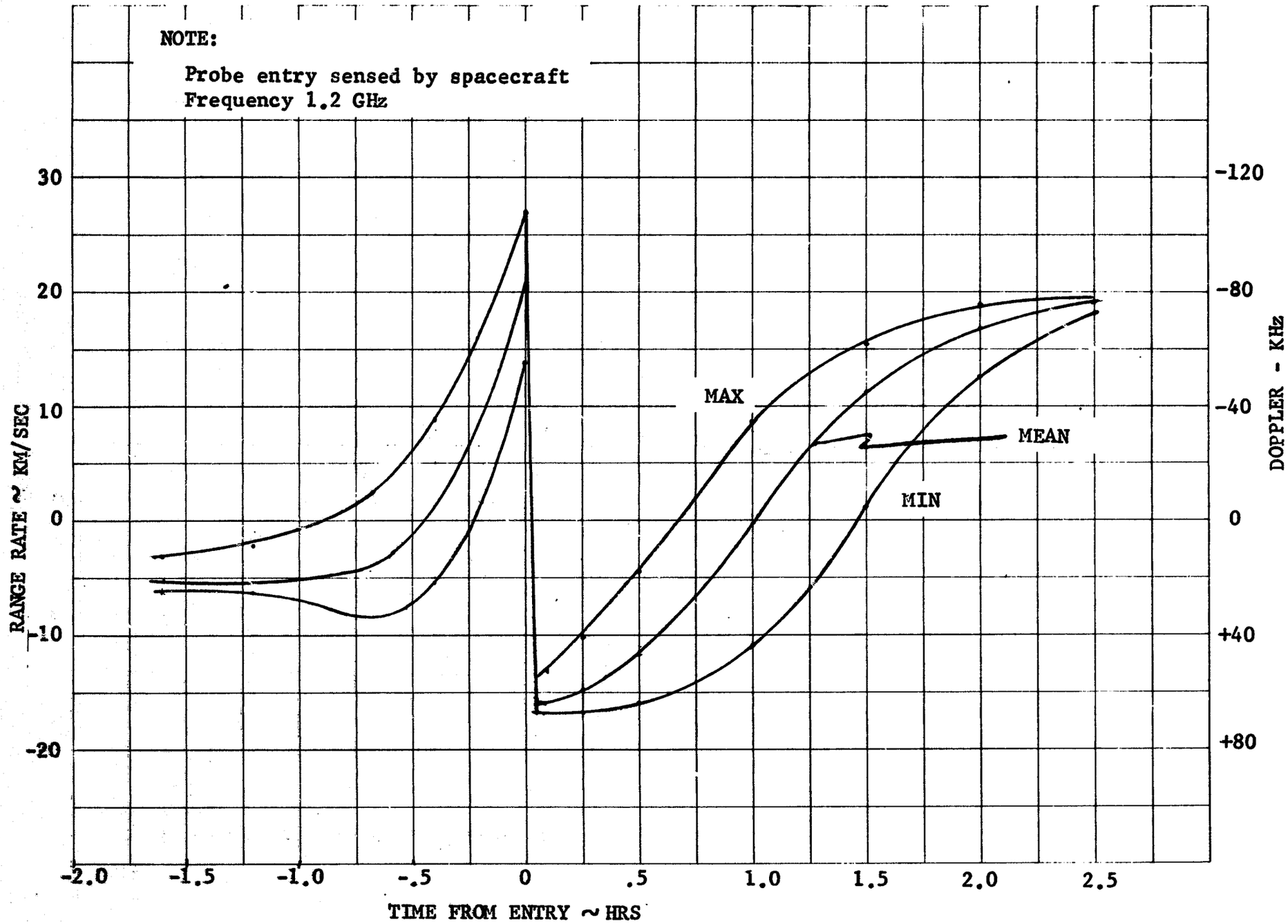
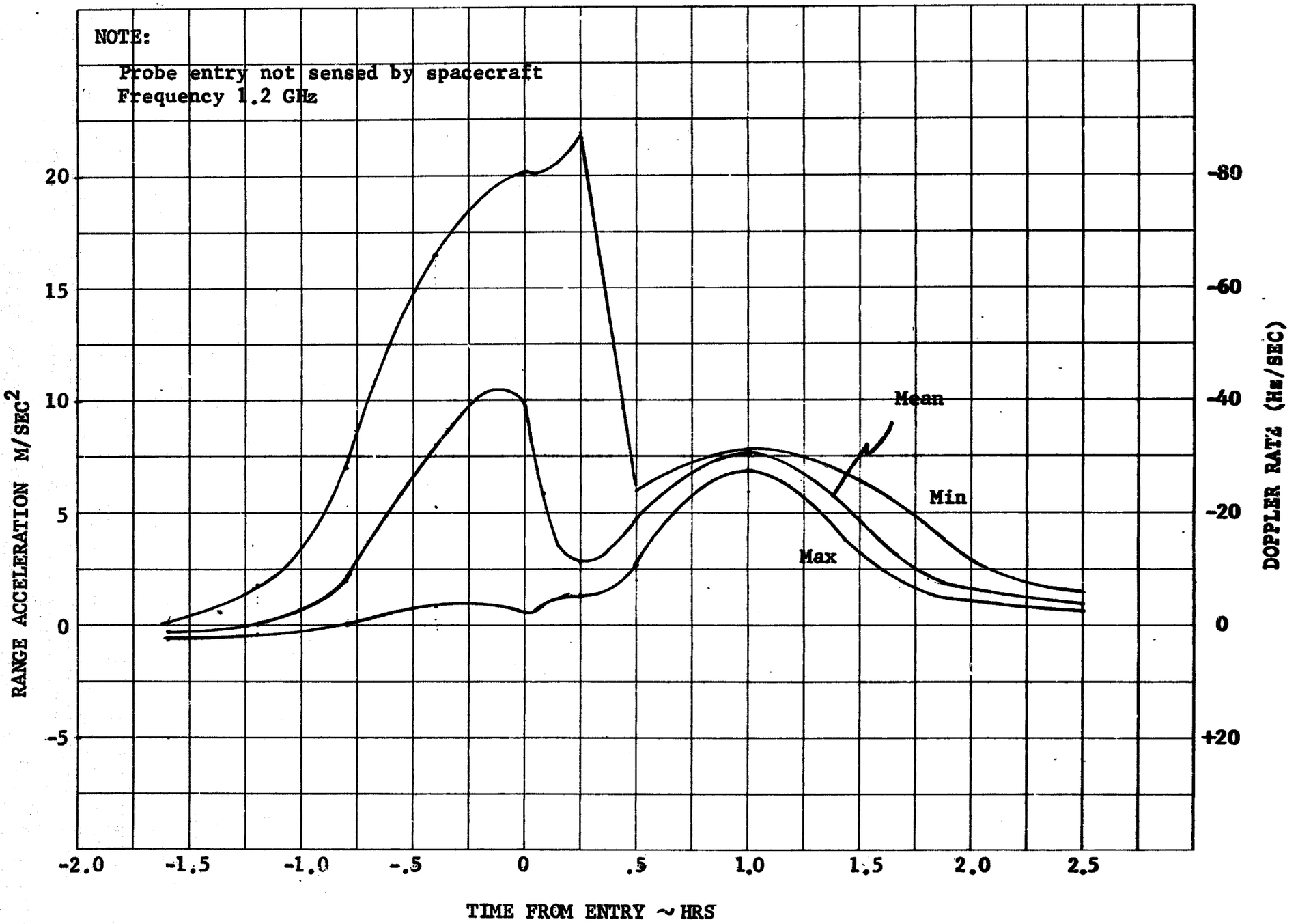


Figure VIF-5B Design Example Mission Range Rate and Doppler vs Time

Figure VIF-6A Design Example Mission Range Acceleration and Doppler Rate vs Time



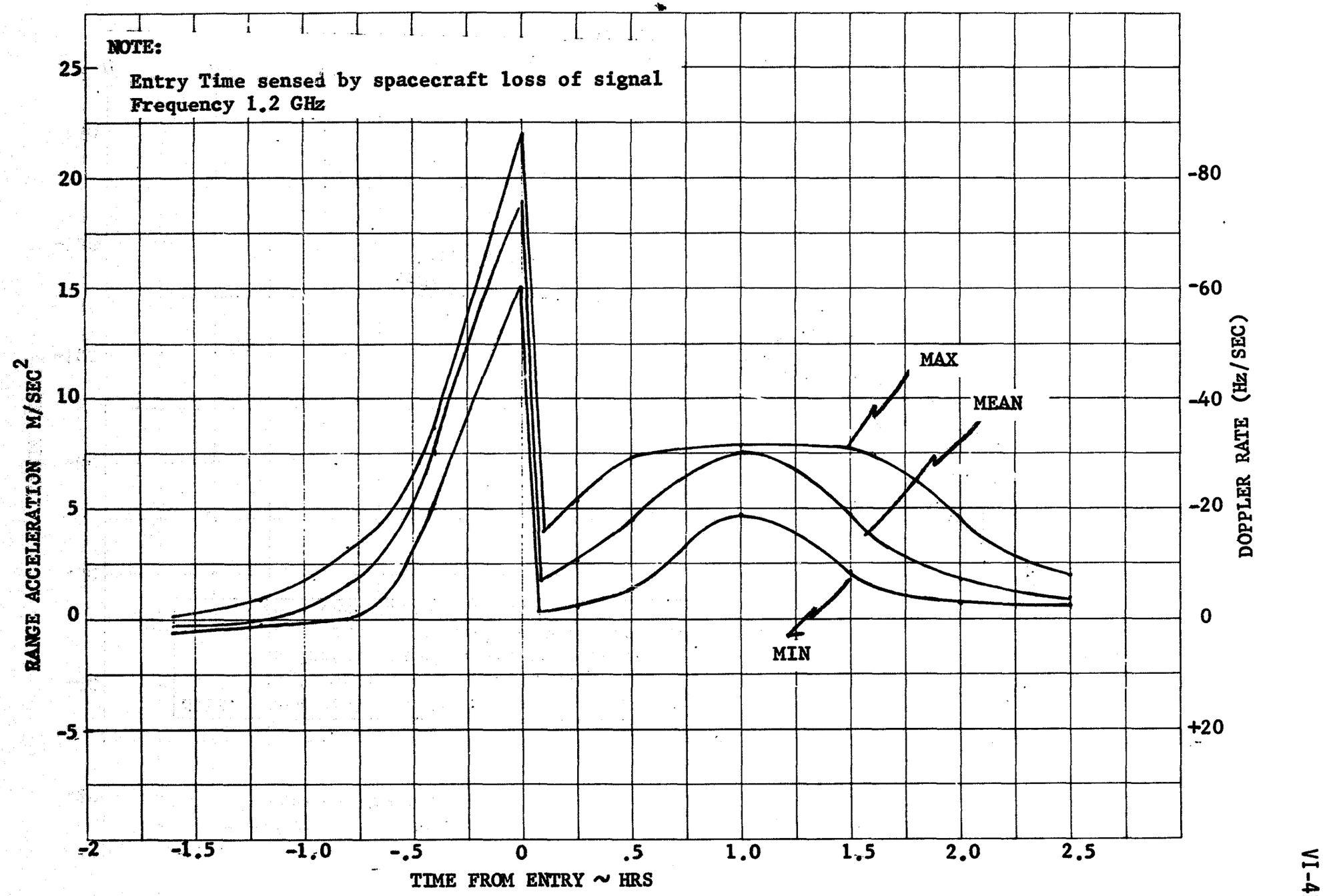
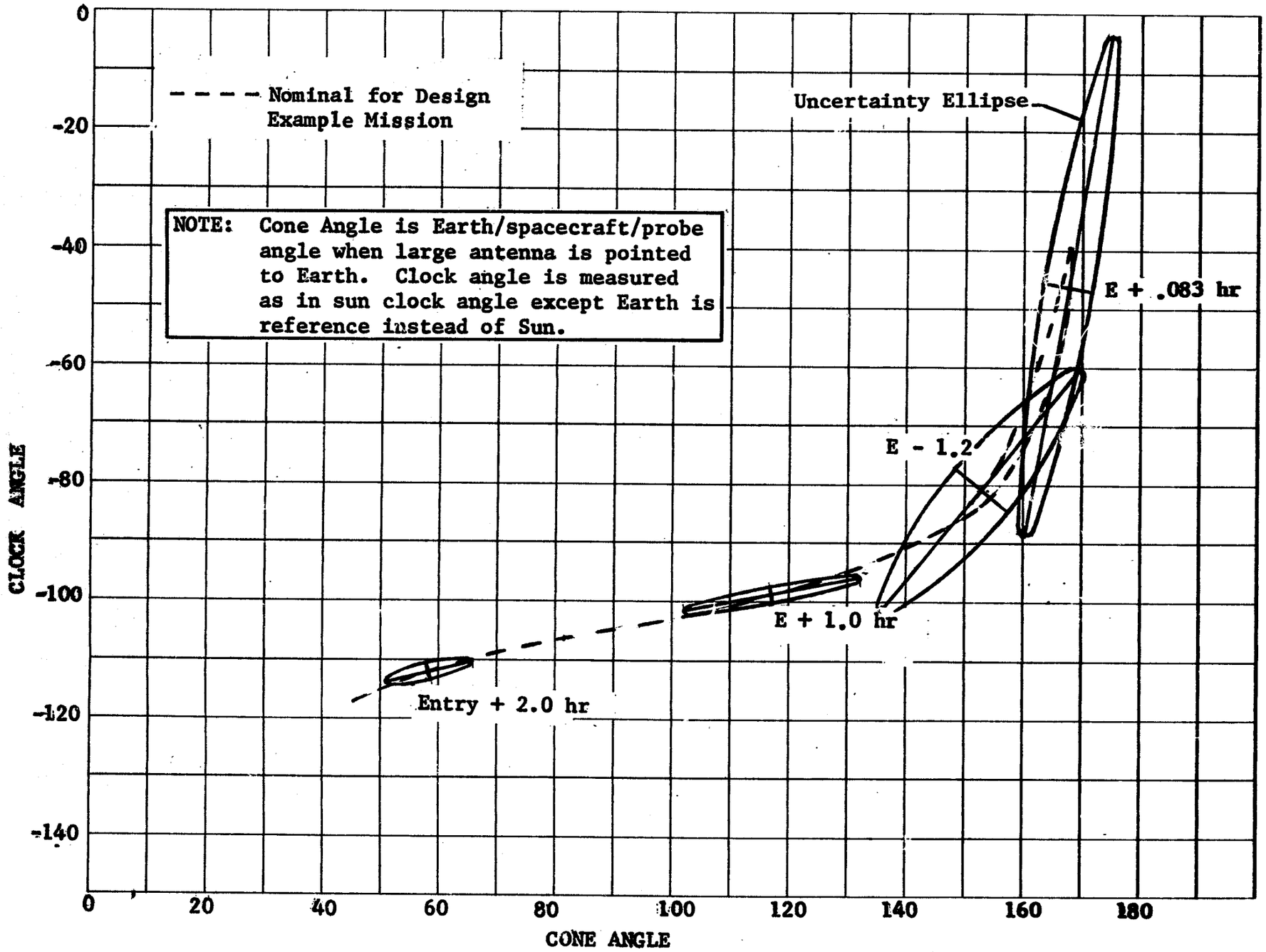


Figure VIF-6B Design Example Mission Range Acceleration and Doppler Rate

Figure VIF-7 Spacecraft Relay Antenna Pointing Angles (Nominal and Uncertainty)



shows uncertainty in pointing of the spacecraft antenna toward the probe during any period for initial acquisition. Acquisition search time at nominal post entry time assuming no knowledge of actual entry requires 3 minutes for one complete search over 3 beam positions. Using the knowledge that entry occurred, one search with 99% probability over the 3 σ pointing uncertainty requires 1.27 minutes. Detailed discussion of the signal acquisition and tracking is given in Volume III Chapter IVG.

d. The Spacecraft Telecommunications - DE Mission

Telecommunications required for either the TOPS or PIONEER spacecraft to support a probe relay link for this mission is tabulated in Table VIF-3.

2. Data Handling System - Design Example Mission

a. General Approach

The data handling system will include the sequencer and timer, data storage, engineering and science interfaces, data digitization and format generator-control subsystems. A generalized data handling system block diagram is shown in Figure VIF-8. This system will be used to handle data from both the basic internal probe engineering and science payloads and the external Ion Mass Spectrometer (IMS), which is jettisoned with the aeroshell. This will provide a reduced IMS package weight, size, and complexity at the expense of an increased number of pressure shell penetrations. The science payload of Figure VIF-8 includes one Ion Mass Spectrometer, one range switched digital pressure transducer, one range switched digital temperature transducer, one accelerometer, one six channel photometer and one Gas Chromatograph Mass Spectrometer with digital outputs. The output data rates will be 180, 40 and 10 bps. These instrument outputs more than fill the available data space at the 10 bps data rate and some instruments are dropped to provide space for the higher priority data.

Generally the engineering data has a lower priority than the science payload and lower data sampling rates with subcommutation used to reduce the required data space. Table VIF-4 shows the

TABLE VIF-3

TOPS AND PIONEER

TELECOMMUNICATIONS DATA HANDLING AND POWER

FOR DESIGN EXAMPLE MISSION

Telecommunications - TOPS or PIONEER	Wt (lb)	Power (Watts)
Relay Data Receiver	5	5
Subcarrier Demodulator	2	2
Viterbi Algorithm Decoder and Bit Synchronizer	1	1
Multilobing Receiver and Switch	3	3
Antenna Feed, Gimbals and Servos	Note 1	13
Despin Motor and Servo for PIONEER Only	Note 1	Note 2
	11	24
Data Handling - TOPS		
Frequency and Beam Search Programer (Relay link)	2	2
Miscellaneous Mods for Programing Spacecraft Operations and Storing and Retrieving Data	3	2
	5	4
Data Handling - PIONEER		
Frequency and Beam Search Programer	2	2
Data Storage for Relay Link Data	15	Note 2 15
Miscellaneous Mods for Programing and Control of S/C & Data Store	5	5
	22	22
Power Subsystem - TOPS		
Additional Switching and Control	3	-
Cabling	Note 1	-
Power Subsystem - PIONEER		
Power Conditioning Switching & Control	2.5	5.0
Remote Activated Primary Battery (4.0 hrs x 50 = 200 watt hours)	9.7	-

NOTES:

1. Weights shown under mechanical subsystems
2. It is assumed that the mechanically despun boom for the antenna and other telecommunications equipment is despun using spacecraft power.

   Data storage for the spacecraft is assumed to be read after the probe mission using spacecraft power. It will be battery operated during receipt of data.

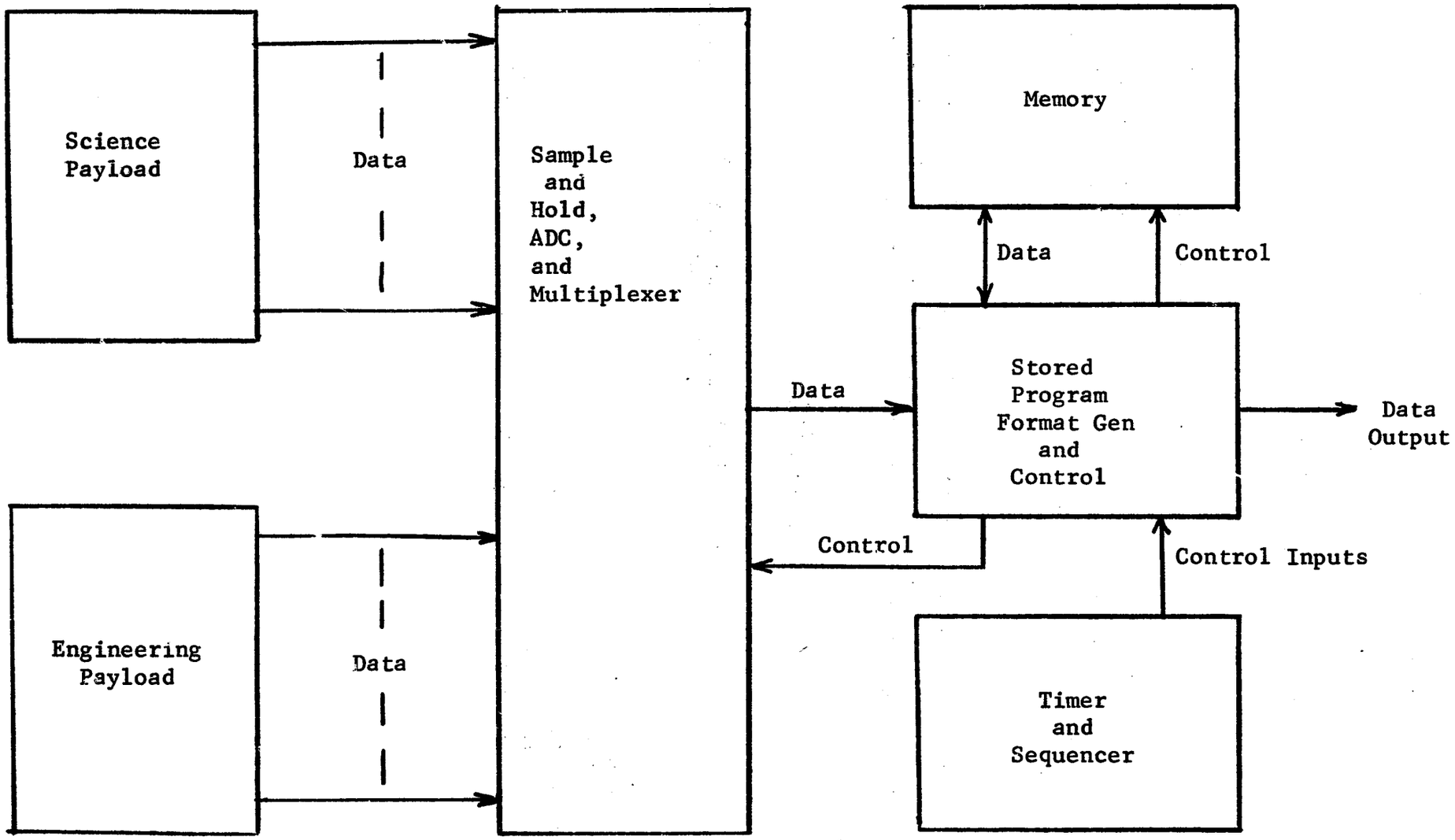


Figure VIF-8 Generalized Data Handling System

TABLE VIF-4

ENGINEERING PAYLOAD INSTRUMENTATION
DESIGN EXAMPLE MISSION

Engineering Data Bit Rates Available

Period #	Period in Mission	Bit Rate (BPS)	
1.	Pre entry	11	
2.	First 20 seconds of entry	412	(stored in probe)
3.	Entry + 20 sec to staging from aeroshell	226	(stored in probe)
4.	Post entry plus 1.75 hours	3.2	See Note
5.	Last 0.75 hour of mission	1.67	See Note

NOTE:

The above rates are adequate to provide 30 channels of engineering data each sampled every 75 seconds during period 4 and once every 144 seconds during period 5. Other options are obviously available.

Entry Sampling Rates

MEASUREMENT	# of Sources	SAMPLING RATE (SPS)	
		Entry Period #2	Entry Period #3
Probe internal temperature	2	1	0.1
Probe internal wall temp	2	1	0.1
Heat shield recession	3	4	-
Heat shield subsurface temp	3	1	0.1
Exterior Aeroshell temperature	3	1	0.1
Other Subsystems	2	1	

engineering payload sample data rates for the various mission phases.

The sample and hold (S/H), analog-to-digital converter (ADC) and multiplexer shown in Figure VIF-8 will operate under control of the format generator and control unit. These three units will operate at speeds in excess of the data rate and will not require special handling such as data buffering or multiple word lead times. The formats will be stored in memory and be special for each mission phase and data rate. All output data will be serial in nature and under direct control of the format generator.

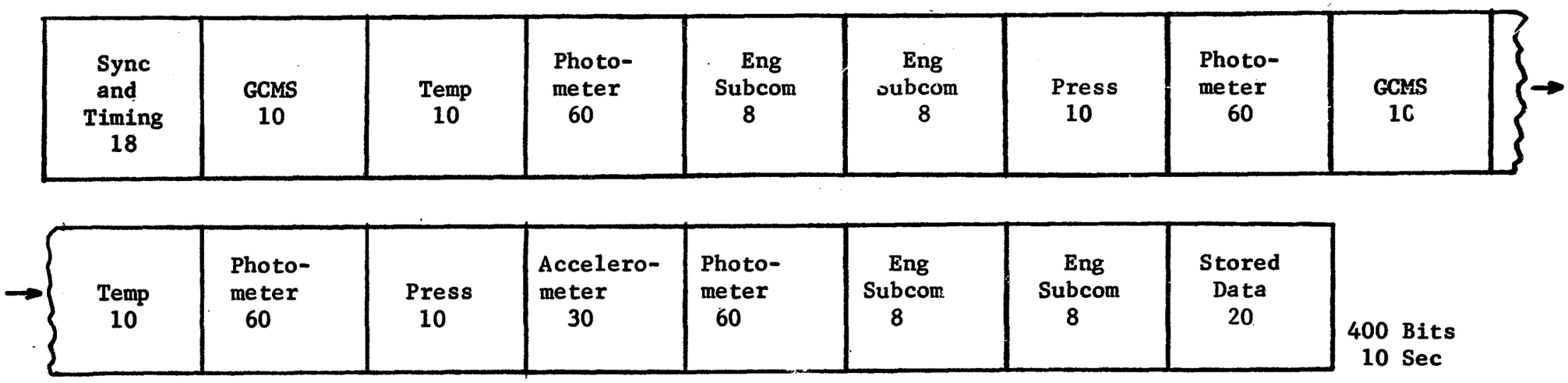
The timer will be an oscillator and set of electronic counters with the capability to count until the end of the entry phase. Primary use will be for timing of the coast phase. The sequencer is another set of electronic counters with decoders, which can be reset and combined with other events to provide time referenced control of sequencial operations.

The sequential operations for this example are summarized in Table VIC-1. These operations will be controlled by using the time reference supplied by the counted down oscillator and a secondary resetable 100 second counter for the sequencing of each arm, fire and safe pyro function, ΔV, other functions as required. These same signals will be used to either activate the transmitter or any other time referenced function.

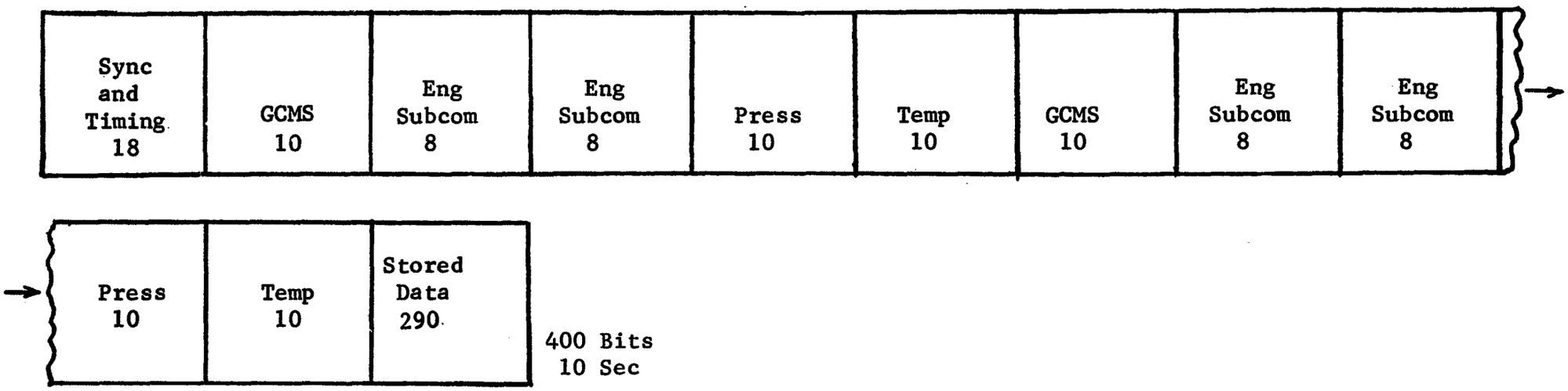
Weight and power allocations for the data handling subsystems are given in Table VIF-2.

b. Descent Phase

This phase starts immediately after aeroshell/heat shield staging with the reacquisition of probe to spacecraft signal. Transmission and storage of the first 3 minutes of data will be done according to the format shown in Figure VIF-9. This same format will be used to transmit real time data after this initial 3 minute period and until 30 atm is reached where the photometer and accelerometer data is omitted. This format has a 300 second main frame length which is the sample interval of the GCMS. The portion shown in Figure VIF-9 is one of the 30, 10 second sub frames per



DESCENT FORMAT BEFORE 30 ATM



DESCENT FORMAT AFTER 30 ATM

Figure VIF-9 Data Formats

each main frame. After the initial 3 minute combined store and transmit interval, the real time data transmission will continue without interruption. However, the stored data channel will then start being used to transmit 2.0 bps of data, starting with the 3 minutes of stored descent data. The total stored data, entry data and descent data, will be 26175 bits. At 2.0 bps the total stored data will require 218 minutes to transmit, which is longer than this mission phase. The 30 atm pressure point is reached 79 min after start of descent and at this point there remains 16695 bits in memory to be transmitted. However, at 30 atm the bit rate remains the same (40 bps) but the science output is reduced by omitting the photometer and accelometer. This increases the format space available for stored data transmission from 2 bps to 28 bps. The transmission of stored data is then completed 9 minutes 56 seconds later. The stored data is then re transmitted to guarantee that all the pre entry and all the first 3 minutes of post entry data is obtained. Retransmission will require another 15 minutes and 34 seconds. This will leave a very small unused space in the transmission format for other data. However, since it appears later in the mission the probability of receiving it is lower. In this example this space will be left unused for system expansion of the stored data. This 30 seconds of transmission represents the time between stored data transmission complete until data bit rate changes at 105 atm, and 105 minutes. Approximately 840 bits of stored data expansion is available. With the uncertainties of the atmospheres this choice of leaving this data space open is probably the best one.

At 105 atm the data rate changes to 10 bps and the format changes to that shown in Figure VIF-10. This format is used until mission end at 300 atm. There is no room in this format at this data rate to include stored data.

The required sequential operations during this phase are included in Table VIC-1 which shows all phases from separation to mission end. The first sequence of this phase is the deployment of the decelerator (chute) at entry plus 62.0 seconds. This will be done by decoding

Sync 18	Event 2	Eng Subcom 8	GCMS 10	Temp 10	Press 10	Eng Subcom 8	GCMS 10	Temp 10	Press 10

96 Bits
9.6 Sec

DATA FORMAT AFTER 105 ATM

Sync 18	Eng 10	Eng 88	Heat Shield Recession 96	Accelo-Meters 200

1 Sec
412 Bits

ENTRY 0-20 SEC FORMAT

Sync 18	Accelero-meter 200	Eng Subcom 8

1 Sec
226 Bits

ENTRY 20-67.5 SEC FORMAT

Figure VIF-10 Data Formats

the resetable sequencer at 62. seconds and logically combining this function with the 0.1 g sensor output to start the required pyro sequencer which deploy the chute, stage the aeroshell and start the transmission of data. All other sequential operations, staging the decelerator, changing the data mode and rate will be functions of pressure and be actuated by a pressure level sensor. This pressure level sensor will continuously monitor the pressure transducer output and provide switch signals at 15, 30 and 105 atm. Thus some automatic compensation for the various atmospheric models is built into the system.

c. Entry Phase

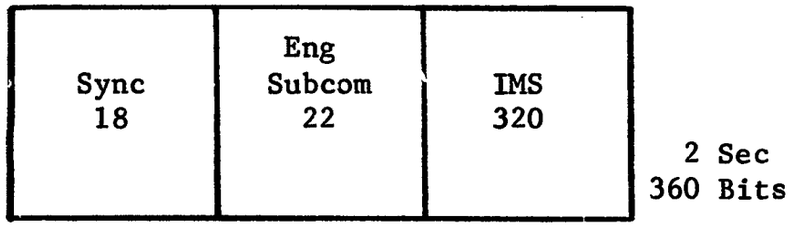
This phase consists of the ballistic portion of the flight to a radius where the chute deploys and descent phase data is acquired. The start of entry is a timed function pre-programmed before separation from the spacecraft. The nominal time used for this example mission is 40 days. The time decoder will be a digital comparator with this variable time set on registers and compared to the timer output. At 40 days this digital comparator output will activate the data system to collect and store the accelometer and engineering entry data. This same timer will continue to run and at .1 g the sequencer will be reset by the acceleration sensor and another digital comparator will indicate the end of entry and start the aeroshell/heat shield staging sequence which uses this same resetable counter. At this time the entry data is complete and is in storage. This data is collected and stored as per the formats shown in Figure VIF-10. The use of two formats. one for the first 20 seconds and another thereafter, reduces the stored data to only that high priority engineering data and the entry accelerometer data. Total stored data during entry is then 26175 bits when the 0 to 20 second engineering data is sampled at the minimum rate. The data format change will also be a timed function activated by the resetable sequencer and the .1 g sensor. This entry data will require the use of the S/H, ADC, memory and format generator which will require a complete power up of the total data system.

d. Pre-entry Phase

This phase consists of the transmission of Ion Mass Spectrometer data for 1.2 hours just prior to the entry phase. This transmission is started by the timer at entry minus 1 hour and 5 minutes, with the initial 5 minutes used to transmit unmodulated carrier. This 5 minute transmission helps in the establishment of the spacecraft to probe link. After this 5 min period the Ion Mass Spectrometer is operated at 2 seconds per scan with an output of 320 bits per scan. The format generator and multiplexer are activated to provide the serial bit stream to the modulator. The required format is shown in Figure VIF-11 with the engineering subcom channel format. At entry minus 17 minutes pyros are armed, fired and safed by the sequencer, which is activated by a time decoder (digital comparator), to despin the probe by the extension of weights. This same sequencer then continues with another arm, fire, safe sequence to jettison the despin weights. This phase is stopped by the timer just as the entry phase is beginning. This phase will provide data from 800, 2 second scans during the 1 hour transmission time.

e. Separation and Deflection Phase

The entire separation maneuver will be under control of the spacecraft. This will require 1) numberous electrical penetrations through the probe shell, and 2) that all probe systems be designed to operate from the probe control system and from spacecraft stimuli. The requirement for numerous shell penetrations tends to justify our use of one data system for the probe science and the IMS. Many of the penetrations used to provide spacecraft stimulation can also be used for IMS data handling and provide a saving in penetration number. The separation sequence is started with a preparation sequence by the spacecraft at entry minus 40 days plus the sequence time. This sequence includes the establishment of spacecraft-earth link, the determination of deflection burn duration and the input of the data to the probe, a probe system checkout and the attitude maneuver to separate the probe at the correct angle. These commands are sent through the spacecraft. At the time of actual separation the probe attitude control system will be active. However, the data handling system is not required and can



PRE-ENTRY FORMAT

Battery Voltage 8 Probe Temp 8 Battery I* 4	Battery I* 4 Battery Temp 8 Excitev Pwr 8	Calibrate 8 VCO Temp 4 Xmit Pwr 8	Probe Temp 4 Probe Press 8 Events 8

ENG SUBCOM FORMAT

*Half of Data Word

Figure VIF-11 Pre-entry Formats

be powered down until separation plus 20 minutes where the deflection burn is initiated by a time decoder. The resetable sequencer then takes over and outputs the required arm, fire and safe signals. Deflection burn stop is initiated by an acceleration level sensor circuit which triggers the sequencer for the arm, fire and safe functions. This acceleration level is also set before separation by the spacecraft as is the ACS data. The ACS system then orients the probe to a zero angle of attack just prior to probe spin up which is initiated by the ACS system and sequenced by the resetable electronic sequencer. The ACS is then shutdown for the coast portion (40 days) of the flight. The data handling system can then be powered down until entry minus one hour and 12 minutes when the pre-entry phase starts.

f. The Spacecraft Data Handling - Design Example Mission

General data handling requirements and modifications for the spacecraft(s) are discussed in Volume III Chapter IV. Weight and power allocations for spacecraft data handling for the design example mission are given in Table VIF-3.

Electrical Power - Design Example Mission

a. General

Electric power for the entry vehicle and descent probe is required for all phases of the mission following launch.

The power profile for the mission beginning at deflection of the probe from the spacecraft is shown in Figure VI.F-12. It is assumed here that preheating of the probe to maintain temperatures during the deflection to entry coast period was accomplished using spacecraft power which is the case for the TOPS spacecraft. For the Pioneer spacecraft case, electrical energy is required to keep the entry vehicle up to temperature during the deflection to entry period. This energy is provided by the battery carried in the aeroshell of the entry vehicle.

b. Entry Vehicle and Probe Power

Conventional power conditioning equipment is proposed for regulation of battery power and power isolation. Non-dissipative high efficiency regulators and converters will operate at better than 80% efficiency at maximum load. Solid state switching will be used for most loads. Switching of transmitter input power may require a relay.

The power profile Figure VI.F-12 represents an energy requirement of 640 watt hours with a peak load of 180 watts in one duty cycle. This load is split between two batteries, one in the aeroshell to handle coast through entry (171 watt hours) and one in the probe for post entry power (469 watt hours). Remotely activated primary batteries are proposed for this application as discussed in Volume III, Chapter IV.

The battery would comprise a cell configuration of dry charged plates and microporous separators capable of a wet stand life of 40 days. Electrolyte would be stored in a container so designed that gas generated from an electrically activated double base propellant would eject the electrolyte into the cells. Battery and power conditioning weight

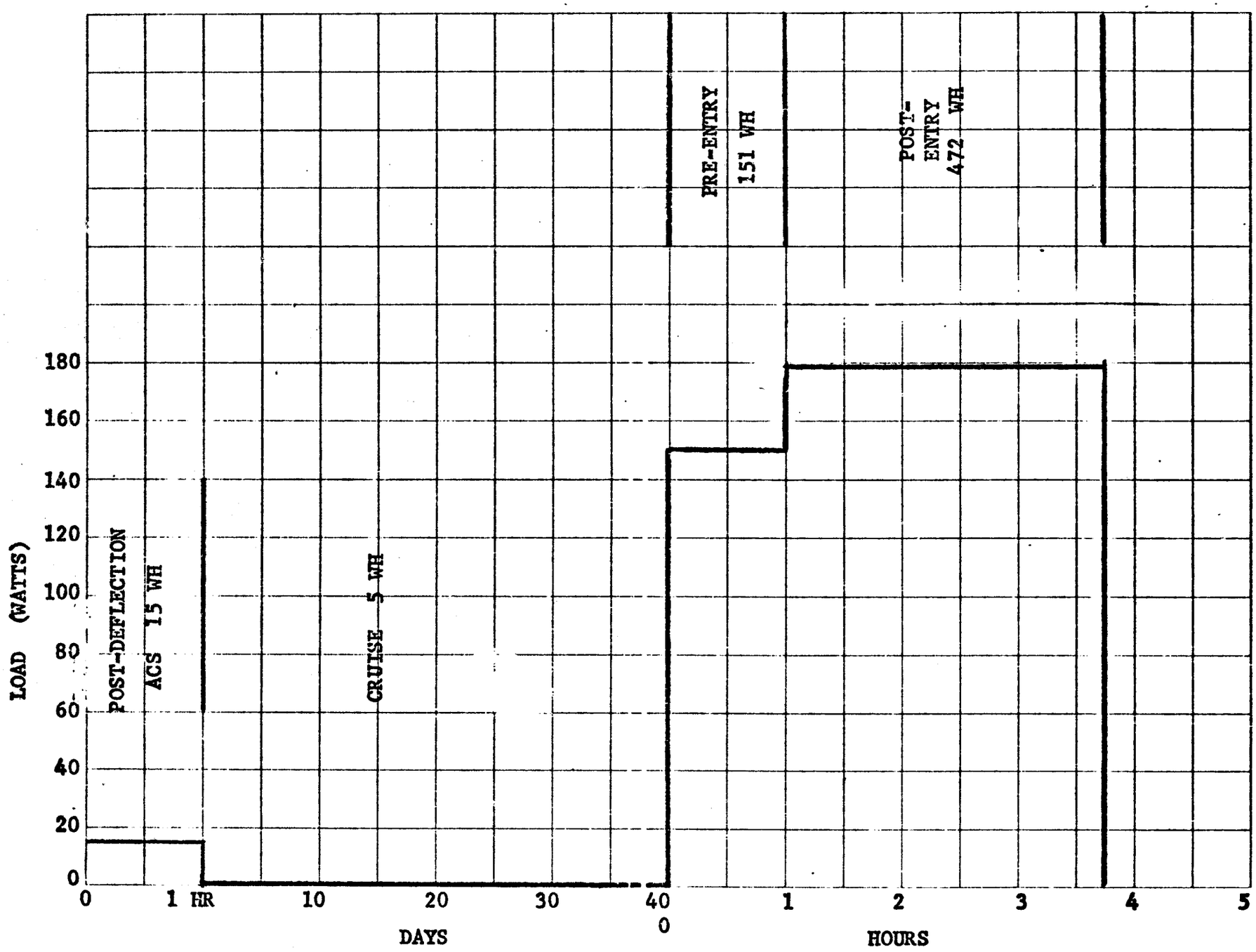


Figure VIF-12 Power Profile, Design Example Mission

allocation are given in Table VI.F-2, assuming 27.5 watt hours per lb to include degradation allowance.

c. Spacecraft Power Subsystem

The TOPS spacecraft power subsystem is required to supply from 0 to 2.3 watts of electrical power for active thermal control of the probe and approximately 1 watt for thermal control of spacecraft mounted telecommunications probe support equipment for the cruise phase and 7500 watt hours during a 3 day interval prior to separation of the entry vehicle from the spacecraft for preheating of the entry vehicle. For the pre-entry through the probe descent phase 31 watts are required for TOPS spacecraft telecommunications and data handling relay link support equipment. For the case of the TOPS spacecraft all power is assumed available from the "existing" spacecraft power subsystem.

For the Pioneer spacecraft an additional continuous power capacity of 1.1 watts must be provided to maintain the entry vehicle at a higher temperature during cruise to eliminate a requirement for preheating. Fifty watts are required for pre-entry and entry relay communications support phases. Remotely activated primary batteries (zinc silver oxide) are recommended for supplementing spacecraft power for the probe entry support phase. Battery and other power subsystems weights are given in Table VI.F-3 based on 200 watt hours for support of probe relay communications.

VII. SAMPLE MISSIONS

A series of Sample Missions were selected to illustrate various aspects of potential Jupiter missions in addition to those of the Design Example Probe of the previous chapter.

These are:

Mission A	A nominal science probe in combination with a 1979 Grand Tour Mission.
Mission B	A probe with a reduced probe-to-spacecraft aspect angle geometry to facilitate Pioneer tracking.
Mission C	A Pioneer Orbiter Mission.
Mission D	A dual miniprobe mission on a 1979 Grand Tour Mission.
Mission E	A probe combined with a 1978 Grand Tour.
Mission F	A direct link mission.

The science payloads for these missions are shown in Table VII-1, and descriptions of each are contained in the following paragraphs.

A. Mission A Selection Rationale

Sample Mission A was selected to examine the feasibility of using the TOPS spacecraft on a 1979 Grand Tour mission to carry an atmospheric entry probe to Jupiter. The Type I trajectory results in a reduced payload capability (1900 lbs) compared to a Type II trajectory. The planetary approach geometry is radically different from the Design Example mission because of the large periapsis radius (= 6.8 R_J) associated with the 1979 J_PUN Grand Tour.

1. Mission Profile

The approach geometry for sample Mission A is shown in Figure VIIA1-1. Two versions of the descent profile were studied:

In version A_1 a single probe with a ballistic coefficient of .05 sl/ft^2 descends to 10 atmospheres in approximately 55 minutes.

In version A_2 an upper probe has the same profile as for A_1, and a lower probe with a ballistic coefficient of 1.1 sl/ft^2 descends to 100 atmospheres in the same time interval.

The descent profiles are shown in Figure VIIA1-2.

2. Sequence of Events

Major sequenced events and design parameters for sample Mission A are tabulated in Table VIIA2-1.

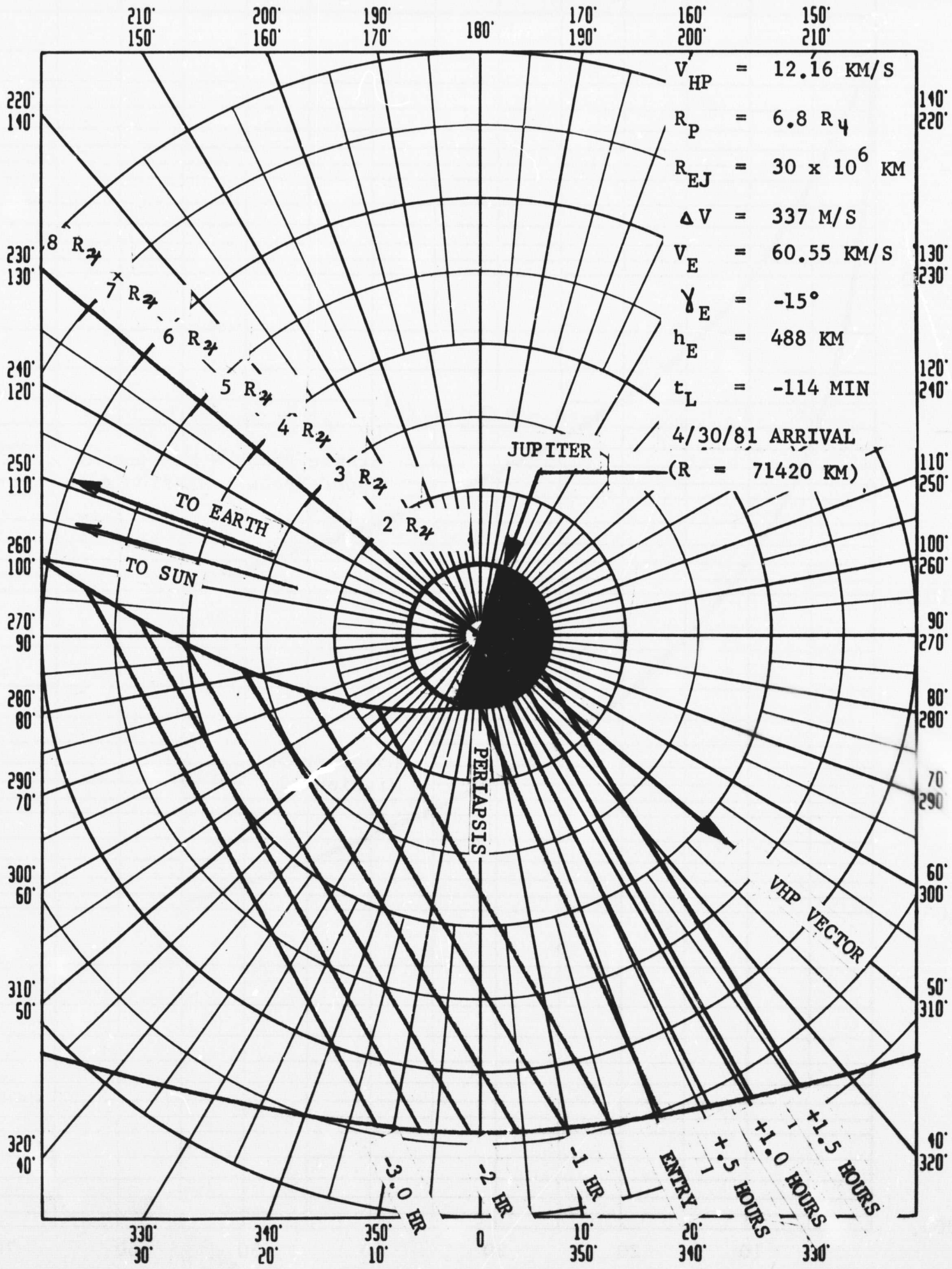


FIGURE VIIA1-1
APPROACH GEOMETRY
SAMPLE MISSIONS A AND D

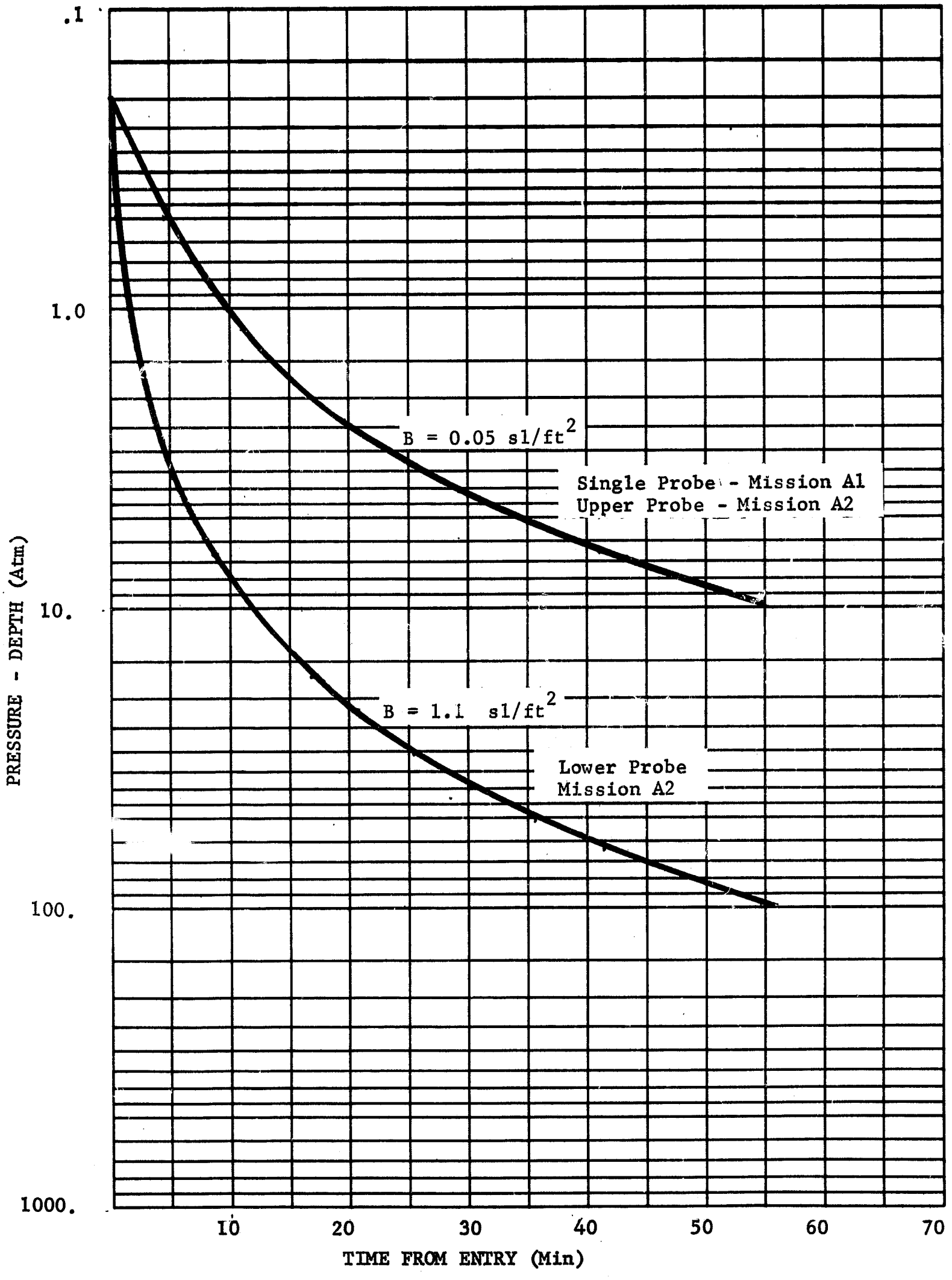


Figure VIIA1-2 Descent Profile - Sample Mission A

TABLE VIIA2-1

LAUNCH PARAMETERS

LAUNCH DATE (NOMINAL)	11/6/79
LAUNCH VEHICLE	TITAN III D CENTAUR (7 SEG WITH BURNER II)
LAUNCH PERIOD	30 DAYS
PARKING ORBIT ALTITUDE	100 NAUTICAL MILES
SPACECRAFT	TOPS
SPACECRAFT WEIGHT	1450. LBS
PAYLOAD WEIGHT (INCL S/C)	1900 LBS
FAIRING SEPARATION	CORE 2 IGNITION PLUS 10 SEC
MAX LAUNCH AZIMUTH	115 DEG

INTERPLANETARY CRUISE PARAMETERS

TRAJECTORY	TYPE 1/GRAND TOUR
DECLINATION OF LAUNCH ASYMPTOTE DLA	24.9 DEGREES
RIGHT ASCENSION	139.5 DEGREES
INJECTION ENERGY, C3	111.7 KM2/SEC2
FLIGHT TIME	541 DAYS (NOMINAL)
SEMI-MAJOR AXIS	6.0 A.U.
RADIUS OF APHELION	NOT TRAVERSED
ECCENTRICITY	0.835
INCLINATION TO ECLIPTIC	2.3 DEGREES
CENTRAL ANGLE OF TRAVEL	145.1 DEGREES
TRUE ANOMALY AT DEPARTURE	357.9 DEGREES

ENCOUNTER PARAMETERS

JUPITER ARRIVAL DATE	4/30/81 (NOMINAL)
TRUE ANOMALY AT ARRIVAL	143.0 DEGREES
EXCESS VELOCITY, VHP	12.154 KM/SEC
DEC OF VHP VECTOR	6.53 DEGREES
RIGHT ASC OF VHP VECTOR	164.7 DEGREES
(WITH RESPECT TO VERNAL EQUINOX, EARTH EQUATORIAL SYSTEM)	
DEC OF VHP VECTOR	0.22 DEGREES
(WITH RESPECT TO EQUATOR OF JUPITER)	
COMMUNICATION RANGE	4.6 A.U.

DEFLECTION PARAMETERS

BUS TRAJECTORY	FLYBY
PERIAPSIS RADIUS OF BUS	483969. KM= 6.8 JUPITER RADII
DEFLECTION RADIUS	30,000,000. KM
INCLINATION OF TRAJECTORY (WITH RESPECT TO EQUATOR OF JUPITER)	1.0 DEGREES
DEFLECTION VELOCITY	337 METERS/SEC
DEFLECTION ANGLE	-126.5 DEGREES
CAPSULE COAST TIME	26 DAYS
LEAD TIME	-114 MINUTES
LEAD ANGLE	19.53 DEGREES

* *

* * * * ENTRY PROBE DESIGN DATA * * * *

RELATIVE ENTRY VELOCITY	48.05 KM/SEC = 157604 FT/SEC
ENTRY ANGLE	-15. DEGREES (SKIPOUT AT -4 DEG)
ENTRY ALTITUDE (TIME=0)	487.7 KM = 1,600,000. FEET
ENTRY RADIUS	71907.7 KM
ENTRY LATITUDE	-0.6 DEGREES
ENTRY LONGITUDE	105.2 DEGREES
(RELATIVE TO MERIDIAN OF SUN)	

* *

* * * * AEROSHELL DATA * * * *

* *

ALTERNATE 1

ENTRY BALLISTIC COEFFICIENT	.78 SLUGS/FT2
TIME TO .1 G POINT	12.5 SECONDS
TIME OF MAXIMUM DECELERATION AND MAX DYNAMIC PRESSURE	26.5 SECONDS
MAXIMUM DECELERATION	714 G
MAXIMUM DYNAMIC PRESSURE	15069 LB/FT2
TIME OF MACH 1 OCCURRENCE	51.5 SECONDS
AEROSHELL STAGING	
ALTITUDE	33 KM=200 MB
MACH NUMBER	.50
DYNAMIC PRESURE	76.8 LB/FT2
TEMPERATURE	203.4 DEG R
DENSITY	.00009726 SLUG/FT3
TIME (TS)	92.0 SECONDS

* *

ALTERNATE 2

ENTRY BALLISTIC COEFFICIENT	.88 SLUGS/FT2
TIME TO .1 G POINT	13.0 SECONDS
TIME OF MAXIMUM DECELERATION AND MAX DYNAMIC PRESSURE	27.0 SECONDS
MAXIMUM DECELERATION	724 G
MAXIMUM DYNAMIC PRESSURE	16,643 LB/FT2
TIME OF MACH 1 OCCURRENCE	51.5 SECONDS
AEROSHELL STAGING	
ALTITUDE	33 KM=200 MB
MACH NUMBER	.52
DYNAMIC PRESSURE	83.4 LB/FT2
TEMPERATURE	203.4 DEG R
DENSITY	.00009726 SLUG/FT3
TIME (TS)	88.0 SECONDS

3. Configuration Summary - Mission A-1 and A-2

The configuration for the single probe concept of A-1 and the split probe concept of A-2 are shown in Figures VIIA-3-1 and VIIA-3-2 respectively. System characteristics are given in Table VIIA-3-1 and weight breakdown in Table VIIA3-2 and VIIA3-3.

Descriptions of the systems are contained in Sections 4 and 5 which follow:

4. Mechanical and Support Systems

a) Mission A-1

The descent probe structural/thermal design concept is an evacuated titanium pressure vessel exposed to the ambient environment since at the 10 atmosphere maximum depth point the temperature is only 190°F. The inner wall is lined with multilayer insulation. The concept of equipment support, shell penetrations, and shell closure of the Design Example configuration is also applicable to this design. Since the low initial descent ballistic coefficient required, 0.05 slugs/ft^2, is maintained throughout the descent, the probe stays suspended beneath a parachute which allows the pressure vessel shape to be selected independent of aerodynamic configuration considerations. A sphere is therefore selected.

The entry aeroshell is a 55 degree half angle cone, 3.0 feet in diameter. Aeroshell construction and arrangement is typical of the Design Example.

The probe is mounted to the TOPS spacecraft as is shown previously in Figure VI-D-3. The integration of the planetary vehicle within the booster fairing envelope and adaptations to the booster is also the same as in the Design Example case.

b. Mission A-2

The structural/thermal concept of an evacuated pressure vessel thermally insulated applies to both the upper and lower descent probes. The internal structural arrangement concept of equipment

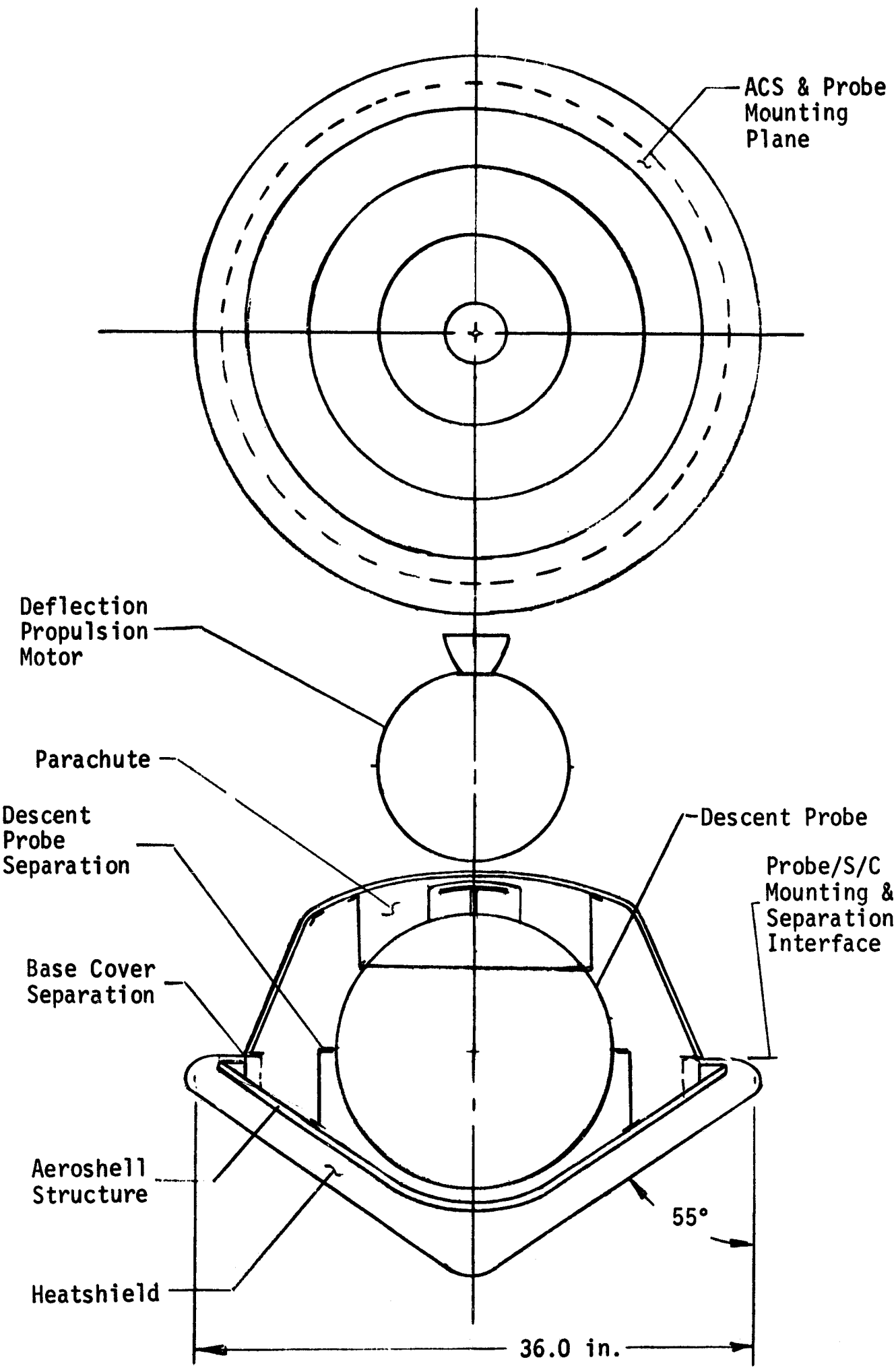


Fig. VII-A-3-1 Entry Probe Inboard Profile, Mission A_1

TABLE VIIA3-1

MISSION A MAJOR PROBE CHARACTERISTICS SUMMARY

	A-1	A-2
Type Probe	Single	Split
Maximum Depth	10 atm	100 atm
Entry Angle	-15°	-15°
Data Return Mode	Relay	Relay
Spacecraft Radius of Periapsis	6.8	6.8
Science Payload	10 lbs	10 lbs
Bit Rate - Descent	40	40
Transmitter Power	40 watts	40 watts (upper) 2 (lower)
Spacecraft Antenna Dish Diameter	4.5 feet	4.5 feet
Descent Time	.93 hr	.93 hr
Entry Ballistic Coefficient	.78	.88
Probe Diameter	3.0	3.5
Entry Weight	239.0 lbs	367.0
Probe as Installed	311.5	459.5
Total Probe System Weight (including spacecraft mods)	399.5	562.5
Total Liftoff Weight	1849.5	2012.5
Launch Vehicle Capability (7 segment TIIID Centaur with Burner II)	1900.0	1900.0

TABLE VII A-3-2

MISSION A-1 SYSTEM WEIGHT SUMMARY

ITEM		WEIGHT (LBS)
Science	18.0	
Communications & Power	41.7	
Pressure Shell	6.6	
Internal Structure	5.6	
Insulation (Multi-Layer)	0.2	
Accelerometer Trial	1.9	
Pyro Vent Valve Inst'l.	1.5	
Antenna	1.4	
Misc. External Structure	4.0	
Descent Probe Wt.		(80.9)
Parachute & Harness	4.1	
Parachute Canister	1.3	
De-Spin (Fixed)	1.0	
Separation Mechanisms	3.0	
Auxiliary Structure	3.0	
Entry Veh. ACS (Gyro, Jets, etc.)	25.0	
Cabling & Umbilicals	3.0	
Equipment Inst'l. Structure	4.0	
Total E. V. Misc.		(44.4)
Aeroshell Structure (3.0'D.)		(32.0)
Heatshield		(81.7)
Entry Weight		239.0
Deflection Propulsion Module	61.0	
De-Spin System (Spent)	1.5	
Separation Mechanisms	2.0	
Thermal Blanket	8.0	
		(72.5)
Probe Installed Wt.		311.5
Spacecraft Mods		88.0
Total Probe System Weight		399.5
TOPS Spacecraft		1450.0

TABLE VII A-3-3

MISSION A-2 WEIGHT SUMMARY

		UPPER PROBE	LOWER PROBE
Science		18.0	15.3
Communication & Power		41.7	15.1
Pressure Shell		11.5	13.6
Internal Structure		5.6	3.1
Multi-Layer Insulation		.8	.5
Phase Change Material		- -	- -
Antenna/s	(2)	2.5	1.4
Pyro Vent Valve		1.5	1.5
Aero Stabilizer Structure		4.0	8.5
Descent Probes Complete		(85.6)	(59.0)
			(85.6)
De-Spin Yo-Yo System (Fixed)		2.0	
Parachute & Canister		8.4	
Separation Mechanisms		3.0	
Auxiliary Structure		3.0	
Entry Vehicle ACS		25.0	
Cabling and Umbilicals		4.0	
Equipment Inst'l Structure		5.0	
Total E. V. Misc.			(49.4)
Aeroshell Structure (3.5' Dia)			(48.0)
Heatshield			(125.0)
Entry Weight			367.0
Deflection Propulsion Module		80.0	
De-Spin System (Spent)		2.0	
Separation Mechanisms		2.5	
Thermal Blanket		8.0	
			(92.5)
Probe Installed Wt.			459.5
Spacecraft Mods			103
Total Probe System Weight			562.5
TOPS Spacecraft			1450.0
Total			2012.5

support is the same in both probes based on the entry g-load requirements. The design philosophy discussed for the Design Example probe is also applicable to these designs.

Upper Probe

The upper probe is an evacuated titanium pressure vessel exposed to the ambient environment with the inside surface of the shell lined with multi-layer insulation. To facilitate packaging in the aeroshell while minimizing entry weight, the upper probe is reconfigured from a sphere to a modified oblate spheroid. Since the terminal pressure is low (10 atmospheres) the weight penalty associated with this configuration does not impact the total weight situation as compared to increasing the aeroshell size to accommodate a spherical upper probe.

The three-module upper probe configuration presented in the Volume III parametric study is not compatible with the aeroshell size because it results in an impractical cross-section size from a packaging standpoint, as well as necessitating nearly a complete torus to provide the volume required. Since this concept would result in an appreciably heavier probe, the single-module modified oblate spheroid configuration was selected.

The upper probe's required descent rate is low necessitating a parachute for velocity control, consequently the probe shape is not critical from an aerodynamic standpoint.

The upper probe has two antennas both turnstile types but of different size because of the different operating frequencies required. The upper antenna is protected by an RF transparent domed cover which also serves to provide a smooth receptacle for parachute packaging.

The lower antenna retracts for mounting the probes in the aeroshell and is deployed by an extension spring when the probes are separated.

Lower Probe

The lower probe is an evacuated titanium spherical pressure vessel exposed to the ambient environment. The inner wall is lined with multi-layer insulation and the shell closure-dome is inverted to effect a shallower total probe depth.

An external ring on the pressure shell serves to mount both probes at the aeroshell ring beam and transmit the entry loads to the aeroshell. Since the pressure shell is inherently rigid for the pressure loads little shell reinforcement is necessary for entry loads. A ring skirt outside the closure dome provides an adapter and separation joint for the upper probe.

The descent ballistic coefficient of 1.0 slugs/ft^2 for the lower probe is achieved by adding a drag ring that deploys to a more aft position, after separation from the entry vehicle, to provide directional stability.

Aeroshell

The entry aeroshell is a 55 degree half angle cone forebody 3.5 feet in diameter. Construction and general arrangement is typical of the Design Example. The entry ballistic coefficient is .88 slugs/ft^2 at an entry angle of -15 degrees.

The probe is mounted to the TOPS spacecraft as previously shown (Figure VIB-3).

Probe Weight vs Launch Vehicle Capability

The weight of this probe, 562.5 lbs, is greater than the 450 lb capability of the 7 segment launch vehicle. However, the launch vehicle capability is constrained by the R_P = 6.8 R_J associated with the 1979 JUN Grand Tour mission. In the previous chapter, it was found that extending R_P to slightly larger values increases the payload capability faster than it increases the split probe system weight. An R_P of 7.8 was found to provide approximately the needed match between probe weight and L.V. capability (Figure VG-2). Thus if the other objectives of the Grand Tour mission are not compromised by the increased flyby distance, the split probe mission at R_P = 7.8 appears to be the best way to achieve a substantial survival depth. It should be noted that some reduction in the 100 ATM probe survival depth would have to be made to offset the increased communications range at R_P = 7.8 vs 6.8 (if the 40 watt transmitter power limit is adhered to).

a. Telecommunications Data Handling and Power for Mission A-1

Telecommunications data handling and power concepts for mission A-1 are based on those for the design example missions with the exception that pre-entry data transmission over the relay link is not attempted due to adverse entry vehicle antenna angles and the long range. A 3 db deficiency in link margin exists during this period for rapid acquisition of an unmodulated carrier if one designs for post entry conditions. Post entry communications require a 40 bps data rate for a period of 1 hour while the single descent probe descends to a pressure depth of 12 earth atmospheres.

A 40 watt 2.3 GHz probe transmitter and a 4.55' S/C auto track antenna are used to attain the bit rate. Communications geometry, range and antenna aspect angles, relative link losses, and communications link margin as a function of time are shown in Figures VIIA1-1 and VIIA5a-1, 2 and 3.

Initial signal acquisition is accomplished by searching in frequency in only the mean antenna position based on the small antenna pointing uncertainty dispersions shown in Table VII-A5a-1. See Volume III, Chapters IIIE and IV for a discussion of search and acquisition and antenna uncertainty ellipses.

TABLE VII-A5a-1

CONE AND CLOCK ANGLE DISPERSIONS - ALTERNATE MISSION A-1

Time From Nominal Entry	Mean Cone Angle (deg)	Mean Clock Angle (deg)	3σ Ellipse		
			Semi-axis 1 (deg)	Semi-axis 2 (deg)	0 (deg)
.0833	44.0	-104.7	2.82	.564	3.3
.25	43.3	-104.7	1.62	.532	4.5
.5	41.9	-104.8	1.58	.525	5.0
.75	40.6	-104.9	1.56	.517	5.2
1.0	39.3	-104.9	1.52	.509	5.4

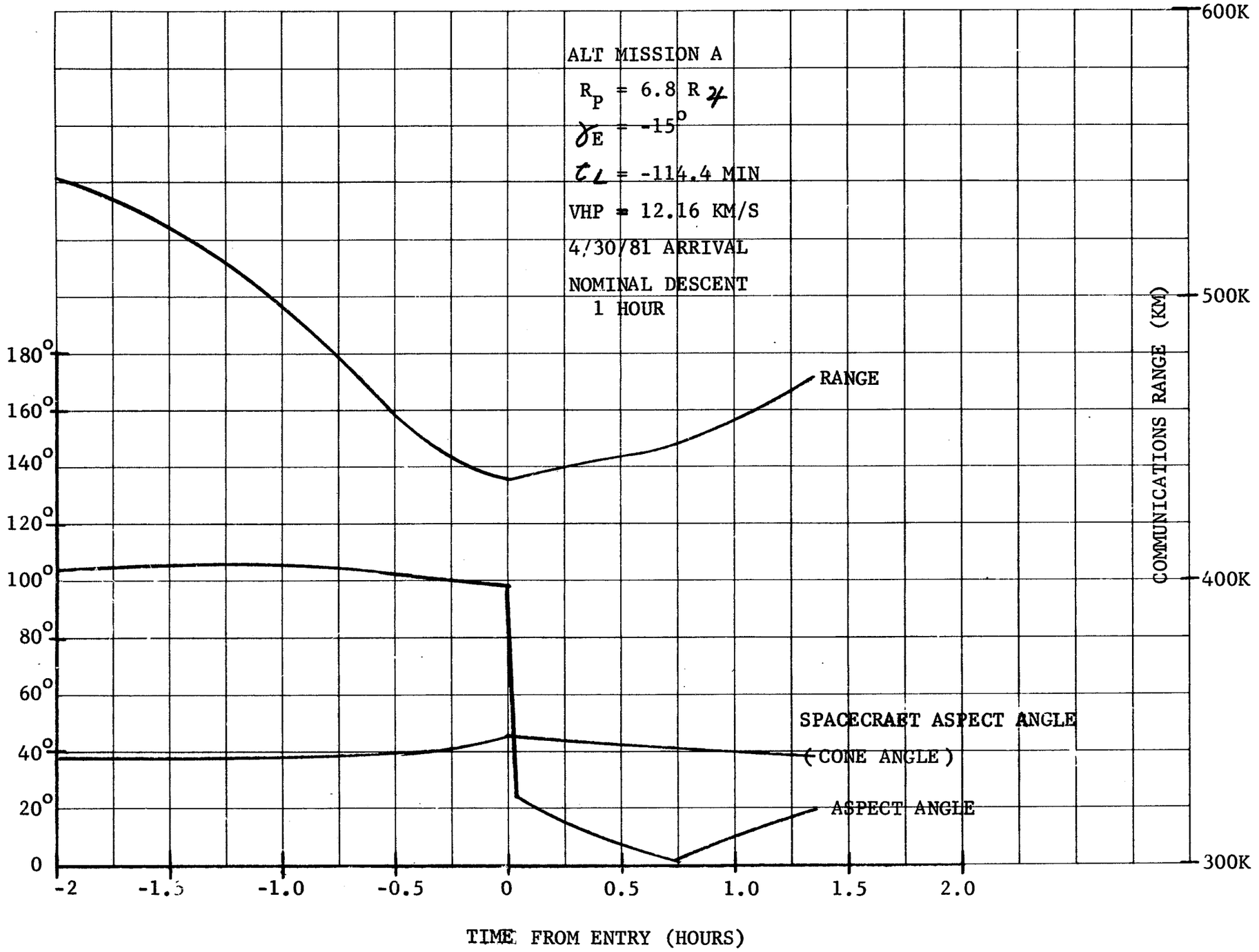


Figure VIIA5a-1 Alternate Mission A - Aspect Angles and Range vs Time

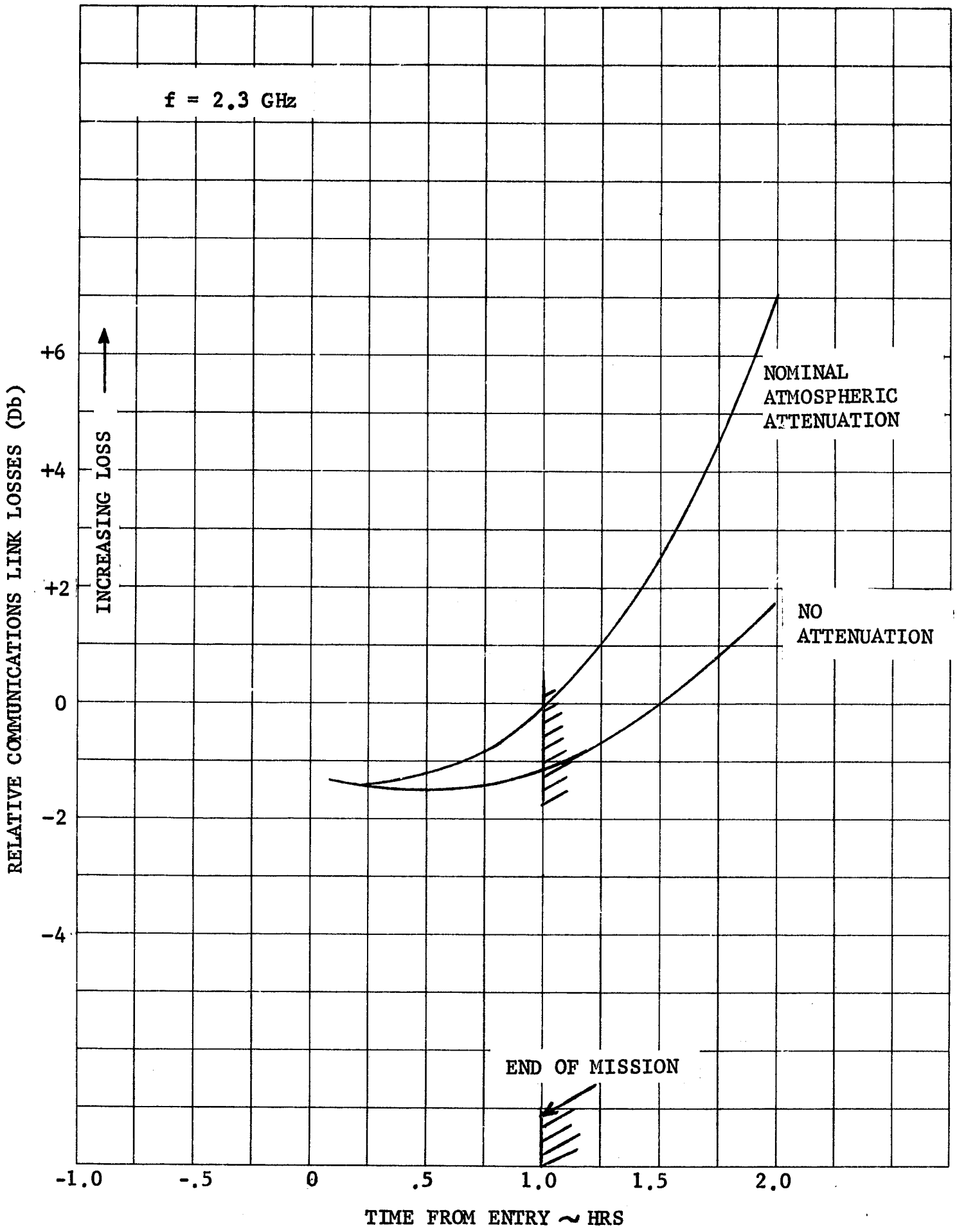


Figure VIIA5a-2 Relative Relay Link Losses vs Time Probe to Spacecraft.

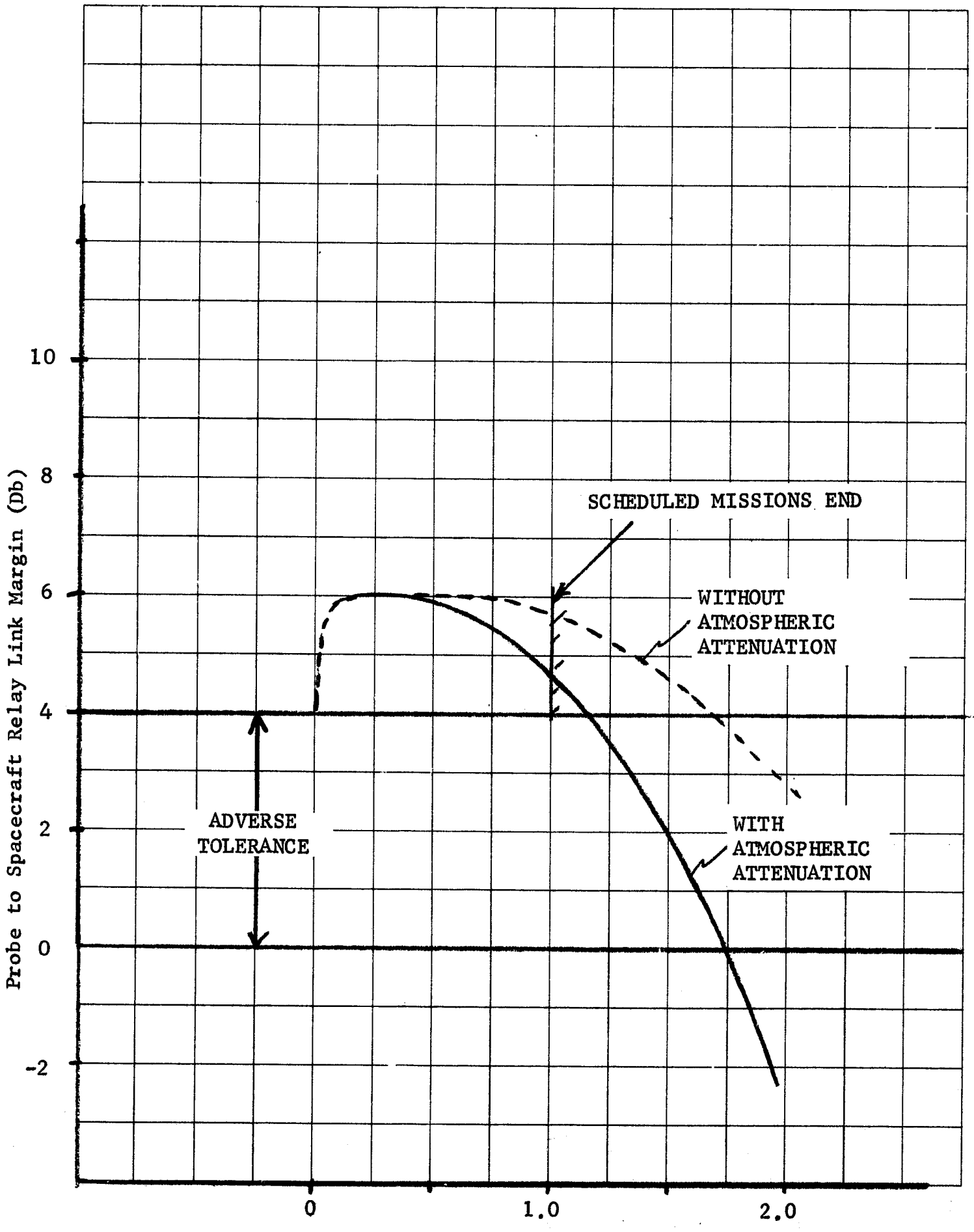


Figure VIIA5a-3 Probe to Spacecraft Relay Link Margin Mission A1 and A2.

Storage of 26175 bits of science and engineering data occurs during entry and for 3 minutes after entry in the same manner as for the design example mission. The 40 bps transmission data rate following entry is made up of 25 bps of real time science, 8 bps of stored data and 8 bits of engineering and timing data.

Power for the probe is supplied by a remotely activated zinc silver oxide primary battery located in the probe pressure shell. No aeroshell mounted battery is required since the probe transmitter is not used during pre-entry coast. A battery weight allocation of 9 lbs is based on the following power requirements:

Subsystem	Power (Watts)	Total Watt Hours
Telecommunications	130	130
Data Handling	12	17
Science	33	33
Power Conditioning	19	30
Entry Vehicle - ACS	10	10
	204	220

Total weight of the telecommunications, data handling and power subsystems based on similarity to the design example mission less an 8-pound difference in battery weight is as follows:

	Weight (lb)
Telecommunications	10
Data Handling	12
Power	13
	35

Spacecraft support requirements for this mission are the same as for the design example mission except that relay data bits to be handled are 40 x 3600 coming to a total of 144,000 as compared to over 600,000.

b. Telecommunications Data Handling and Power - Mission A-2

Telecommunications data handling and power concepts for this mission are in general based on those used in the baseline parametric study for a split probe arrangment in which the upper probe descends to 10 atmospheres in a 1 hour period while the lower probe is descending to 100 atmospheres in the same period. Data acquired by the lower probe is transmitted to the upper probe via a 1.0 GHz wide-band non-coherent PCM link. This data is in turn combined with data acquired by the upper probe and transmitted in a single data stream using a coherent PCM/PSK/PM coded link to the flyby S/C. Post entry bit rates for the two links are 40 and 9.85 bps for the lower and upper probes respectively using the same combination of 40 watt, 2.3 GHz probe transmitter and 4.55 ft diameter S/C antenna as required for mission A-1. Pre-entry data is not acquired.

Relay communications geometry, range, antenna aspect angles and link margin for the upper probe to S/C link is the same as for mission A-1.

A communications design control table for the probe to probe link is shown as Table VII-A5a-2. Lower probe transmitter power output is 2 watts at 1.0 GHz. Low gain circularly polarized curved turnstile antennas are used for both ends of the probe to probe link. Selection of the 1.0 GHz frequency was based on lowering the frequency until antenna size became the limiting factor. See Volume III, Chapter VII for this tradeoff which is common for this mission and the trial mission.

A receiver and bit synchronizer completes the probe to probe link equipment requirement for the upper probe.

Data handling for the upper probe as compared to the A-1 mission probe requires in addition, the synchronization of the 9.85 bps data stream being received from the lower probe

TABLE VIIA5a-2

PROBE TO PROBE COMMUNICATION LINK CALCULATIONS

WIDE BAND FSK

		Adverse (db)
Transmitter Power (2 W, 1 GHz)	+33 dbm	0
Transmit Antenna Gain (Max)	+5.0 db	0
Transmit Antenna Pointing Loss(@ 45°) Note 3	-1.5 db	8.0 Note 2
Receive Antenna Gain	+5.0 db	0
Receive Antenna Pointing Loss (@ 45°)	-1.5 db	6.0 Note 2
Transmit Circuit Loss	-0.5 db	0.5
Receive Circuit Loss	-0.2 db	0.2
Atmospheric Losses	-3.5db	3.0
Polarization and Miscellaneous	-1.0 db	0.3
Space Loss (295 km, 1.0 GHz) Note 3	-141.9db	3.1
Total Gains and Losses	-140.1db	21.1
Received Signal Power	-107.1dbm	21.1
Receive Noise Power Density (System Temp = 2130°k)	-165.3 dbm	1.0
Filter Bandwidth (13 kHz)	+41.1 db	0
Required Input S/N (Bit Error Probability 1×10^{-5})	-5.0 db	0
Required Input Signal Power	-129.2 dbm	22.1
Margin	+22.1db	22.1db

NOTES:
1. Set margin equal to adverse tolerance where adverse tolerance is equal to worst case expected.
2. Transmit antenna and receive antenna aspect angles of 120° and 90° respectively can be accommodated in turbulence without exceeding margin.
3. Nominal antenna aspect angle of 45° is assumed to accommodate drift due to wind variations. Range assumes $\sqrt{2}$ times vertical separation.

with the upper probe data stream. The upper probe data train consists of the following:

Source	Data Rate (BPS)
Real time upper probe science	17
Resynchronized lower probe data	10
Upper probe stored data (entry and first 3 minutes of post entry)	8
Real time engineering and timing data (upper probe data)	5
	40

The lower probe data train consists of 8 bps of science and 1.95 bps of engineering and timing data.

Power for the upper and lower probes are provided by primary battery. Energy requirements are 44.3 watt hours for the lower probe and 193.3 watt hours for the upper probe.

Weight and power for the subsystems are shown in Table VII-A5a-3.

The S/C mounted support equipment and modifications to the S/C are identical to the requirements for mission A-1.

TABLE VII-A5a-3

WEIGHT AND POWER FOR MISSION A-2 PROBES

	Upper Probe		Lower Probe	
	Lbs	Watts	Lbs	Watts
Antennas				
Relay to S/C	0.5	-		
Probe/Probe	1.4	-	1.4	
FSK Receiver	1.5	0.5		
Modulation/Exciter	1.5	1.5		
Power Amplifier	8.0	130.0		
FSK Transmitter			0.8	8.0
Times and Sequences	3.0	2.0	1.0	2.0
Format Generator, and Memory	6.0	4.0	2.0	1.0
ADC and Multiplexers	3.0	2.0	2.0	2.0
Power Conditioning	4.0	15.0	3.0	4.0
Battery	9.0	-	1.5	-
	37.9	158.0	11.7	17.0
Other				
Science Instruments	-	20.3	-	27.3
TOTAL POWER		178.3		44.3

NOTE: Energy for entry ACS and the coast period following probe deflection is 15 watt hours. It is supplied by the upper probe battery.

B. Mission B Selection Rationale

Sample Mission B was selected to define the design requirements associated with a single atmospheric entry probe carried by the PIONEER F/G spacecraft. A payload weight of 1550 pounds and a Type II trajectory permit the use of the five segment version of the TITAN IIID launch vehicle. The launch date was not critical though a September 1978 date was chosen.

1. Mission Profile

The approach geometry for sample mission B is shown in Figure VIIB1-1. The descent profile is shown in Figure VIIB1-2.

2. Sequence of Events

Major sequenced events and design parameters for sample mission B are tabulated in Table VIIB2-1.

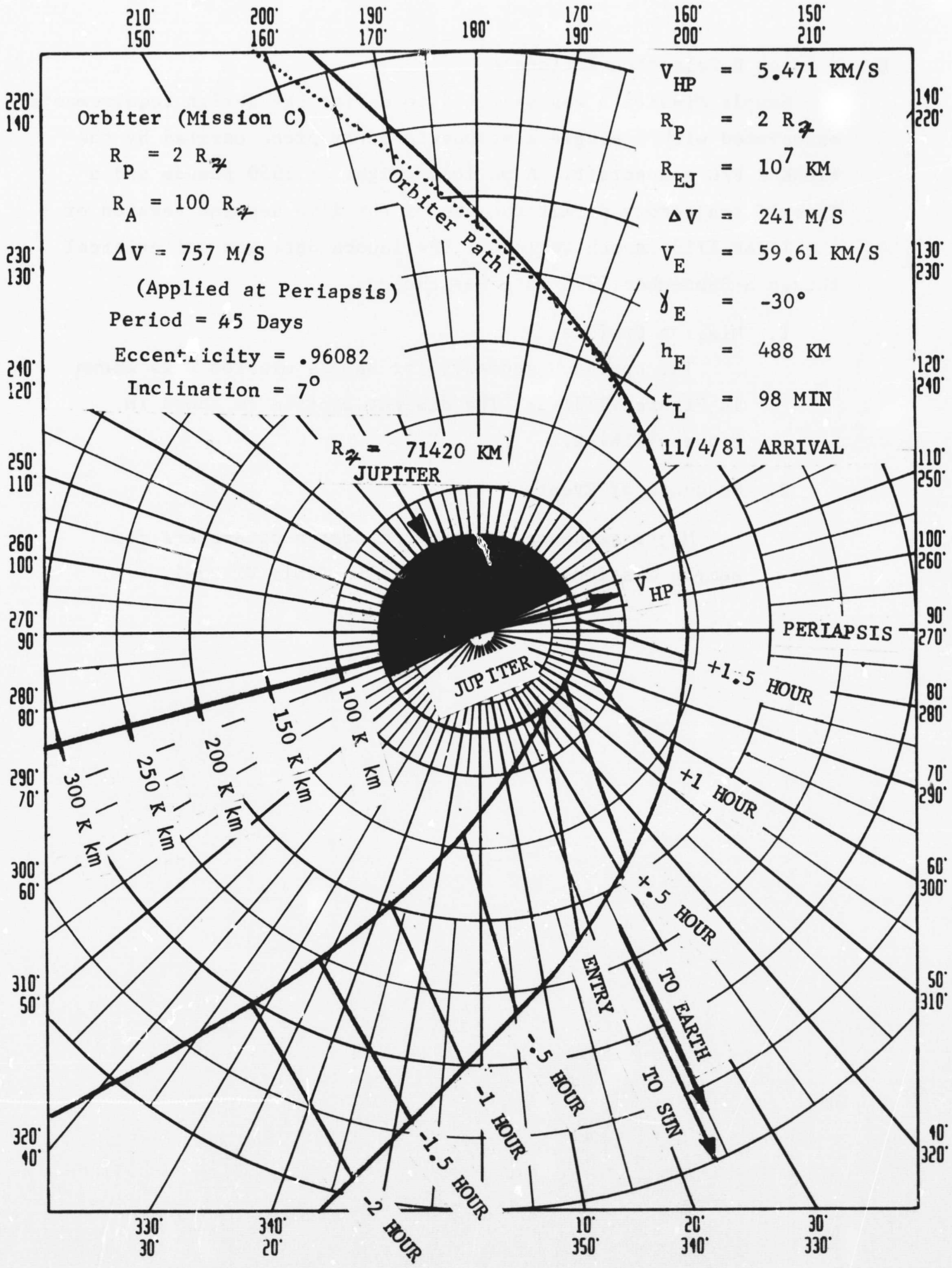


FIGURE VIIB1-1
APPROACH GEOMETRY
SAMPLE MISSIONS B AND C

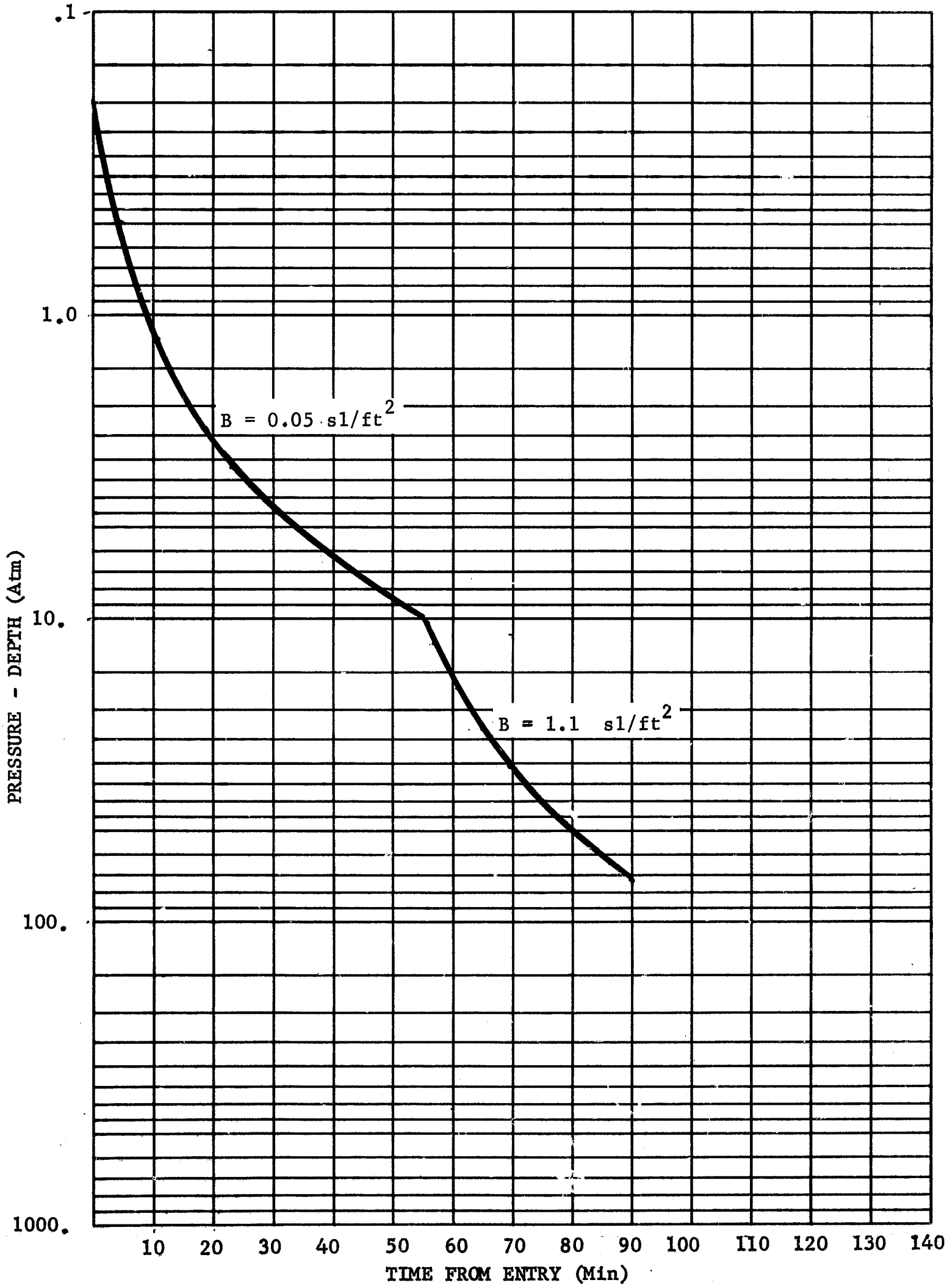


Figure VIIB1-2 Descent Profile - Sample Mission B and C

LAUNCH, INTERPLANETARY CRUISE, AND ENCOUNTER PARAMETERS
FOR JUPITER
MISSION B

* * * * * * * * * * TABLE VIIB2-1 * * * * * * * * * * * * * * * * *

* * * * LAUNCH PARAMETERS * * * *

LAUNCH DATE (NOMINAL)	9/25/78
LAUNCH VEHICLE	TITAN III D CENTAUR (5 SEG WITH BURNER II)
LAUNCH PERIOD	20 DAYS
PARKING ORBIT ALTITUDE	100 NAUTICAL MILES
SPACECRAFT	PIONEER
SPACECRAFT WEIGHT	547 LBS
PAYLOAD WEIGHT (INCL S/C)	1550 LBS
FAIRING SEPARATION	CORE 2 IGNITION PLUS 10 SEC
MAX LAUNCH AZIMUTH	115 DEG

* *

* * * * INTERPLANETARY CRUISE PARAME * * * *

TRAJECTORY	TYPE II
DECLINATION OF LAUNCH ASYMPTOTE	
DLA	6.6 DEGREES
RIGHT ASCENSION	118.4 DEGREES
INJECTION ENERGY, C3	99.0 KM2/SEC2
FLIGHT TIME	1136 DAYS (NOMINAL)
SEMI-MAJOR AXIS	3.22 A.U.
RADIUS OF APHELION	5.5 A. U.
ECCENTRICITY	0.695
INCLINATION TO ECLIPTIC	3.6 DEGREES
CENTRAL ANGLE OF TRAVEL	200.7 DEGREES
TRUE ANOMALY AT DEPARTURE	342.0 DEGREES

* *

* * * * * ENCOUNTER PARAMETERS * * * * *

JUPITER ARRIVAL DATE	11/4/81 (NOMINAL)
TRUE ANOMALY AT ARRIVAL	182.8 DEGREES
EXCESS VELOCITY, VHP	5.47 KM/SEC
DEC OF VHP VECTOR	27.4 DEGREES
RIGHT ASC OF VHP VECTOR	106.8 DEGREES
(WITH RESPECT TO VERNAL EQUINOX, EARTH EQUATORIAL SYSTEM)	
DEC OF VHP VECTOR	3.2 DEGREES
(WITH RESPECT TO EQUATOR OF JUPITER)	
COMMUNICATION RANGE	6.4 A.U.

* *

* * * * DEFLECTION PARAMETERS * * * *

BUS TRAJECTORY	FLYBY
PERIAPSIS RADIUS OF BUS	143000. KM = 2 JUPITER RADII
DEFLECTION RADIUS	10,000,000. KM
INCLINATION OF TRAJECTORY	7.0 DEGREES
(WITH RESPECT TO EQUATOR OF JUPITER)	
DEFLECTION VELOCITY	241 METERS/SEC
DEFLECTION ANGLE	-107.0 DEGREES
CAPSULE COAST TIME	12 DAYS
LEAD TIME	98 MINUTES
LEAD ANGLE	-20.8 DEGREES

* * * * ENTRY PROBE DESIGN DATA * * *

RELATIVE ENTRY VELOCITY	49.0 KM/SEC = 160,720 FT/SEC
ENTRY ANGLE	-30 DEGREES (SKIPOUT AT -4 DEG)
ENTRY ALTITUDE (TIME=0)	487.7 KM = 1,600,000. FEET
ENTRY RADIUS	71907.7 KM
ENTRY LATITUDE	7.0 DEGREES
ENTRY LONGITUDE (RELATIVE TO MERIDIAN OF SUN)	16.2 DEGREES

* *

* * * * AEROSHELL DATA * * * *

ENTRY BALLISTIC COEFFICIENT	1.09 SLUGS/FT2
TIME TO .1 G POINT	6.5 SECONDS
TIME OF MAXIMUM DECELERATION AND MAX DYNAMIC PRESSURE	14.5 SECONDS
MAXIMUM DECELERATION	1,532 G
MAXIMUM DYNAMIC PRESSURE	44,078 LB/FT2
TIME OF MACH 1 OCCURRENCE	26.5 SECONDS
AEROSHELL STAGING	
ALTITUDE	33 KM = 200 MB
MACH NUMBER	.68
DYNAMIC PRESSURE	143.5 LB/FT2
TEMPERATURE	203.4 DEG R
DENSITY	.0000891 SLUG/FT3
TIME (TS)	33.0 SECONDS

3. Configuration Summary - Mission B

The Inboard Profile of the Entry Probe is shown in Figure VIIB3-1. Major Characteristics and Weights are summarized in Tables VIIB3-1 and -2 respectively, and system descriptions are contained in the following sections (4 and 5).

4. Mechanical and Support Systems

Descent Probe

The descent probe structural/thermal concept is an evacuated titanium pressure vessel exposed to the ambient environment. The inner surface of the shell is lined with multi-layer themal insulation. The concept of equipment support, shell penetrations, and shell closure characteristic of the Design Example configuration is applicable to this design.

The descent profile prescribed has two-stages where the first stage employs a parachute descent down to 10 atmospheres and requires no specific aerodynamic configuration for the probe. After separation from the parachute, the remainder of the descent requires a ballistic coefficient of 1.1 slugs/ft^2. This is achieved with a symmetrical 40 degree half angle skirt of ring-shell construction.

The antenna is a curved turnstile type mounted external to the pressure vessel on the closure dome. It is protected by an RF transparent domed cover similar to that of the Design Example Probe.

Entry-Aeroshell

The entry aeroshell is a 55 degree half angle cone forebody 3.5 feet in diameter. Aeroshell construction and arrangement is the same as that of the Design Example except for the descent probe support. structure. Since the pressure shell is exposed, its stiffness is

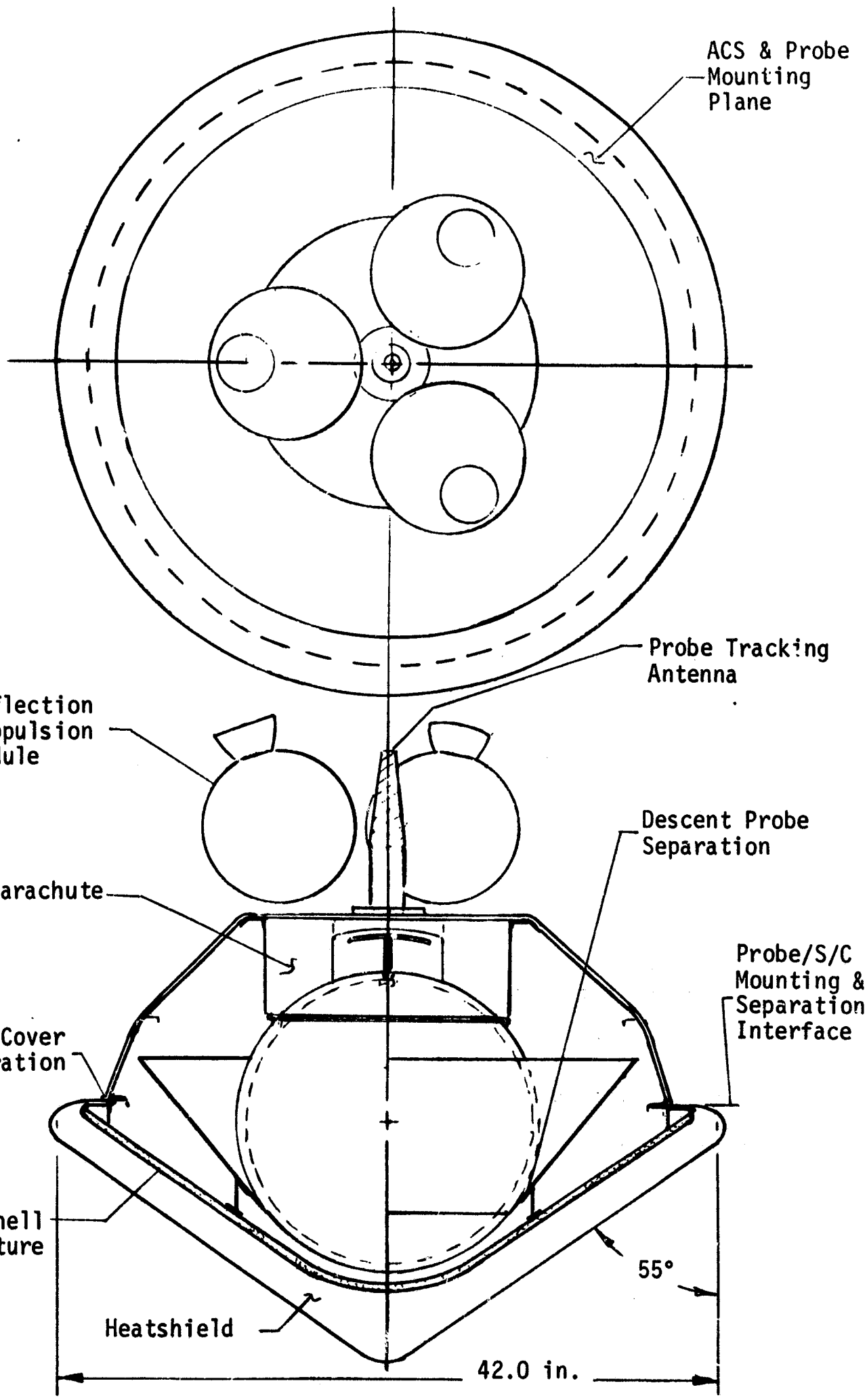


Fig. VII-B-3-1 Entry Probe Inboard Profile, Mission B

TABLE VIIB3-1

MISSION B CHARACTERISTICS SUMMARY

Type Probe	Single
Maximum Depth	73 Atm
Entry Angle	-30° Deg
Data Return Mode	Relay
Spacecraft	Pioneer
Spacecraft Radius of Periapsis	2.0 R
Science Payload	27 lbs
Bit Rate-Descent	40 B/S
Bit Rate - Pre Entry	100 B/S
Transmitter Power	40 watts
Spacecraft Antenna Dish Size	3.5 ft
Descent Time	1.5 hrs
Entry Ballistic Coefficient	1.09 slugs/ft^2
Probe Diameter	3.5 ft
Entry Weight	457 lbs
Probe Installed Weight	552 lbs
Total Probe System (including spacecraft mods)	743 lbs
Total Lift-off Weight	1300 lbs
Launch Vehicle Capability (5 Segment TIIID Centaur with Burner II)	1550 lbs

TABLE VIIB3-2

MISSION B PROBE WEIGHT SUMMARY

	Wt. (lbs.)		
Science	26.0		
Communication & Power	50.0		
Insulation (Multi-Layer)	0.8		
Pressure Shell	19.6		
Internal Structure	11.3		
Pyrotechnic Vent Valve Inst'l	1.5		
Antenna	1.5		
External Aerodynamics & Misc. Structure	9.5		
Descent Probe Weight		(120.2)	
Parachute	5.5		
Parachute Canister	1.5		
Despin (Fixed)	1.0		
Separations Mechanisms	3.0		
Auxiliary Structure	4.0		
Entry Vehicle ACS (Gyro, Jets, etc.)	25.0		
Pre-Entry Communication Elects & Power	17.0		
Equipment Inst'l Structure	6.0		
Probe Thermal Control During Approach (Fixed Wt)	33.0		
		(96.0)	
Aeroshell Structure (3.5' Dia.)		(86.0)	
Heatshield		(155.0)	
Entry Weight		457.0	
Deflection Propulsion Module	80.0		
Despin System (Spent)	2.0		
Separation Mechanisms	2.5		
Ion Mass Spectrometer	3.0		
Thermal Blanket (Jettisoned)	8.0		
		(95.5)	
Probe Installed Weight		552.5	
Spacecraft Mods		190.5	264.5*
Total Probe System Weight		743.0	817.0*
Pioneer Spacecraft		557.0	557
Total Liftoff Weight		1300.0	1374*

*With added propellant weight to retain 200 m/s ΔV capability for midcourse corrections. (Not required if launch vehicle system includes Burner II).

utilized in transmitting loads to the aeroshell. By nesting the probe in the aeroshell nose in a pad of high ($\sim$ 30 lb/ft^3) density foam rimmed with a shallow ring beam, the load is transmitted directly to the aeroshell. As the high g loads of entry are reached, the pad deflects causing the ring beam to carry the over-load above the pad s capability. The beam also serves as the primary attach and separation plane for the descent probe.

The entry ballistic coefficient is 1.09 slugs/ft^2 and the entry angle, -30 degrees.

Deflection and Approach

The probe is released, spinning, with the spacecraft still in its earth pointing orientation. A Phased Lock Loop preprogrammed precession system reorients the probe to the ΔV direction and that attitude is maintained during ΔV burn by virtue of the spin momentum. After ΔV, precession is again used to orient the probe for entry. ΔV implementation accuracy with this method is not anticipated to be as good as for the 3-axis system used for the non-spinning (TOPS) probes, but no quantitative assessment is available. Entry dispersion due to the potentially large ΔV errors are one of the reasons for selecting a smaller ejection range for the Pioneer Probes. The precession control system situation is discussed further in Volume III Chapter V.

Thermal control during the approach phase is provided by battery operated heaters as described in Volume VI Chapter V. This mode was selected since the "pre-heat and insulate" concept of the Design Example probes requires much more power than is available on the Pioneer spacecraft. This is the other reason for the relatively close-in probe ejection range, 10 x 10^6 km. The ΔV propulsion system penalty incurred, $\sim$50 lbs, due to the short ejection range, in combination with the heater battery weight, $\sim$ 30 lbs, would probably pay for adding power to the Pioneer (for probe preheating) but the entry dispersion aspects would still have to be resolved before using larger probe ejection ranges.

Adaptation to Spacecraft

The entry probe mounting to the Pioneer spacecraft is shown in Figure VIIB3-2. The probe mounts symmetrically with its roll axis on the spacecraft spin axis. It stands off from the spacecraft body because of a dish type probe tracking antenna located between the probe and spacecraft. The stand-off distance is minimized by folding the antenna feed system and deploying after probe separation.

The probe is mounted to the spacecraft body through a cylindrical envelope of a truss structure which also adapts and supports the spacecraft for booster loads. The spin axis is maintained as the maximum moment of inertia axis. Inertia and c.g. changes are shown in Figure VIIB3-2.

The probe tracking antenna is a mechanically despun dish of limited scan range capability. The feasibility and the mechanics of the despun system is described and discussed in Volume III, Chapter V.

Table VIIB3-3 gives the weight breakdown for the spacecraft modifications.

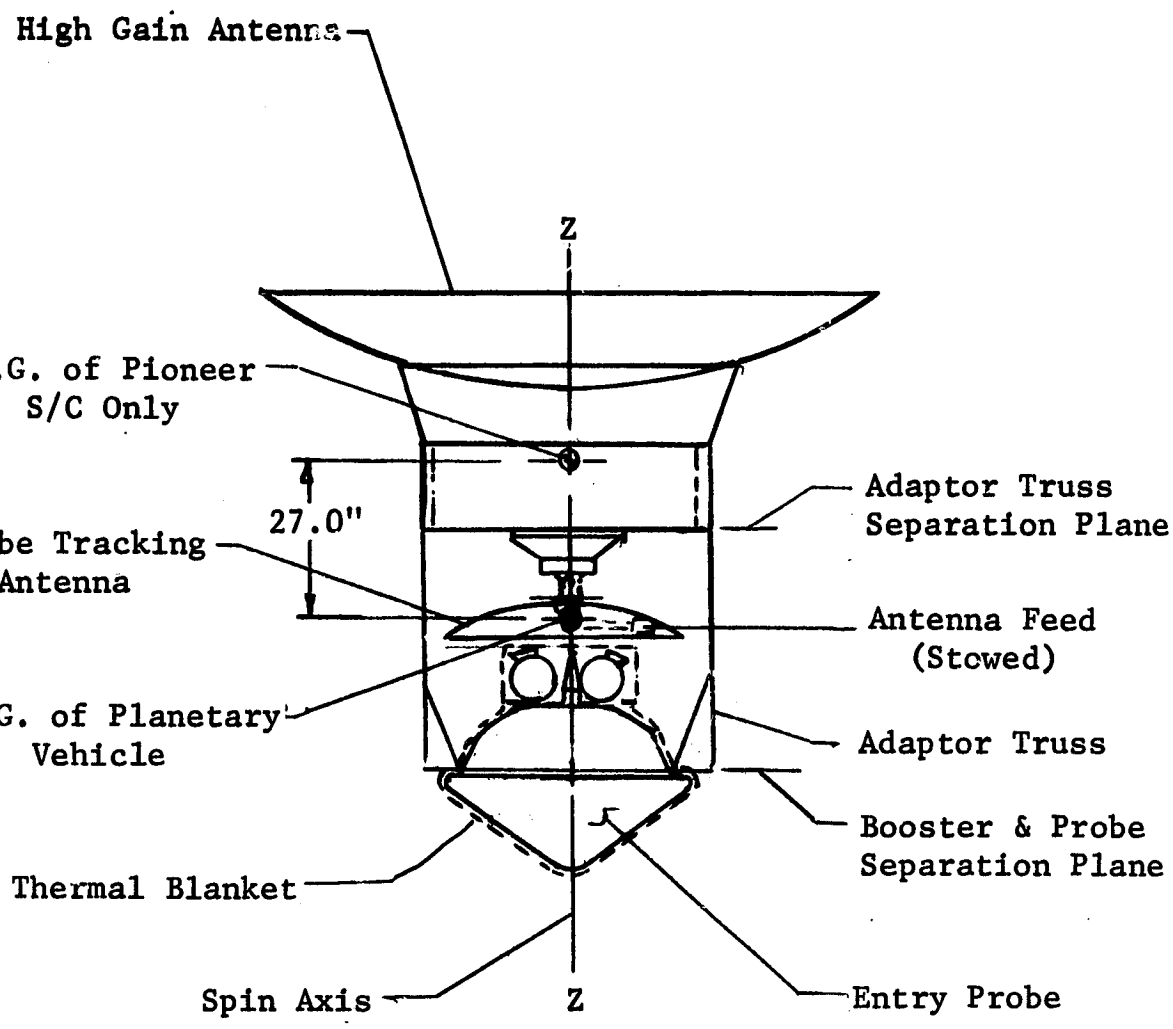
Adaptation to Booster

The planetary vehicle installation on the booster vehicle is shown in Figure VIIB3-3. Due to the addition of the probe and antenna, the new c.g. location violates the limits imposed by the existing spin table*. This situation dictates modifications to the payload spin-up provisions which are beyond the scope of this study to examine.

The total lift-off weight of 1300 lbs is well within the capability of the 5 segment TIIID Centaur, 1550 lbs.

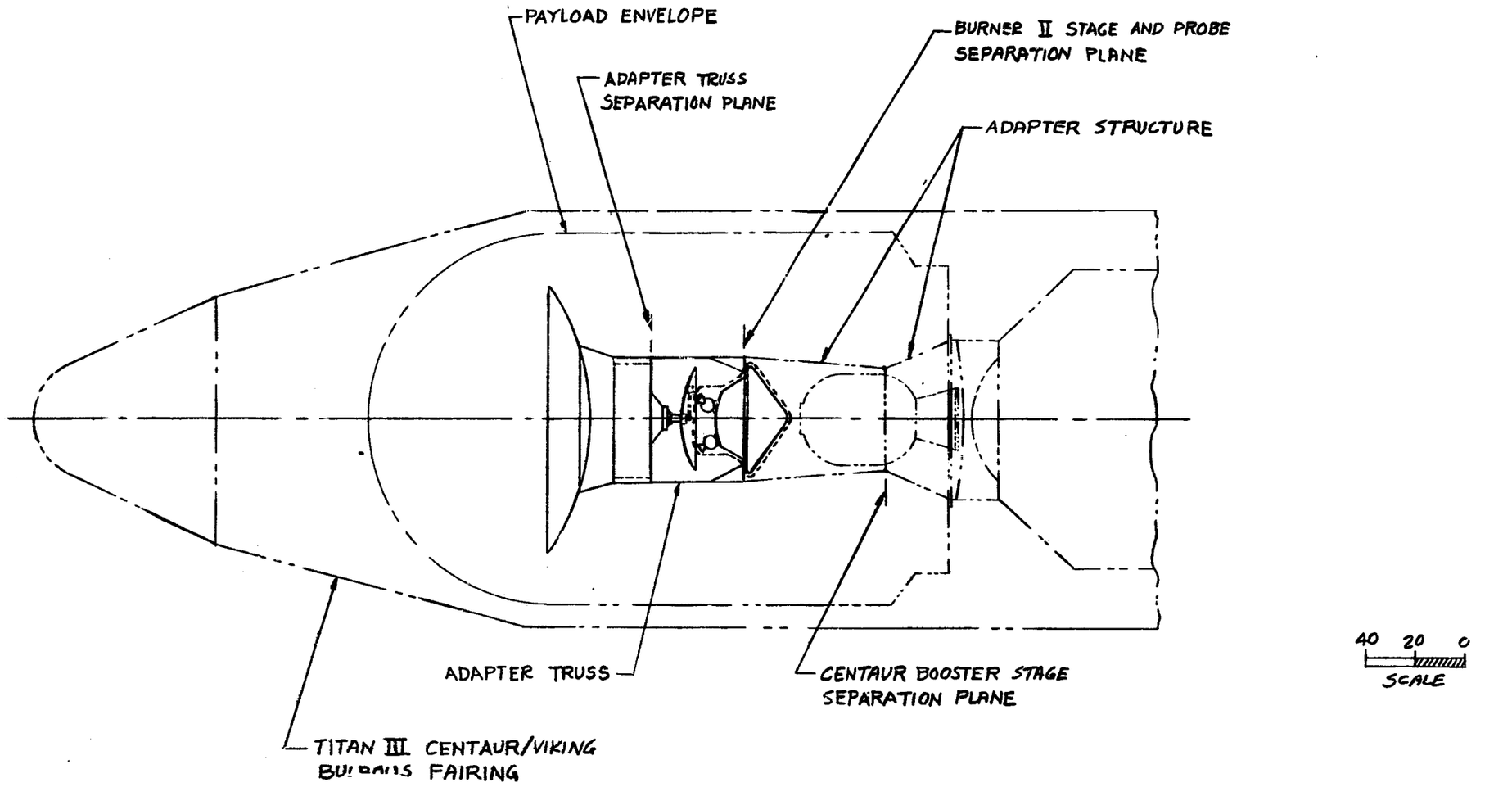
---

*JPL Section Document containing data on Pioneer Spacecraft as furnished by: Ames Research Center



	Condition	Wt. (lbs)	Moment of Inertia (Slug/ft^2)		
			I_z	I_x	I_y
Pioneer S/C Only	Stowed	547	93.3	62.5	58.1
	Deployed	547	424.4	282.8	168.9
Planetary Vehicle (S/C with Probe)	Deployed	1130	465.0	452.0	345.0
			$2\,I_z/(I_x + I_y) = 1.17$		

Mission B
Planetary Vehicle Configuration
Pioneer F & G Spacecraft)
Figure VII-B-3-2



MISSION B
PIONEER PLANETARY VEHICLE/BOOSTER INSTALLATION

FIGURE: VII-B-3-3

TABLE VIIB3-3

MISSION B PIONEER SPACECRAFT MODIFICATIONS WEIGHTS

Item		Weight (lbs)
Power:	Battery, Switching and Control for Data System during Probe Spacecraft Communications.	13.2
Probe Adaptor System		
	Fixed Portion of Truss	16
	Jettisonable Portion of Truss	54
	Separation at Spacecraft	2.5
	Probe Attachment and Separation Mech.	4.8
Asteroid/Meteoroid Detection Instrument Relocation		3.0
Low Gain Antenna Relocation		1.2
Electronics for Telecommunications		11.0
Data Storage System		22.0
Cabling		7.0
Thermal Control Mods		5.0
±45° Angle Mechanically Despin Antenna System		51.0
		190.7

	With Burner II	Without Burner II
Added Midcourse Propellant Weight	0*	74

*Use of Burner II reduces the required magnitude of ΔV corrections by more than the probe addition increases the spacecraft mass.

5 Telecommunications, Data Handling and Power, Mission B

a. General

Mission B has the same instrument complement as Mission C, which is expanded by three instruments compared to the design example. Its trajectory has been modified to minimize the spacecraft relay antenna scan angle requirements. This was done in order to facilitate the use of the spin-stabilized Pioneer spacecraft. The spacecraft aspect angle coverage is centered on the spin axis, looking away from Earth. The maximum departure from this axis is 45°. A mechanically despun two-axis gimballed dish 3.5 ft in diameter was selected for the spacecraft antenna. The tradeoff leading to this selection is described in Volume III, Chapters IV and V. As described in Chapter V, it was subsequently found that this antenna concept could be extended to give essentially unrestricted coverage with an increase in weight of only 20 lbs. This diminishes the original motivation for Mission B. However, it has been analyzed to the same depth as the other missions. Results are given below.

Pre-entry communications lasts for a period of 1.2 hours at a bit rate of 100 bps. The post-entry mission lasts for 1.5 hours, penetrating to a depth of 75 atmospheres. Bit rate is 40 bps, 6 bps of which is used for data stored during entry. This bit rate is not switched but is held at 40 bps throughout the post-entry mission. 1.8 GHz was selected as the transmission frequency.

This mission was initially worked assuming a phased array antenna or the spacecraft, operating at 1.2 GHz. Transmitter power requirement was found to be 40 watts. Battery, thermal control, and probe sizing was based on this value. The change-over to the despun dish and the higher frequency would permit the lowering of this to 20 watts. However, in view of the work already done on the 40 watt system, it was decided to leave the power at this higher level and show an additional 3 db margin in the links.

b. The Probe Telecommunications System

Coherent signalling is used for the relay link. Data rates are 100 bps pre-entry and 40 bps post entry. Convolutional coding is used, with decoding at the spacecraft. Spacecraft PLL bandwidth is 40 Hz. A communication frequency of 1.8 GHz, was selected to optimize the link. A low-gain turnstile antenna is used on the probe. Transmitter power is 40 watts.

Figure VIIB5-1 shows probe aspect angles, spacecraft cone angle and range for a November 4, 1981 arrival date. Lead time can be chosen such that the 45^{o} antenna excursion limit is not exceeded over all arrival dates.

Figure VIIB5-2 shows communication link margins over the mission for a typical arrival date. The worst-case margin is seen to be 4 db. Margins for other arrival dates do not vary significantly from this value. These margins are based on design control tables similar to the one shown for the design example mission in Chapter VI. Figure VIIB5-3 shows relative link losses versus time. Communications geometry is shown in Figure VIIB1-1.

The search and acquisition problem is treated in Volume III. Chapter IVG gives a general discussion. Mission B is considered specifically in Chapter IVJ2.a. It was found that the complete two-dimensional search consisted of an angular search of four beam positions and a frequency search over 12 KHz pre-entry and 24 KHz post-entry. Search time is calculated to be 1 and 2 minutes respectively.

c. Spacecraft Interface and Modifications

The principal modification to the Pioneer spacecraft is the installation of the mechanically despun dish antenna. This is treated in detail in Chapters IV and V of Volume III. Total weight of this installation is given in Chapter IV, Vol III as 59 lbs.

Other modifications include the data receiver, data storage, and interface electronics to put the stored probe data into the spacecraft data system as described for the design example mission. See Chapter VI and Volume III, Chapter IV.

ALT MISSION B AND C -
ASPECT ANGLE AND RANGE VS. TIME

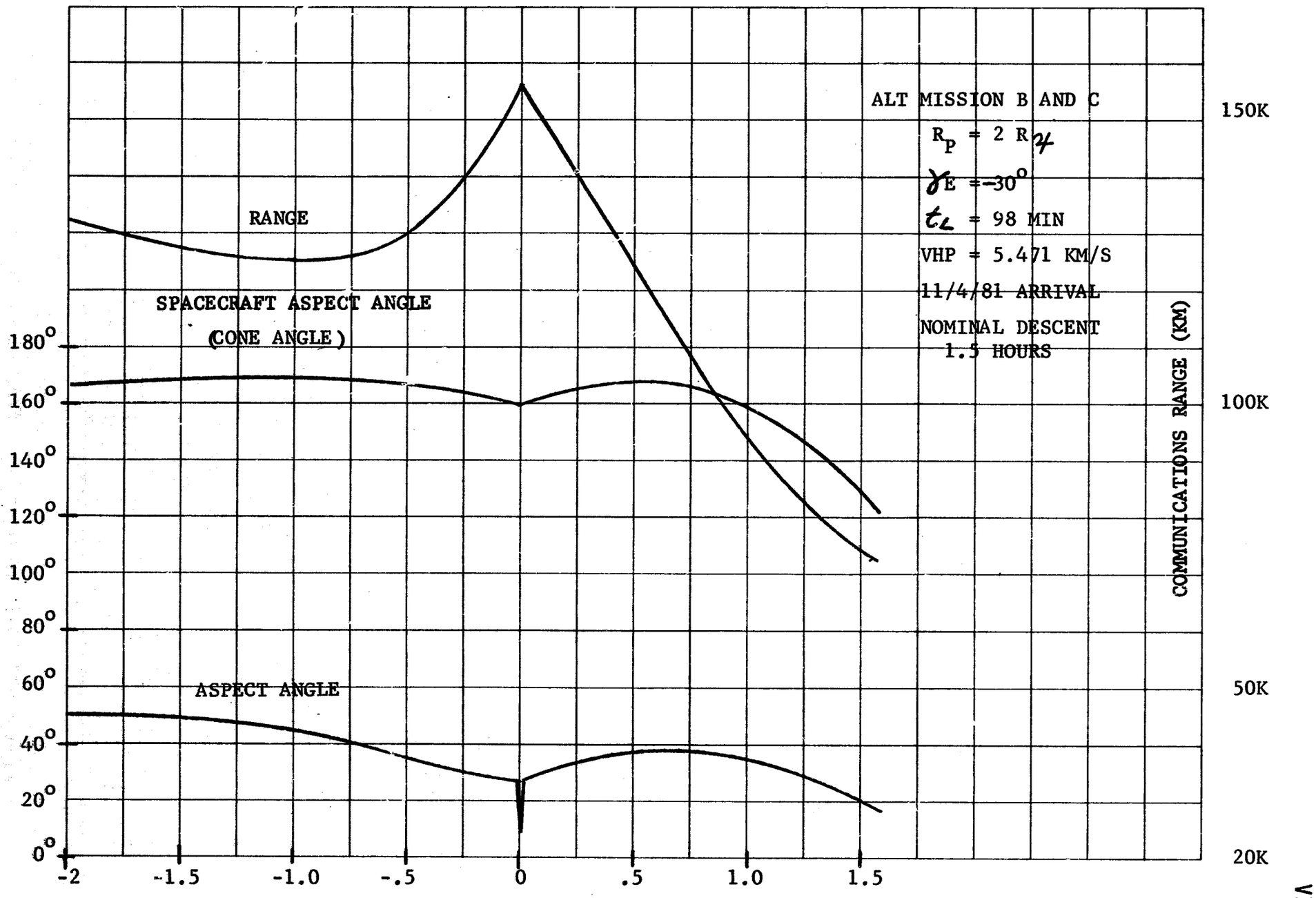


Figure VIIB5-1

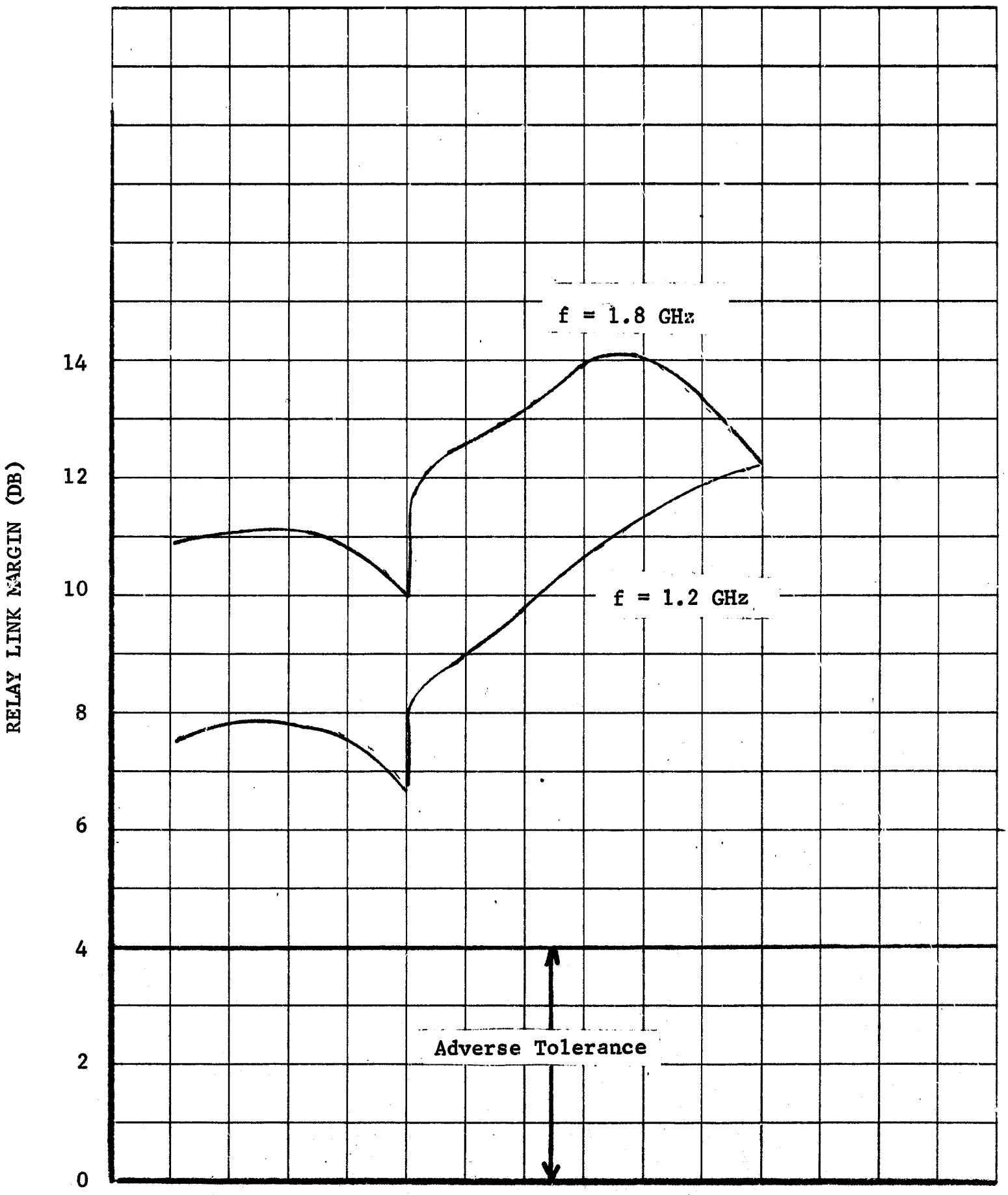


Figure VII B5-2 Mission B Relay Link Margin vs Time

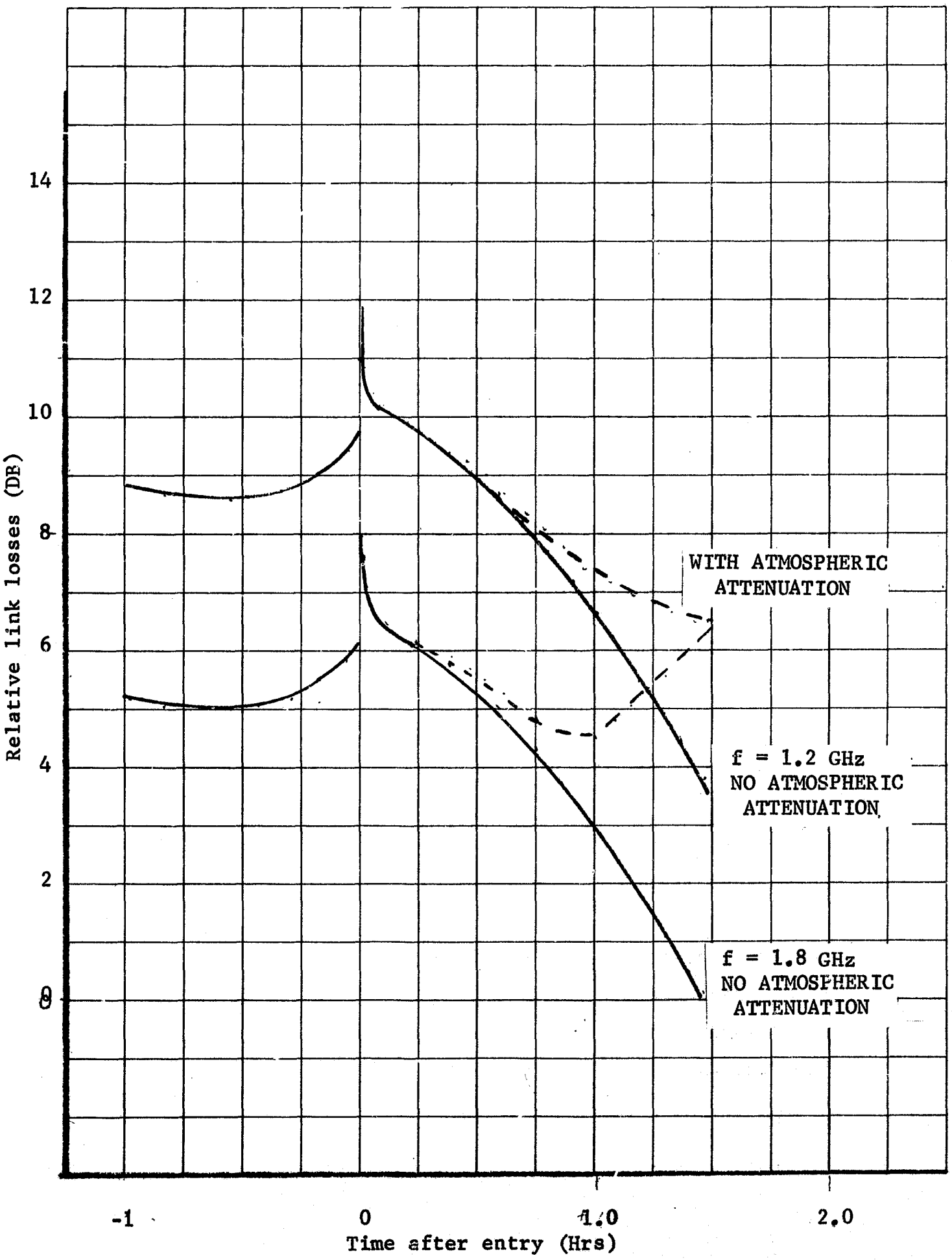


Figure VIIB5-3. Mission B Relative Relay Link Losses Versus Time

d. Data System

A detailed description of the data system was given for the design example mission. This detail will not be repeated here. The data system for Missions B and C are identical. They are similar to the system described for the design example mission, except that they are slightly larger to accommodate the additional instruments listed for these missions. Weight and power consumption estimates are increased accordingly. See Table VIIB5-2.

e. Probe Power System

The probe power profile is similar to that shown in Figure VIF-12 for the design example mission except that the post-entry mission has a shorter duration, 1.5 hours. The pre-entry period is set at 1.2 hours. Total energy consumption for post-deflection, cruise, and pre-entry is 201 watt-hours. Power consumption for the post-entry period is tabulated below. Total energy consumption for this period is 285 watt-hours. This requires a battery weight of 11 lbs. Pre-entry energy is supplied by a 6 lb aeroshell mounted battery.

TABLE VIIB5-1

POWER CONSUMPTION, POST-ENTRY, MISSION B

Item	Power, watts
Modulator/Exciter	2
Power Amplifier	130
ADC & Multiplexers	4
Format Generator, Control and Memory	6
Timer and Sequencer	2
Power Conditioning	16
Instruments	30
Total	190

f. Probe Weights

The weights of the components of the telecommunications data handling, and power systems for the Mission B probe are tabulated below.

TABLE VIIB5-2

PROBE ELECTRONICS SYSTEM WEIGHTS, MISSION B

Item	Weight, lbs
Antenna	1.0
Modulator/exciter	1.5
Power Amplifier	8.0
Timer and Sequencer	3.0
Format Generator, Control and Memory	6.0
ADC and Multiplexer	4.0
Inverter	4.0
Battery	11.0
Cabling	See Note
Total	38.5

Note:

Cabling for all subsystems is lumped and shown in final weight summary.

C. Mission C Selection Rationale

Sample mission C was selected to demonstrate the feasibility of using the PIONEER F/G as an orbiter after completion of the atmospheric entry mission as in sample mission B.

1. Mission Profile

The approach geometry for sample mission C is the same as for sample mission B shown in Figure VII B1-1 The spacecraft orbits the planet as shown by the orbiter path. The probe descent profile is as shown in Figure VII B1-2.

2. Sequence of Events

Orbiter data for sample mission C is tabulated in Table VII C2-1.

LAUNCH, INTERPLANETARY CRUISE, AND ENCOUNTER PARAMETERS
FOR JUPITER
MISSION C

* * * * * * * * * * * TABLE VIIC2-1 * * * * * * * * * * * * * * * * * *

MISSION C IS SAME AS MISSION B EXCEPT THAT BUS IS INSERTED
INTO AN ELLIPTIC ORBIT AT PERIAPSIS OF THE HYPERBOLA

ELLIPTIC ORBIT DATA	
PERIAPSIS RADIUS	143000 KM=2 JUPITER RADII
APOARSIS RADIUS	7142000 KM=100 JUPITER RADII
INSERTION DELTA V	757 M/SEC=2480 FPS
ECCENTRICITY	0.961
ORBIT PERIOD	45 DAYS
ORBIT INCLINATION	7 DEGREES

3. Configuration Summary - Mission C

The Probe Systems of Mission C are identical to those for Mission B since the Probe mission is complete prior to orbit insertion. However the configuration of the orbiter design must take into consideration the probe and probe tracking antenna in the location of the deorbit propulsion system. The orbiter might utilize the despin-system provided for the probe tracking antenna, if not nearly all of the probe systems can be jettisoned prior to orbit insertion.

If we assume that after the probe system jettisoning, the modified Pioneer - less orbit insertion system - has a weight of 550 lbs, (including any instrumentation for the orbiting mission) the propellant required for orbit insertion would be $\sim$ 240 lbs based on an I_{sp} of 230 (for hydrazine monopropellant). With an estimated additional propulsion system weight of 60 lbs for fixed hardware, the total orbit insertion system would be of the order of 300 lbs.

Consequently the liftoff weight of Mission B, 1300 lbs, would increase to at least 1600 lbs, exceeding the 1550 lb capability of the 5 segment TIIID Centaur with Burner II but still falling within the capability of the larger launch vehicles.

D. Mission D Selection Rationale

Sample Mission D was selected as a dual probe extension of sample Mission A on a 1979 Grand Tour mission and atmospheric entry probe capabilities at both Jupiter and Uranus.

1. Mission Profile

The approach geometry at Jupiter for sample Mission D is the same as for sample Mission A shown in Figure VIIA1-1. The descent profile for the Jupiter probe is shown in Figure VIID1-2.

2. Sequence of Events

Major sequenced events and design parameters are tabulated in Table VIID2-1.

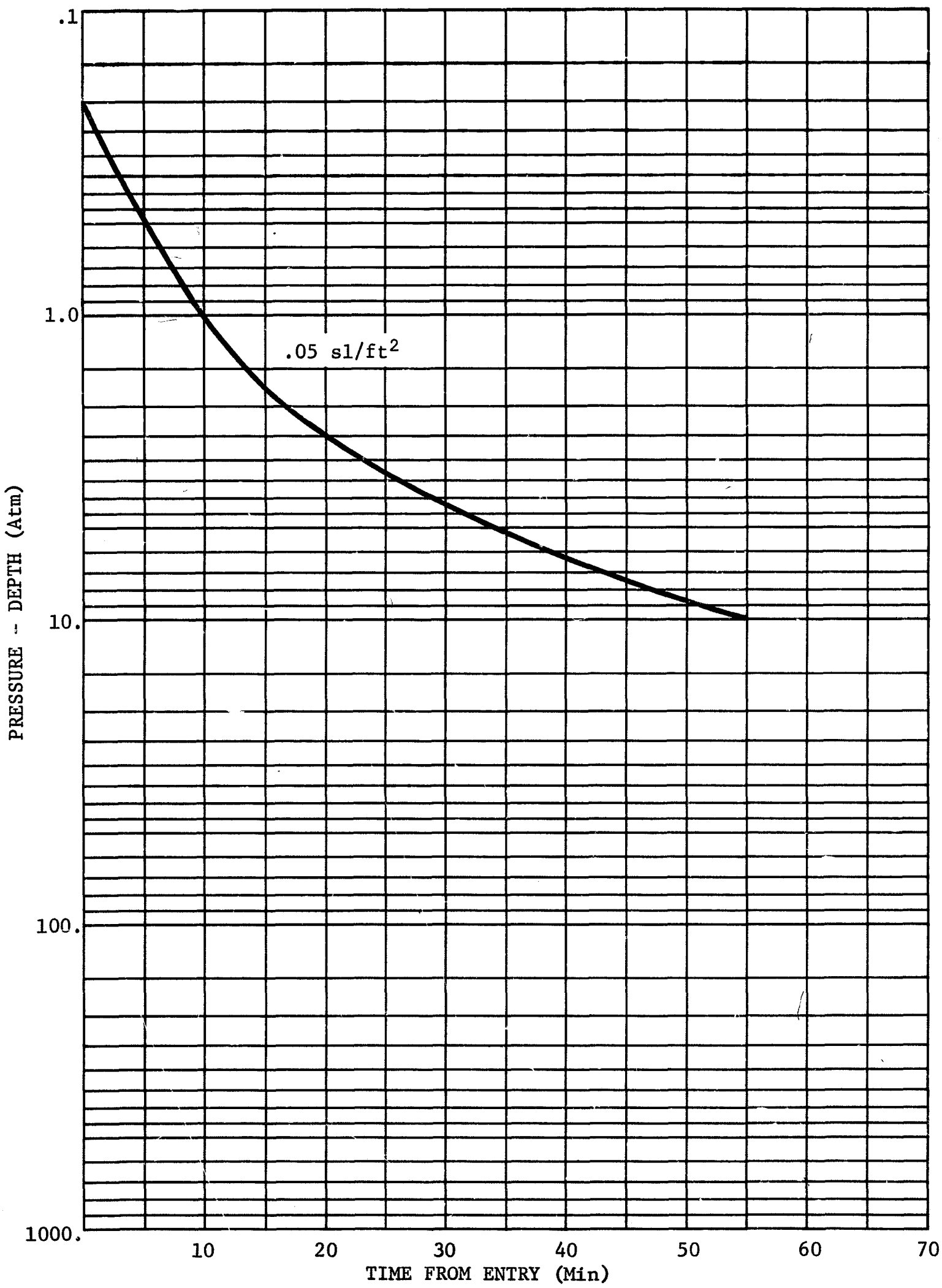


Figure VIID1-2 Descent Profile - Sample Mission D

LAUNCH, INTERPLANETARY CRUISE, AND ENCOUNTER PARAMETERS
FOR JUPITER
MISSION D

* * * * * * * * * * * * TABLE VIID2-1. * * * * * * * * * * * * * *

* * * * LAUNCH PARAMETERS * * * *

LAUNCH DATE (NOMINAL)	11/6/79
LAUNCH VEHICLE	TITAN III D CENTAUR (7 SEG WITH BURNER II)
LAUNCH PERIOD	30 DAYS
PARKING ORBIT ALTITUDE	100 NAUTICAL MILES
SPACECRAFT	TOPS(2 MINI PROBES)
SPACECRAFT WEIGHT	1450. LBS
PAYLOAD WEIGHT (INCL S/C)	1900 LBS
FAIRING SEPARATION	CORE 2 IGNITION PLUS 10 SEC
MAX LAUNCH AZIMUTH	115 DEG

* *

* * * * INTERPLANETARY CRUISE PARAMETERS * * * *

TRAJECTORY	TYPE 1/GRAND TOUR
DECLINATION OF LAUNCH ASYMPTOTE	
DLA	24.9 DEGREES
RIGHT ASCENSION	139.5 DEGREES
INJECTION ENERGY, C3	111.7 KM2/SEC2
FLIGHT TIME	541 DAYS (NOMINAL)
SEMI-MAJOR AXIS	6.0 A.U.
RADIUS OF APHELION	NOT TRAVERSED
ECCENTRICITY	0.835
INCLINATION TO ECLIPTIC	2.3 DEGREES
CENTRAL ANGLE OF TRAVEL	145.1 DEGREES
TRUE ANOMALY AT DEPARTURE	357.9 DEGREES

* *

* * * * * ENCOUNTER PARAMETERS * * * * *

JUPITER ARRIVAL DATE	4/30/81 (NOMINAL)
TRUE ANOMALY AT ARRIVAL	143.0 DEGREES
EXCESS VELOCITY, VHP	12.16 KM/SEC
DEC OF VHP VECTOR	6.53 DEGREES
RIGHT ASC OF VHP VECTOR	164.7 DEGREES
(WITH RESPECT TO VERNAL EQUINOX, EARTH EQUATORIAL SYSTEM)	
DEC OF VHP VECTOR	.22 DEGREES
(WITH RESPECT TO EQUATOR OF JUPITER)	
COMMUNICATION RANGE	4.6 A.U.

* *

* * * * DEFLECTION PARAMETERS * * * *

APPROACH TRAJECTORY TYPE	FLYBY
PERIAPSIS RADIUS OF BUS	483969 KM = 6.8 JUPITER RADII
DEFLECTION RADIUS	30,000,000. KM
INCLINATION OF TRAJECTORY	1.0 DEGREES
(WITH RESPECT TO EQUATOR OF JUPITER)	
DEFLECTION VELOCITY	312 METERS/SEC
DEFLECTION ANGLE	-126.5 DEGREES
CAPSULE COAST TIME	26 DAYS
LEAD TIME	-114 MINUTES
LEAD ANGLE	19.53 DEGREES

* *

* * * * ENTRY PROBE DESIGN DATA * * * *

RELATIVE ENTRY VELOCITY	48.05 KM/SEC = 157604 FT/SEC
ENTRY ANGLE	-15. DEGREES (SKIPOUT AT -4 DEG)
ENTRY ALTITUDE (TIME=0)	487.7 KM = 1,600,000. FEET
ENTRY RADIUS	71907.7 KM
ENTRY LATITUDE	-0.6 DEGREES
ENTRY LONGITUDE (RELATIVE TO MERIDIAN OF SUN)	105.2 DEGREES

* *

* * * * AEROSHELL DATA * * * *

ENTRY BALLISTIC COEFFICIENT	.71 SLUGS/FT2
TIME TO .1 G POINT	12.5 SECONDS
TIME OF MAXIMUM DECELERATION AND MAX DYNAMIC PRESSURE	26.5 SECONDS
MAXIMUM DECELERATION	708 G
MAXIMUM DYNAMIC PRESSURE	12,971 LB/FT2
TIME OF MACH 1 OCCURRENCE	51.5 SECONDS
AEROSHELL STAGING	
ALTITUDE	35.1 KM= 179 MB
MACH NUMBER	.50
DYNAMIC PRESSURE	67.0 LB/FT2
TEMPERATURE	203.4 DEG R
DENSITY	.0000861 SLUG/FT3
TIME (TS)	92.4 SECONDS

3. Configuration Summary - Mission D

The Inboard Profile of the Mission D entry probe is shown in Figure VIID3-1. Probe Characteristics and total system weight summaries are presented in Tables VIID3-1 and 2. The total system is weight constrained to the payload weight available and considers two probes of equal size. System descriptions are given in the following sections.

4. Mechanical and Support Systems

Descent Probe

The descent probe structural/thermal concept is an evacuated titanium pressure vessel exposed to the ambient environment. The inside surface of the shell is lined with multi-layer thermal insulation. The concept of equipment support, shell penetrations, and shell closure characteristic of the Design Example configuration is applicable to this design.

Since the initial descent ballistic coefficient of 0.05 slugs/ft^2 is retained throughout the mission, the probe is supported on a parachute allowing the pressure vessel shape to be a sphere.

The antenna is a curved turnstile type mounted to the closure dome. It is protected by an RF transparent domed cover.

Entry Aeroshell

The entry aeroshell is a 55 degree half angle cone forebody 2.5 feet in diameter. Aeroshell construction and arrangement is the same as that of the Design Example except for the descent probe support. Since the pressure shell is exposed its stiffness is utilized in transmitting axial entry loads directly to the aeroshell by nesting it in a high density foam pad within the aeroshell nose. A shallow ring beam provides probe attachment and separation. The nested design is capable of supporting the major portion of the entry g load however the ring carries an increasing higher portion as the pad compresses.

Deflection and Approach

The extremely critical weight situation for this probe - a total

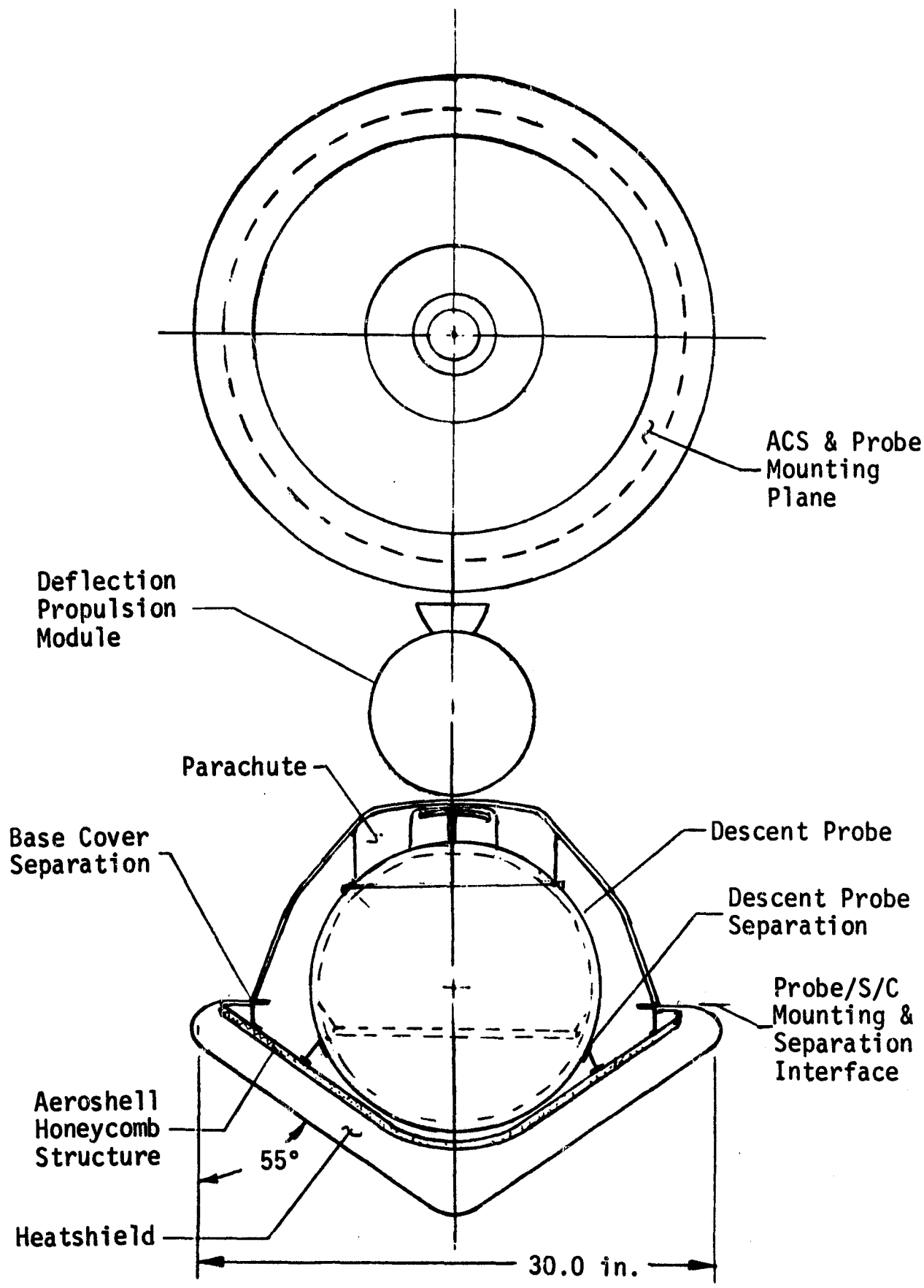


Fig. VII-D-3-1 Entry Probe Inboard Profile, Mission D

TABLE VIID3-1

MISSION D PROBE CHARACTERISTICS SUMMARY

Type Probe	Single (Unstaged)
Maximum Depth	17 atm
Entry Angle	-15 Deg
Data Return Mode	Relay
Spacecraft Radius of Periapsis	6.8 R
Science Payload	10 lbs
Bit Rate Descent	20 B/S
Bit Rate Pre-Entry	0
Transmitter Power	40 watts
Spacecraft Antenna Dish Diam.	4.14
Descent Time	.93 hr
Entry Ballistic Coefficient	.71 slugs/ft^2
Probe Diameter	2.5 ft
Probe Entry Weight	150.5 lbs
Probe Installed Weight	185.0 lbs
Total Probe System Weight - 2 probes (including spacecraft mods)	450 lbs
Total Lift-off Weight	1900 lbs
Launch Vehicle Capability (7 Segment TIIID Centaur with Burner II)	1900 lbs

Figure VIID3-2

Mission D Weight Summary

	Wt. (lbs.)		
Science	10.0		
Communications and Power	38.4		
Pressure Vessel	6.6		
Int'l Structure	5.7		
Insulation (Multi-Layer)	.1		
Antenna	1.2		
Parachute and Harness	3.0		
Descent Probe Wt.			(65.0)
Parachute Canister	1.2		
Despin (Fixed)	1.2		
Separation Mechanisms	1.5		
Auxiliary Structure	1.5		
Entry Vehicle Misc.		(5.4)	
Aeroshell Structure		(22.0)	
Heatshield Wt.		(51.1)	
Pre-entry ACS System		(7.0)	
Entry Wt.		150.5	
Deflection Propulsion Module	30.0		
Thermal Blanket	3.0		
Despin (Spent)	1.5		
		(34.5)	
Probe Installed Wt.	2 @	185.0	= 370
Spacecraft Modifications			80
Total Probe Systems Wt.			450
TOPS Spacecraft			1450
Total Liftoff Weight			1900

of 150 lbs including the approach G&C system is all that is available for the entry probe - requires that a very efficient system be developed to control the ΔV maneuver and subsequent reorientation for entry. Only 7.0 lbs is available for that function where as 25 lbs has been allocated for probes using the 3-axis system and 20 lbs for the potentially less accurate spin stabilized system.

Adaptation to Spacecraft and Booster

Two probes of equal size would be mounted to the TOPS spacecraft directly opposite each other on the sides of the spacecraft equipment compartment in the y-y plane. This results in essentially no c.g. shift and a symmetrical installation on the booster. After delivery of one probe to the first planet, the remaining probe will cause a c.g. shift. Loads associated with spacecraft reorientation are of low magnitude since acceleration rates are low. The assessment of the changes to the spacecraft will depend on its maneuver requirements after the first probe separates.

The total lift off weight of 1900 lbs coincides with the available capability of the 7 segment TIIIC Centaur with Burner 2. As noted, at least one of the probe subsystems requires some development to meet this weight constraint.

5. Mission D - Telecommunications, Data Handling and Power

Telecommunications requirements for Mission D are to provide a relay link from a single descent probe to a flyby spacecraft for a total period of 1 hour after separation of the probe from the aeroshell. Pre-entry data is not acquired due to the excessive communications link gain required during this period. A post entry data rate of 20 BPS is required to accommodate the payload.

A 40 watt 2.3 GHz phase modulated probe transmitter and a 4.14 ft diameter spacecraft antenna are required to provide this bit rate to a probe descent depth of 18.6 Earth atmospheres.

Communications geometry, antenna aspect angles and range are the same as for the Mission A-1.

Relative link losses as a function of time are shown in Figure VIID5-1. Margin as a function of time is shown in Figure VIID5-2. These parameters vary from those of Mission A-1 because of the difference in probe ballistic coefficient and descent depth versus time which is reflected in atmospheric attenuation.

Entry data is stored as well as the first 3 minutes of post entry data as in Mission A except storage is restricted to a total of 21,600 bits to allow readout and transmission of stored data at 6 bps in a total period of 1 hour. The 20 bps rate is divided among sources as follows:

Source	Data Rate
Real time science	10
Stored entry and post entry	6
Engineering and timing	4
TOTAL	20 bps

Weight for the probe telecommunications data handling and power subsystems including the 40 watt transmitter and battery is 38.5 lbs.

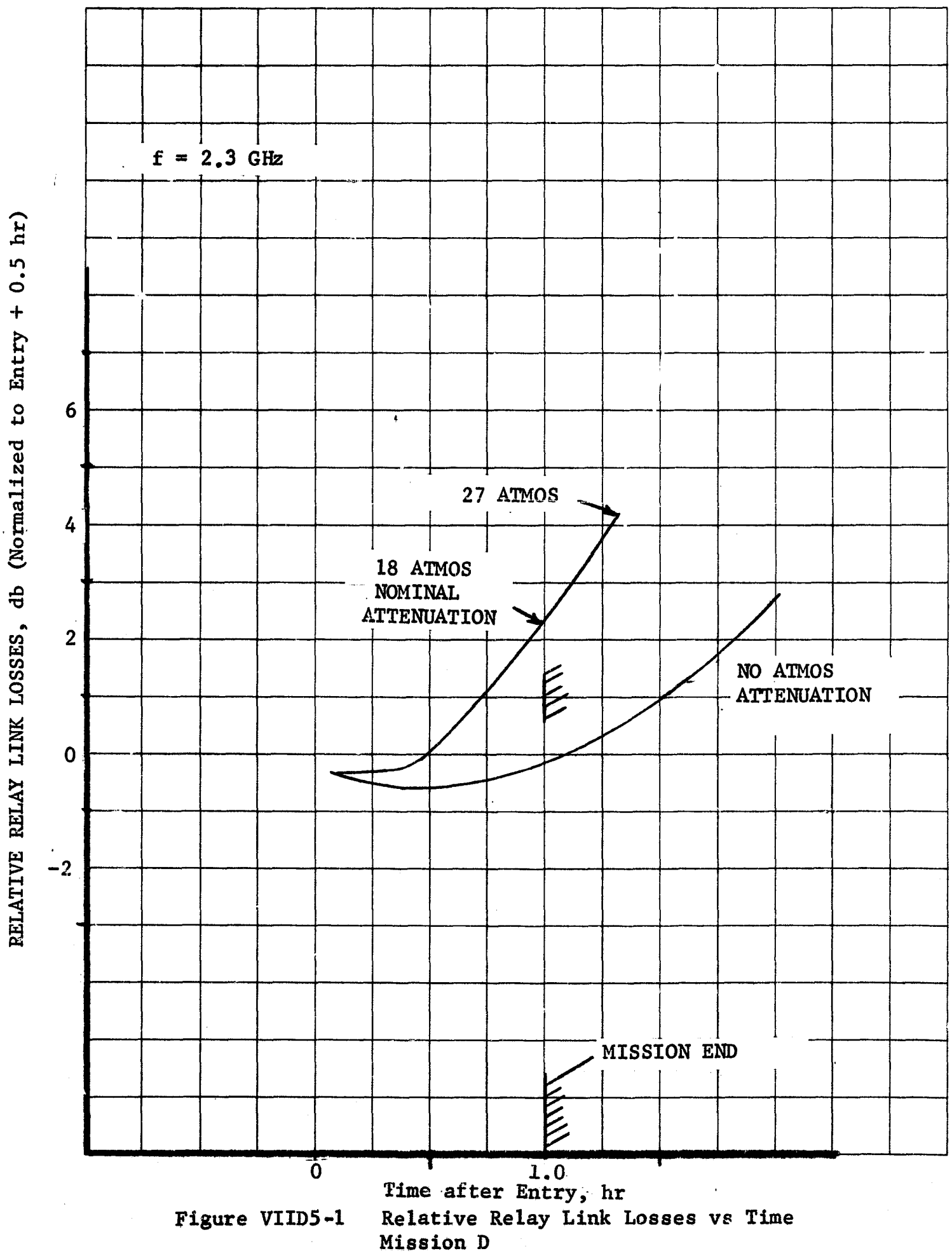


Figure VIID5-1 Relative Relay Link Losses vs Time
Mission D

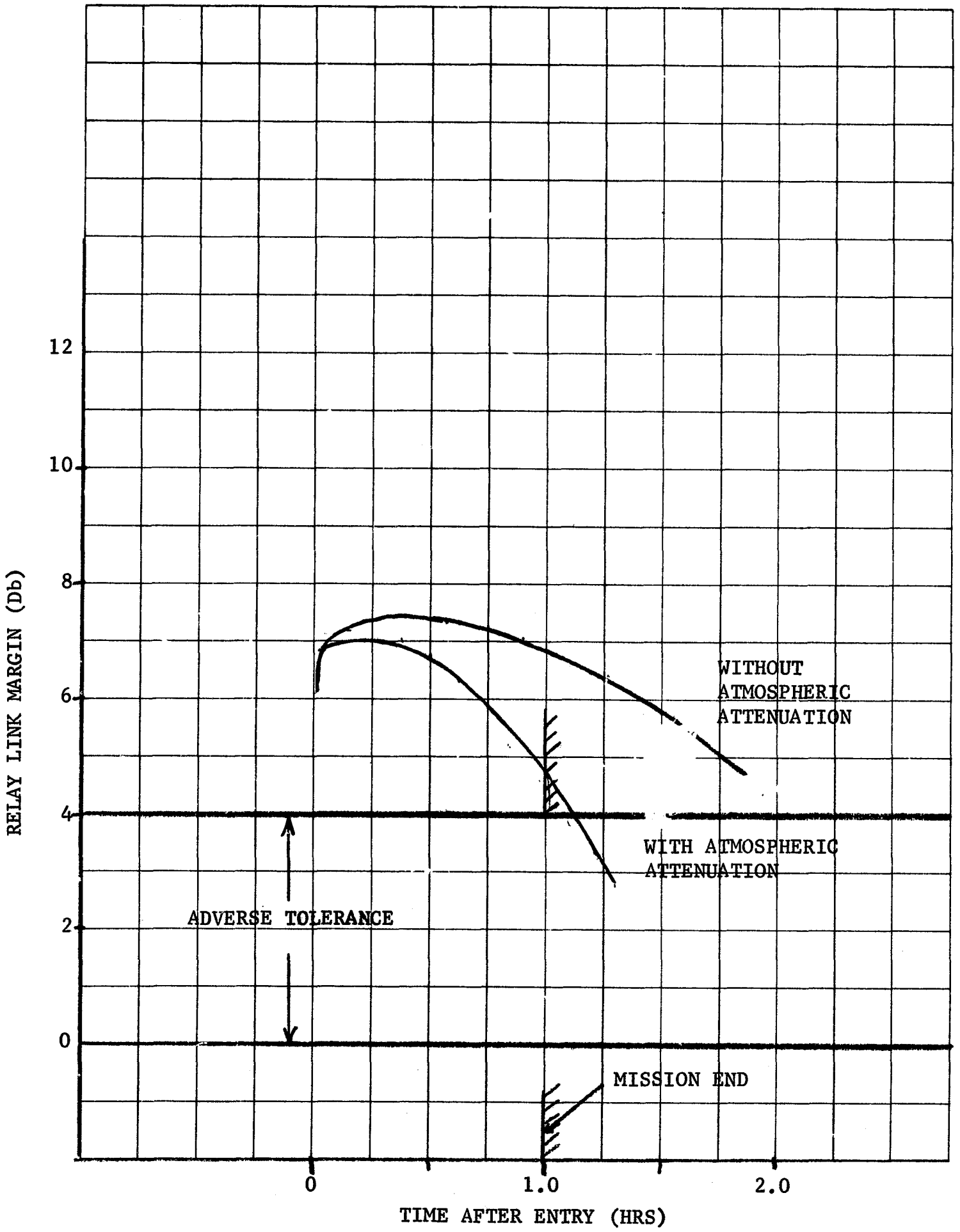


Figure VIID5-2 Relay Communications Link Margin vs Time Mission D

Spacecraft relay support systems and modifications are the same as for Mission A-1.

E. Mission E Selection Rationale

Sample mission E was selected as a Ground Tour mission with a launch date in October 1978 and Jupiter approach geometry much more favorable (R_P = 1.6 R_j) than the other Grand Tour missions considered.

1. Mission Profile

The approach geometry for sample mission E is shown in Figure VIIE1-1. The descent profile is shown in Figure VIIE1-2. Although less constrained in depth than the 1979 Grand Tour situation, Mission A-1, the rapidly changing probe/spacecraft angle limits the time of this mission and, consequently, the depth to 100 bars.

2. Sequence of Events

Major sequenced events and design parameters for sample Mission E are tabulated in Table VIIE2-1.

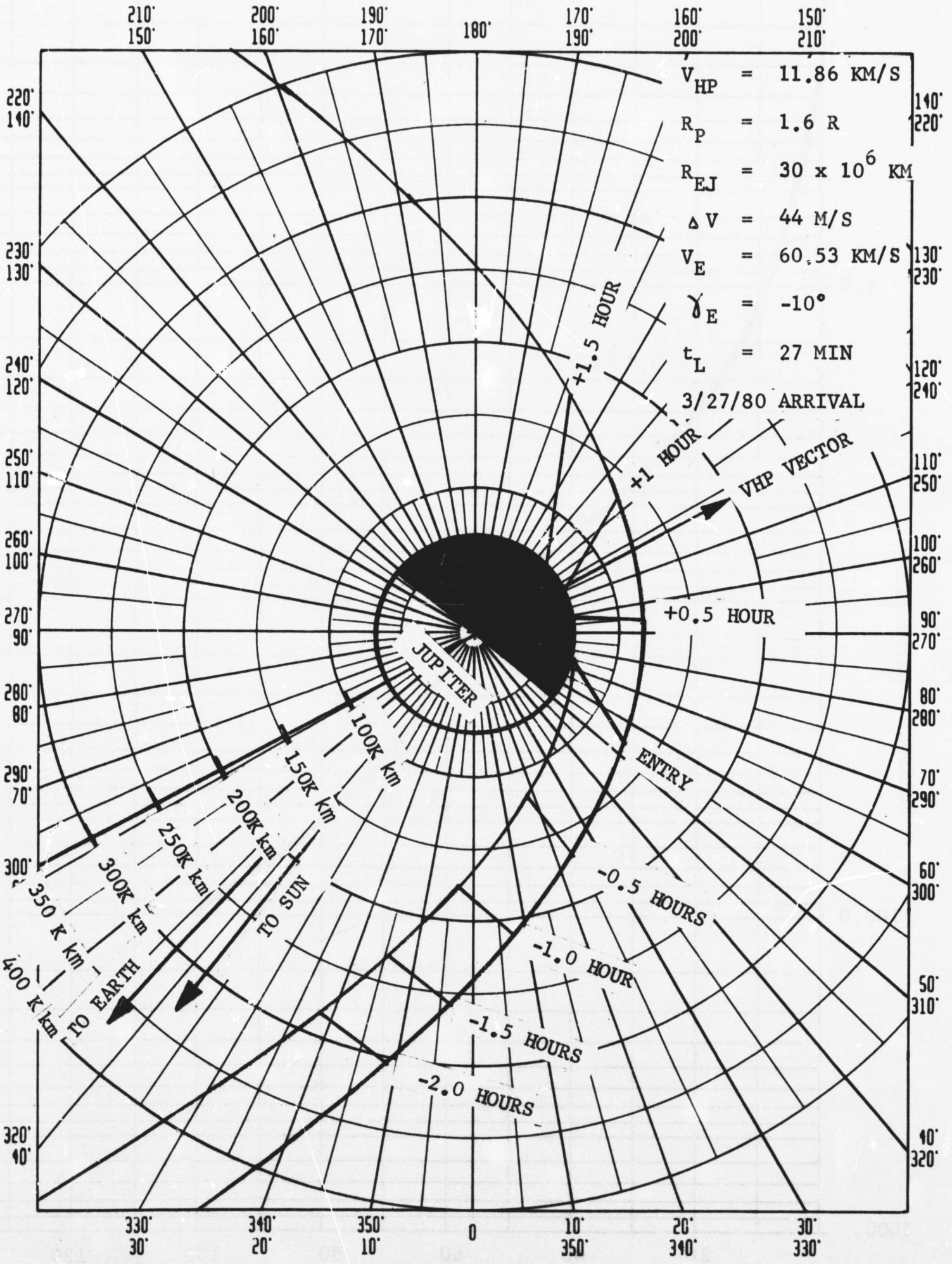


FIGURE VIIE1-1
APPROACH GEOMETRY
SAMPLE MISSION E

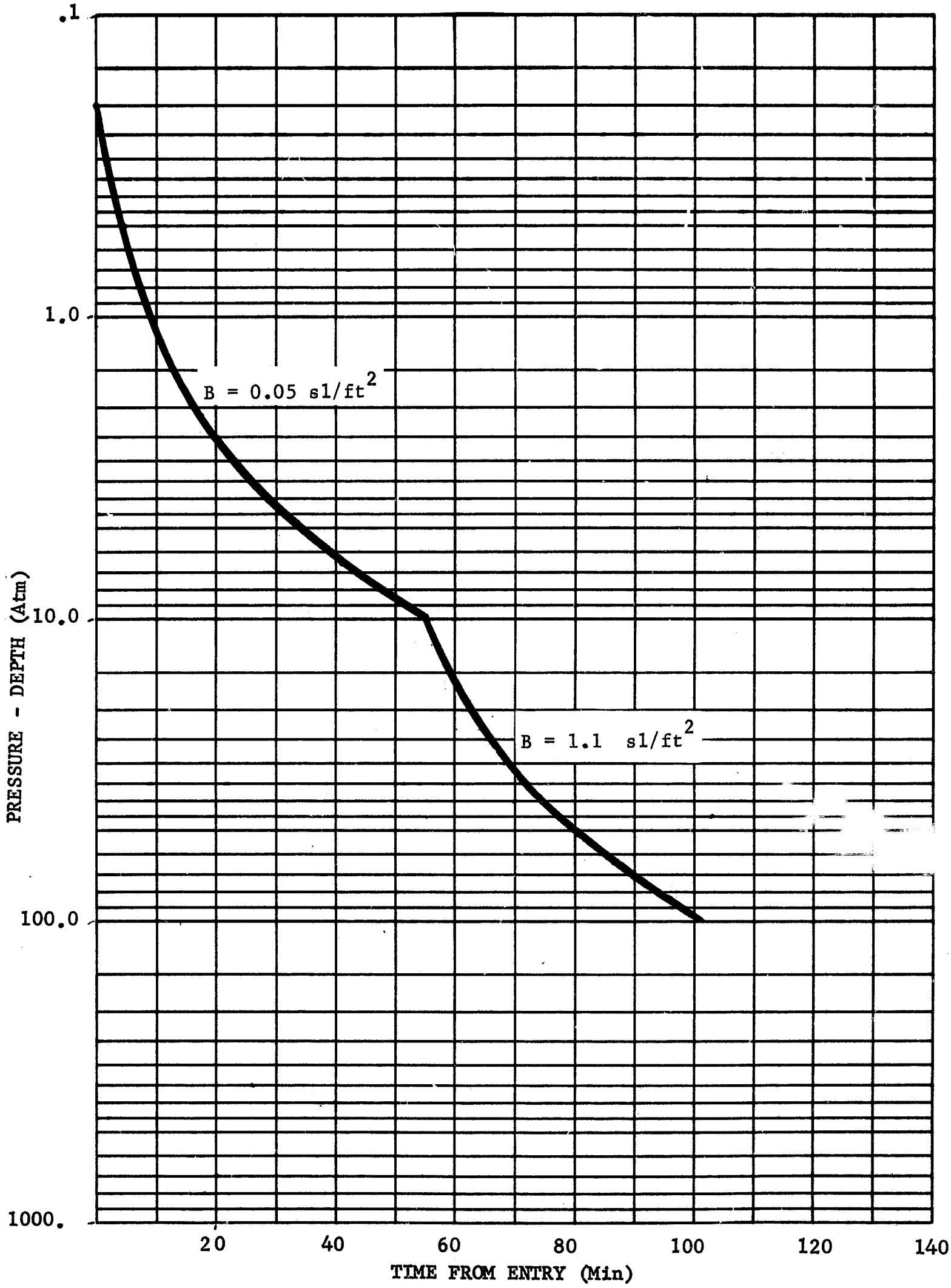


Figure VIIE1-2 Descent Profile - Sample Mission E

LAUNCH, INTERPLANETARY CRUISE, AND ENCOUNTER PARAMETERS
FOR JUPITER
MISSION E

* * * * * * * * * * * TABLE VIIE2-1 * * * * * * * * * * * * * * *

* * * * LAUNCH PARAMETERS * * * *

LAUNCH DATE (NOMINAL)	10/10/78
LAUNCH VEHICLE	TITAN III D CENTAUR (7 SEG WITH BURNER II)
LAUNCH PERIOD	30 DAYS
PARKING ORBIT ALTITUDE	100 NAUTICAL MILES
SPACECRAFT	TOPS
SPACECRAFT WEIGHT	1450. LBS
PAYLOAD WEIGHT (INCL S/C)	1900 LBS
FAIRING SEPARATION	CORE 2 IGNITION PLUS 10 SEC
MAX LAUNCH AZIMUTH	115 DEG

* *

* * * * INTERPLANETARY CRUISE PARAMETERS * * * *

TRAJECTORY	TYPE 1/GRAND TOUR
DECLINATION OF LAUNCH ASYMPTOTE	
DLA	29.65 DEGREES
RIGHT ASCENSION	102.6 DEGREES
INJECTION ENERGY, C3	112.4 KM2/SEC2
FLIGHT TIME	534 DAYS (NOMINAL)
SEMI-MAJOR AXIS	5.9 A.U.
RADIUS OF APHELION	NOT TRAVERSED
ECCENTRICITY	0.831
INCLINATION TO ECLIPTIC	1.76 DEGREES
CENTRAL ANGLE OF TRAVEL	141.3 DEGREES
TRUE ANOMALY AT DEPARTURE	1.49 DEGREES

* *

* * * * * ENCOUNTER PARAMETERS * * * * *

JUPITER ARRIVAL DATE	3/27/80
TRUE ANOMALY AT ARRIVAL	142.8 DEGREES
EXCESS VELOCITY, VHP	11.86 KM/SEC
DEC OF VHP VECTOR	16.54 DEGREES
RIGHT ASC OF VHP VECTOR	134.4 DEGREES
(WITH RESPECT TO VERNAL EQUINOX, EARTH EQUATORIAL SYSTEM)	
DEC OF VHP VECTOR	-1.56 DEGREES
(WITH RESPECT TO EQUATOR OF JUPITER)	
COMMUNICATION RANGE	4.5 A.U.

* *

* * * * DEFLECTION PARAMETERS * * * *

BUS TRAJECTORY	FLYBY
PERIAPSIS RADIUS OF BUS	114372 KM = 1.6 JUPITER RADII
DEFLECTION RADIUS	30,000,000. KM
INCLINATION OF TRAJECTORY	2.0 DEGREES
(WITH RESPECT TO EQUATOR OF JUPITER)	
DEFLECTION VELOCITY	44 METERS/SEC
DEFLECTION ANGLE	-106.3 DEGREES
CAPSULE COAST TIME	26.5 DAYS
LEAD TIME	27.0 MINUTES
LEAD ANGLE	-23.1 DEGREES

* * * * ENTRY PROBE DESIGN DATA * * * *

RELATIVE ENTRY VELOCITY	48.0 KM/SEC = 157440 FT/SEC
ENTRY ANGLE	-10. DEGREES (SKIPOUT AT -4 DEGREES)
ENTRY ALTITUDE (TIME=0)	487.7 KM = 1,600,000. FEET
ENTRY RADIUS	71907.7 KM
ENTRY LATITUDE	-2.0 DEGREES
ENTRY LONGITUDE	114.1 DEGREES
(RELATIVE TO MERIDIAN OF SUN)	

* *

* * * * AEROSHELL DATA * * * *

ENTRY BALLISTIC COEFFICIENT	0.84 SLUGS/FT2
TIME TO .1 G POINT	19.0 SECONDS
TIME OF MAXIMUM DECELERATION AND MAX DYNAMIC PRESSURE	40.0 SECONDS
MAXIMUM DECELERATION	446 G
MAXIMUM DYNAMIC PRESSURE	9,715 LB/FT2
TIME OF MACH 1 OCCURRENCE	79.0 SECONDS
AEROSHELL STAGING	
ALTITUDE	33 KM=200 MB
MACH NUMBER	.52
DYNAMIC PRESSURE	82.3 LB/FT2
TEMPERATURE	203.4 DEG R
DENSITY	.00009726 SLUG/FT3
TIME (TS)	124.0 SECONDS

3. Configuration Summary - Mission E

The Inboard Profile of the Mission E entry probe is shown in Figure VI-E3-1. The system characteristics and total system weight summaries are presented in Tables VIIE-1 and 2.

4. Mechanical and Support Systems

Descent Probes

The descent probe structural/thermal concept is an evacuated titanium pressure vessel exposed to the ambient environment. The inside of the pressure shell is lined with multi-layer thermal insulation. The concept of supporting the equipment on a shelf, shell penetrations, and the pressure shell closure characteristic of the design example configuration is applicable to this design.

The descent profile prescribed for the science mission is two stage where a parachute is required initially down to 10 atmospheres requiring no specific probe aerodynamic configuration. After separation from the parachute, the remainder of the descent to 100 atmospheres is ballistic at an m/C_DA of 1.1 slug/ft^2. This is achieved with a 40 degree half angle skirt of fabricated ring-shell construction.

The spacecraft communications antenna is a curved turnstile type external to the pressure vessel mounted to the closure dome. It is protected by an RF transparent domed cover as it is for the Design Example.

Entry Aeroshell

The entry aeroshell is a 55 degree half angle cone forebody 3.5 feet in diameter. The aeroshell construction and arrangement is the same as that of the Design Example except for the descent probe support. Since the pressure shell is exposed, its stiffness is utilized in transmitting entry loads to the aeroshell. Nesting the probe in a high density foam pad conforming to the probe's shape allows the entry g-loads to be transmitted directly to the aeroshell. A shallow ring beam provides the probe attachment and separation points and will carry the over-load above the pads capability. The beam also

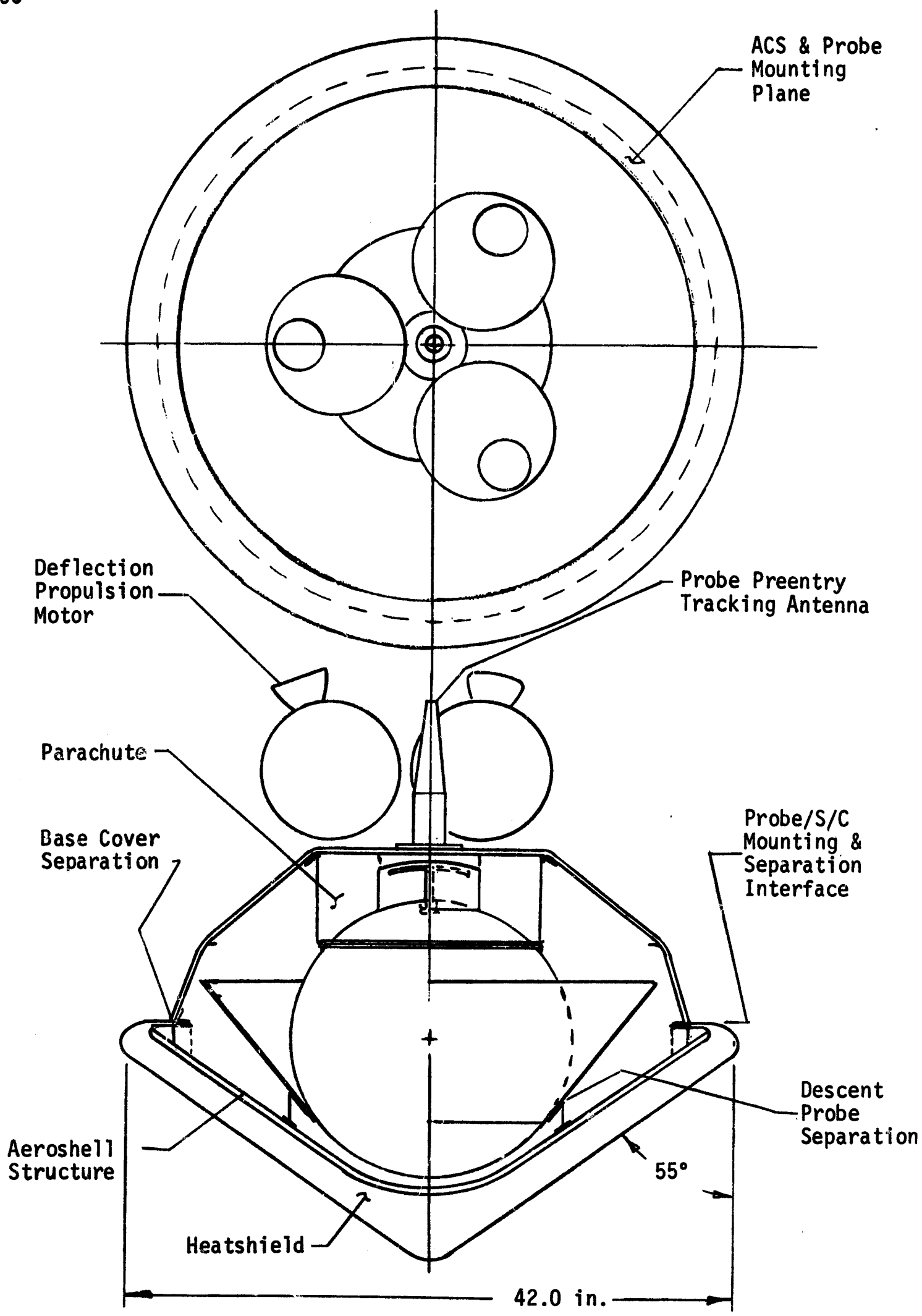


Fig. VII-E-3-1 Entry Probe Inboard Profile
Mission E

TABLE VIIE3-1

Type Probes	Single (staged)
Maximum Depth	100 atm
Entry Angle	-10 deg
Data Return Mode	Relay
Spacecraft Radius of Periapsis	2.0 R
Science Payload	26 lb
Bit Rate	
Descent	40/20 B/S
Pre-entry	180 B/S
Transmitter Power	40 watts
Spacecraft Antenna Dish Diam.	3.4 ft
Descent Time	1.65 hrs
Entry Ballistic Coefficient	.84 slugs/ft^2
Probe Diameter	3.5 ft
Entry Weight	353 lb
Probe Installed Weight	381 lb
Total Probe System Weight (Including Spacecraft Mods)	468 lb
Total Lift-off Weight	1918 lb
Launch Vehicle Capability (7 Segment TIIID Centaur with Burner II)	1900 lb

TABLE VIIE3-2

MISSION E WEIGHT SUMMARY

	Wt. (lbs.)	
Science	26.0	
Communication Electronics & Power	50.0	
Pressure Shell	24.8	
Internal Structure	7.3	
Insulation (Multi-Layer)	0.9	
Phase Change Material	1.0	
Pyrotechnic Vent Valve	1.5	
Antenna	1.5	
External Aerodynamics & Adapter Hardware	8.0	
		(121.0)
Parachute & Harness	6.0	
Parachute Canister	1.8	
Spinup/Despin System (Fixed)	3.0	
Separation Mechanisms	3.0	
Auxiliary Structure	3.5	
Entry Vehicle ACS (Gyro, Data, etc.)	25.0	
Pre-entry Communication Electronic & Power	17.0	
Equipment Inst'l Structure	5.0	
Total Entry Vehicle Misc.		(63.3)
Aeroshell Structure		(45.0)
Heatshield		(124.0)
Entry Weight		353.0
Deflection Propulsion Module	12.0	
Despin Systems (Spent)	3.0	
Thermal Blanket	8.0	
Separations Mechanisms	2.5	
Ion Mass Spectrometer	3.0	
Expended or Jettisoned Equipment		(28.5)
Probe Installed Weight		381.5
Spacecraft Modifications		86.5
Total Probe System Weight		468.0
TOPS Spacecraft		1450.0
Total Lift Off Weight		1918.0

serves as the primary attach and separation plane for the descent probe.

Adaptation to Spacecraft

The entry probe mounting to the TOPS spacecraft is the same as for the Design Example Probe. The probe mounts to the -y side of the equipment compartment in the y-y plane tilted downward 40 degrees in the booster installation. The mounting rationale and the resultant effects to the spacecraft are discussed in the Design Example configuration description.

The Booster Installation Sketch for the Design Example also applies to this configuration.

The 1918 lb total weight is 18 lbs over the 1900 lb capability of the 7 segment TIIID Centaur with Burner II indicating a slight compromise in descent depth or payload would be required.

5. Mission E Telecommunications, Data Handling and Power

Mission E requires a single descent probe to descend to a pressure of 100 earth atmospheres while transmitting data to a flyby S/C passing the planet at an R_p of 1.6 R_j. Pre-entry data for an hour before probe entry is also acquired.

The communications link is required to provide a 180 bps pre-entry rate, a 40 bps rate for 68 minutes following entry and a 20 bps rate for the balance of the 1-3/4 hour descent period. This is accomplished with a 40 watt phase modulated probe transmitter operating at 1.2 GHz and a 3.4 ft diameter S/C antenna.

Communications geometry, antenna aspect angles and range, relative link losses and communication link margin, all as a function of time, are shown in Figures VIIE1-1 and Figure VIIE5-1. 2, 3. The communications geometry associated with the smaller Rp becomes unfavorable in probe antenna aspect angle as the post entry time approaches 1.65 hours; thus, the mission is designed to terminate at this point.

Radio frequency selection is based on minimizing probe transmitter power at the end of the mission time since power requirements at this time are greater than for any other period. Doppler and Doppler rates as a function of time for the nominal case are shown in Figure VII.E.5-4.

Trajectory error analysis data is not available for this mission; therefore, antenna pointing and Doppler uncertainties (as a function of geometry dispersion) is likewise not available. The procedure assumed for the S/C system acquiring the probe radio signal is the same as for the other missions although it is felt intuitively that the acquisition procedure will be more time consuming due to the higher Doppler and Doppler rates.

The relay link telemetry data transmitted for pre-entry and stored during entry are the same as described for the design example mission. Storing of entry data plus 3 minutes of post entry data requires 26,175 bits of storage as used in the DE mission.

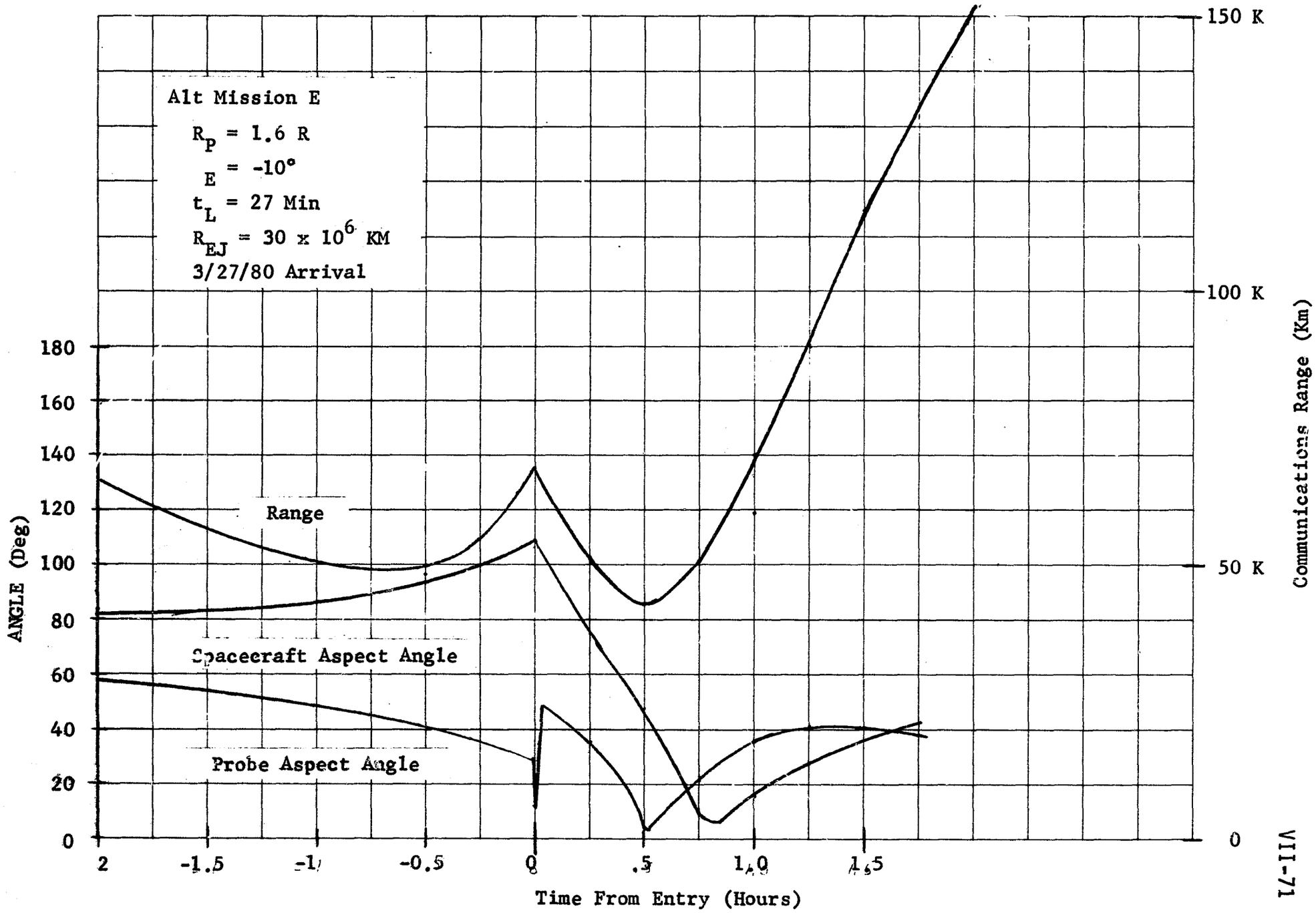


Figure VIIE5-1 Aspect Angles and Range vs Time

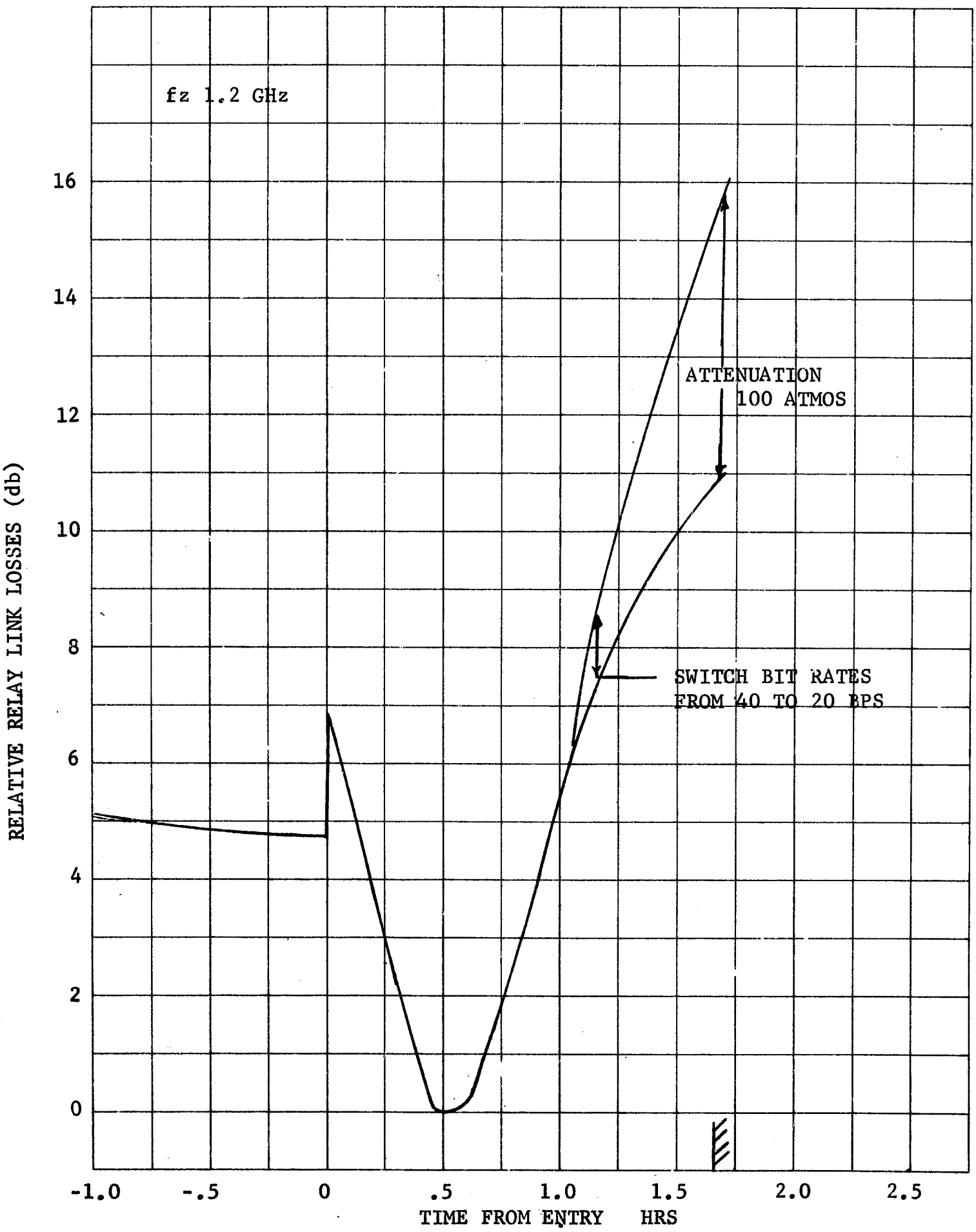


Figure VIIE5-2 Mission E Relative Relay Link Losses vs Time

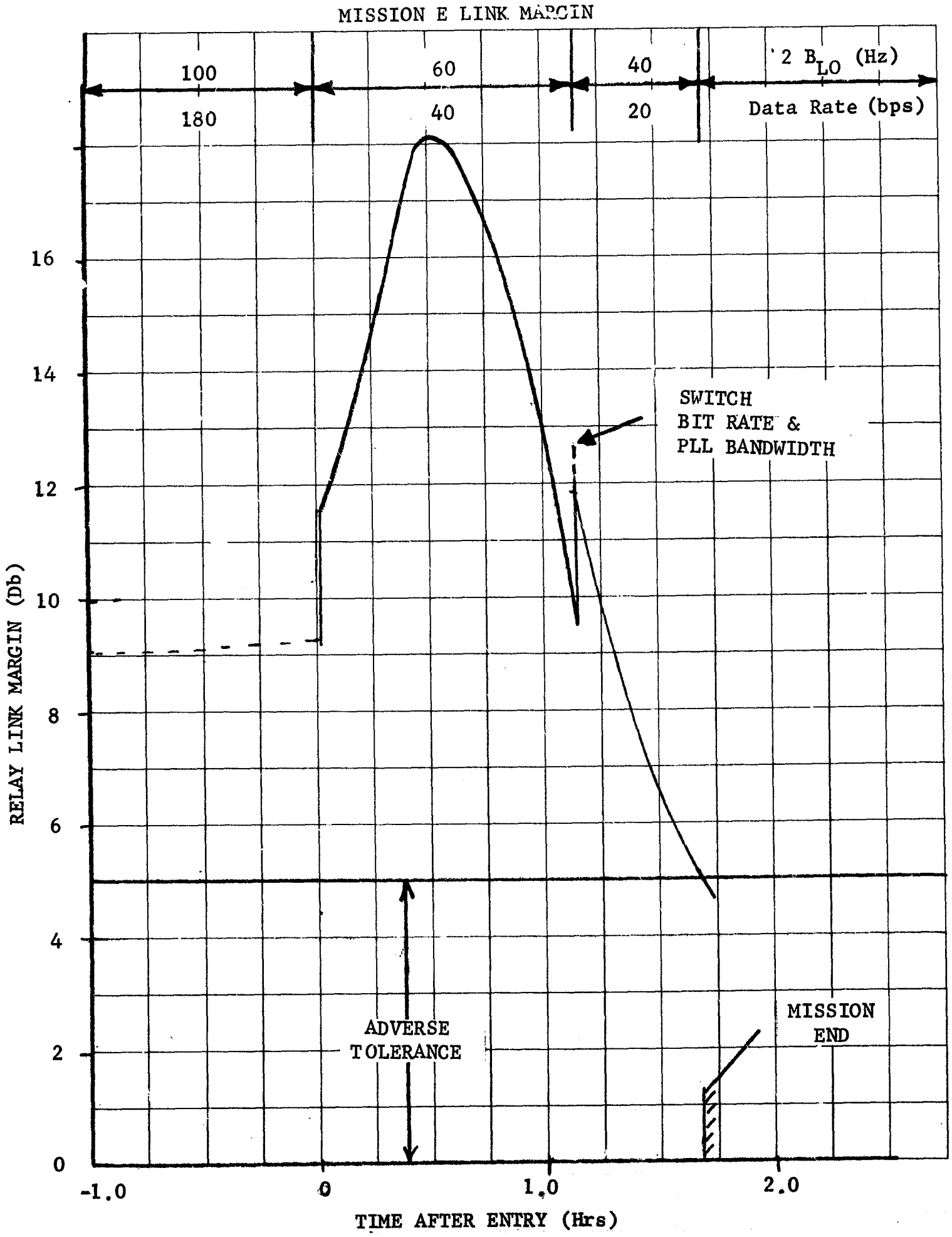
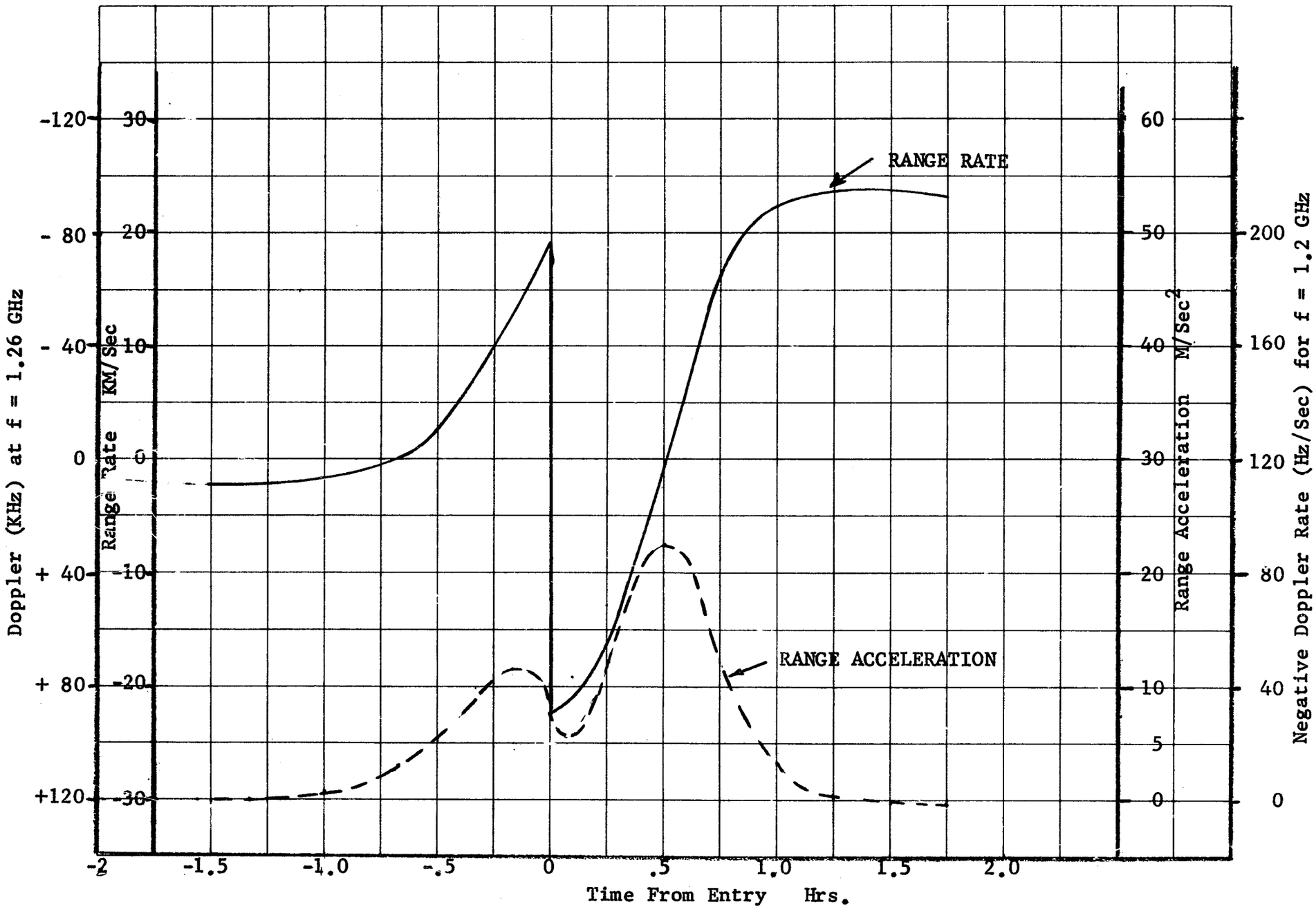


Figure VIIE5-3 Relay Link Margin vs Time

Figure VIIE5-4 Nominal Doppler and Doppler Rates for Mission E Relay Link



The telemetry data stream content for the post entry periods are apportioned as follows:

Aeroshell Staging to Staging Plus 68 Minutes

Source	Data Rate
Science	24
Stored Data	12.5
Engineering & Timing	3.5
	40.0 bps

Aeroshell Staging Plus 68 Min. to End of Mission

Source	Data Rate
Science	14
Engineering & Timing	3.5
Reread of Stored Data	2.5
	20.0 bps

Power for the system is supplied by batteries, one each in the aeroshell and probe. The aeroshell battery weighs 6 pounds as for the DE mission. The probe battery must accommodate a peak load of 188.9 watts and supply 311 watt hours of power. This requires a battery weight allocation of 10 lbs.

Probe subsystem weight and power allocations for the telecommunications, data handling and power subsystems are shown in Table VII.E.5-1.

Spacecraft mounted support equipment and modification is essentially the same as for the DE mission. See Chapter VI.

TABLE VIIE5-1

MISSION E

TELECOMMUNICATIONS DATA HANDLING AND POWER SUBSYSTEMS

WEIGHT AND POWER

Aeroshell Mounted	Wt (lb)
Relay Antenna	1.5
Battery	6.0
Power Conditioning	2.0
Total	9.5 (Note 2)

Probe Mounted Equipment	Wt (lb)	Power (Watts)
Modulator/Exciter	1.5	1.5
Power Amplifier	8.0	130.0
Data Handling	12.0	11.0
Power Conditioning	4.0	17.0
Battery	10.0	-
Subtotal	35.5	159.5
Other		
Science	See Note 1	29.0
Cabling	See Note 1	
Total		188.5 watts

NOTES:

1. Weight included elsewhere
2. Ion Mass Spectrometer not shown

F. Mission F Selection Rationale

Sample Mission F was selected to examine the feasibility of a direct radio link to Earth. The TOPS spacecraft is used and the approach geometry is similar to that of the design example shown in Figure VIB-1. The descending probe goes to a depth of approximately twenty atmospheres with the profile shown in Figure VIID1-2.

3. Configuration Summary - Mission F

Figures VIIF3-1 and -2 show the configuration. Mission characteristics and subsystem weight summaries are given in Tables VIIF3-1 and VIIF3-2 respectively.

4. Mechanical and Support Systems

The Mission F descent probe establishes a direct link with the earth by means of a retrodirective phased array antenna. A slow descent rate on a parachute precludes any requirement for aerodynamic characteristics of the descent probe. The equipment canister is a 2 to 1 oblate spheroid shape to facilitate its mating with the phased array antenna and packaging in the aeroshell. This system is different from the other probes in that the transmitter and the antenna are integral and external to the canister. The high entry g-loads due to a 49 degree entry angle impact the internal equipment mounting and support structure for the phased array antenna.

The entry aeroshell is a 4.0 feet diameter 60 degree cone half angle body since the shallow payload allows use of a blunter cone to stay below the required maximum ballistic coefficient of .80 slugs/ft^2 imposed due to the steep entry (to achieve M.8 at or above .2 atm altitude).

The mission duration of .93 hours results in a traverse of 32° by the probe. A 49° entry angle is selected to permit the mission to start with the probe 25° up-stream of the subearth point so that at the end of the mission, the greatest attenuation point, the aspect angle to earth will be small. This results in a significant entry aeroshell weight penalty. This penalty could be reduced by moving the end-point of the mission farther from subearth, but probe transmitter power and antenna weight would increase fairly rapidly.

Probe Deflection Systems are similar to the Design Example Probe, and the probe adaption to the spacecraft is likewise similar except that the spacecraft tracking antenna is of course deleted.

The total probe system weight is quite large relative to the Mission D probes which perform a similar descent profile mission by

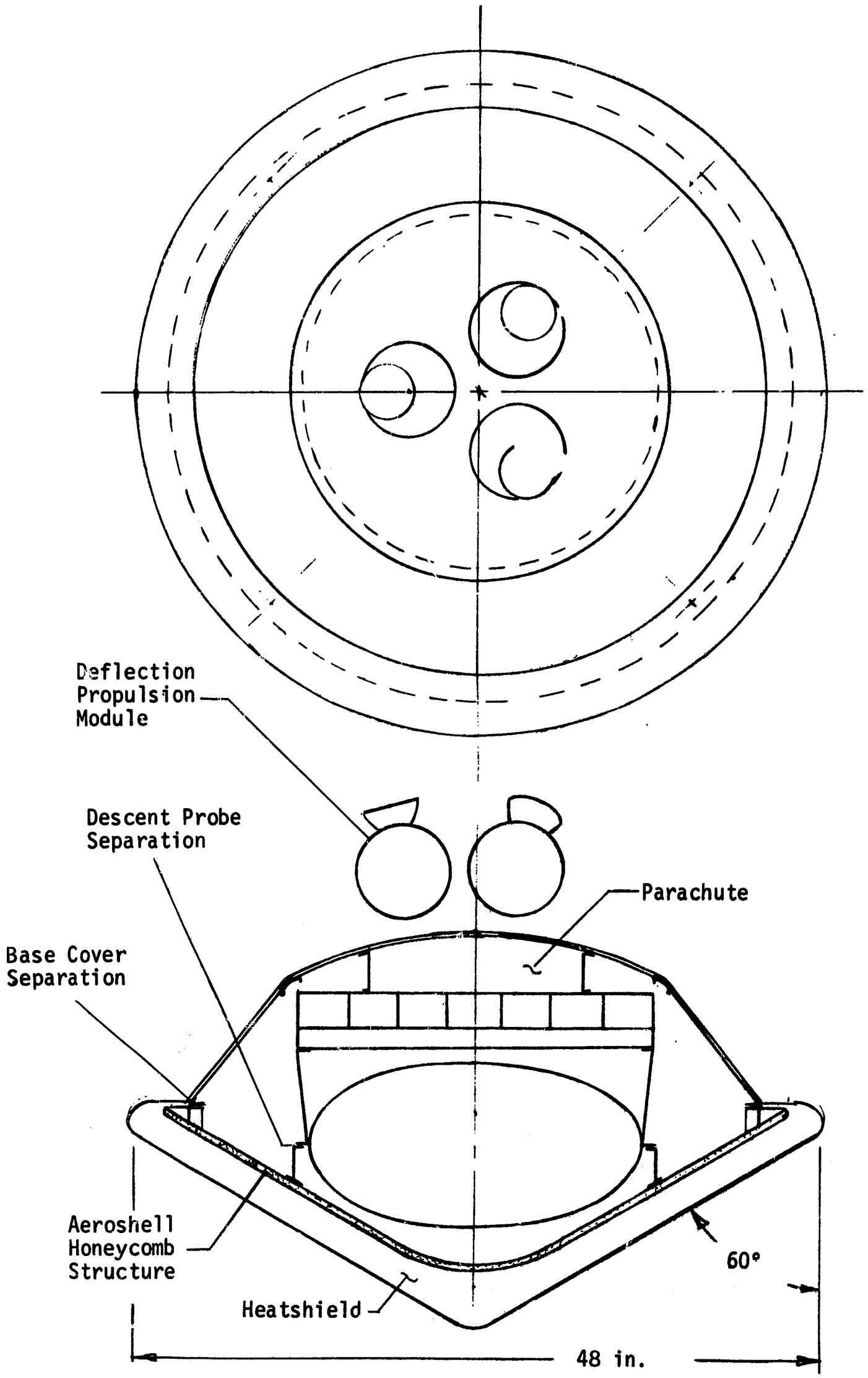


Fig. VII-F-3-1 Entry Vehicle Inboard Profile, Mission F

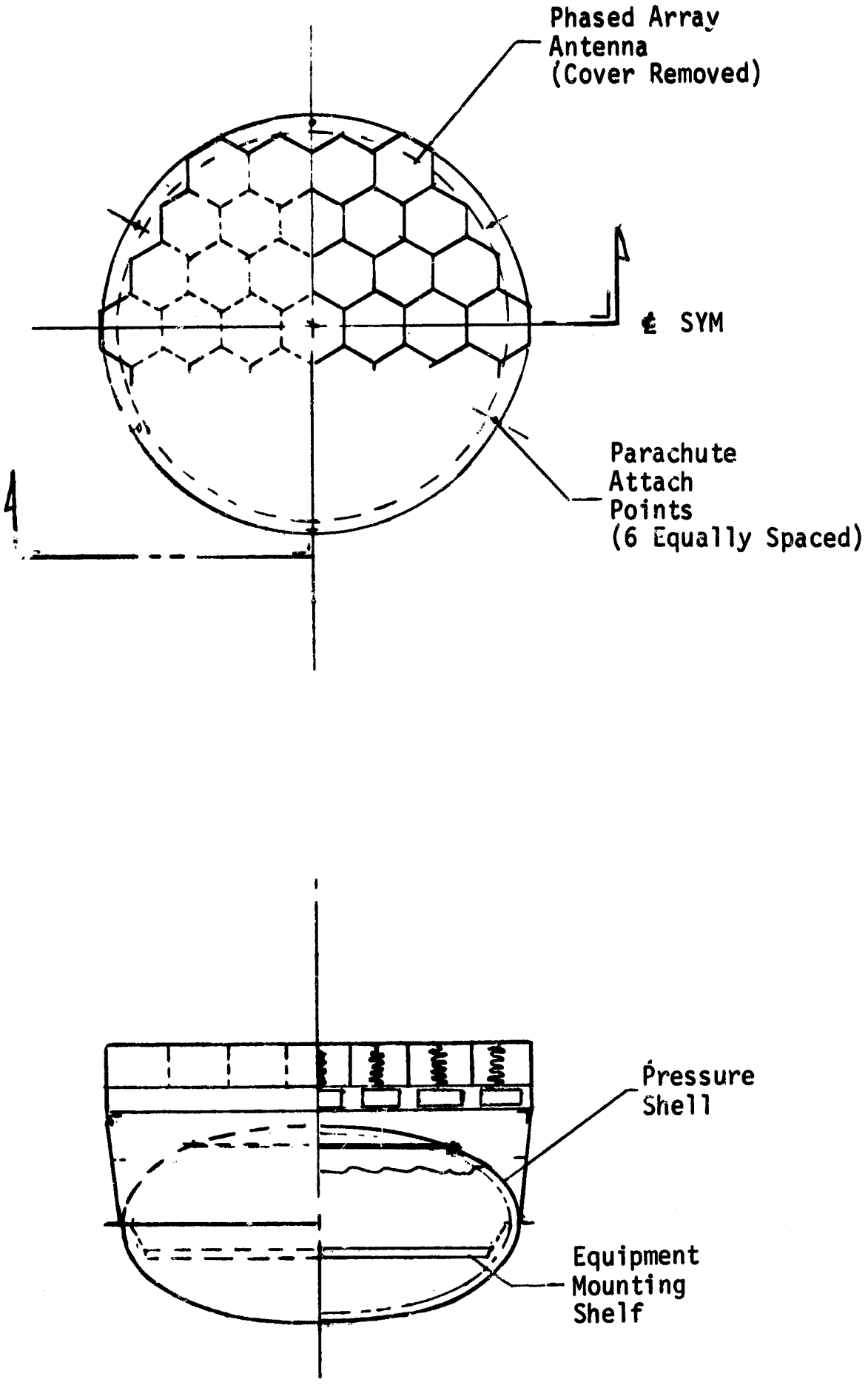


Fig. VII-F-3-2 Descent Probe Inboard Profile
Mission F

TABLE VIIF3-1

MISSION F CHARACTERISTICS SUMMARY

Type Probe	Single (Unstaged)
Maximum Depth	17 Atm
Entry Angle	-49°
Data Return Mode	Direct Link
Science Payload	10 lbs
Bit Rate Descent	20 B/S
Bit Rate Pre Entry	-0
Transmitter Power	15 watts
Descent Time	.93 hr
Entry Ballistic Coefficient	.80 slugs/ft^2
Probe Diameter	4.0 ft
Entry Weight	497 lbs
Probe Installed Weight	552 lbs
Total Probe System Weight	617 lbs
Total Lift-off Weight	2067 lbs
Launch Vehicle Capability (7 segment TIIID Centaur with Burner II)	2420 lbs

TABLE VIIF3-2

MISSION F WEIGHT SUMMARY

Items	Wts. (lbs)	
Science Instruments	10.0	
Communication Electronics	21.0	
Power	5.0	
Multi-Layer Insulation	.4	
Pressure Vessel Structure	12.5	
Internal Structure	7.2	
Internal Equipment and Canister		(56.1)
Phased Array Antenna	51.0	
Interconnecting Structure	5.5	
Antenna Installation		(56.5)
Descent Probe		(112.6)
Parachute and Harness	6.0	
Parachute Canister	1.2	
De-Spin Yo-Yo System (Fixed)	2.0	
Separation Mechanisms	3.0	
Entry Vehicle ACS	25.0	
Equipment Inst'l Structure	4.0	
		(41.2)
Aeroshell Structure (4.0 D, 60° 1/2)		(152.0)
Heat Shield		(191.2)
Entry Weight		497.0
Deflection Propulsion Module		47.0
Thermal Control Blanket		8.0
Probe Installed Weight		552.0
Spacecraft Mods		65.0
Total Probe System Weight		617.0
TOPS Spacecraft		1450.0
Total		2067.0

using the Relay Mode. This is because the added weight of the phased array factored through the aeroshell weight (which is almost twice as heavy to start with due to the 49° entry) way more than offsets the deletion of the probe tracking antenna on the spacecraft.

The total lift-off weight of the Mission F systems, 2067 lbs requires a 7 segment TIIID Centaur or a 5 segment TIIIC Centaur with Burner II launch vehicle. (The maximum Type I trajectory payload capability would be 1950 lbs which is too small even without considering that Type I would dictate an even steeper entry angle $\gamma = -90°$, and thus increase probe weight drastically.)

5. Telecommunications, Data Handling and Power, Mission F

a. General

This mission uses a direct communication link to Earth. The instrument package, flight time, penetration depth, and data rate are the same as Mission D (miniprobe). The post entry bit rate is 20 bps. This includes 6 bps for readout of data stored during entry. There is no pre-entry communications. Mission duration is 0.93 hours, terminating at a depth of 17 atmospheres. Targeting is designed to keep the probe as close as possible to the subearth point during its 0.93 hour mission. Communication angles are sketched in Figure VIIF5-1A. Probe attitude excursions due to turbulence are assumed to be limited to 20° at post-entry, decreasing to 10° at the end of the mission.

Communications frequency is constrained to the DSN frequency, 2.3 GHz. A high-gain phased array antenna is used to permit a reasonable transmitter power level. Several modulation formats are compared, and a coded noncoherent system is selected.

The weight of this probe is such that either the TOPS or the Pioneer could be used as the spacecraft. Modifications to the spacecraft are minimal since it is not used as a relay.

The DSN antenna feed configuration is dependent on the selected spacecraft. The S-band feed appropriate for the Pioneer gives somewhat better performance than the combined X-band, S-band feed required for the TOPS. The Pioneer configuration has been assumed for the link design control tables. The difference in performance between the two configurations is 1.3 db.

b. The Probe Telecommunications System

The probe telecommunications system uses a high-gain (22 db) steerable phased array antenna radiating 15 watts RF power. The selected signalling format is 32 ary FSK using a rate 1/5, constraint length 8 convolutional encoder. Predetection recording, noncoherent detection, and Viterbi decoding are assumed at the DSN ground station. The tradeoffs leading to this system design are discussed below.

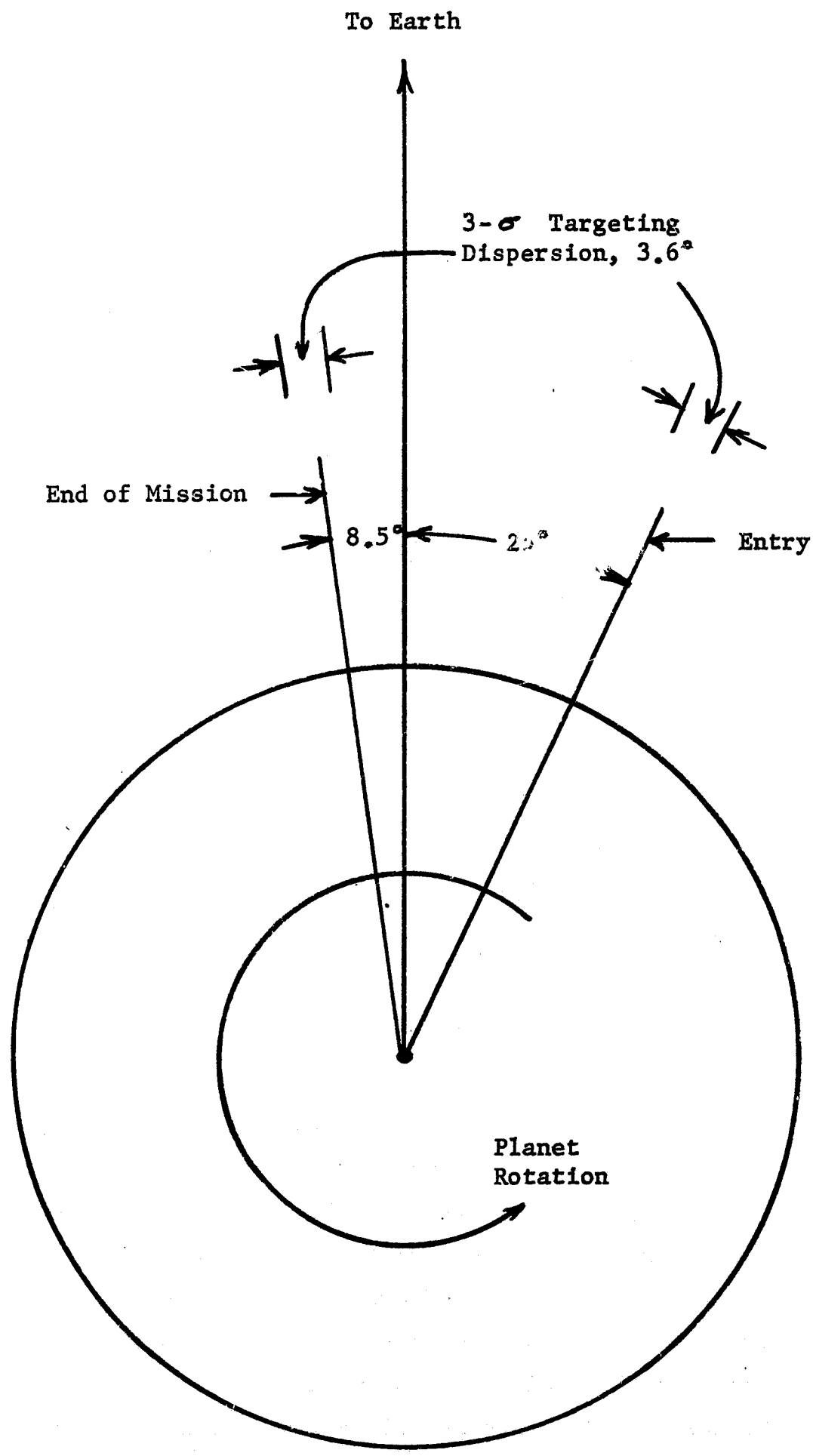


Fig. VIIF5-1A Communication Angles, Direct Link, Mission F

(1) Real-Time Acquisition and Tracking, Coherent Links

It is assumed that transmission will begin immediately after parachute deployment. At that point the nominal velocity is around 100 m/sec. Uncertainty in this velocity, due primarily to uncertainty in the pressure at the time of deployment, is estimated to be 35 m/sec. The nominal initial deceleration is 0.12 m/sec^2 with an uncertainty estimated to be 0.024 m/sec^2. For entry 22.2° from subearth, the earth-directed component of these values would all be reduced by cos 22.2° = 0.925. The reduced values are tabulated below along with their resulting doppler values.

The trajectory-related uncertainty in the doppler rate is overwhelmed by the turbulence-related uncertainty. Earth-directed accelerations as high as 10 m/sec^2 could occur, and even higher values cannot be ruled out, since Jupiter gravity is 2.5 times this value. Doppler rates corresponding to 10 m/sec^2 are also tabulated below.

		One way, up	One way, down	Two-way
92.5	m/sec, nominal	646 Hz	710 Hz	1356 Hz
32.4	m/sec, uncertainty	226 Hz	248 Hz	474 Hz
0.111	m/sec^2, nominal	0.78 Hz/sec	0.86 Hz/sec	1.64 Hz/sec
0.022	m/sec^2, uncertainty	0.155 Hz/sec	0.170 Hz/sec	0.325 Hz/sec
10.	m/sec^2, turbulence	70 Hz/sec	77 Hz/sec	147 Hz/sec

These values all decrease sharply as the probe descends into denser atmosphere.

The doppler rate fixes the minimum bandwidth PLL that can can be considered. The doppler rate that can be tracked by a loop is given by $k B_N^2$, where B_N is the loop noise bandwidth. Selection of k depends on a number of factors, including loop SNR, desired static phase offset, and desired cycle-slipping probability. A good rule-of-thumb value for k is 0.1. From [1], and assuming a 9 db loop SNR, this value of k gives a static phase offset of 20°. The loss of lock rate at this offset and SNR is estimated to be once in 250 seconds on the average. The rate without the phase

offset is once in 800 seconds. A loop can stand momentary rates somewhat higher than this, but loss of lock probability increases sharply. Also, signal degradation equal to the cosine of the phase offset will result even if lock is not lost. Assuming 10 m/sec^2 peak turbulence, the rule-of-thumb indicates a minimum B_L of around 28 Hz for a one-way link and 38 Hz for a two-way link. These bandwidths are prohibitively large for the direct down link, so we will assume a 12 Hz loop, and accept the possibility of some brief periods of signal loss early in the mission if high turbulence should be encountered. This is the narrowest loop that should be considered. A narrower loop could be out of lock thruout most of the early part of the mission.

This same $0.1\ B_N^2$ can be used as a rule-of-thumb for selecting a search rate that will permit signal acquisition by the loop as it scans past the signal. The total frequency uncertainty is composed of doppler uncertainty and probe frequency reference uncertainty. Uncertainty in the probe frequency reference is estimated to be $2{:}10^6$ or at S-band, 4600 Hz. If a one-way (down only) link were assumed, the ground station would have to search through the uncertainty of 4800 Hz. Using the rule-of-thumb for search rate, $0.1\ B_N^2$, a 12 Hz loop could search at 14.4 Hz/sec, which would require a search time of 5.3 minutes.

This time can be markedly reduced by using a two-way link. The strong up-link can operate into a 40 Hz loop in the probe giving a search rate of 160 Hz/sec. Its search would be completed in 30 seconds. Once lockon is established, the only uncertainty remaining in the down-link is the 474 Hz doppler. This could be searched in 33 seconds with a 12 Hz loop.

The 40 Hz loop in the probe can readily track the one-way doppler on the up link. The use of a two-way link has the unfortunate effect of doubling the doppler rates due to turbulence that must be tracked by the DSN receiver. It would be possible to consider a two-oscillator system in the transponder, with a second oscillator frequency-locked to the phase-locked oscillator after some intervening smoothing. However, this would increase the initial lockup time and the complexity

of the transponder. This option will not be considered further at this time, but could be investigated when more information is available on the expected turbulence levels on Jupiter.

A design control table for a link using a 12 Hz loop is shown in Table VIIF5-1. A table for the up-link is shown in Table VIIF5-2.

(2) Predetection Recording

Based on rather limited experimental data on the planned DSN capability for predetection recording*, a SNR degradation of 1.25 db has been estimated for predetection recording. This is believed to be an upper limit, applicable to wideband multi-subcarrier signals with coherent detection. Better performance is expected for narrow band signals, and noncoherent signalling is expected to be somewhat better than coherent signalling. Accordingly, we will assume 1.2 db for coherent signalling and 1.0 db for noncoherent signalling. These values are shown on line 11 of Table VIIF5-1.

It will be assumed that by using predetection recording the PLL bandwidth can be made much narrower than that required for real-time demodulation. Tracking through the high doppler rate regions caused by turbulence would be carried out by a iterative process, with successive playbacks used to improve the estimate of the carrier frequency vs time trajectory. The prior estimate would be programed into the tracking system for each playback, and the PLL error signals generated during the playback would be used to improve this estimate for the next playback. This estimate should converge after a number of iterations, and the final estimate would be used to demodulate the data. A 3 Hz loop will be assumed.

A 1 Hz loop (the narrowest now being considered for the DSN) could in principal also be used with this iterative demodulation technique, giving further improvement in performance for the price of more iterations. However, there are limitations imposed by the quality of the reference oscillator used in the probe. Given the constraints of the probe environment and size, it is not realistic to assume oscillator linewidths less than about 2 Hz at S-band. This signal would

---

*Telecon with Carl Johnson of JPL, December 1970.

not have sufficient coherence to be tracked by a 1 Hz loop. The carrier would appear as a noise-like input to any loop whose bandwidth is narrower than the oscillator linewidth. Therefore, a 3 Hz loop is the narrowest that could be considered, even with predetection recording and the iterative demodulation procedure described above.

In theory, predetection recording avoids the whole problem of real-time signal acquisition. However, there is some advantage in reducing the frequency uncertainty. It allows a narrower-band recording, giving a higher recorded SNR and reducing the required searching needed during processing. Given the finite dynamic range of the tapes, the higher recorded SNR should improve performance. Accordingly, it would be desirable to use an up-link as described in the previous section to remove the oscillator frequency uncertainty from the down-link signal. Since the recommended down-link antenna is a retrodirective array, lockon to an up-link signal is required in any event to focus the antenna, so this signal would also be used to fix the down-link oscillator frequency.

A design control table using a 3 Hz loop is shown in VIIF5-1. Predetection recording is also used for noncoherent signaling. A calculation for this signalling mode is also shown in Table VIIF5-1.

(3) Noncoherent Signalling

The advantage of noncoherent signalling over coherent signalling is that it avoids the loss required by diverting power into the carrier, and it also avoids the noisy carrier loss. This saving outweighs the loss due to the less efficient detection operation for low data rates, giving an advantage to noncoherent signalling at these low rates. The crossover data rate depends on a number of factors, including the coding system used and the oscillator spectral linewidth.

Performance is calculated using the techniques described in [2] and [3]. Figures VIIF5-1B and 2 are taken from [3]. It is assumed that the oscillator spectral linewidth 2a is equal to 2 Hz (a = 1 Hz). This may be somewat conservative. A fast-fourier-transform (FFT)

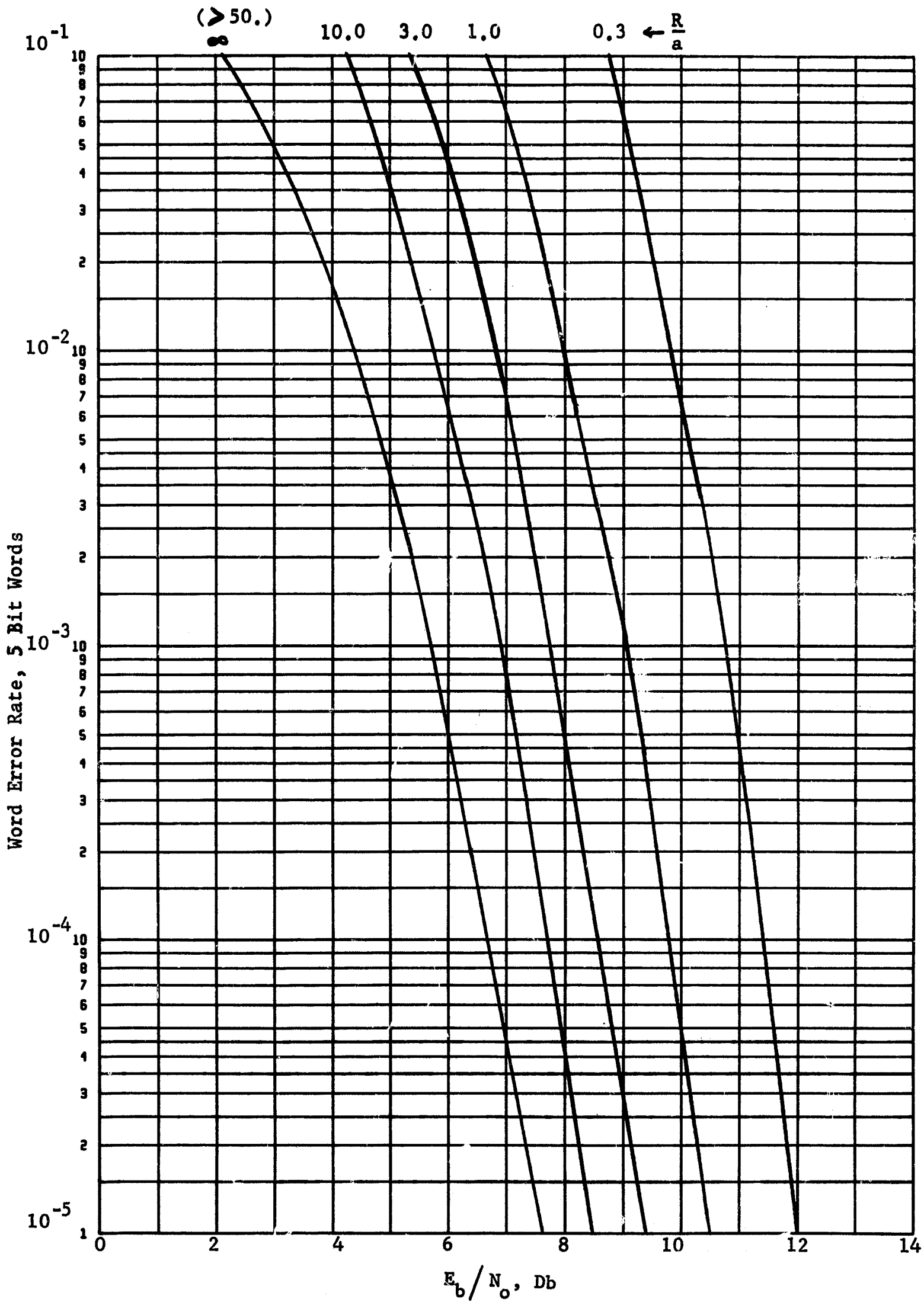


Figure VIIF5-1B Performance of Uncoded 32ARY FSK, Noncoherent Detection

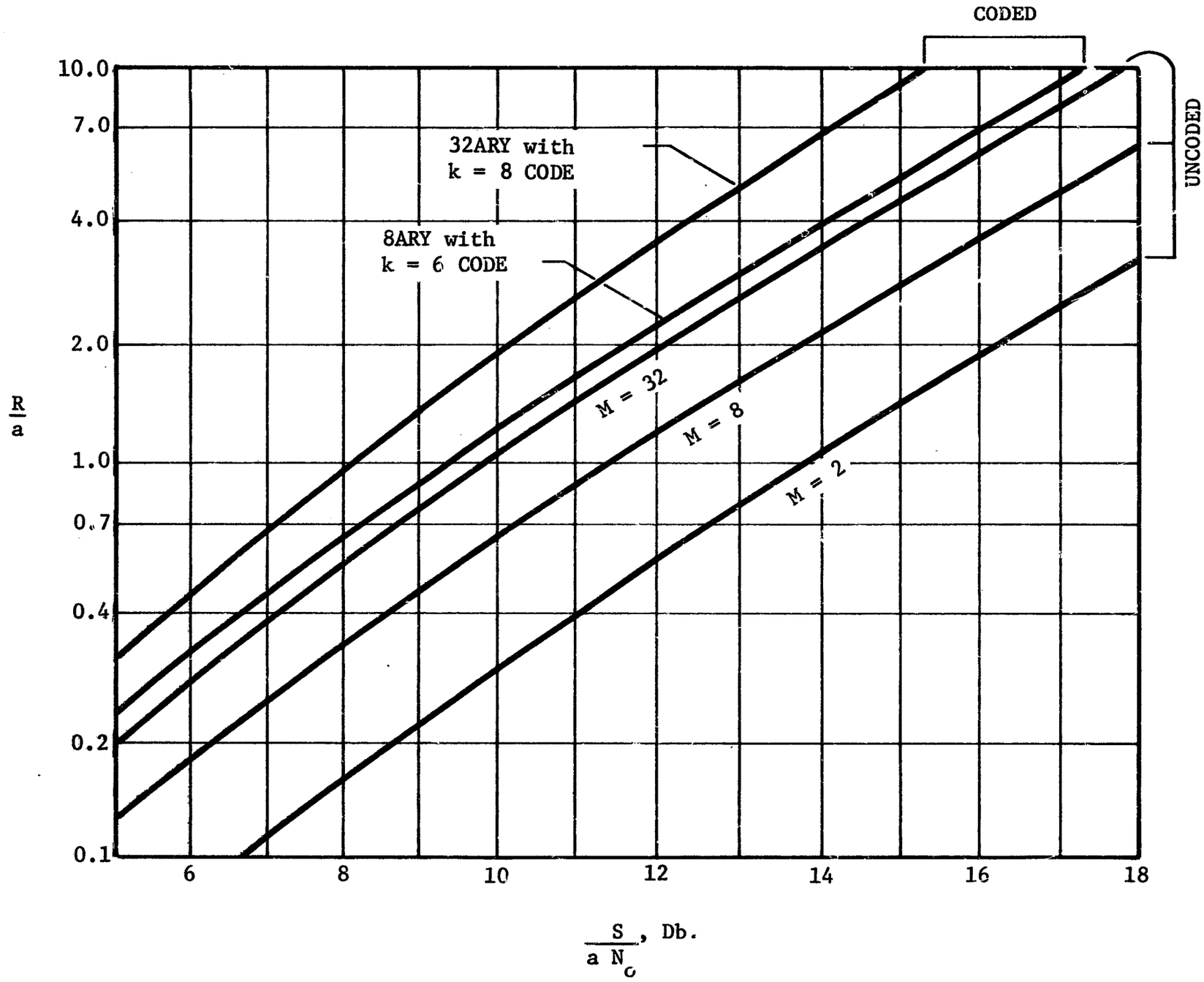


Figure VIIF5-2 Normalized Signalling Rate vs Normalized Signal Power for Bit Error Rate of 5×10^{-5}.

receiver configuration is assumed. Repeated iterations through the data, using decision feedback, is used to reduce the frequency uncertainty to a small residue that is included in the 2 Hz linewidth. With these assumptions, performance is a function of the ratio of the data rate R to the signal linewidth. This is shown in Figure VIIF5-2, which shows performance curves for 32 ary FSK, with R/a as a parameter. From this figure, with a = 1 Hz and R - 20 bps, an E_b/N_o of +7.4 db will give a word error rate of 10^{-4}. As shown in Figure VIIF5-3, (which assumes Viterbi decoding) the convolutionally encoded 32 ary format will give an improvement of 2.5 db (holding the data rate constant and reducing power) or, E_b/N_o = 4.9 db. The improvement in the other dimension, holding the power constant and increasing data rate, is 2.9 db.

The R/a = ∞ curve in figure VIIF5-2 shows the performance that would be calculated if signal linewidth effects were neglected. This (erroneous) assumption would give an improvement in E_b/N_o of 0.7 db, or E_b/N_o = 4.2 db. This curve can be used with good accuracy for R/a $>$ 50. This very low E_b/N_o is comensurate with that given by coherent detection and good coding. This is a reflection of the results shown by Lindsey [4] and others that, given sufficiently elaborate coding, the difference in performance between noncoherent and coherent detection becomes vanishingly small.

A block diagram of the encoder is shown in Figure VIIF5-3. It is not appreciably more complicated than a convolutional encoder that would be used with a coherent communication system, and the decoding operation is a straightforward extension of techniques now being proposed for binary Viterbi decoding. Accordingly, it seems reasonable to assume that an equivalent capability will exist at the time this mission is flown.

Chadwick and Springett [5] have estimated demodulation losses of around 2 db for the MFSK signalling format due to imperfect frequency and symbol synchronization tracking. These losses assume real-time demodulation, and they should be markedly reduced by the iterative processing of predetection recordings assumed by us. However, we have arbitrarily degraded the expected performance by 1.6 db, and will use E_b/N_o = 6.5 db for our link design.

(4) Coherent Signalling

The modulation and noisy carrier losses inherent in conventional coherent signalling could be reduced somewhat for low signalling rates by the use of suppressed carrier modulation and some carrier reconstruction scheme such as frequency doubler in the receiver. However, there does not appear to be any firm plans to equip the DSN to handle this signalling mode, and performance is hard to estimate in the absence of a specific configuration, so the conventional modulation demodulation system was assumed.

The use of advanced coding and decoding systems such as the rate 1/3, constraint length 8, Viterbi decoder system evaluated by Heller [6] will give a bit error probability of 5×10^{-5} for E_b/N_o = 3.9 db, and workers in this field [7] are now estimating improvements of as much as 2.6 db over this figure. A value of 4 db will be assumed for our calculations. Assuming that these estimates are largely realized by 1975, this gives a margin of around 2 db.

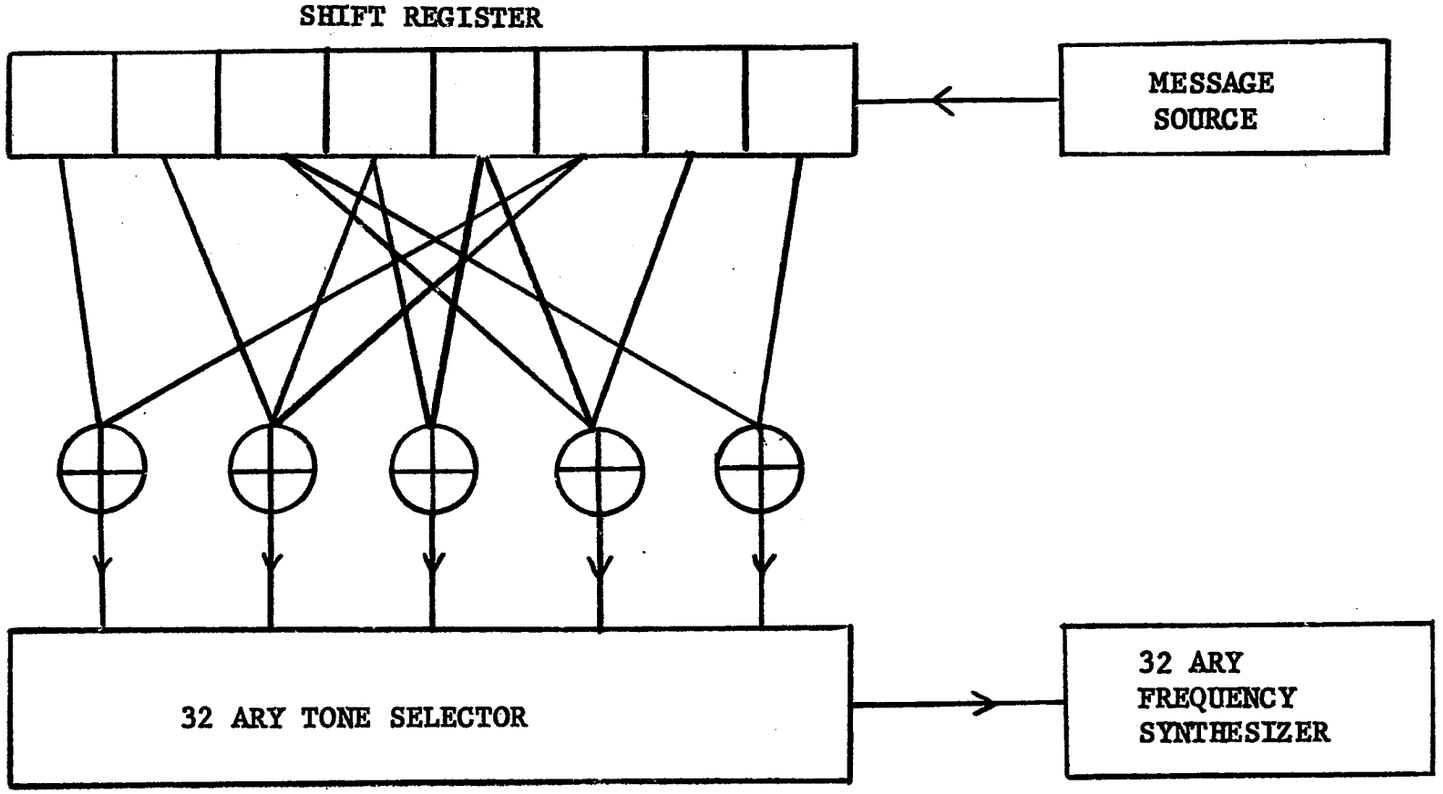


Figure VIIF5-3 Convolutional Encoder
K = 8, M = 32

Loop thresholds are set at + 9 db for the DSN receiver and + 20 db for the up-link. A coherent transponder is assumed. The high loop threshold on the up-link is set to minimize the noisy carrier loss for a two-way link. This, combined with the + 9 db loop threshold SNR on the down-link gives the noisy carrier receiver loss shown in the down-link calculations, 1.5 db. (From [8]).

(5) The Probe Antenna

A steerable high gain antenna is required to hold the transmitter to a reasonable power level. Size of this antenna is limited by vehicle size. The vehicle will be an oblate spheroid with the minor diameter pointing upward. The major diameter will be around 26" to 29". A dish or an array of this size will give a gain of around 20 to 22 db, with the higher aperture efficiency of the array giving the higher figure.

A comparison between a dish and an array was made for the spacecraft antenna on mission B. A dish was selected for that mission. The requirements of this mission are markedly different. Pointing information for either type of antenna would be derived from the up-link signal from Earth. This signal is strong enough to permit the use of a self-focusing array, giving automatic rapid acquisition and highly agile tracking. This seems preferable to the mechanical search and track that would be required of a dish, particularly in view of the unknown turbulence environment on Jupiter. In either case the frequency search and acquisition would be done via a fixed low-gain antenna, which could be one element of the array. Beam position search would begin after frequency acquisition. For a self-focusing array, this would be almost instantaneous.

The array would be similar to the one discussed in Mission B, a honeycomb of hexagonal cavities having a hexagonal envelope. However, because of the limited scan range, fewer, higher gain

elements could be used. A 37 element array (which also gives a hexagonal envelope) of 0.5 λ cavity helices is recommended. The element pattern is shown in Figure VIIF5-4. Cavity areas would be scaled by 61/37 to give the same total aperture and the same gain, 22 db. The aperture would be scaled by frequency ratio 1.2/2.3, giving a point-to-point diameter of 25.2". Gain would decrease as Cos θ for scanning off boresite. The pattern of Figure VIIF5-4 is used for the up-link antenna gain.

Microelectronic transceiver modules similar to those now being developed for airborne phased-array radars would be used at each element. Assuming 1975 technology, it is estimated that the weight of antennas and associated electronics would be on the order of 1.1 lbs per element, or 41 lbs for the whole array. This assumed RF power amplifiers at each element, so this 41 lbs includes the transmitter weight. The feed and the central control electronics would add 5 lbs and the supporting structure would be another 5 lbs, for a total of 51 lbs.

Power consumption is estimated at 0.5 watt per element for low-power functions, or a total of 19 watts, an additional 5 watts for common functions, plus RF power amplification at 20% efficiency. For 15 watts radiated RF power this component would be 75 watts, giving a total for the whole system of 99 watts.

A lower-gain fixed antenna could also be considered. Given the angular range of look angles over the mission, including allowances for turbulence and uncertainties, the antenna of Figure VIIF5-4 is about the highest gain fixed antenna that could be used. This gives a gain at the end of the mission that is 14.2 db less than that given by the array. Matching the ERP given by the 15 watts transmitted power of the array would require 400 watts RF power. This could only be realized by a tube. Assuming a 0.93 hour mission, 40% efficiency for the transmitter, and 25 watt-hrs/lb for the batteries, estimated weights for the two systems are compared below.

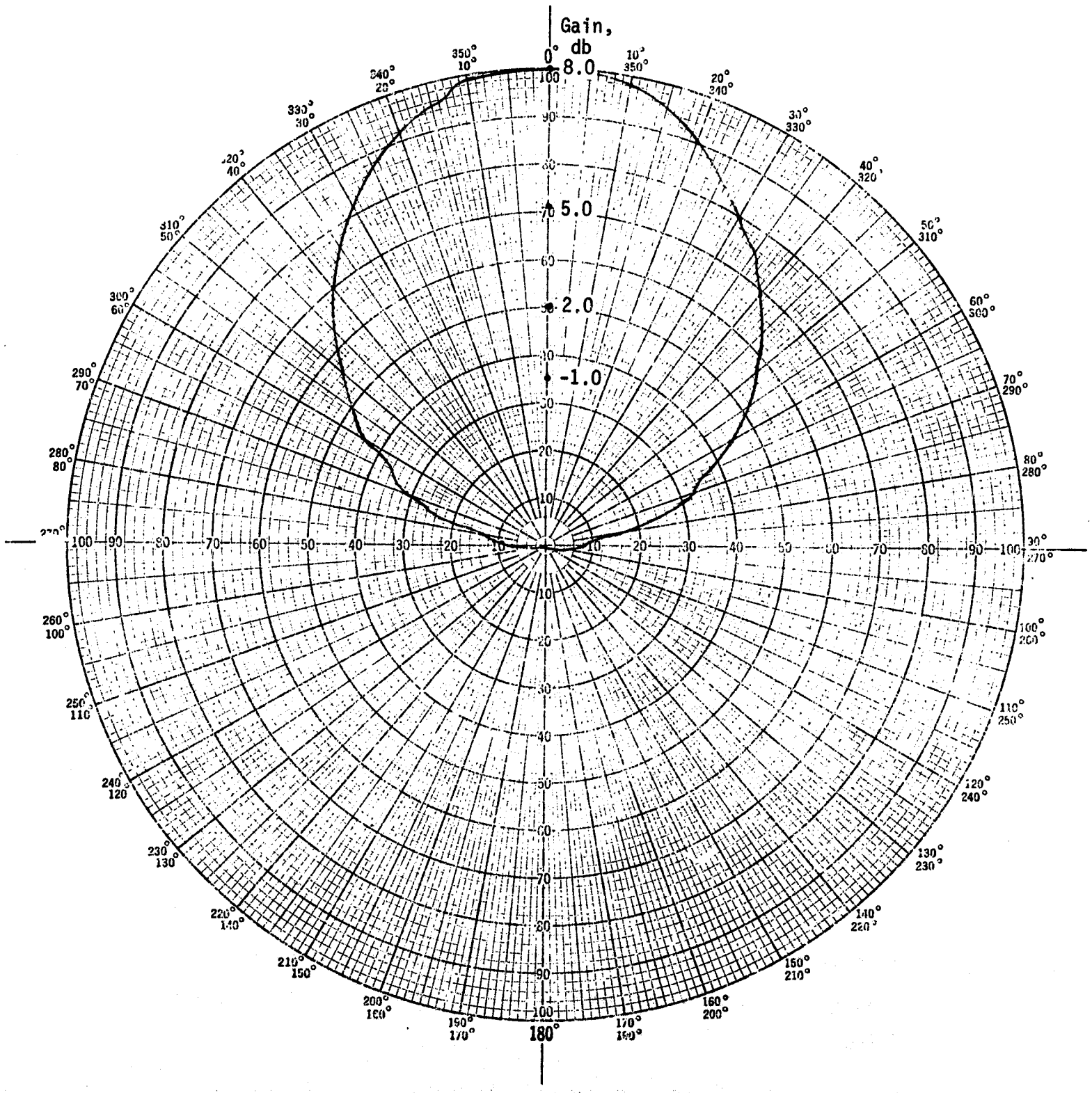


Fig. VIIF5-4 Radiation Pattern, 0.5λ Cavity Helix; Peak Gain, 8 db

TABLE VIIF5-1

ESTIMATED WEIGHTS. ARRAY VS FIXED ANTENNA

A. Array

Item	Weight, lbs
Antenna plus transmitter	51
Battery	4
Total	55

B. Fixed Antenna

Item	Weight, lbs
Antenna	1
Transmitter and power supply	60
Battery	37
Total	98

These estimates are not highly refined. No consideration is given to the thermal control problems that would be caused by a 400 watt transmitter. Even without this consideration, it is clear that the array system is the preferred choice. Estimated weight for the 400 watt transmitter is taken from [9].

(6) Link Calculations

The antenna gains and temperatures given by the 210 ft DSN dish vary with the antenna feed configuration. S-band receiving gains and zenith temperatures for several configurations are listed below.*

A. Transmit X-band, Receive S and X-band.	$G = 60.8 \begin{smallmatrix} + 0.4 \\ - 0.4 \end{smallmatrix}$ db
	$T = 27.0 \pm 3.0$ deg K
B. Transmit S-band, Receive S-band.	$G = 61.4 \pm 0.4$ db
	$T = 23.0 \pm 3.0$ deg K
C. Receive only, S-band	$G = 61.4 \pm 0.4$ db
	$T = 18.0 \pm 2.0$ deg K

*Murray Koerner, personal communication.

Configuration A would be used with the TOPS spacecraft and Configuration B with the Pioneer spacecraft. Configuration C could be used with either spacecraft, but it would not allow an occultation experiement to be carried out so it will not be considered. The combined G and T difference between configurations A and B is 1.3 db. Our design contro' tables assume a Pioneer spacecraft, Configuration B. If a TOPS is used, margins would be reduced (or power should be increased) by 1.3 db.

The antenna temperature must be augmented by 4° to account for the contribution of Jupiter in the main beam. Also, temperature must be increased for scanning off zenith. This contribution is 6° for 65° off zenith [10]. Adding these items to the Configuration B temperature gives 33 ± 3°k. This is the value used in our calculations.

Calculations were made comparing three signalling formats,

(1) Coherent signalling, 12 Hz PLL, real-time demodulation.
(2) Coherent signalling, 3 Hz PLL, predetection recording.
(3) Noncoherent signalling, 32 ary FSK, predetection recording.

Data rate is held constant at 20 bps, and power is varied to give equivalent performance. Results are shown in Table VIIF5-1. Performance relative to (1) is

(2) 1.2 db improvement,
(3) 2.2 db improvement,

Accordingly, (3) is selected as the preferred signalling format. The indicated minimum transmitter power is + 39.2 dbm or 8.3 watts. This is increased to 15 watts in our system, giving an additional margin of 2.6 db.

The communications range used in the design control tables is the maximum over a 30 day launch window. The atmospheric loss is based on the nominal atmosphere, at a depth of 17 atmospheres (elevation -117 km) and a look angle of 8.5° with an adverse tolerance of 1.8°. Probe antenna pointing loss assumes an additional 10° due

TABLE VIIF5-1

DESIGN CONTROL TABLES, DIRECT DOWN LINK,
JUPITER ENTRY PROBE, MISSION F

Parameter	a. 12 Hz. PLL, Real-Time Demodulation		b. 3 Hz. PLL, Pre-detection Recording		c. Noncoherent, Pre-detection Recording	
	Nominal, db	Adverse tol, db	Nominal db	Adverse tol, db	Nominal, db	Adverse tol, db
1. Minimum Transmitter Power	+ 41.4 dbm	0.4	+ 40.2 dbm	0.4	+*39.2 dbm	0.4
2. Transmitter Circuit Loss	- 0.5	0.5	- 0.5	0.5	- 0.5	0.5
3. Transmitter Antenna Gain	+ 22.0	0	+ 22.0	0	+ 22.0	0
4. Transmitter Antenna Pointing Loss	0	0.3	0	0.3	0	0.3
5. Space Loss, 2297 MHz, 9.5×10^8 km.	-279.2	0	-279.2	0	-279.2	0
6. Atmospheric Loss	- 2.4	0.2	- 2.4	0.2	- 2.4	0.2
7. Polarization Loss	0	0.5	0	0.5	0	0.5
8. Receiver Antenna Gain, 210-Ft Dish	+ 61.4	0.4	+ 61.4	0.4	+ 61.4	0.4
9. Receiver Pointing Loss	0	0	0	0	0	0
10. Receiver Circuit Loss	- 0.1	0	- 0.1	0	- 0.1	0
11. Recorder Loss	0	0	- 1.2	0	- 1.0	0
12. Net Circuit Loss	-198.8	1.9	-200.0	1.9	-199.8	1.9
13. Total Received Power	-157.4 dbm	2.3	-159.8 dbm	2.3	-160.6 dbm	2.3
14. Received Noise Spectral Density, 33° ± 3° K	-182.8 dbm	0.4	-182.8 dbm	0.4	-182.8 dbm	0.4
Carrier Performance, Data Demodulation						
15. Carrier Power to Total Power	- 2.5	0.4	- 6.1	0.4		
16. Received Carrier Power	-159.9 dbm	2.7	-165.9 dbm	2.7		
17. Carrier Threshold Bandwidth, 12 Hz PLL	+ 10.3	0.5	+ 4.3	0.5		
18. Threshold S/N in 2 B_{LO}	+ 9.0	0	+ 9.0	0		
19. Threshold Carrier Power	-163.5 dbm	0.9	-169.5 dbm	0.9		
20. Margin, Carrier	+ 3.6	3.6	+ 3.6	3.6		
Data Channel Performance						
21. Receiver Loss	- 1.5	0.2	- 1.5	0.2	0	0
22. Data Channel Power/Total	- 3.6	0.4	- 1.2	0.4	0	0
23. Total Data Power	-162.5 dbm	2.9	-162.5 dbm	2.9	-160.6 dbm	2.3
24. Data Threshold E/NO	+ 4.0	0	+ 4.0	0	+ 6.5	0
25. Data Rate, 20 bps	+ 13.0	0	+ 13.0	0	+ 13.0	0
26. Data Channel Threshold	-165.8 dbm	0.4	+165.8 dbm	0.4	-163.3 dbm	0.4
27. Data Channel Margin	+ 3.3	3.3	+ 3.3	3.3	+ 2.7	2.7

* 15 watts (+41.8 dbm) actually used in system design, giving a margin of 2.6 db.

TABLE VIIF5-2

DESIGN CONTROL TABLE, DIRECT UP-LINK
JUPITER ENTRY PROBE, MISSION F

	Parameter	Carrier Only	
		Nominal, db	Adverse Tol, db
1.	Total Transmitter Power, 400 kw	+ 86.0 dbm	0
2.	Transmitter Circuit Loss	- 0.4	0
3.	Transmitter Antenna Gain	+ 59.9	0
4.	Transmitter Antenna Pointing Loss	0	0
5.	Space Loss, 2116 MHz	-278.5	0
6.	Atmospheric Loss	- 2.0	0.2
7.	Polarization Loss	0	0.5
8.	Receiver Antenna Gain	+ 8.0	0
9.	Receiver Pointing Loss	- 0.1	0.4
10.	Receiver Circuit Loss	- 0.3	0.3
11.	Net Circuit Loss	-213.4	1.4
12.	Total Received Power	-127.4 dbm	1.4
13.	Received Noise Spectral Density, 1750° K	-166.2 dbm	0
	Carrier Performance		
14.	Carrier Power to Total Power	0	0
15.	Received Carrier Power	-127.4 dbm	1.4
16.	Carrier Threshold Bandwidth, 40 Hz	+ 16.0	0
17.	Threshold S/N in 2 B_{LO}	+ 20.0	0
18.	Threshold Carrier Power	-130.2 dbm	0
19.	Margin, Carrier	+ 2.8	1.4

attitude swings caused by turbulence. The initial pointing angle is larger than this (26.8° + 20° adv. tol.), but there is more margin in the link at this initial point. The conditions at 17 atmospheres are the worst-case on which the link calculations are based.

The up-link calculation assumes a carrier-only transmission using the full 400 kw power capability of the DSN. The up-looking probe antenna temperature at the 17 atmosphere level is computed to be 550°k, due largely to the magnetosphere temperature. This temperature assumes a low-gain antenna. This is augmented by the receiver temperature. A receiver with a low-noise RF amplifier giving a temperature of 1200° k is assumed. This should be well within the state-of-the-art at the time the probe is designed.

It is interesting to consider what would happen if it were possible to lower the DSN frequency to 960 MHz, retaining the 210 ft dish. Given a link having a fixed aperture at one terminal and a fixed gain (e.g. a near-omni low gain antenna) at the other terminal, the link calculation becomes independent of frequency, with the decrease in gain of the fixed aperture antenna exactly compensated by the decrease in space loss. If this were the case in the link under consideration it would be advantageous to lower the frequency because this would reduce the atmospheric absorption loss, the doppler rates, and the frequency uncertainty. However, the link being examined here uses substantial gain in the probe antenna, and is essentially a link with a fixed aperture at both ends. Under these circumstances, combined losses go as $\left(\frac{f_1}{f_2}\right)^2$. Using f_1 = 2300 MHz and f_2 = 960 MHz, this amounts to a loss of 7.6 db, much more than can be saved by the reduction in atmospheric absorption. Now if deeper probe penetrations were considered for a direct link mission, (which would be impractical because of the enormous transmitter power required), the tradeoff could go the other way. For penetration to 1000 atm for example, the saving in atmospheric absorption would be 30 db, much more than the 7.6 db loss due to reduced antenna gains.

Because of these two opposing effects, there is an optimum frequency for every depth of penetration, with deeper penetrations corresponding to lower frequencies. It turns out that for the 17 atm penetration selected for this mission the S-band frequency is not far from optimum. Going to X-band, for example, gives a net loss of around 27 db compared to S-band.

c. Spacecraft Interface and Modifications

The principal advantage of a direct link system is that it minimizes the modifications required for the spacecraft. The electrical interface will consist of a connection into the spacecraft power and data system to carry out engineering monitoring during interplanetary flight. Storage and execution electronics will be required for the probe separation maneuver.

d. Data System

The probe data system is identical to that used for the Mission D probe.

e. Power System

Power consumption is summarized below.

TABLE VIIF5-3

POWER CONSUMPTION, MISSION F

Item	Power, watts
Sequencer	3
Data Handling	5
Memory	2
Power Conditioning	11
Phased Array Antenna and Transmitter	99
Instruments	15
Total	135

Power system design is similar to that for the other missions. Silver-zinc batteries are assumed. Total energy consumption for the 0.93 hour mission is 125 watt-hours. This gives a battery weight of 5 lbs.

f. Weights

The weights of the components of the telecommunications, data handling, and power systems for Mission F are tabulated below.

TABLE VIIF5-3

ELECTRONIC SYSTEM WEIGHTS, MISSION F.

Item	Weight, lbs
Sequencer	4
Data Handling	5
Memory	2
Power Conditioning	4
Cabling	6
Phased Array Antenna and Transmitter	51
Battery	5
Total	77

References, Section VIIF5

1 JPL Document 831-1, Rev. A, 1 Oct 1968, pg 3-32

2 R. J. Richardson, "Analysis of a Weak-Signal Noncoherent MFSK Deep Space Telemetry System", Presented at SWIEECO, Houston, July 1968.

3 R. J. Richardson, C. C. Korgel, R. B. Blizard, "Coding for Low Data Rate Noncoherent Channels", to be published, 1971 NTC (Record).

4 W. C. Lindsey, "Coded Noncoherent Communications", IEEE Transactions, SET-11, No. 1, March 1965.

5 H. D. Chadwick and J. C. Springett, "The Design of Low Data Rate MFSK Communication Systems." IEEE Transactions, COM-18, No. 6, December 1970.

6 J. A. Heller, "Short Constraint Length Convolutional Codes", JPL-SPS 37-54, Vol III, p 171, December 31, 1968,

7 Phase II Final Report, Contract NAS9-9852 (Martin-Marietta Corporation), "Study of Potential Applications of Digital Techniques to Appolo USB System", November 1970, pg IV-14.

8 W. C. Lindsey, JPL Tech Report 32-986, "A Theory for the Design of Phase-Coherent Communication Systems", July 1969.

9 Phase I Final Report, Contract NAS8-21886, Volume II, "Multikilowatt Transmitter Study for Space Communications Satellites", 10 June 1967, (General Electric Co.), pg 3-78.

10 JPL Document 910-5, "DSN Standard Practice", March 1, 1970.

VIII. RELIABILITY REQUIREMENTS AND MAGNETIC CLEANLINESS REQUIREMENTS

A. Reliability Requirements

A cursory evaluation of the reliability requirements for a Jupiter atmospheric probe can be made by comparing the probe systems and anticipated environments to those of well defined systems. Current and proposed spacecraft systems encompass the mission duration required. As a general comparison of long life mission design, the following categories are representative:

Spacecraft	Approximate Design Lifetime
Mariner	2 yrs
Pioneer	2 - 5 yrs
TOPS	5 -12 years

The Jupiter atmospheric probe mission duration may vary from about 2 years for the Type I trajectories, to about 3 years for the Type II trajectories. This would imply reliability requirements typical of the Pioneer spacecraft and, therefore, state-of-the-art hardware would, in some instances, be sufficient.

The probe systems would essentially be "on the shelf" and completely inactivated for nearly the full duration of flight. This inactive status will improve the reliability of certain subsystems such as the mechanical systems; however, the integrated circuit equipment reliability essentially remains the same whether the circuits are on or off because very little heat is generated during operation. Independent of the inactive status of the probe equipment during the life of the mission, the category of mechanical equipment is considered the greatest threat to reliability. The unreliability of mechanical equipment compared with electronic equipment is basically due to the difficulty of establishing a sufficient design margin. With mechanical equipment the design margin is more difficult to analytically establish during early design, is more costly and time consuming to verify by testing, is more costly and time consuming to achieve by redesign, and inadequacies are less apt to show up in ground testing[1].

---

(1) Burrows, R. W., Martin Marietta Corporation, Denver, "The Long-Life Spacecraft Problem", AIAA Paper No. 67-880, AIAA 4th Annual Meeting and Technical Display, Anaheim, California, October 1967.

These problems are solvable by expanding the usual scope of Margin Testing (both functional and environmental) and to accomplish this testing during the Development Phase prior to Qualification Testing.

Martin Marietta, under the Viking Program, is currently conducting tests in support of a long-term vacuum exposure materials evaluation. The test facility enables exposure of materials to a vauum at various temperatures, and properties testing while still in the vacuum environment. It is expected that by early 1974, three years of real-time vacuum testing will have been accomplished. These data will provide important background information to be used for the selection of the non-metallic materials for a Jupiter Probe. An important goal of this program is the development of valid techniques to predict the long term effects of the environment based on accelerated test techniques.

B. Magnetic Cleanliness Requirements

A primary requirement for the probe and its components to be "magnetically clean" exists only if its mission includes measurements of the Jovian magnetic field during the descent through the atmosphere. However, it is probably adequate to conduct any such magnetic measurements in the upper parts of the atmosphere, i.e., in the general region of the visible cloud top "Surface" of the planet. If one uses a split probe, only its upper, more slowly descending part would have to be magnetically clean, and this is easier to achieve than for the deeply penetrating lower part which will probably need a pressure shell of steel, i.e., be ferromagnetic.

Going much deeper with the magnetic experiment, and in particular down to the deepest technically accessible ($p \sim 10^3$ atm, $T \sim 1400^{\circ}K$) - level some 600 km below the clouds would only be desirable if one had good reasons to expect already appreciable field distortions from magneto-hydrodynamic effects at this depth. However, this is fairly unlikely because the best guess for magnetic Reynold's number even at 1000 kilometers in depth is less than 10^{-4} (see Appendix D).

The scientific instruments in the probe, namely its

gas chromatograph and mass spectrometer
pressure and temperature gauges
visual photometers
accelerometers
nephelometer
I. R. radiometers
R. F. lightning detector, and
microphone

are very little affected by small and spurious magnetic fields, and the same is true for its data processing and transmitting electronics. There is, therefore, no particular requirement for a great magnetic cleanliness of the probe, as far as the major part of its payload is concerned.

With the exception of the mass spectrometer, the insensitivity of these instruments and of their associated electronics against magnetic fields is even great enough to dispose of a need for particular precautions against interference from the Jovian magnetic field which seems to be about twenty times stronger than that of the earth (order of 10^{-3} volt sec m^{-2}, or 10 gauss at the surface of Jupiter).

The mass spectrometer will, however, very likely need either some light magnetic shielding of an essentially conventional instrument, or else a special design with stronger and more compact electrical and/or magnetical RF-fields, in order to avoid unacceptable defocussing by the gyration of the ions in the magnetic field. Either approach appears feasible. The selection of a particular design is then a question of tradeoffs in weight, complexity, reliability, and development costs.